Microbial Community and Proteomic Analysis of a Mixed Microbial Culture Achieving Bioplastic Production from Fermented Dairy Manure

A Dissertation

Presented in Partial Fulfillment of the Requirements for the

Degree of Doctorate of Philosophy

with a

Major in Microbiology, Molecular Biology, and Biochemistry

in the

College of Graduate Studies

University of Idaho

by

Andrea J. Hanson

Major Professor: Erik R. Coats, P.E., Ph.D.

Committee Members: Andrzej Paszczynski, Ph.D.; Eva Top, Ph.D.;

Armando McDonald, Ph.D.

Department Administrator: James Nagler, Ph.D.

December 2015

Authorization to Submit Dissertation

This dissertation of Andrea J. Hanson, submitted for the degree of Doctorate of Philosophy with a Major in Microbiology, Molecular Biology, and Biochemistry and titled "Microbial Community and Proteomic Analysis of a Mixed Microbial Culture Achieving Bioplastic Production from Fermented Dairy Manure," has been reviewed in final form. Permission, as indicated by the signatures and dates below, is now granted to submit final copies to the College of Graduate Studies for approval.

Major Professor: _____ Date_____
Erik R. Coats, P.E., Ph.D.

Committee Members: _____ Date_____
Andrzej J. Paszczynski, Ph.D.

_____ Date_____
Eva Top, Ph.D.

_____ Date_____
Armando G. McDonald, Ph.D.

Department Administrator: _____ Date_____
James Nagler, Ph.D.

Abstract

Polyhydroxyalkanoates (PHAs) are bio-based, biodegradable polyesters displaying a range of thermoplastic properties. The use of mixed microbial cultures (MMCs) to synthesize PHA from organic-rich waste streams is an alternative strategy for commercial-scale PHA production. For this approach to be effective, MMCs must be enriched for PHA-producing bacteria exhibiting a physiologically-primed metabolism for PHA storage. Microbial enrichment is commonly performed through the application aerobic dynamic feeding (ADF) or feast-famine conditions in a sequencing batch reactor (SBR), after which the MMC is used for fed-batch PHA production. Our research group has developed a multi-stage PHA production process using fermented dairy manure as the feedstock. However, advancement of this PHA production approach is impeded by an incomplete understanding of the microbial community and functional dynamics associated with conventional process observations. The aim of the research presented herein was to explore the microbial composition and proteome of an MMC enriched through ADF in relation to traditional bulk solution variable assessments. MMC protein mixtures collected over an SBR cycle and during fed-batch PHA production were visualized and compared using two-dimensional electrophoresis. Proteins exhibiting large abundance changes during the SBR cycle and fed-batch PHA production were identified using liquid chromatography coupled with tandem mass spectrometry. For the SBR cycle, prominent functions during the feast phase included PHA synthesis, energy generation, and protein synthesis, whereas nutrient transport, acyl-CoA metabolism, energy generation, and housekeeping functions were more pronounced during the famine phase. During fed-batch PHA production, PHA synthesis-related proteins acetyl-CoA acetyltransferase and phasin proteins were in increased abundance relative to the feast phase, supporting the higher

PHA content observed. High-throughput 16S rRNA gene sequencing revealed a diverse microbial community that fluctuated over time, although *Meganema* was the dominant genus in terms of relative abundance throughout SBR operation. While consistent correlations between microbial composition and the feast-to-famine ratio, specific VFA uptake rate, and PHA content in the SBR were not observed, lower microbial diversity appeared to be more favorable for fed-batch PHA production. Collectively, the results corroborated functional responses of MMCs to ADF conditions and provided new insight into multi-stage PHA production using MMCs and waste feedstocks.

Acknowledgements

I thank my major professor, Erik R. Coats, for providing me the opportunity to work and study in his civil engineering laboratory and for his guidance during my time at the University of Idaho. My gratitude is extended to my committee members, Drs. Andrzej Paszczynski, Eva Top, Armando McDonald, as well as former member Dr. Aurelio Briones for their critical review of my research, in addition to their expert guidance and support throughout the course of my studies and research.

Special thanks is extended to my lab mate Nicholas Guho for his trusted assistance, support, and friendship during my time in the Coats' lab. I also wish to thank the faculty and students of the former Microbiology, Molecular Biology, and Biochemistry department, in addition to former and fellow graduate students for collaborate discussions, use of laboratory instruments, and support related to academics and research activities. I am also appreciative for the technical support received from the Mass Spectrometry Core and the Genomics Resources Core at the University of Idaho.

Finally, I gratefully acknowledge the financial support of the National Science Foundation and the Environmental Protection Agency's Science to Achieve Results Fellowship Program.

Dedication

To my parents, John and Jennifer Hanson.

To my brother, Daniel Hanson.

To my sister and brother-in-law, Allison and Maxwell Johnson.

Table of Contents

List of Abbreviations

Abbreviation	
2DE	Two-dimensional electrophoresis
ADF	Aerobic dynamic feeding
ADF	Anaerobic digestion
AEBSF	4-(2-aminoethyl)benzenesulfonyl fluoride hydrochloride
AGC	Accudenz gradient centrifugation
CBB	Coomassie Brilliant Blue
CHAPS	3-[(3-Cholamidopropyl)dimethylammonio]-1-propanesulfonate hydrate
CL	Cycle length
CoA	Coenzyme A
COD	Chemical oxygen demand
DGGE	Denaturing gradient gel electrophoresis
DO	Dissolved oxygen
DTT	Dithiothreitol
EBPR	Enhanced biological phosphorus removal
EDTA	Ethylenediaminetetraacetic acid
F:F	Feast-to-famine ratio
FDML	Fermented dairy manure liquor
FISH	Fluorescence in situ hybridization
GC-MS	Gas chromatography-mass spectrometry
HB	Hydroxybutyrate
HRT	Hydraulic retention time

HV	Hydroxyvalerate
IEF	Isoelectric focusing
IPG	Immobilized pH gradient
LC-MS/MS	Liquid chromatography-tandem mass spectrometry
MMC	Mixed microbial culture
NGS	Next-generation sequencing
OLR	Organic loading rate
PHAs	Polyhydroxyalkanoates
PHB	Polyhydroxybutyrate
PHBV	Poly(3-hydroxybutyrate-co-3-hydroxyvalerate)
PHV	Polyhydroxyvalerate
QTOF	Quadrupole-time of flight mass spectrometry
RDP	Ribosomal database project
SBR	Sequencing batch reactor
SRT	Solids retention time
TSS	Total suspended solids
VFA	Volatile fatty acid
VSS	Volatile suspended solids

List of Tables

List of Figures

Introduction

Polyhydroxyalkanoates (PHAs) are intracellular carbon and energy storage granules synthesized by numerous bacterial species. PHAs are also considered bioplastics, exhibiting material properties comparable to many conventional petroleum-based thermoplastics with the added benefits of being biodegradable and produced from renewable feedstocks. An attractive strategy for the production of PHAs utilizes organic-rich waste streams derived from industrial or agricultural processes as feedstocks and ecological selection principles to obtain mixed microbial cultures (MMCs) with a high PHA production capacity. To obtain these MMCs, cyclic feast-famine conditions are imposed by alternating substrate availability to enrich MMCs for PHA-producing bacteria; this process is also referred to as aerobic dynamic feeding (ADF) and is commonly applied using a sequencing batch reactor (SBR) configuration. Typically for an ADF operational cycle, the feast phase is characterized as a brief period of substrate excess, whereas the famine phase represents a long period of time devoid of exogenous substrate. Once MMCs are appropriately enriched for PHA-producing bacteria exhibiting a desirable feast-famine response, a portion of the MMC is then used for PHA production, after which PHA is extracted from MMC biomass and processed.

Our research group has advanced an MMC PHA production technology using fermented dairy manure as the feedstock, with the motivation stemming from the desire to establish and advance core process fundamentals associated with a ‘waste-to-products’ vision centered on bio-converting dairy manure to PHAs. Not only does this integrated process exhibit potential to produce PHA in a commercially viable manner, but it provides an environmentally-benign alternative for the treatment of dairy manure.

Most of the research concerning PHA production using MMCs and waste feedstocks, including fermented dairy manure, has focused on the empirical "black box" evaluation and optimization of varied operating conditions, as opposed to elucidating the underlying microbiology driving the observed biochemical changes. Although a traditional engineering approach may facilitate inferences regarding microbial physiology, implicit challenges remain as bulk solution investigations would require the analysis of hundreds of different bioreactor configurations. More importantly, bulk solution factorial analyses would not biologically identify the microbial composition and corresponding functionality of MMCs specifically during the feast phase compared to the famine phase, and collectively over the course of an operational cycle.

Conversely, investigating this process at a functional, or proteomic level would strengthen our fundamental knowledge regarding the PHA metabolism in MMC exposed to ADF conditions in the presence of mixed substrates. Because no proteomic profiling has been completed for MMC cultivated under ADF conditions using waste feedstocks (including fermented dairy manure), basic research questions in this context still linger: What proteins are functional in an MMC exposed to ADF conditions? What proteins are more or less abundant in the feast phase compared to the famine phase of an ADF cycle? To what extent are these proteins more or less abundant? How does the MMC proteome profile change over an ADF operational cycle? Associated with this functionality is the microbial community composition; however, no prior microbial community characterization has been performed for MMC cultivated under ADF conditions using fermented dairy manure as a feedstock in an SBR, therefore, basic research questions also remain: What is the microbial composition of the MMC? Does the microbial composition change over time? Are there potential

relationships between microbial composition and PHA process performance? Considering these collective research questions, the aim of the research presented herein was to investigate MMC composition and proteome profiles in an ADF enrichment SBR cultivated on fermented dairy manure with respect to conventional bulk solution observations and in regard to ultimately advancing this PHA production technology. As such, microbial community and proteomic profiling techniques were applied to an MMC maintained in a SBR under ADF conditions using fermented dairy manure as the feedstock. This dissertation presents and discusses the findings associated with these research objectives.

Chapter 1 presents a review of the literature relevant to the research presented herein and overviews the research objectives. The main topics discussed include general characteristics of PHAs as bioplastic materials, the occurrence and synthesis of PHA in bacteria, the use of MMCs for PHA production, and an overview of the "omics" technologies that were used in the applied experimental approaches. The chapter ends with a summary of the research objectives.

Chapter 2 describes the optimization of proteomic methods that was required prior to commencing proteomic investigations. To monitor and quantify MMC protein profiles, two-dimensional protein electrophoresis was selected as the protein separation method; however, the complexity of the fermented dairy manure sample matrix posed many challenges to effective protein resolution. As such, an original biomass purification and sequential protein extraction workflow was developed to alleviate the shortcomings associated with the sample matrix. The optimized method greatly improved the quality of the two-dimensional electrophoresis, facilitating successful MMC protein separation and protein identification.

Chapter 3 reports the original work describing the characterization of MMC composition and proteome profiles with respect to given ADF conditions and process performance. In addition to conventional bulk solution parameter assessments, 16S rRNA gene sequencing was used to identify taxa present in the MMC. Two-dimensional protein electrophoresis was used to resolve MMC protein mixtures and quantify protein abundance changes during an SBR cycle, as well as fed-batch PHA production tests. Liquid chromatography coupled with tandem mass spectrometry was used to identify proteins of interest. Ninety protein spots of interest were selected for identification, and proteins of functional relevance with respect to ADF were identified.

Chapter 4 describes the original work characterizing the temporal dynamics of the microbial community (in the same enrichment SBR as in Chapter 3) with respect to traditional bulk solution observations. During SBR start-up, equilibration, and stable operation, biomass samples were taken approximately every equivalent solids retention time (SRT) for microbial community profiling based the bacterial 16S rRNA gene. Select bulk solution parameters including the feast-to-famine ratio, substrate utilization, and maximum PHA content were monitored, and the microbial composition was investigated with respect to these process performance observations.

Chapter 5 provides a summary of the research activities, in addition to conclusions that were made upon integrating research findings. To close, future perspectives and research activities are outlined.

Chapter 1. Literature Review

This literature review is comprised of four main sections, each with sub-sections denoted by underlined headings. To begin, a broad overview of PHA in relation to bioplastics, material properties, large-scale production, and applications is first presented. Once a general idea of PHA and its uses has been overviewed, the occurrence and biosynthesis of PHA in bacteria is described in greater detail in reference to investigations completed in pure cultures, given this information is adapted to MMCs. With an understanding of PHA synthesis in pure cultures established, the discussion turns to PHA production using MMCs and ADF, followed by PHA production using fermented dairy manure. To conclude the literature review, the discussion transitions to the experimental approaches applied for the research presented herein, namely, microbial community and proteomic profiling. Lastly, a summary is provided.

1.1 Polyhydroxyalkanoates

This first section presents a brief overview of polyhydroxyalkanoates (PHAs) as bioplastic materials. The section begins with a brief and broad summary of some of the concerns associated with conventional petroleum-based plastics, followed by the need for and development of bioplastic alternatives. The discussion then specifically targets PHAs and provides a summary of commercial production, material properties, and applications.

Petroleum plastic pollution

Petroleum-derived thermoplastics have improved our everyday lives thanks in part to their low costs, diverse material properties, and associated uses. Despite their convenience and versatility, conventional plastics have contributed to our society's enormous generation of waste. The U.S. Environmental Protection Agency reported 33 million tons of plastic waste

was generated in the US in 2013; nearly 63% of this plastic waste was classified as containers and packaging, or nondurable goods (EPA, 2012). The aforementioned categories of plastics are broadly characterized as being disposable, one-time use products, and since conventional petroleum-based thermoplastics used for these applications are considered to be non-biodegradable (Mueller, 2006), these materials inevitably continue to accumulate in the environment. In addition to waste accumulation concerns, the U.S. Energy Information Administration reported that plastic production consumed 191 million barrels of petroleum and natural gas liquids in 2010 (EIA, 2010), a number further reinforcing the need for bioplastic alternatives manufactured from renewable resources as opposed to non-renewable fossil fuels. Notably, the numbers presented above are only in reference to the United States; far more staggering figures accompany plastic consumption and pollution relative to the entire world (Chen & Patel, 2011).

Plastic pollution occurs in both terrestrial and aquatic environments. A well-documented instance of plastic pollution concerns the ocean; substantial plastic accumulation in gyres (natural collection points in the ocean created by swirling currents) has been reported (Moore *et al.*, 2001). In addition to accumulating in the environment and causing aesthetic issues, petroleum-based plastics (e.g., polyethylene) can fragment into particles known as microplastics (Sivan, 2011). Microplastics can be easily disbursed and inadvertently consumed by both terrestrial and marine animals, likely causing health hazards to animals, in addition to penetrating and accumulating in the food chain (Derraik, 2002; Frias *et al.*, 2010; Teuten *et al.*, 2009). Apart from accidental ingestion, plastic debris in terrestrial or marine environments can pose risks to animals such as choking, suffocation, or entanglement (Barnes *et al.*, 2009; Gregory, 2009). Furthermore, the dispersal of plastics or microplastics has been

shown to facilitate the movement of invasive species (Barnes, 2002a; Barnes, 2002b; Thiel & Gutow, 2004). The environmental impacts of plastic waste (including resulting microplastics) in both terrestrial and aquatic environments is undeniable, and the consequences of plastic pollution are becoming more apparent and accepted. To address some of the aforementioned concerns related to conventional petroleum-based plastics, the development of bioplastic alternatives has been pursued.

Bioplastics

Bioplastics comprise a large family of polymeric materials with differing origins, properties, and applications. Bioplastics can be bio-based, meaning polymers are derived from biological and renewable feedstocks, as well as being biodegradable (Chee *et al.*, 2010; Lagaron & Lopez-Rubio, 2011; Luengo *et al.*, 2003; Pilla, 2011; Queiroz & Collares-Queiroz, 2009). Several bioplastics can be found in today's market, such as PHAs, poly(lactic acid), poly(ethylene terephthalate), polyethylene, polypropylene, polyamides, and cellulosic derivatives (Bugnicourt *et al.*, 2014; Chen & Patel, 2011; Garlotta, 2001; Madison & Huisman, 1999; Mekonnen *et al.*, 2013). Of the bioplastics currently produced, PHAs offer great application potential along with being bio-based and biodegradable (Chen & Patel, 2011; Mekonnen *et al.*, 2013).

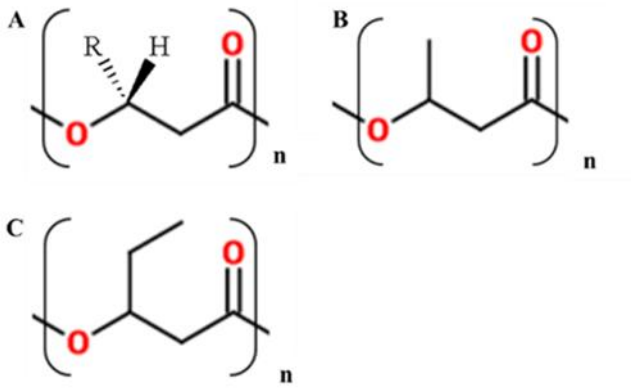

Figure 1.1. Various PHA structures. A) general PHA structure; B) PHB; C) PHV; and D) PHBV.

PHAs are linear polyesters synthesized by microorganisms. The basic PHA structure is shown in Figure 1.1A and can have many variable side-chains. The simplest and best-characterized member of the PHA family, poly(3-hydroxybutyrate) (PHB, Figure 1.1B) was first discovered in bacteria in 1925 (Lemoigne, 1926). Since then, more than 150 different monomer structures have been reported (Agnew & Pfleger, 2013; Steinbüchel & Lütke-Eversloh, 2003), which contribute to the wide the application range discussed later. Furthermore, copolymers can be formed (e.g., poly(3-hydroxybutyrate-co-3-hydroxyvalerate, PHBV), resulting in altered or in some instances improved material properties (Dekoning, 1995). Life cycle assessments have been used as a tool compare costs associated with PHAs, mainly directed at evaluating costs associated with various polymers beginning with raw materials and progressing through end of life processing; PHAs have been found to have superior life cycle assessments compared to conventional plastics (Akiyama *et al.*, 2003; Gurieff & Lant, 2007; Shahzad *et al.*, 2013; Tabone *et al.*, 2010). In summary, of the different bioplastics available and developed for different applications, PHAs offer great application potential.

PHA material properties

The material properties of PHAs depend on the polymer origin and are of special interest to the commercial market. Generally, PHAs share many mechanical and thermal properties (Table 1.1) with conventional petroleum-based plastics, namely, polyethylene and polypropylene, apart from being biodegradable (Bugnicourt *et al.*, 2014; Sudesh *et al.*, 2000; Thellen *et al.*, 2008). Differences in material properties may arise from biological variances

Table 1.1. Properties of PHB and PHBV compared to conventional plastics. (Sudesh et al., 2000)

Polymer	Melting temperature (°C)	Glass-transition temperature (°C)	Young's modulus (GPa)	Tensile strength (MPa)
P(3HB)	180	4	3.5	40
P(3HB-co-HV)*	145	-1	0.8	20
Polypropylene	176	-10	1.7	38
Low-density polyethylene	130	-30	0.2	10

* 20 mol% 3HV content

associated with polymer synthesis, or polymer recovery and processing dissimilarities. While different material properties exist for the many different PHA polymers comprised of many different monomers, the focus of this discussion will be on PHB, poly(3-hydroxyvalerate) (PHV) and resulting copolymer PHBV since they are the most relevant to the research presented herein.

For PHB, PHV, and the resulting copolymer PHBV, the relative monomeric distributions affect the material properties. The tensile strength and Young's Modulus (the force per unit area that is required to stretch or compress a material) of PHB and PHBV are comparable to polypropylene as shown in Table 1.1. Pure PHB exhibits poor temperature stability, accompanied by molecular weight loss and overall decomposition at its melting temperature, collectively making processing difficult (Sudesh *et al.*, 2000). Moreover, pure PHB is brittle due to its crystallinity, resulting in poor toughness. Interestingly, when HV monomers are incorporated with HB to form the copolymer PHBV, the material properties can be improved and thermal processing made easier through reducing the melting temperature without affecting the decomposition temperature (Dekoning, 1995; Gogolewski *et al.*, 1993; Lee, 1996). Furthermore, incorporating higher fractions of HV with HB can reduce the stiffness of the copolymer, as well as improve the toughness and flexibility (Avella

et al., 2000). PHBV films have also been shown to have an improved oxygen barrier compared to other polyolefin films (Thellen *et al.*, 2008). The thermal and mechanical properties associated with PHBV make it comparable to conventional petroleum-based plastics, but with the added benefit of biodegradability.

The biodegradation of PHA in the environment largely depends on the monomeric composition, physical dimensions, and disposal conditions. Generally, PHAs have been shown to be readily biodegradable in many natural environments such as soil, fresh water, composts, and sewage sludge (Braunegg *et al.*, 1998; Reddy *et al.*, 2003; Shah *et al.*, 2008; Sudesh *et al.*, 2000), with the biodegradation rates being contingent upon the specific environmental conditions (e.g., temperature, pH, water content, soil type). The rate of PHA degradation has been shown to range from a few weeks (Luzier, 1992) to nearly one year (Mergaert *et al.*, 1995). PHA degradation in different soil types (e.g., sandy, clay, and loam) at different temperatures has been investigated. Key findings included the loss of polymer mass was found to be zero-order, copolymers typically degraded at a higher rate compared to homopolymers, and higher temperatures increased the overall degradation rate (Mergaert *et al.*, 1993); for example, at 15°C, PHB and PHBV experienced mass losses ranging from 6-28%, whereas at 28°C, PHB and PHBV exhibited mass losses ranging from 9-46% during the same 200-day period. The distribution of microbial and fungal species also exerts an influence on the rate of PHBV degradation, including the extent of colonization of polymer surfaces (Sang *et al.*, 2002).

PHA degradation in aquatic environments is more variable. In one study involving freshwater ponds from December until June, both PHB and PHBV were shown to have slow degradation rates; mass losses ranged from just 4-7% in 178 days (Mergaert *et al.*, 1995).

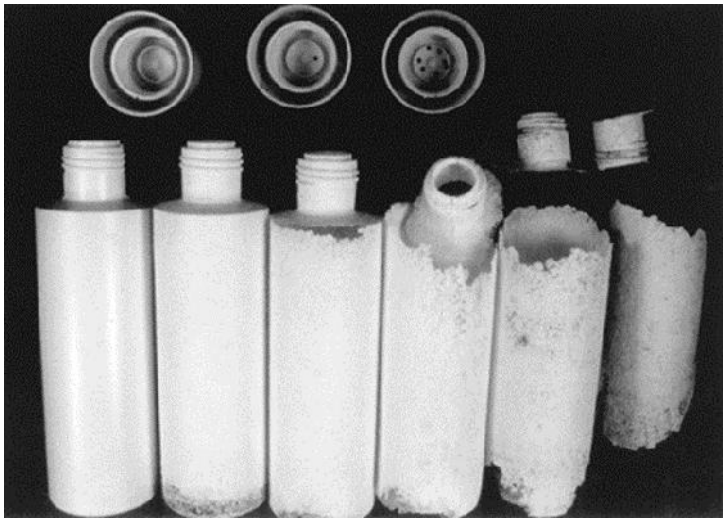

Figure 1.2. PHBV degradation in aerobic sewage sludge. From left to right, PHBV bottle at 0, 2, 4, 6, 8 and 10 weeks exposure to aerobic sewage sludge (average temperature of 20°C). (Madison and Huisman, 1999).

However, when PHB and PHBV were immersed in a freshwater canal for 358 days from January to January, 25-100% mass losses were reported (Mergaert *et al.*, 1995). In another study involving PHA degradation in fresh water where the temperature did not exceed 6°C, a PHA film lost 85% of its initial mass after 254 days (Reddy *et al.*, 2003). PHA degradation in sea water has been investigated; from April to January (270 days), PHB and PHBV lost 23-52% of their initial polymer masses (Mergaert *et al.*, 1995). In another study of PHB and PHBV in sea water with temperatures ranging from 27-30°C, after 160 days, polymers lost 62-87% of their initial mass (Volova *et al.*, 2011). In a study that simulated dynamic ocean conditions, 33-50% degradation was reported after only 49 days (Thellen *et al.*, 2008). Factors including water temperature, salinity, pH, inorganic content, and distribution of microorganisms have been implicated in the variable nature of PHA degradation in aquatic environments.

PHA degradation in engineered environments such as sewage sludge or landfills is of particular interest, as many PHA products could certainly be disposed of in these types of settings. An example of PHBV degradation in aerobic sewage sludge is shown in Figure 1.2;

degradation of a PHBV bottle was clearly visible after just 4 weeks, and more pronounced at 10 weeks; in activated sludge, the high microbial activity and temperatures are thought to significantly contribute to the rapid degradation (Madison & Huisman, 1999). The degradation of PHBV in anaerobic digesters has been investigated, albeit with different results. In one study, PHBV was completely degraded in just 42 days (Luzier, 1992). In another anaerobic digestion study, PHBV degradation was less pronounced after a comparable number of days (29% mass loss in 40 days), however, the authors noted appreciable methane production (Day *et al.*, 1994). In another case, PHBV degradation was even less, with mass losses ranging from 7-15% after a much longer digestion time (123 days) (Mergaert *et al.*, 1996). Differences in anaerobic digester operation (e.g., temperature, pH, retention time, mixing intensity, microbial composition) have been implicated in affecting PHA degradation rates, in addition to the chemical nature of the digester contents (e.g., acid content) (Byrom, 1994). Despite the physical and chemical differences in the aforementioned environments, a commonality shared with respect to PHA degradation is the presence PHA-degrading bacteria and fungi.

The ability to degrade PHA in the environment is widely distributed among bacteria and fungi. The first observation of PHA-degrading microorganisms included the genera *Bacillus*, *Pseudomonas*, and *Streptomyces* (Chowdhury, 1963), and since then, a number of bacteria and fungi capable of degrading PHA from a variety of ecosystems have been documented (Jendrossek, 1998; Lee, 1996; Tokiwa & Calabia, 2004). Regarding PHA-degrading fungi, 95 genera have been identified from a variety of environments (Kim & Rhee, 2003; Neumeier, 1994). The degradation of PHBV was shown to be a concerted effect of a microbial consortium including fungi, bacteria, and actinomycetes that colonized the PHBV film surface

(Sang *et al.*, 2002). The presence of extracellular, secreted PHA depolymerases facilitates the enzymatic hydrolysis of PHA polymers, which occurs in two main steps: i) the PHA depolymerase binds to the polymer substrate, and ii), the enzyme catalyzes a hydrolytic cleavage, generating water-soluble monomers and/or oligomers (Jendrossek & Handrick, 2002). Notably, microorganisms that secrete PHA depolymerases do not necessarily accumulate intracellular PHA (Jendrossek & Handrick, 2002); rather, PHA depolymerases are excreted in order to utilize exogenous carbon sources in the form of PHA monomers. A number of extracellular depolymerases have been isolated and purified (Bachmann & Seebach, 1999; Jendrossek *et al.*, 1993; Nakayama *et al.*, 1985; Schober *et al.*, 2000), revealing similarity to all known hydrolases. Considering the aforementioned breadth of material properties and biodegradability of PHAs, a wide range of applications is permitted, which is discussed in the next section after establishing the means of PHA production on a larger scale.

Large-scale PHA production

With the positive attributes of PHA materials, commercial-scale production has been established. Currently, commercial production of PHA is accomplished using pure, axenic cultures of genetically modified *Cupriavidus necator* exposed to a macronutrient limitation (P) in the presence of excess carbon in the form of glucose (derived from corn) and propionic acid; this combination of carbon sources permits the synthesis of the desirable PHBV copolymer (Byrom, 1992; DiGregorio, 2009). Beginning the 1970s, PHBV was produced using *C. necator* and commercialized under the name Biopol™ (Holmes, 1985), but since then a number of sales and acquisitions have been made, and the number of companies worldwide that have at one point been researching, developing, and producing PHA whether

at a pilot or industrial has exceeded twenty (Chen, 2009). For example, in the U.S., Metabolix has produced PHA polymers under the name Mirel at an industrial scale, and in China, Tianjin Green Bio-Science (GreenBio) has established a large PHA production base.

As alluded to previously, the most common strategy for commercial PHA production involves the use of genetically modified *C. necator* exposed to macronutrient limitation in the presence of excess carbon. Once a critical cell concentration has been achieved (using glucose as the sole carbon source and no P limitation), excess glucose and propionic acid, (but limited P) are fed into the bioreactor until the intracellular PHBV accumulation reaches its maximum, typically in a range of 70-80% of the total biomass weight (Byrom, 1992). Other bacterial species have been evaluated for commercial scale PHA production. The *Psuedomonas* genus offers the advantage of synthesizing medium-chain-length PHAs that exhibit different material properties, all while being cultivated on un-related carbon substrates (e.g., alkanes or fatty acids) (Van der Walle *et al.*, 2001). Genome sequencing coupled with advances in genetic and metabolic engineering have facilitated the employment of other bacterial species for PHA production. As a specific example, *Pseudomonas putida* was modified through the introduction of a suicide plasmid to disrupt β-oxidation genes, and when grown on tetradecanoic acid, the synthesis of medium-chain-length PHA reached up to 84% of the biomass, which was considerably higher than the wild-type (Liu & Chen, 2007). Recombinant *Escherichia coli* harboring PHA biosynthetic genes from *C. necator* has been reported to accumulate high amounts of PHA ranging from around 70% up to 90% of the total biomass (Dias *et al.*, 2006b; Lee, 1997; Wang & Lee, 1998). Interestingly, entirely unrelated components such as *Vitreoscilla* haemoglobin and lytic genes have been introduced in recombinant strains to improve culturing conditions and PHA recovery (e.g., higher oxygen

uptake and inducible cell lysis) (Yu *et al.*, 2003). Indeed, genetic modification is a powerful tool to address engineering challenges associated with the large-scale production of PHA, although challenges remain regarding the widespread expansion of processes that rely on recombinant bacteria.

Although pure cultures can achieve high intracellular PHA yields, the costs associated with these processes are a barrier to prevalent application. The price of commercially-produced PHA is widely acknowledged as a primary issue (Dias *et al.*, 2006a; Mudliar *et al.*, 2008; Reis *et al.*, 2003; Van Wegen *et al.*, 1998) and has been estimated to be in a range of 4-9 times higher compared to conventional petroleum-based plastics (Serafim *et al.*, 2008b). Moreover, given the current landscape surrounding petroleum extraction and processing (EIA, 2013), conventional plastics will remain much less expensive to produce and consume. The type of feedstock used for commercial PHA production is a primary expense, and the use of refined substrates can account for nearly 40% of production costs (Choi & Lee, 1997). Moreover, when food crops (e.g., corn) are used as raw materials for PHA precursors, direct competition is established. Maintaining the axenic conditions required for pure cultures is another expense (Mudliar *et al.*, 2008; Serafim *et al.*, 2008b), along with downstream processing procedures including PHA extraction from microbial biomass and purification (Pollet & Avérous, 2011). Despite the barriers commercial PHA production faces, PHA is estimated to account for about 2.4% of the 6.2 million tons of bioplastics produced by 2017 (EBA, 2013), reiterating the need for developing innovative PHA production strategies. Though the expansion of large-scale PHA production is limited to an extent, the applications and uses of PHA are vast.

PHA applications and uses

The unique material properties of PHA permit a wide range of applications and uses for this group of bioplastics. With physiochemical properties similar to conventional thermoplastics and the added benefit of biodegradability, PHAs have been touted as ideal functional replacements for many one-time use products such as containers (e.g., shampoo bottles, plant containers, milk cartons), packaging materials (e.g., bubble wrap, packing peanuts, moisture barrier coatings), or grocery bags (Keshavarz & Roy, 2010; P.J. Hocking, 1994; Philip *et al.*, 2007). Other consumable products such as writing utensils, adhesives, toner compositions, personal hygiene products, and diaper materials have utilized PHAs (Madison & Huisman, 1999). PHAs have also been used in more durable goods such as razors or holding trays (Chen, 2009; Gerngross & Slater, 2000), or automotive interior panels when blended with other polymers (Holbery & Houston, 2006). Related to agricultural applications, PHAs have been used as controlled-release agents for pesticides or insecticides (Philip *et al.*, 2007; Reddy *et al.*, 2003), in addition to mulches, irrigation tubes, components of greenhouse structures (Chiellini *et al.*, 2003; Kasirajan & Ngouajio, 2012), inoculant carriers (Kadouri *et al.*, 2005), and horticulture crop containers (Madbouly *et al.*, 2014).

Due to the biocompatible and "dissolving" nature of PHAs, applications in the medical and pharmaceutical industries have experienced growth. PHAs have been used for the development of many biomedical products such as surgical sutures, bone plates, and tissue scaffolds (Brigham & Sinskey, 2012; Chen & Wu, 2005; Guzmán *et al.*, 2011; Misra *et al.*, 2006; Valappil *et al.*, 2006; Williams & Martin, 2005). PHAs have also contributed to the development of cardiovascular-related materials such as pericardial patches, stents, grafts, or heart valves (Philip *et al.*, 2007; Williams & Martin, 2005). Drug delivery methodologies

have also incorporated PHAs into transport vesicles, capitalizing on the biocompatibility and ability to modulate drug release characteristics based on specific polymer formulations (Pouton & Akhtar, 1996; Wang *et al.*, 2003). Even though PHAs offer great flexibility regarding the design and implementation of biomedical and pharmaceutical products, the quality and purity of PHAs must be unequivocally high (e.g., PHAs must be devoid of residual bacterial lipopolysaccharides, proteins, surfactants, or toxins), requiring careful consideration concerning synthesis and purification procedures (Sevastianov *et al.*, 2003; Shishatskaya *et al.*, 2002). One proposal suggested the use of Gram-positive bacteria as opposed to the currently employed Gram-negative bacteria for the production of PHAs specifically for medical use as a potential means of addressing the presence of endotoxins synthesized by Gram-negative bacteria (Valappil *et al.*, 2007). With continued research and development, future applications of PHAs will continue to progress, delivering products that are renewable, biodegradable, and non-toxic, thus addressing many of the concerns related to the environmental burden plastic pollution places on the planet. Arguably, the application range of PHAs is largely attributed to its synthesis by microorganisms, which is the topic of the next section.

1.2 Microbial occurrence and synthesis of PHA

PHAs accumulate naturally in bacteria and some archaea. A great deal of literature describing PHA biosynthesis in different bacterial species is available (Anderson & Dawes, 1990; Lee, 1996; Lenz & Marchessault, 2005; Reddy *et al.*, 2003; Steinbüchel & Valentin, 1995; Urtuvia *et al.*, 2014; Verlinden *et al.*, 2007). In this section, the occurrence of PHAs in bacteria is discussed relative to microbial ecology, chemical structures, and microbial

physiology. With PHA occurrence established, the discussion transitions to biosynthetic considerations including PHA synthesis induction mechanisms, enzyme-catalyzed synthesis, relevant metabolic pathways, PHA granule architecture, intracellular PHA mobilization, and finally regulatory factors governing PHA-related metabolisms.

PHA occurrence in bacteria

PHA synthesis is common, though not ubiquitous, in bacteria. Since the discovery of PHB in *Bacillus*, more than 90 genera (Gram negative and Gram positive) in both aerobic and anaerobic environments have been reported to synthesize PHA (Findlay & White, 1983; Steinbüchel, 1991; Zinn *et al.*, 2001). The evolutionary history of PHA synthesis and formation has been discussed (Madison & Huisman, 1999; Reddy *et al.*, 2003); generally, PHA synthesis in the first PHA-accumulating microorganisms has been regarded as a likely minor metabolic pathway, with the purpose being different from the storage of excess substrate (Haywood *et al.*, 1990; Madison & Huisman, 1999). As the ability to synthesize PHA became advantageous, PHA-producing species were selected. Concerning the evolution of the PHA biosynthetic pathways, one hypothesis suggested pathways may have originated from fatty acid metabolism, given similarities between PHA monomers and intermediates of fatty acid metabolism (Madison & Huisman, 1999).

PHA-producing bacteria have been identified or isolated from a range of natural environments including soil (Brämer *et al.*, 2001; Mizuno *et al.*, 2010), marine environments (López-Cortés *et al.*, 2008), and Antarctic environments (Ayub *et al.*, 2004; Ciesielski *et al.*, 2014), as well as engineered environments such as activated sludge (Ciesielski *et al.*, 2006; Ciesielski *et al.*, 2008). PHA-producing bacteria have also been identified as part of symbioses including a gutless marine worm (Kleiner *et al.*, 2012), and plants (Gasser *et al.*,

2009). Though many bacteria synthesize PHA, a relatively small number of bacteria have been used as model organisms; *Cupriavidus necator* (former names include *Alcaligenes eutrophus, Wautersia euthropha* and *Ralstonia eutropha*) is one of the most-studied model organisms (Steinbüchel & Schlegel, 1991), in addition to *Azotobacter vinelandii* (Page *et al.*, 1992), and *Psuedomonas putida* (Nelson *et al.*, 2002).

Held in common by all PHA-producing bacteria is the presence of PHA biosynthetic enzymes, which are often clustered in bacterial genomes. The organization of the genes encoding PHA biosynthetic enzymes have been reviewed in great detail (Rehm & Steinbüchel, 1999; Steinbüchel *et al.*, 1992; Steinbüchel & Schlegel, 1991), and loci encoding PHA biosynthetic genes have been characterized from at least 18 different bacterial species (Madison & Huisman, 1999). Interestingly, the organization of PHA biosynthetic genes varies from species to species, implying *pha* loci have diverged. The selective pressures at the time may have resulted in the clustering of PHA biosynthetic genes into slightly different operons, in addition to a second evolutionary force that may have impacted the organization of individual genes, as some loci are interrupted by other genes (Haywood *et al.*, 1990; Hein *et al.*, 1998; Madison & Huisman, 1999; Reddy *et al.*, 2003; Umeda *et al.*, 1998). To provide an example of operon organization, considering the model organism *C. necator*, the genes for PHA synthesis, namely, PHA synthase (*phaC*), β-ketothiolase (*phaA*), and NADPH-dependent acetoacetyl-CoA reductase (*phaB*) comprise the *phaCAB* operon in tandem on the chromosome with a promoter upstream (Peoples & Sinskey, 1989; Schubert *et al.*, 1988; Slater *et al.*, 1988). In some cases, additional genes involved in PHA synthesis are present in the same locus. For example, *Chromatium vinosum*, *Thiocystis violacea*, and *Synechocystis* sp. encode PHA synthase as two separate sub-units (*phbE* and *phbC*); the *phbAB* and *phbEC*

genes are clustered in one locus, but divergently oriented (Hein *et al.*, 1998). In other instances, genes encoding enzymes or proteins (e.g., regulators or structural proteins) have been identified, further highlighting the divergence of *pha* loci (Reddy *et al.*, 2003). Despite differences concerning the clustering and orientation of PHA biosynthetic genes, the enzymes most directly implicated in PHA synthesis (i.e., β-ketothiolase, NADPH-dependent acetoacetyl-CoA reductase, and PHA synthase) show a high degree of sequence similarity across bacterial species, share structural features contributing to PHA synthesis (Reddy *et al.*, 2003; Steinbüchel & Hein, 2001), and influence PHA polymer structures.

PHA polymers exist as many different structures in bacteria, both naturally and as a result of synthetic biology. Commonly, PHAs are divided into two groups based on the number of constituent carbon atoms in the monomeric units, namely, short-chain-length and medium-chain-length; short-chain-length PHA contain monomers with 3-5 carbon atoms, whereas medium-chain-length PHA contain 6-14 carbon atoms (Khanna & Srivastava, 2005). The chain length is dependent on the substrate specificity of PHA synthase as well as the number of carbons in the 3-hydroxyalkanoate precursors (Gumel *et al.*, 2013). For example, the PHA synthase of *C. necator* can polymerize 3-hydroxyalkanoates with 3-5 carbon atoms, whereas the PHA synthase of *P. putida* can polymerize precursors with 6-14 carbon atoms, resulting in different PHA structures (Khanna & Srivastava, 2005). To date, more than 150 different monomers have been documented (Agnew & Pfleger, 2013; Steinbüchel, 2003), and naturally occurring monomeric units are in the D(-) configuration given the stereospecificity of the biosynthetic enzymes (Dawes & Senior, 1972). The molecular mass of PHA polymers can range from 50,000-1,000,000 Da and varies across bacterial species (Anderson & Dawes,

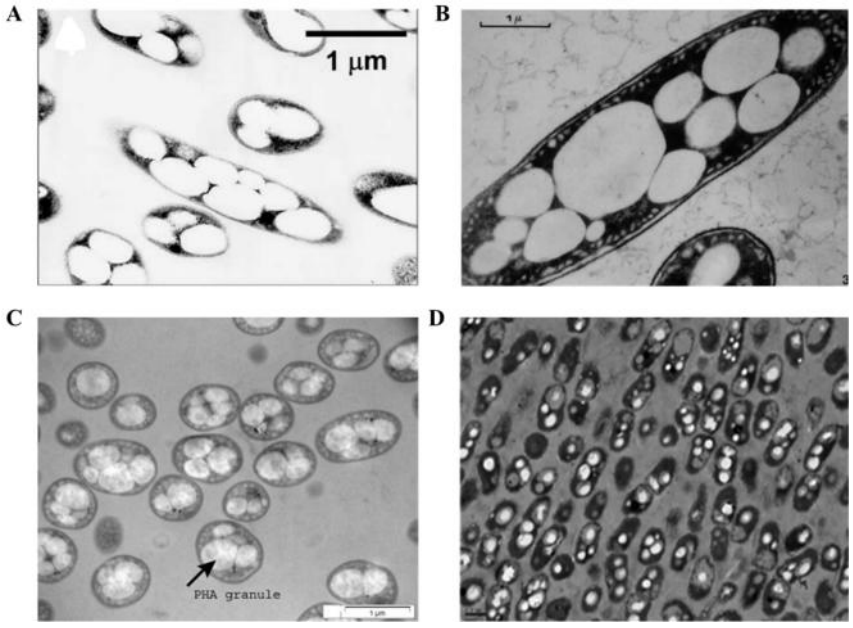

Figure 1.3. PHA inclusions in bacteria. A) *Ralstonia eutropha* (Stubbe and Tian, 2003); B) *Azotobacter chroococcum* (Nuti *et al.*, 1972); C) *Pseudomoas putida* CA-3 (Ward, 2005); D) mixed culture, (Scherson 2013).

1990; Madison & Huisman, 1999; Reddy *et al.*, 2003). Depending on the substrate conditions, homopolymers (i.e., a single, distinct monomeric unit comprises the PHA polymer) or copolymers (i.e., more than one distinct monomeric unit comprises the PHA polymer) can be synthesized. Though limited types of homopolymers have been reported, examples include PHB, PHV, poly(3-hydroxypropionate), polyhydroxyoctanoate, and poly(3-hydroxydodecanoate) (Meng *et al.*, 2014; Tripathi *et al.*, 2013). Copolymers are often random, meaning the sequence of incorporated monomeric units is random, and examples include PHBV, poly(3-hydroxybutyrate-*co*-3-hydroxypropionate), poly(3-hydroxybutyrate-co-3-hydroxyhexanoate), and poly(3-hydroxybutyrate-co-3-hydroxy-4-methylvalerate) (Andreeßen & Steinbüchel, 2010; Jeon *et al.*, 2014; Tanadchangsaeng *et al.*, 2009). Copolymers may also exist in a block form, wherein two or more homopolymer subunit "blocks" are connected (Chen & Thouas, 2015). The natural synthesis of block copolymers is less common in bacteria, although the careful modulation of periodic substrate availability

has facilitated the production of specific block copolymers (Li *et al.*, 2011; Pederson *et al.*, 2006; Tripathi *et al.*, 2013).

Biosynthesis of PHA and relevant metabolic pathways

In bacteria PHA synthesis is typically induced by some type of imbalance in growth, and PHA granules accumulate in bacterial cells as insoluble inclusions (examples in Figure 1.3). Under imbalanced growth conditions, PHA granules serve as a sink for excess carbon substrates and reducing equivalents that would be otherwise wasted if growth continued (Byrom, 1994; Doi, 1990; Steinbüchel, 1991), and have been likened to a metabolic equivalent to fat in animals (Smit *et al.*, 2012). PHA synthesis has frequently been described to occur solely under non-carbon limited situations (Dias *et al.*, 2006a; Khanna & Srivastava, 2005; Salehizadeh & van Loosdrecht, 2004; Serafim *et al.*, 2008a; Verlinden *et al.*, 2007); when the growth imbalance is lifted (e.g., when a limiting nutrient is restored), the endogenous PHA stores can be mobilized as a carbon and energy source. However, PHA synthesis has been observed under balanced growth conditions (Babel, 1992; Doi *et al.*, 1988; Matin *et al.*, 1979; Östling *et al.*, 1993; Tal & Okon, 1985; van Loosdrecht *et al.*, 1997). As such, the induction of PHA synthesis in bacteria should be considered enhanced, rather than predicated on a growth imbalance.

An imbalance in bacterial growth that induces PHA synthesis can arise from a number of environmental factors. A common growth imbalance leading to PHA synthesis includes the limitation of an essential nutrient (e.g., N or P) in the presence of excess carbon. For example, in a situation where N or P becomes limiting while excess carbon (e.g., glucose or acetate) is present, intermediates of the TCA cycle begin to accumulate because biomass precursors (e.g., α-ketoglutarate and oxaloacetate) are not assimilated into new biomass (e.g.,

amino acids, nucleotides, or proteins/enzymes) due to the lack of N or P, leading to feedback inhibition of the TCA cycle (Gottschalk, 1986; White, 2007). Furthermore, the ratio of acetyl-coenzyme A to coenzyme A (CoA) begins to increase, signifying the energy supply in the cell is high, which can inhibit citrate synthase in catalyzing the first step of the TCA cycle (White, 2007). In relation to PHA synthesis, the result is the diversion of acetyl-CoA and excess reducing equivalents to PHA as opposed to continued oxidation through the TCA cycle (Lenz & Marchessault, 2005).

PHA synthesis can also be induced in situations wherein a terminal electron acceptor becomes limiting, most commonly oxygen. When an oxygen limitation is imposed in the presence of excess carbon substrate, electron flow from electron donors to oxygen as the terminal acceptor is restricted, and reducing equivalents accumulate quickly, resulting in uncoupled respiration. Under such conditions, PHA-producing organisms can divert acetyl-CoA and excess reducing equivalents (NADH or NADPH) to PHA (Dawes, 1983; Ward *et al.*, 1977). Though acetoacetyl-CoA reductase requires NADPH, excess NADH can be converted to NADPH by different mechanisms (Madigan, 2006), thus excess NADH can still be used in PHA synthesis. When the oxygen concentration is eventually increased and is no longer limiting, oxygen consumption resumes concurrent with electron flow, and PHA content decreases (Tal *et al.*, 1990; Ward *et al.*, 1977). PHA synthesis under anaerobic conditions is most commonly observed in the engineered process known as enhanced biological phosphorus removal (EBPR).

As another induction mechanism, PHA synthesis can be induced in response to transient substrate availability or feast and famine conditions without any external nutrient limitation. This mechanism is the most complicated (biochemically and metabolically) and the least

understood. Generally, feast-famine conditions refer to the cyclic exposure to periods of carbon excess (i.e., feast) followed by an extended duration of carbon limitation (i.e., famine). Macronutrients (e.g., nitrogen and phosphorus) required for growth can be supplied in addition to a terminal electron acceptor (e.g., oxygen or nitrate) during feast-famine cycles. Regarding the induction of PHA synthesis under feast-famine conditions, the storage response is widely attributed to a reduction in anabolic capacity resulting from extended exposure to carbon-limited conditions (i.e. famine), which renders bacterial cells unable to grow at a rate commensurate upon exposure to excess substrate availability (i.e., feast) (Dias *et al.*, 2006a; Krishna & Van Loosdrecht, 1999; Serafim *et al.*, 2008a; van Loosdrecht *et al.*, 1997); a situation that has been referred to as an intracellular limitation (Daigger, 1979). As such, upon exposure to a feast phase, the majority of the exogenous substrate is diverted to PHA for temporary storage as opposed to growth, despite the availability of all nutrients required for growth. Upon exogenous substrate depletion, the famine phase ensues, and bacteria with PHA stores begin to mobilize their endogenous substrate stores to support growth and cellular maintenance. More specifically, the absence of exogenous substrate for an extended length of time was proposed to decrease the intracellular levels of RNA and enzymes (Daigger & Grady, 1982). Following a starvation period, when substrate becomes available, the amount of protein synthesis machinery is insufficient to facilitate achieving a maximal growth rate, thus the storage of excess substrate is the dominant response (Daigger & Grady, 1982).

Although widely accepted, the reduced anabolic capacity concept that serves as the basis for the physiological explanation for the feast-famine PHA storage response has yet to be experimentally validated. Moreover, this lack of validation is exacerbated because PHA storage was not observed in the experiments that led to the proposition of a reduced anabolic

capacity driving the PHA storage response under feast-famine conditions (Daigger, 1979). Related to this reduction in anabolic capacity, rRNA and PHB dynamics in *C. necator* were investigated with respect to feast-famine cycles (Frigon *et al.*, 2006). Unfortunately, the results were inconclusive with respect to rRNA pools during exposure to feast-famine conditions, however, the results did provide evidence to support the notion in that the ability to synthesize PHB promoted enhanced metabolic responsiveness to feast-famine conditions. In a different study, flow cytometry was used to investigate the adaptive responses of a particular strain of *C. necator* to feast-famine conditions by measuring the dynamics of DNA, rRNA, and PHB content (Müller *et al.*, 1999). The authors found that under balanced growth conditions, multiplication was favored, whereas under unbalanced growth conditions (i.e., feast-famine conditions) an overflow metabolism was exhibited, accompanied by PHB accumulation. Though the results of this study provided evidence to support a storage response occurs under feast-famine conditions, the physiological impetus driving the storage response was not definitively determined. With a general rationale concerning the induction of PHA synthesis established, biosynthetic mechanisms and regulatory factors of PHA metabolism will be further discussed.

Regardless of induction mechanism, PHA synthesis generally follows a three-reaction pathway that can be reversed when conditions require the mobilization of stored substrate. An example set of reactions leading to the synthesis of PHB and subsequent hydrolysis is outlined in Figure 1.4. Two acetyl-CoA moieties are condensed by β-ketothiolase (PhaA). The resulting four carbon intermediate, acetoacetyl-CoA, is stereo-specifically reduced by NADPH-dependent acetoacetyl-CoA reductase (PhaB). The resulting 3-hydroxybutyrl-CoA

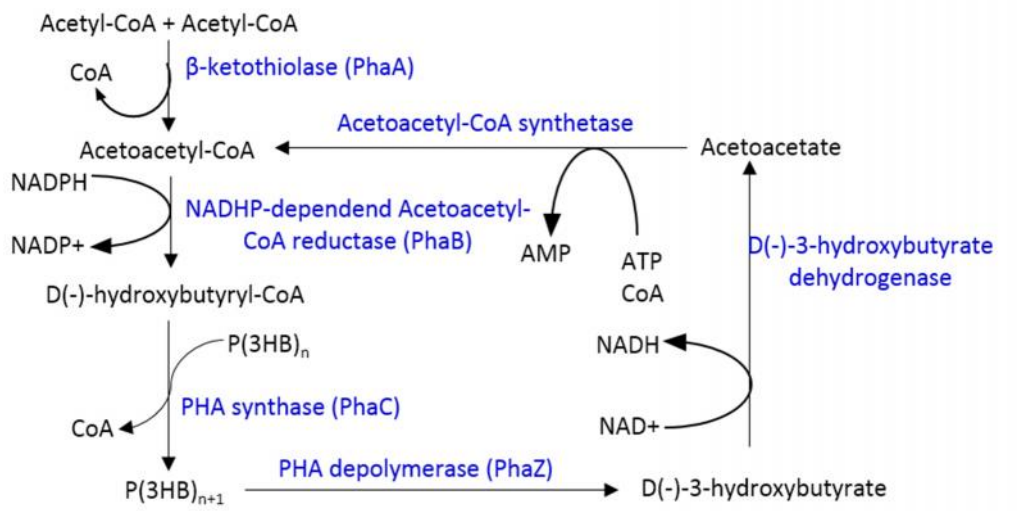

Figure 1.4. PHB synthesis and degradation in *Cupriavidus necator*. Redrawn from Johnson, 2010.

intermediate is then polymerized into PHB by PHA synthase (PhaC). Though acyl-CoA moieties serve as immediate precursors, PHA synthesis in bacteria is possible from a number of un-related carbon substrates. To date, 14 naturally occurring metabolic pathways for PHA synthesis are known and shown in Figure 1.5 (Meng *et al.*, 2014). Even though differences exist in each biosynthetic route, commonalities are shared, such as the generation of acyl-CoA intermediates and their incorporation into growing PHA polymer chains previously described and shown in Figure 1.4. The discussion of biosynthetic pathways will focus on sugars and organic acids, as these substrates are most relevant to the research presented herein.

When sugars (e.g., glucose) are substrates, the route to PHA begins with converting sugars to pyruvate via glycolysis or the Enter-Doudoroff pathway. Pyruvate is subsequently converted to acetyl-CoA via the pyruvate dehydrogenase complex, which is then used for PHA synthesis. When short-chain volatile fatty acids (VFAs) including acetate, propionate, butyrate, valerate, and caproate are substrates, PHA synthesis is more direct, as these substrates (depending on the number of carbon atoms) can either be directly activated with

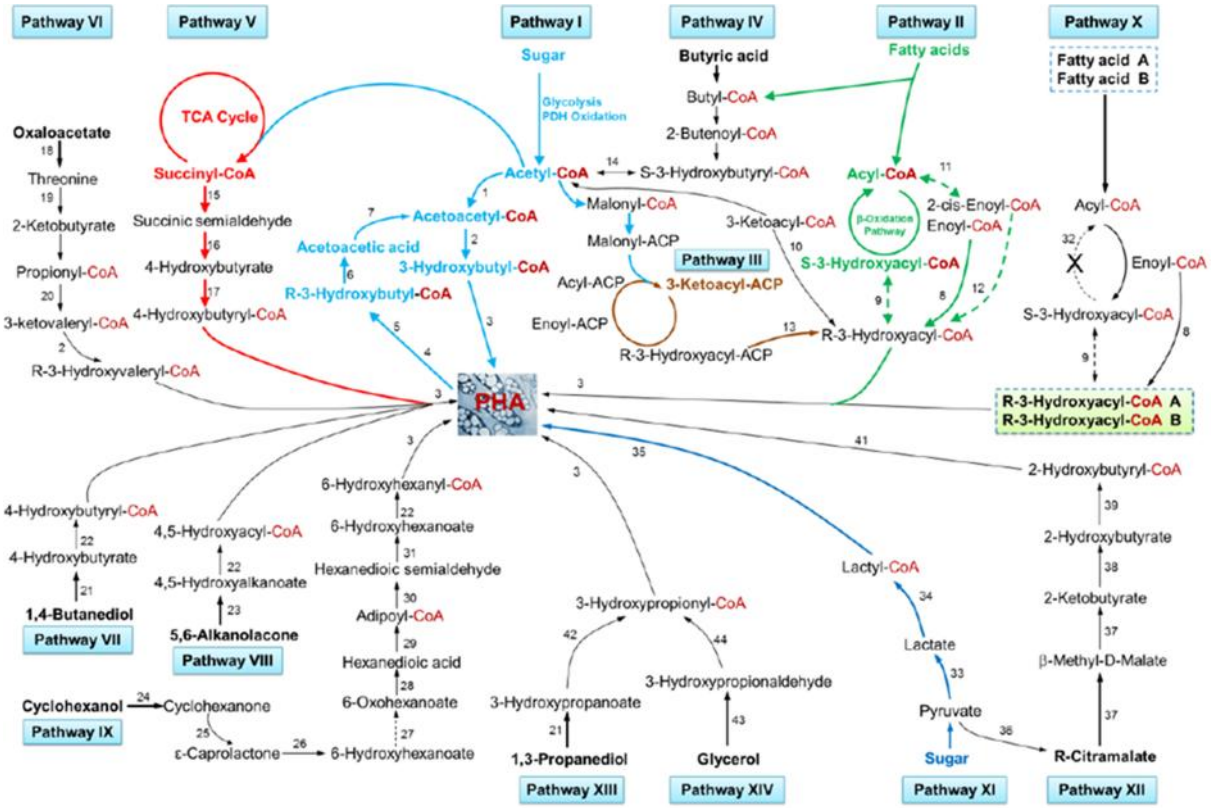

Figure 1.5. Known PHA synthesis pathways in bacteria. Adapted from Meng, *et al*., 2014 and Wei, 2015.

CoA or oxidized via β-oxidation to yield acyl-CoA moieties (White, 2007). Acetate and propionate are directly activated with CoA to yield acetyl-CoA and propionyl-CoA, respectively, whereas VFAs with four or more carbons pass through β-oxidation, yielding additional acetyl-CoA and propionyl-CoA; VFAs with an even number of carbon atoms yield acetyl-CoA, while VFAs with an odd number of carbon atoms yield both acetyl-CoA and propionyl-CoA. As alluded to previously, two acetyl-CoA moieties can condense to form acetoacetyl-CoA (the precursor to HB), however, acetyl-CoA can also condense with propionyl-CoA, yielding 3-ketovaleryl-CoA (the precursor to HV). Furthermore, butyrate can be converted to acetoacetyl-CoA, and valerate to 3-ketovaleryl-CoA. In other cases when fatty acids (acids with at least 4 carbon atoms) are substrates, (R)-specific enoyl-CoA hydratase (PhaJ) can catalyze the oxidation of enoyl-CoA to a corresponding (R)-3-hydroxyacyl-CoA (direct precursors of PHA) (Fukui *et al.*, 1998). Alternatively,

intermediates of fatty acid *de novo* synthesis can be diverted to PHA synthesis by the action of transacylase (PhaG), which involves the transfer of the (R)-3-hydroxyacyl moiety of the respective acyl carrier protein thioester to CoA, resulting in a suitable precursor to PHA (Hoffmann *et al.*, 2002; Rehm *et al.*, 1998; Rehm *et al.*, 2001). With the enzyme-catalyzed biosynthesis of PHA established, aspects related to PHA granules as intracellular inclusions will be discussed.

PHA granule architecture

PHA granules are complex cytoplasmic inclusions. In fact, arguments have been made that PHA granules are complex enough to be considered bacterial organelles, on par with carboxysomes or magnetosomes (Jendrossek, 2009; Uchino *et al.*, 2007). The diameter of PHA granules ranges from 200-500 nm (Anderson & Dawes, 1990). Concerning the chemical composition of PHA granules, analyses have shown the inclusions contain approximately 97.5% PHA polymer, 2% protein, and 0.5% lipid material (Steinbüchel *et al.*, 1995). Essentially two competing models exist regarding the formation of PHA granules and are represented in Figure 1.6. The "budding" model (Figure 1.6, top panel A), depicts PHA synthase dimers linked to growing PHA chains located near the inner side of the cytoplasmic membrane or bound at these sites. As PHA synthesis proceeds and granules enlarge, the inner cytoplasmic membrane envelopes the granule until this intermediary structure is sufficiently large to "bud" off, taking part of membrane (Stubbe & Tian, 2003). Given the observed phospholipid monolayer observed on granules (Griebel *et al.*, 1968) and supporting experimental data indicating granules are located close to the inner membrane, the "budding" model has been favored (Jendrossek *et al.*, 2007; Jurasek & Marchessault, 2004; Rehm, 2007;

Thomson *et al.*, 2010). Another model for PHA granule formation, the "micelle" model (Figure 1.6, bottom panel B), proposes the amphiphilic properties of PHA synthase-PHA chain complexes induce the aggregation of growing PHA chains; the aggregations enlarge as PHA synthesis proceeds, forming micelle-like structures that are further covered by phospholipids and other PHA-related proteins (Gerngross *et al.*, 1994; Stubbe & Tian, 2003).

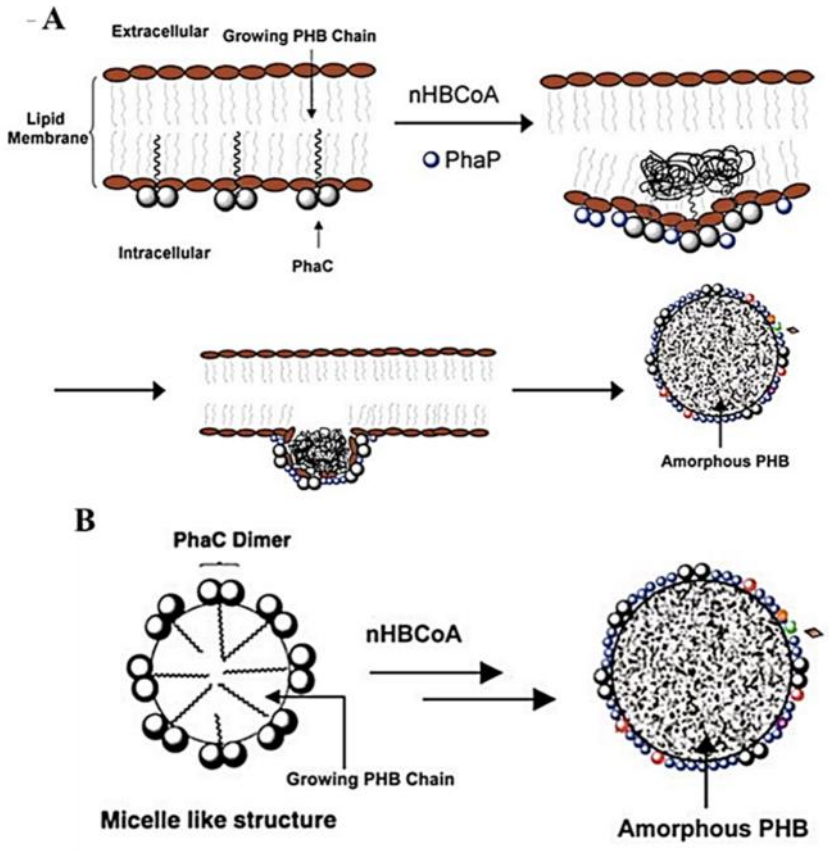

Figure 1.6. Existing models of PHA granule formation. A) the "budding" model; and B) the "micelle" model. Adapted from Stubbe and Tian, 2003.

However, the "micelle" model originated from *in vitro* PHA granule assembly studies, therefore, the distribution of sizes of PHA synthase-PHA chain complexes that affect micelle-like structures, in addition to how phospholipids envelope growing granules were not established, thus this model carries drawbacks (Thomson *et al.*, 2010). NMR studies have indicated the PHA polymer within growing granules is maintained in an amorphous state

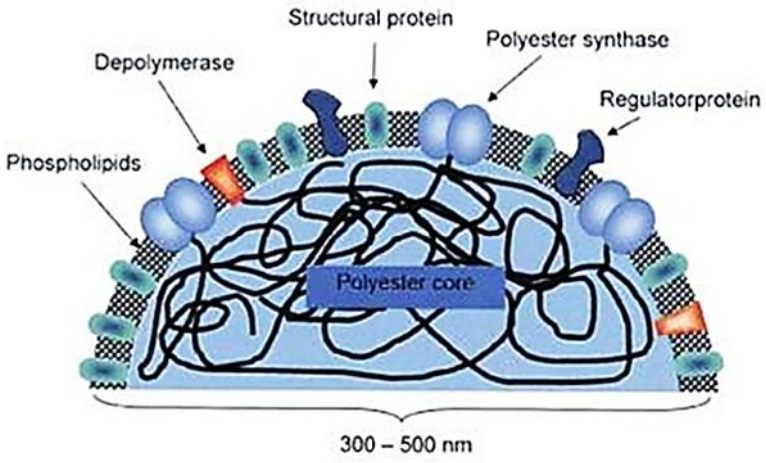

Figure 1.7. Theoretical PHA granule structure. (Grage *et al.*, 2009)

(Barnard & Sanders, 1989; Horowitz & Sanders, 1994), therefore, granules must be protected from the cytoplasm.

PHA granule protection is achieved by a complex outer layer of phospholipids and proteins that envelop granules, as depicted in Figure 1.7. As stated previously, PHA granules are surrounded by a phospholipid membrane with proteins embedded or bound to the surface (Stuart *et al.*, 1998), including PHA synthase (Gerngross *et al.*, 1994), phasin proteins (Jurasek & Marchessault, 2002; Pieper-Furst *et al.*, 1995; Potter & Steinbüchel, 2005; York *et al.*, 2001a), PHA-specific regulator proteins (Maehara *et al.*, 2002; Prieto *et al.*, 1999; York *et al.*, 2002), intracellular PHA depolymerase (Handrick *et al.*, 2000), as well as additional proteins with uncharacterized functions (Klinke *et al.*, 2000). Indeed, PHA synthase is a key granule-bound protein as the enzyme catalyzes polymerization and determines PHA composition (Rehm, 2006), however, other granule-bound proteins play important roles in PHA metabolism.

Phasin proteins constitute a large fraction of the PHA granule-bound proteins and play a primary role as structural proteins (Rehm, 2006). However, phasin proteins have been shown to be involved in many other facets of PHA homeostasis. Phasin proteins have been

shown to promote PHA biosynthesis and impact PHA granule size and number (Potter *et al.*, 2005; York *et al.*, 2001b), and influence the intracellular localization and distribution of PHA granules (Galan *et al.*, 2011). Phasin proteins have also been reported to possess regulatory activity in both the synthesis (Prieto *et al.*, 1999) and degradation of PHA (Handrick *et al.*, 2004). Results of PHA granule self-assembly simulations indicated phasin proteins may also impact the kinetics of granule formation (Jurasek & Marchessault, 2004). Phasin proteins have also been reported to enhance the specific activity of PHA synthase (Qi *et al.*, 2000), in addition to affecting the transcription of *phaC* (Tian *et al.*, 2005). In studies involving recombinant *E. coli*, phasin proteins were also shown to exhibit chaperone-like activity, aiding cytoplasmic proteins that come in contact with PHA granules to prevent protein misfolding or aggregation (de Almeida *et al.*, 2011; Mezzina *et al.*, 2015). Other PHA granule-bound proteins also play key roles in maintaining PHA homeostasis, and aspects of such regulation are discussed in the next section.

PHA metabolism regulatory factors

The regulation of PHA metabolism in bacteria is complex. As alluded to previously, the environmental and physiological conditions play a crucial role in regulating PHA synthesis and subsequent mobilization, depending on the growth and energetic state of the cell at a given time. In addition to regulation at a physiological level, regulation of PHA synthesis can occur at enzymatic level, depending on the availability of intermediate metabolites, as well as transcriptional regulation of PHA biosynthetic genes. Furthermore, PHA granules themselves possess regulatory features as previously overviewed. Aspects associated with each of these levels of regulation in relation to PHA metabolism, as well as the interdependence of each regulatory level will be further discussed.

Physiological conditions arguably impart the greatest level of regulation with respect to the induction of PHA synthesis and intracellular degradation. Since such physiological conditions that induce PHA synthesis have been previously described, aspects of this regulation will be briefly reviewed. As stated previously, PHA synthesis typically commences upon a departure from balanced growth conditions, with PHA acting as a reserve material for excess carbon and reducing equivalents; when the growth imbalance is relieved, PHA stores are then mobilized as endogenous carbon substrates that can be used for energy and biomass precursor generation. Nutrient limitation or absence of electron acceptor in the presence of excess carbon are among the most common physiological conditions that modulate PHA synthesis. Additionally, feast-famine conditions can induce PHA synthesis. In summary, the physiological conditions largely dictate the energetics (e.g., $NADH/NAD^+$ ratio) and intracellular metabolite pools (e.g., NADPH, acetyl-CoA) that directly modulate PHA metabolism.

Related to physiological conditions, regulation of PHA synthesis can occur at an enzymatic level. Enzymatic regulation is largely dependent on the availability of PHA precursors (e.g., acetyl-CoA, propionyl-CoA, acetoacetyl-CoA, and 3-ketovaleryl-CoA), reducing equivalents, and free coenzyme A (denoted CoA). Considering PHA synthesis in the model organism *C. necator*, PHA synthesis from acetyl-CoA and propionyl-CoA is highly regulated by the activity of β-ketothiolase and citrate synthase in relation to the quantities of free CoA, NADH, and NADPH (Doi *et al.*, 1992; Kessler & Witholt, 2001; Trotsenko & Belova, 2000). Under conditions conducive for PHA synthesis, CoA will be less readily available as it is consumed for substrate activation, however, continual use of CoA is facilitated as CoA is liberated upon polymerization of 3-hydroxyacyl-CoA intermediates.

When physiological conditions change such that carbon substrate is no longer present in excess quantities, CoA begins to accumulate (since less substrate is available to be activated), resulting in the inhibition of β-ketothiolase (Haywood *et al.*, 1988). The second enzyme involved in PHA synthesis, NADPH-dependent acetoacetyl-CoA reductase, has been shown to experience substrate inhibition from acetoacetyl-CoA (Haywood *et al.*, 1988). Finally, PHA synthase has been shown to be inhibited by CoA (Haywood *et al.*, 1989). However, the availability CoA is not the only means of regulating PHA synthesis, as the condensation of acetyl-CoA and oxaloacetate by citrate synthase releases CoA, which could facilitate further substrate activation. Citrate synthase has been considered a potentially important control point in PHA synthesis as the enzyme largely determines the fate of acetyl-CoA (Henderson & Jones, 1997). Citrate synthase has been shown to be inhibited by NADH (Henderson & Jones, 1997) and NADPH (Lee *et al.*, 1995), both of which would begin to accumulate under suboptimal growth conditions. As such, the inhibition of citrate synthase would prevent acetyl-CoA from entering the TCA cycle, thus diverting it to PHA.

PHA synthesis can be regulated at a transcriptional level and varies across bacterial species. The expression of PHA biosynthetic genes can be activated by specific environmental signals (Kessler & Witholt, 2001), and various promoters have been experimentally identified or proposed based on gene sequences upstream of PHA biosynthetic operons (Huisman *et al.*, 1991; Liebergesell & Steinbuchel, 1992; Matsusaki *et al.*, 1998; Timm & Steinbuchel, 1992). Interestingly, a phosphate starvation inducible promoter identified in a species of *Acinetobacter* isolated from activated sludge was implicated in regulating the transcription of PHA biosynthetic genes (Schembri *et al.*, 1995), and nitrogen regulation genes (*ntrB* and *ntrC*) were shown to involved in the regulation of the PHB

synthesis in strain of *Azospirillum brasilense* (Sun *et al.*, 2000), highlighting the role of nutrient limitation in PHA synthesis. In *Vibrio harveyi* the LuxR regulatory protein was shown to regulate the synthesis of PHB at high cell densities in the presence of the autoinducer *N*-(3-d-hydroxybutanoyl) homoserine lactone, further demonstrating the diversity of transcriptional control across different bacterial species.

To provide an example of other mechanisms of transcriptional control, the model organism *Cupriavidus necator* will be considered. In *C. necator*, a transcriptional repressor protein (PhaR) is encoded downstream of the *phaCAB* operon, which can bind to at least three different areas, namely, the promoter region of PhaP1 (encodes phasin protein PhaP1), the promoter region of PhaR (i.e., its own promoter region), and the surface of PHA granules (Potter *et al.*, 2002; Potter & Steinbüchel, 2005; Reinecke & Steinbüchel, 2009; York *et al.*, 2002). As such, models of regulation were proposed with respect to PhaR. In the absence of PHA granules (i.e., when environmental conditions do not induce PHA synthesis), the cytoplasmic concentration of PhaR is sufficiently high to repress the transcription of PhaP1. In contrast, under conditions conducive for PHA synthesis, PHA synthase initiates polymerization, during which PHA polymer chains remain covalently linked to the enzyme; as PHA granules become increasingly large, PHA synthase no longer occupies the entire polymer surface. As such, PhaR can bind to the surface of the granules, therefore, decreasing the cytoplasmic concentration of PhaR, thus relieving the repression of additional PHA biosynthetic genes, including PhaP1. PHA granules continue to increase in size until the maximum size is reached, with phasin proteins covering nearly the entire granule surface. Consequently, PhaR is displaced from the granule surface, resulting in an increase of the cytoplasmic concentration of PhaR. As such, PhaR can once again repress the transcription

of additional PHA biosynthetic genes. Furthermore, since PhaR can bind its own promoter region, when PhaR is in sufficiently high concentration, PhaR can auto-regulate its own expression, thus imparting an auto-control mechanism (Potter & Steinbüchel, 2005). As mentioned previously, when a growth imbalance that initially induced PHA synthesis is relieved, PHA stores are mobilized as endogenous substrates to support energy generation for growth and cellular maintenance; this mobilization requires the action of intracellular PHA depolymerases.

The regulatory factors governing the intracellular degradation of PHA are not fully established. Intracellular PHA depolymerases (distinct from extracellular PHA depolymerases) are required for the hydrolysis and mobilization of PHA stores, given self-hydrolysis rates of PHA granules are low (Jendrossek & Handrick, 2002), and multiple PHA depolymerases have been identified in a number of bacterial species (Briese *et al.*, 1994; Knoll *et al.*, 2009; York *et al.*, 2003). However, mechanisms and factors that influence PHA depolymerases in relation to PHA hydrolysis are poorly understood; for example, no particular substrate binding domain for intracellular PHA depolymerases has been described to date, little sequence similarity exists between extracellular and intracellular PHA depolymerases, and the characteristic lipase-box of extracellular PHA depolymerases is not present in all intracellular PHA depolymerases (Knoll *et al.*, 2009). Adding to the enigmatic activity of PHA depolymerases is the evidence indicating PHA depolymerases are constitutively expressed, and that PHA synthesis and degradation occur simultaneously (Doi *et al.*, 1992; Ren *et al.*, 2009).

The enzymatic activity of intracellular PHA depolymerases has been shown to be affected by physiological conditions including ionic strength and pH (Handrick *et al.*, 2000;

Saito *et al.*, 1995), but, relatively little is known concerning other factors that may contribute to the functionality and kinetics of these enzymes. In the model organism *Cupriavidus necator*, PHA depolymerase (*phaZ*) has been cloned and characterized, and reported to best hydrolyze amorphous PHB granules into oligomers and monomers of HB (Saegusa *et al.*, 2001). It was suggested multiple PHA depolymerases were encoded by *C. necator* with the possibility for both constitutive and inducible activity (Handrick *et al.*, 2000; Saegusa *et al.*, 2001), and eventually two additional candidate PHA depolymerase genes (*phaZ2* and *phaZ3*) were identified (York *et al.*, 2003); however, as with previous studies, the details regarding the hydrolysis and regulatory mechanisms were elusive. Studies in *Paracoccus denitrifcans* indicated this organism likely contains two PHA depolymerases, possibly acting in concert with one enzyme hydrolyzing granules into HB oligomers, and the other enzyme converting oligomers to monomers; though enzyme inhibition studies were performed, the catalytic mechanisms could not be determined (Gao *et al.*, 2001). In studies of *Pseudomonas putida* KT2442, a PHA depolymerase was found to be expressed and translated concurrent with the PHA synthase, bound to the PHA granule, and likely to require some type of interfacial activation in order to hydrolyze PHA polymers, further highlighting the complexities of intracellular PHA mobilization (De Eugenio *et al.*, 2008; de Eugenio *et al.*, 2007).

In summary the occurrence of PHA is widespread across many different bacterial species. Synthesized under different physiological conditions through multiple biosynthetic routes from multiple carbon substrates, the unique “buffering” capacity PHA polymers provide to bacterial species is apparent. Though the regulatory mechanisms concerning PHA metabolism in bacteria have not been fully established, experimental evidence supports a complex combination of physiological and molecular-level regulation. In the context of the

research presented herein, systems have been engineered to leverage the collective biosynthetic capabilities of PHA-producing bacteria in mixed microbial cultures, which is the topic of the next section.

1.3 PHA synthesis in mixed microbial cultures

Though mixed microbial cultures (MMCs) can be found essentially anywhere in the environment, in the context of the research presented herein, MMCs will be in reference to occurring in an engineered system. The use of MMCs for PHA production has been reviewed in great detail in relation to process configuration and performance (Dias *et al.*, 2006b; Reis *et al.*, 2003; Salehizadeh & van Loosdrecht, 2004; Serafim *et al.*, 2008a). Concerning PHA synthesis in MMCs, all aspects of PHA metabolism has been adapted from pure cultures as previously discussed to MMCs; however, since undefined MMCs are often used for PHA production, the exact genetic and physiological factors associated with PHA metabolism in specific pure cultures are nearly impossible to extrapolate to MMCs. In relation to the commercial-scale production of PHA, the processes employed to produce PHA by MMCs are necessarily different than pure cultures, most notably, the use of MMCs requires the enrichment of PHA-producing bacteria prior to PHA production. As such, in this section PHA synthesis in MMCs is discussed in greater detail. First, the appeal of using MMCs for PHA production is overviewed. The discussion then transitions to PHA production in MMCs using a staged process that comprises i) MMC enrichment for PHA-producing bacteria through the application of aerobic dynamic feeding (ADF), and ii) fed-batch PHA production. Finally, a multi-staged PHA production strategy using MMCs and waste feedstocks is discussed, including dairy manure, as this feedstock is the focus of the research presented herein.

The use of MMCs for commercial-scale PHA production offers advantages over pure cultures. Along with cost savings, abundance of possible feedstocks, and operational flexibility, PHA synthesis by MMCs can be integrated with other resource recovery and conversion technologies, as part of the greater area of mixed culture biotechnology (Akaraonye *et al.*, 2010; Dias *et al.*, 2006a; Kleerebezem & van Loosdrecht, 2007; Nikodinovic-Runic *et al.*, 2013; Reddy *et al.*, 2003; Reis *et al.*, 2003). Unlike pure cultures, MMC bioreactors can be operated under non-axenic conditions, requiring less energy input and equipment costs (Reis *et al.*, 2003). MMC bioreactors experience minimal concern over strain degeneration or contamination in comparison to pure cultures that rely on genetically manipulated bacteria (Johnson, 2010). Depending on the MMC process configuration, nearly any feedstock containing organic material could potentially be used as a substrate for PHA production by MMCs, encompassing waste or surplus feedstocks that are considerably less expensive than refined carbon substrates, further contributing to overall cost savings (Dias *et al.*, 2006a; Reis *et al.*, 2011; Serafim *et al.*, 2008a). In contrast to pure culture processes, MMC bioreactors offer potential for continuous operation for PHA production, in addition to less restricted process configurations.

Considering these select few advantages, the use of MMCs and mixed substrates (often in the form of fermented organic-rich waste streams) for the large-scale production of PHA has received research attention over the last few decades and is at the center of the research presented herein. As mentioned previously, the most commonly employed strategy for PHA production using MMCs involves a staged process including MMC enrichment and PHA production. Briefly, for the MMC enrichment stage, a sequencing batch reactor (SBR) configuration operated under aerobic dynamic feeding (ADF) conditions is most commonly

used to selectively enrich the MMC for PHA-producing bacteria. For the PHA production stage, the wasted volume from the enrichment SBR is used to inoculate a separate reactor in which the MMC is fed additional substrate in an effort to maximize the PHA capacity and yield of the enriched MMC. Aspects of this staged process are further discussed, beginning with the ADF process.

Aerobic dynamic feeding

The idea of using MMCs specifically for PHA production arose from the observations of PHA granules in bacteria in activated sludge systems designed for EBPR (Wallen & Rohwedder, 1974). Building on preliminary evidence, a significant PHA storage capacity was observed in bacteria in activated sludge exposed to aerobic selectors that had been implemented to control bulking sludge (Majone *et al.*, 1996). In contrast to the alternating anaerobic/aerobic systems conventionally found in EBPR systems, this aerobic process in the selector imposed alternating periods of exogenous carbon substrate. The resulting periods of carbon excess (i.e., feast) and carbon depletion (i.e., famine) were further simulated in lab-scale reactors, and the enhanced PHA storage capacity under feast-famine conditions was confirmed, thus leading to the process known as aerobic dynamic feeding (ADF) (Majone *et al.*, 1996). MMC enriched under ADF conditions have been reported to accumulate higher amounts of PHA compared to MMC enriched under alternating anaerobic/aerobic conditions (Reis *et al.*, 2003; Serafim *et al.*, 2008a), therefore, the ADF process has been the method of choice for the enrichment of PHA-producing bacteria in MMCs for PHA production. As stated previously, MMC enrichment via ADF has most commonly been done using the sequencing batch reactor (SBR) configuration using volatile fatty acids (VFAs) as substrates (Albuquerque *et al.*, 2007; Beun *et al.*, 2002; Dionisi *et al.*, 2005a; Serafim *et al.*, 2004). In

this section, the application of ADF is discussed with respect to the enrichment of PHA-producing bacteria in SBRs.

In relation to the induction of PHA synthesis in MMC under ADF conditions, aspects of the aforementioned feast-famine response are adapted to the ADF process. A schematic of a typical ADF cycle with a broad representation of primary measured bulk solution constituents is shown in Figure 1.8, and a more detailed description of particular metabolic pathways and

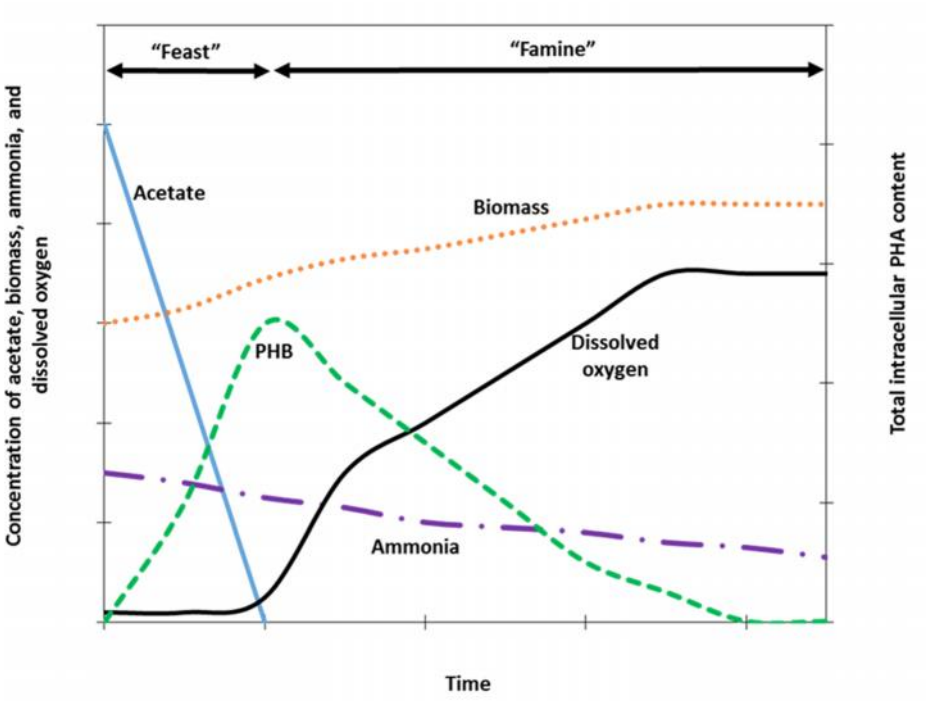

Figure 1.8. Schematic representation of bulk solution parameters during an ADF operational cycle.

intermediates is discussed below and shown in Figure 1.9. Using Figure 1.8 as a reference, substrate (e.g., acetate, along with ammonia) is added at the beginning of an enrichment SBR cycle creating a substrate surplus (i.e., the feast phase); during the feast phase, bacteria able to produce PHA simultaneously synthesize PHA (storage; denoted PHB in Figure 1.8) and new biomass (growth; denoted biomass in Figure 1.8) by quickly assimilating both carbon substrate and ammonia (denoted ammonia in Figure 1.8), whereas bacteria unable to

synthesize PHA simply grow (Dias *et al.*, 2006b; Reis *et al.*, 2003; van Loosdrecht *et al.*, 1997). For the remainder the cycle following exogenous substrate depletion (i.e., the famine phase), bacteria with PHA mobilize their endogenous stores for carbon and energy to support continued growth and cellular maintenance, whereas bacteria lacking PHA stores decay (van Loosdrecht *et al.*, 1997). Oxygen serves as a terminal electron acceptor for the generation of energy in the form of ATP during both the feast and famine phases. During the feast phase, dissolved oxygen is immediately consumed concurrent with substrate oxidation; upon substrate exhaustion, the dissolved oxygen concentration begins to increase (though is still consumed for the oxidation of liberated PHA monomers), and continues to increase for the duration of the famine phase until the next operational cycle starts.

Concerning the biosynthesis of PHA during the feast phase in the presence of VFAs (using Figure 1.9 as a reference, e.g., acetate), VFAs are transported into the cell and activated with CoA to respective acyl-CoA thioesters. The simplest even and odd-numbered carbon acyl-CoA thioesters (acetyl-CoA and propionyl-CoA, respectively), are channeled partially to PHA synthesis (denoted storage in Figure 1.9) and through the TCA cycle for energy generation and biomass production (denoted Growth (feast) in Figure 1.9). The extent to which storage and growth occur simultaneously is typically estimated by carbon and nitrogen mass balancing (Johnson *et al.*, 2009b). Furthermore, during the feast phase, metabolic activity through the central metabolic pathways for carbohydrate catabolism (glycolysis, Enter-Doudoroff, TCA cycle, and the pentose phosphate pathway) is only considered implicitly through assumed stoichiometry. During the famine phase, PHB is hydrolyzed, and the liberated intermediates are oxidized via the TCA cycle to support energy generation for growth and cellular maintenance (denoted Growth (famine) in Figure 1.9). The metabolic

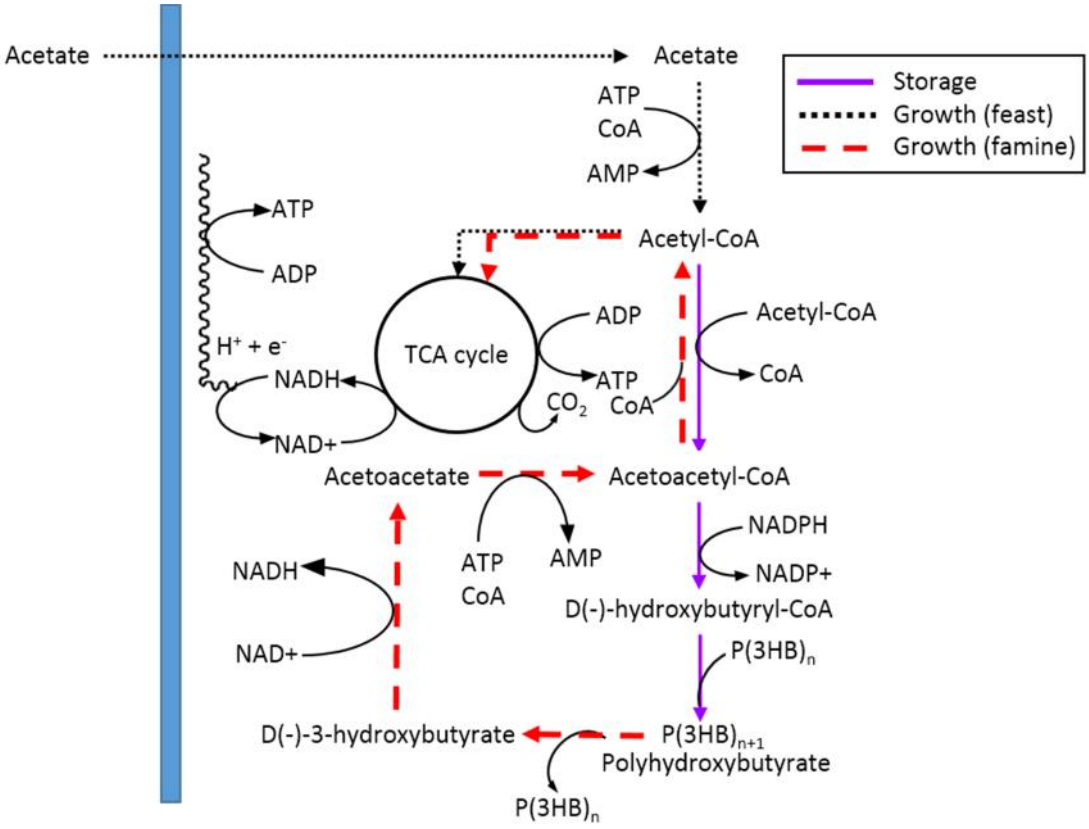

Figure 1.9. Proposed PHA metabolism under feast-famine conditions. Redrawn from Reis, 2003.

activity after exogenous substrate depletion and during the famine phase has received little attention, despite its importance to the culture's "history" that strongly dictates the PHA storage response in the next feast (Majone *et al.*, 1999; Reis *et al.*, 2003). PHA degradation in the famine phase has been observed in many cases, but little evidence is available to describe how or through which pathways liberated PHA monomers are utilized for growth and energy generation. Conversely, the presence of PHA has been reported at the end of an SBR cycle (Morgan-Sagastume *et al.*, 2010), signifying the typical feast-famine metabolic response can be skewed.

The applied ADF conditions influence the microbial composition and metabolic response of the resulting enriched MMC. Two main objectives of MMC enrichment must be met: i) enrich the MMC for PHA-producing bacteria, and ii) enrich a desirable metabolic

response such that PHA storage is dominant. Because PHA-producing bacteria are better equipped to modulate their growth rate, PHA-producing bacteria realize favorable enrichment under ADF conditions over non-PHA producing bacteria (Johnson *et al.*, 2009a; Reis *et al.*, 2003; van Loosdrecht *et al.*, 1997). In relation to microbial physiology, the PHA storage response is widely attributed to the previously described internal limitation of protein synthesis machinery as a result of exposure to the famine phase. To reiterate, the reduced anabolic capacity renders bacteria unable to grow at a rate commensurate with the substrate availability in the subsequent feast phase, thereby inducing the storage of excess substrate as PHA (Dias *et al.*, 2006b; Krishna & Van Loosdrecht, 1999; Serafim *et al.*, 2008a; van Loosdrecht *et al.*, 1997). However, the imposition of ADF conditions does not guarantee successful enrichment of PHA-producing bacteria exhibiting a high PHA storage response, therefore, a primary research focus has been the determination of optimal operating parameters of SBRs.

The choice of substrate and concentration has been a primary consideration for enrichment SBR investigations since the amount of substrate provided can influence the MMC composition, PHA storage response, and PHA material properties. VFAs are considered the best substrates for MMCs to convert PHA as opposed to sugars (e.g., glucose) (Reis *et al.*, 2003), and PHA production from acetic, propionic, butyric, valeric, and caproic acid has commonly been reported (Albuquerque *et al.*, 2007; Bengtsson *et al.*, 2010b; Bengtsson *et al.*, 2008b; Coats *et al.*, 2011). Mixtures of VFAs have commonly been used to produce PHA copolymers, particularly PHBV. Lactic acid has also been evaluated for PHB production by MMC (Jiang *et al.*, 2011c). The organic loading rate (OLR), the substrate concentration and rate at which it is provided to reactors, has been evaluated for enrichment SBRs (Beun *et al.*,

2002; Campanari *et al.*, 2014; Dionisi *et al.*, 2001; Dionisi *et al.*, 2006; Serafim *et al.*, 2004). Commonly, a linear relationship between the amount of substrate consumed and PHA synthesized has been reported, although at higher OLRs, decreased PHA process performance has been observed. The decrease in PHA performance at higher OLRs was attributed to a decrease in the selective pressure of the ADF conditions. As such, fast-growing bacteria with a low PHA storage capacity (i.e., growth was dominant to storage during the feast) were enriched, highlighting the importance of imposing a starvation phase on MMC.

Along those lines, the feast-to-famine (F:F) ratio is a parameter considered to be important for successful enrichment of PHA-producing bacteria. The F:F ratio is the total length of the feast phase compared to the total length of the operational cycle, and a value of 0.2 has been suggested as a potential cutoff between reliable and variable enrichment of PHA-producing bacteria (Dionisi *et al.*, 2007); however, the F:F is a function of multiple parameters (e.g., OLR, specific substrate uptake rate, and cycle length), therefore, the F:F cannot be controlled directly. Additionally, no experimental evidence is available to describe the F:F ratio with respect to MMC composition and physiology, therefore, the parameter can at best be considered a guide.

The solids retention time (SRT), loosely defined as the average time solids are in a system, is another operational parameter that influences MMC enrichment under ADF conditions. The SRT has been evaluated in a number of different SBR studies (Anterrieu *et al.*, 2014; Beun *et al.*, 2002; Beun *et al.*, 2000; Chua *et al.*, 2003; van Aalst-van Leeuwen *et al.*, 1997; Waller *et al.*, 2012). Generally, a shorter SRT is associated with higher cell growth rates and therefore, lower PHA storage (Dias *et al.*, 2006b), but this has not always been the case. Higher PHA content (from the same amount of substrate) was reported for a 3 d SRT

compared to 10 d SRT (Chua *et al.*, 2003), however, significant differences in biomass concentrations between the two SRTs were present, therefore, the PHA content (expressed as the percent PHA per unit biomass) was not necessarily representative. Similarly, in a study involving nutrient-limited waste carbon sources, the PHA content was found to be higher at 4d SRT compared to 6d (Coats *et al.*, 2007a). Formulating an optimal SRT for PHA production using MMCs is challenging, as the SRT must sufficiently low enough to generate PHA-producing biomass at a high rate, and high enough to achieve high PHA yields.

The carbon to nitrogen (C:N) ratio is another operational parameter that has been investigated with respect to the enrichment of PHA-producing bacteria under ADF conditions (Basak *et al.*, 2011; Chua *et al.*, 1999; Dionisi *et al.*, 2005a; Ince *et al.*, 2012; Johnson *et al.*, 2010a; Lemos *et al.*, 2006; Serafim *et al.*, 2004). Depending on the nitrogen availability during both the feast and the famine phases, the C:N ratio can exert an effect on the storage/growth response. For example, if ammonia is limited during the famine phase, bacteria that stored PHA during the feast may not be able to grow as optimally during the famine using their endogenous substrate. The effect of the cycle length on PHA synthesis in MMCs under ADF conditions has been examined (Dionisi *et al.*, 2007; Jiang *et al.*, 2011b; Moralejo-Garate *et al.*, 2013b; Ozdemir *et al.*, 2014; Valentino *et al.*, 2014). While some investigations found shorter cycle lengths (2-8 h) resulted in higher a PHA content, others found the PHA content was higher when the cycle length was longer (18-24 h). Presumably, a longer cycle length would result in a harsher famine phase, thus resulting in a higher PHA storage response. Notably, many of the SBR cycle operational parameters were considerably different (e.g., OLR, SRT, aerobic fill time), therefore, arriving at a consensus concerning the optimal cycle length is challenging.

The effect of the dissolved oxygen concentration on PHA synthesis in MMC has not been extensively evaluated for ADF enrichment SBRs. The common practice has been to operate enrichment SBRs with excess aeration to ensure no oxygen limitation. The effect of reduced aeration (and subsequent decreased oxygen availability) on PHA synthesis in enrichment SBRs cultivated on waste substrates has been assessed. Using crude glycerol as a substrate, oxygen limitation was found to favor glycogen storage during the feast phase in comparison to PHA (Moralejo-Garate *et al.*, 2013a), therefore, reduced aeration resulted in poor PHA process performance. In an investigation using fermented dairy manure as a substrate, reduced aeration did not appear to have a significant impact on PHA storage (Watson, 2015), although reducing aeration could potentially save costs and overall energy input. Microaerophilic conditions were found to support higher PHA yields, but at the expense of the PHA production rate (Pratt *et al.*, 2012); a reduced rate of PHA production would not be ideal, so further optimization of a microaerophilic process would be required. Though unrelated to PHA production using MMCs, the effect of dissolved oxygen availability on PHA synthesis in MMCs has been assessed with respect to post-anoxic denitrification (Third *et al.*, 2003; Third *et al.*, 2004). Interestingly, the PHA yield was found to be higher when oxygen was limiting, in comparison to when oxygen was present in excess; when modeled, at lower dissolved oxygen concentrations, less ATP was available for biomass growth, therefore, PHA storage was higher. In contrast, higher dissolved concentrations resulted in a surplus of ATP, thereby permitting a higher cell growth rate, resulting in decreased PHA storage.

The effects of pH have also been explored with respect to PHA synthesis in MMC under ADF conditions (Chua *et al.*, 2003; Oehmen *et al.*, 2014; Serafim *et al.*, 2004; Villano *et al.*,

2010a). Both PHA content and volumetric productivity was shown to be higher at pH values above 7 (e.g., pH 8.5-9.0), and while continuously controlled in many ADF investigations, when not controlled, the pH changes with the progression of the SBR cycle. Importantly, at lower pH values, the degree of VFA dissociation (e.g., acetate) may become a factor affecting bacterial growth, and thus PHA accumulation. The effects of temperature have also been investigated (Jiang *et al.*, 2011b; Johnson *et al.*, 2010b; Krishna & Van Loosdrecht, 1999). Not surprisingly, the temperature was found to exert a strong influence on the kinetics of PHA storage under ADF conditions. For example, an MMC in an SBR operated at 20°C doubled the amount of PHB stored at 15°C (70% PHB vs. 35% PHB) in a shorter length of time (Johnson *et al.*, 2010b). Apart from influencing PHA storage kinetics, the temperature was also shown to exert a strong influence on MMC composition, as a particular MMC constituent (*Plasticicumulans acidivorans*) was more sensitive to temperature compared to the other dominant genus present (*Zoogloea*), thus *Plasticicumulans acidivorans* was "outcompeted" (Jiang *et al.*, 2011b). The focus on process optimization for enrichment SBRs is understandable, as the process performance in the PHA production stage is necessarily contingent upon the enriched MMC.

The PHA production capacity of MMC enriched using ADF is typically assessed in fed-batch production tests. To review this production stage, the wasted volume from the enrichment SBR is used to inoculate a separate reactor in which different feeding strategies are employed in an effort to fully maximize the PHA accumulation in bacterial cells. Notably, the interdependence of the enrichment and PHA production stages allows for the separate, yet simultaneous optimization of the two stages. Two common feeding regimes have been evaluated for PHA production, namely, continuous-fed and pulse-fed. The pulse-fed (or step-

fed) approach, which ensures sufficient carbon substrate to sustain feast conditions, has typically been regarded as the preferable strategy (Dias *et al.*, 2006a). For the pulse-fed approach, close monitoring is required to ensure the substrate pulses are provided at the right time, and common parameters monitored include the dissolved oxygen (DO) concentration and pH. A rapid increase in DO has commonly been used as a surrogate for VFA depletion, signaling the time to add the next substrate pulse (Dias *et al.*, 2006a; Serafim *et al.*, 2004). Alternatively, the pH may be used as an indicator for substrate depletion, as a linear relationship between VFA concentration and pH has been observed; a change in slope signifies the exhaustion of substrate, therefore, the time at which the next pulse should be fed (Dias *et al.*, 2006b). However, in order for pH monitoring to be effective, the alkalinity in the water must be low enough such that a change in slope can be detected. As such, the DO-based monitoring has been the preferred choice. Another consideration for the PHA production stage has involved imposing an external nutrient limitation (e.g., nitrogen or phosphorus), in an effort to further limit bacterial growth and divert a higher percentage of substrate to PHA storage (Albuquerque *et al.*, 2010b; Johnson *et al.*, 2009a). Though effective, non-growth limiting conditions have generally been shown not to be detrimental to overall PHA process performance.

PHA accumulation performance can be expressed in multiple forms. Obviously the total intracellular PHA content is the primary focus, but polymer yield per unit substrate, PHA composition, as well as specific and volumetric productivities have also been considered as important performance metrics (Serafim *et al.*, 2008a). To date, the highest total PHA content reached using MMC was 89% of the cell dry weight (Johnson *et al.*, 2009a); however, acetate was used as a sole carbon source, therefore, the homopolymer PHB was synthesized. Since

the copolymer PHBV has improved material properties, mixtures of VFAs have been commonly preferred for fed-batch PHA accumulation, and the wide range (anywhere from 20-89% of the cell dry weight) of maximum PHA content has been reviewed (Serafim *et al.*, 2008a). PHA yields been comparable to those in pure cultures, although the volumetric productivities have been lower compared to pure cultures, as the biomass concentration in MMC has been lower (Serafim *et al.*, 2008a). Multiple factors contribute to PHA process performance including the enriched MMC itself, substrate used, feeding strategy, and specific operating conditions, making process optimization a challenging task.

The final component of PHA production is PHA extraction, which requires the separation of PHA granules from other constituents present in the biomass. A number of methods for PHA extraction and processing have been reported (Hahn *et al.*, 1994; Jacquel *et al.*, 2008; Koller *et al.*, 2013; Wei *et al.*, 2014). In many lab-scale investigations involving fermented waste feedstocks, the use of an organic solvent (e.g., chloroform) to selectively dissolve PHA is implemented, followed by PHA recovery by solvent evaporation after filtration (Braunegg *et al.*, 1998; Holmes, 1988). However, at full-scale, the amount of solvent for PHA extraction is enormous (e.g., 20 tons of solvent is required to extract 1 ton of PHA (Byrom, 1994)), requires proper storage and re-use systems, and carries environmental risks, therefore, the use of solvents at large scales is not ideal (Byrom, 1994; Lee, 1996). Alternative extraction methods have included the use of sodium hypochlorite (Berger *et al.*, 1989), combined surfactant-hypochlorite treatment (Ramsay *et al.*, 1990), or alkaline solution digestion (Choi & Lee, 1999), but each method has drawbacks. For example, bleach can degrade PHA, PHA purity can suffer in the presence of surfactants, and alkaline digestion requires a high enough intracellular PHA content such that bacterial cells become fragile. In

contrast, avoiding extraction by blending PHA-rich biomass with other materials to make composite may be a potential option, as demonstrated using PHB-rich biomass obtained from *Azotobacter vinelandii* UWD to make natural fiber-reinforced thermoplastic composites (Coats *et al.*, 2008). PHA extraction and purification methods continue to be developed given efficient and environmentally responsible strategies may greatly increase the applications and value of PHA.

With many operational parameters influencing PHA production by MMCs, the empirical determination of optimal conditions is challenging. As such, in an effort to bolster the optimization of PHA production by MMCs, various mathematical models, metabolic models, and flux balance analysis methods have been developed and applied (Dias *et al.*, 2008; Dias *et al.*, 2005; Jiang *et al.*, 2011a; Lopes Dias *et al.*, 2007; Pardelha *et al.*, 2013; Pardelha *et al.*, 2012; Pardelha *et al.*, 2014; Tamis *et al.*, 2014). A schematic representation of a model for PHA synthesis from multiple VFAs is shown in Figure 1.10 with corresponding intermediates and reaction fluxes (Pardelha *et al.*, 2012). PHA synthesis models share many features and assumptions. For example, material and energetic balances are based on previously elucidated pathways. Similar stoichiometric assumptions for the reactions denoted in Figure 1.10 are made across models. VFAs are assumed to be transported into the cell (via active transport), activated to respective acyl-CoA intermediates (e.g., acetyl-CoA and propionyl-CoA in Figure 1.10) at the expense of ATP, and used for both biomass growth and PHA synthesis. Theoretical yields for both biomass growth and PHA storage are commonly derived as functions of the oxidative phosphorylation efficiency ratio (which must be estimated). Certain kinetic constraints (e.g., growth on acetyl-CoA (R_4 in Figure 1.10)), or cellular maintenance (R_5 in Figure 1.10) are adapted after parameter estimation. Models have

been considerably helpful in determining optimal substrate concentrations and feeding regimes, in addition to providing a baseline for which model calibration and future optimization can be expanded. However, with respect to undefined MMCs and mixed substrates, these models have limitations. For example, only a select few pathway intermediates are taken into consideration, and potential metabolic/kinetic differences across bacterial species are not easily incorporated. Nevertheless, the improvement of metabolic

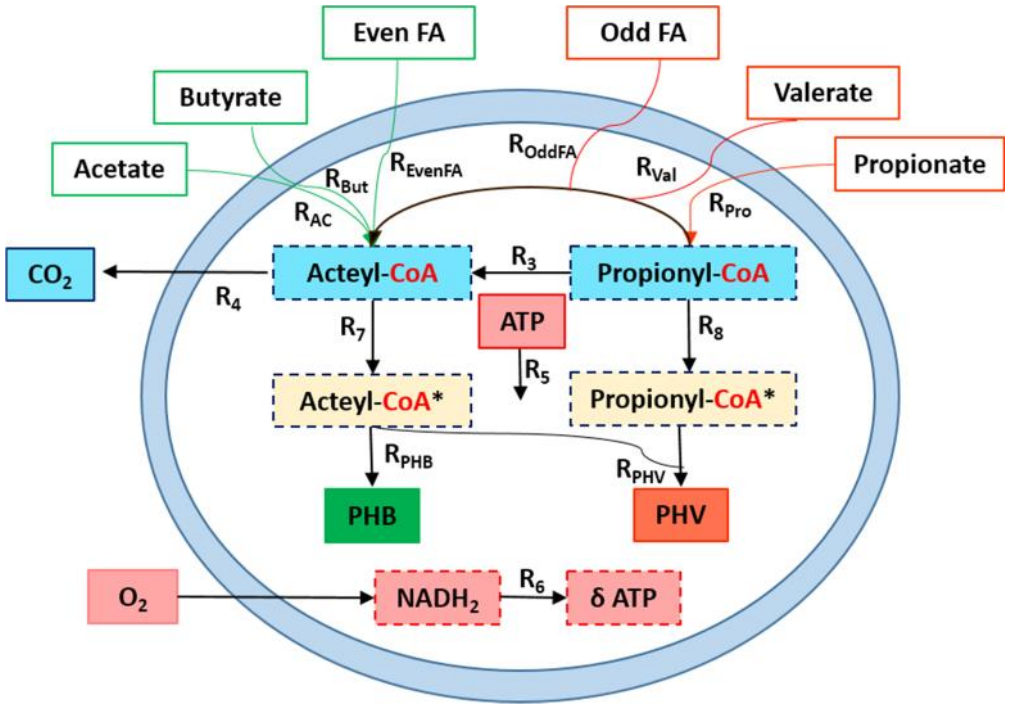

Figure 1.10. Schematic representation of PHA synthesis from multiple VFAs used for modeling purposes. The circular shape depicts a bacterial cell, VFAs are indicated in the grey boxes, reaction intermediates are shown in the dashed boxes, products are shown in shaded boxes, and R indicates a reaction flux included in the model. Redrawn from Pardelha *et al*., 2012.

models as applied to MMCs for PHA production will greatly enhance process optimization strategies. To complement empirical process optimization and modeling, molecular-level methods have been implemented with conventional optimization investigations to interrogate microbial involvement in process performance.

Elucidating the MMC composition and functionality in enrichment SBRs has generally been a secondary research focus. To characterize MMC composition, a suite of

classical molecular techniques have been applied in enrichment SBR studies. Denaturing gradient gel electrophoresis (DGGE) has been a popular method to visualize and monitor MMC dynamics relative to process performance, and in response to the imposition of operational changes using both synthetic and waste substrates (Beccari *et al.*, 2009; Dionisi *et al.*, 2005a; Marang *et al.*, 2013; Valentino *et al.*, 2013; Villano *et al.*, 2010b); although DGGE has provided a visualization of MMC changes relative to operating conditions, the resolving power can be limited, and often only the dominant bands have been sequenced to determine microbial identity. Clone library construction has also been used to characterize the microbial composition of MMCs with pretty good success, as dominant PHA-producing genera have been identified (Albuquerque *et al.*, 2013; Dionisi *et al.*, 2006). Fluorescence *in situ* hybridization (FISH) coupled with PHA staining has been the most commonly used method to estimate the relative fractions of PHA-producing bacteria (and specific genera) present in MMCs (Albuquerque *et al.*, 2013; Lemos *et al.*, 2008; Oehmen *et al.*, 2014; Pardelha *et al.*, 2013; Queiros *et al.*, 2014; Serafim *et al.*, 2006). As FISH is probe-specific, extensive resolution of microbial composition in complex MMCs has been limited. Furthermore, since sequencing was not performed in the studies performing FISH, determining microbial identity was limited. Despite the limitations of these classical molecular characterization techniques, dominant PHA-producing producing genera in ADF enrichment SBRs have been identified, including *Thauera*, *Azoarcus*, and *Paracoccus*, as well as a novel species (*Plasticicumulans acidivorans* (Jiang *et al.*, 2011d)). Though several SBR investigations have alluded to an "ideal" MMC composition, given the differences in reactor operating conditions and configurations across various studies, the likelihood of same MMC composition being "ideal" for all enrichment SBRs is difficult to definitively establish.

Though MMC characterization has provided some insight regarding dynamics and relative abundance of particular PHA-producing bacteria in enrichment SBRs, no enzymatic or protein-level evidence has been obtained to support the concepts of the feast-famine PHA metabolism in MMCs cultivated under ADF conditions. Furthermore, despite multiple references having been made concerning the importance of ecological selection principles in ADF enrichment SBRs, selection mechanisms have not been extensively interrogated. Likewise, aspects of ecological theories concerning microbial diversity and dynamics of MMC in ADF enrichment SBRs have largely been omitted from discussions pertaining to the enrichment process. This lack of molecular-based investigation may be explained by the fact that most ADF enrichment evaluations are done in engineering-centric laboratories/environments, and process optimization is the foremost interest. With a general idea concerning PHA production using MMCs in staged processes established, the discussion will now transition to PHA production using MMC and waste feedstocks.

Three-stage PHA production strategy using waste feedstocks

The use of MMCs and unconventional feedstocks has been proposed as a means to overcome some of the challenges of pure culture PHA production. After nearly two decades of research, the most commonly employed strategy for PHA production using MMCs and waste feedstocks is a three-stage system (outlined in Figure 1.11) that comprises feedstock fermentation, enrichment of PHA-producing bacteria, and PHA production. The fermentation stage (Stage 1) converts the organic material in waste feedstocks to VFAs. The enrichment stage (Stage 2) uses ADF to enrich the MMC for PHA-producing bacteria with a desirable physiological response in an SBR as previously described. The production stage (Stage 3) uses a fraction of the enriched culture in a fed-batch reactor to produce PHA in greater

amounts as previously described. To complete the production process, the PHA-rich biomass is harvested and subjected to downstream handling for polymer extraction and processing. With an overview of this three-stage process provided, components of each separate stage are further discussed in the following section, followed by an examination of waste feedstocks that have been evaluated for PHA production. The discussion then transitions to specific a waste feedstock, namely, fermented dairy manure.

The implementation of fermentation into MMC PHA production strategies permits the

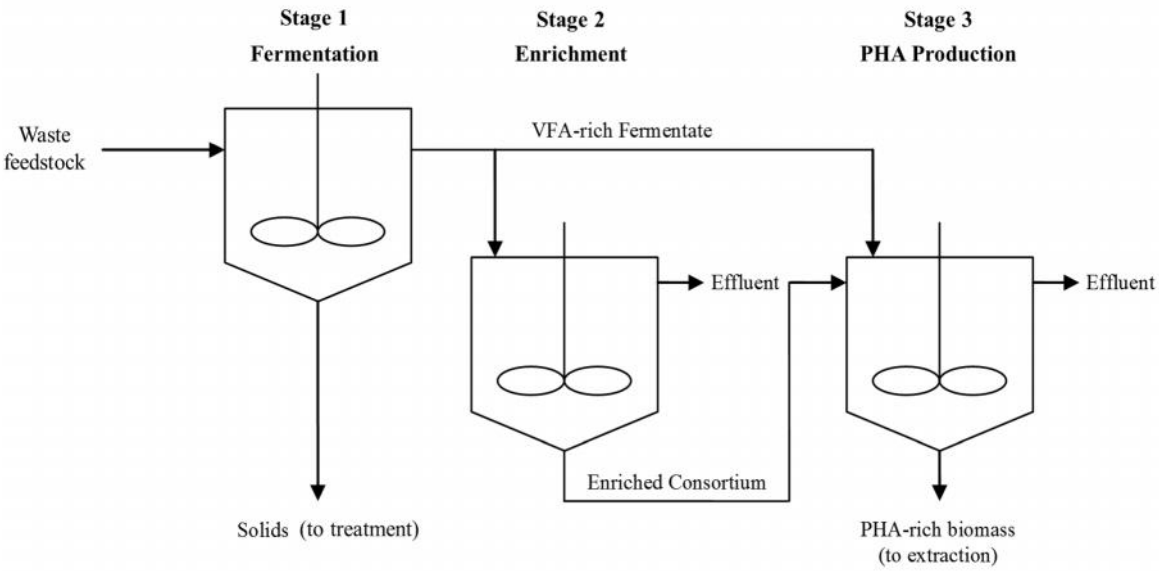

Figure 1.11. Three-stage PHA production process using MMCs and waste feedstocks. Adapted from Guho, 2010.

use of a wide range of potential feedstocks. Moreover, since the carbon substrate accounts for approximately 50% of PHA production costs (Kim, 2000), the use of waste or surplus feedstocks with minimal costs is appealing. The fermentation step is critical for overall PHA process performance as this stage is responsible for generating the VFA substrate, and the main goal of the fermentation step is to maximize the conversion of the organic material in waste feedstocks to VFAs (acidification) without generating methane. Noting this importance, the fermentation potential and performance have been evaluated for a number of

waste feedstocks (Bengtsson *et al.*, 2008a; Chen *et al.*, 2014; Jia *et al.*, 2014; Lee *et al.*, 2014; Ujang *et al.*, 2007; Vergine *et al.*, 2015). The SRT has primarily been used to control the acidification, although the temperature and pH have also been shown to be important in modulating the abundance of fermentative bacteria and methanogenic organisms residing in fermenters, thus affecting VFA yields. As fermentation strategies continue to progress, positive effects on overall PHA process performance will be noted, one of which being the impact on the 2nd stage enrichment process.

Concerning the 2nd stage enrichment process using ADF conditions and waste feedstocks, the same objectives regarding the enrichment of both PHA-producing bacteria and a desirable PHA storage response must be met. However, the optimization of various operating parameters as previously described (e.g., OLR, SRT, cycle length) to achieve effective MMC enrichment is highly challenging as influent waste substrates are often variable in nutrient content (e.g., VFAs, nitrogen, or phosphorus). For example, for waste substrates the OLR is commonly formulated based on VFA chemical oxygen demand (COD; an indirect measurement of organic compounds in water related to the degree of reduction (Roels, 1983)). However, discrepancies have been reported in COD balances relative to VFA content, indicating non-VFA COD is present in waste substrates (Albuquerque *et al.*, 2007; Albuquerque *et al.*, 2010b; Jiang *et al.*, 2012; Morgan-Sagastume *et al.*, 2010). Given waste substrates are derived from complex feedstocks, a range of compounds from readily-biodegradable COD (e.g., simple sugars or other organic acids), to slowly-biodegradable COD (e.g., starch or lignocellulose degradation products) could be present in the media and deleterious to enrichment by reducing the selective pressure of the applied ADF conditions. Non-VFA COD sources could potentially sustain the growth of non-PHA producing bacteria,

or a growth response of PHA-producing bacteria could become dominant to a PHA storage response (Dionisi *et al.*, 2001; van Aalst-van Leeuwen *et al.*, 1997). Indeed, the use of fermented waste feedstocks adds to the difficulty in the MMC enrichment stage. Nevertheless, the enrichment process is critical, as the PHA production performance is highly dependent on the enriched MMC.

The 3rd stage PHA production process is of utmost importance as it is most directly implicated with the economic viability of the technology. Generally, the pulse-fed feeding regime and DO-based monitoring methods as previously described are applied to the PHA production stage using waste feedstocks. Overall, PHA performance metrics (as previously discussed, e.g., maximum PHA content or PHA composition) when using fermented waste feedstocks have been in line with MMC PHA production studies that used synthetic media – values of which that have been reviewed extensively (Dias *et al.*, 2006a; Serafim *et al.*, 2008a). For example, in a PHA production stage assessment that used fermented molasses as a substrate (Dias *et al.*, 2006a), the PHA storage yield was 10% higher compared to an evaluation using acetate and propionate (Lemos *et al.*, 2006), and the maximum PHA content was 6% higher; however, the PHA produced from fermented molasses had a lower HV content, and the PHA production rate was nearly four times slower compared to the MMC cultivated on the synthetic media. Such differences occur frequently and have typically been correlated to the composition of the fermented waste feedstock or microbial community.

Similar methods to improve maximum PHA storage (e.g., external nutrient limitation) are more challenging with waste feedstocks, as modulating nutrient availability is not always easy. Furthermore, potential non-VFA COD present in waste feedstocks may confound the PHA production stage. As illustrated in a study using paper mill wastewater as a substrate,

non-VFA COD accounting for 40% of the total COD was correlated with decreased PHA yields resulting from the enrichment of a so-called “flanking population” that did not accumulate PHA but added to the total microbial biomass (Jiang *et al.*, 2012). Conversely, PHA content higher than theoretical maxima has been observed; the higher PHA yields were attributed to non-VFA COD that was used as PHA substrates (Albuquerque *et al.*, 2011; Dionisi *et al.*, 2005b; Guho, 2010; Gurieff, 2007). In short, addressing differences in process performance is more challenging compared to synthetic media-based PHA production using MMC, as the influent substrate is inherently variable.

A number of waste feedstocks have been assessed for use in a three-stage PHA production scheme. Sugar cane molasses has been the most extensively evaluated waste substrate (Albuquerque *et al.*, 2013; Albuquerque *et al.*, 2010a; Albuquerque *et al.*, 2007; Albuquerque MGE, 2008; Albuquerque *et al.*, 2010b; Bengtsson *et al.*, 2010a; Bengtsson *et al.*, 2010b; Carvalho *et al.*, 2013; Oehmen *et al.*, 2014; Pisco *et al.*, 2009). Overall, PHA process performance using this fermented waste substrate has exhibited great potential; stable 2nd stage enrichment SBRs have been maintained and high PHA accumulation has been consistently reached, the highest approaching nearly 80% (Carvalho *et al.*, 2013). Paper mill effluent has also been assessed as a potential feedstock (Bengtsson *et al.*, 2008a; Bengtsson *et al.*, 2008b; Jiang *et al.*, 2012); high PHA amounts have been reported using this feedstock (up to 77%), although the need for further process optimization has been noted. Olive mill effluents have been investigated (Beccari *et al.*, 2009; Campanari *et al.*, 2014; Dionisi *et al.*, 2005b; Waller *et al.*, 2012), and while PHA content has been above 50%, incomplete fermentation, the need for pre-treatment, and low HV content has been observed. Municipal wastewater has been evaluated for PHA production (Coats *et al.*, 2007b; Morgan-Sagastume

et al., 2015), with maximum PHA contents in a range of approximately 40-53%. Other investigations have included palm oil effluent (Mumtaz *et al.*, 2010; Sudesh *et al.*, 2011), tomato cannery wastewater (Liu *et al.*, 2008), wood mill effluent (Ben *et al.*, 2011), pyrolysis by-products (Moita & Lemos, 2012), and hardwood spent sulfite liquor (Queiros *et al.*, 2014), although sub-optimal process performance was reported for each of these feedstocks. Nevertheless, these studies highlight the range of possible feedstocks for PHA production.

Extensive investigation of temporal bulk solution changes has established many macro kinetic and stoichiometric parameters describing the exhibited PHA storage response under given feast-famine conditions in the presence of waste feedstocks. Conversely, minimal research has been conducted to verify or elucidate the role of microbial composition and physiology as related to observed process performance. Similar molecular methods (e.g., DGGE and FISH) have been applied to MMC cultivated on fermented waste substrates, but the same limitations remain concerning the extent of microbial community resolution and identification. Moreover, depending on the chemical composition of the waste substrate, the sample matrix may interfere with some methods, reducing the reliability (e.g., non-specific PHA staining with Nile blue A). Some studies have sought to quantify how specific operating conditions affected MMC dynamics. For example, in an investigation involving fermented molasses, FISH was coupled to microautoradiography to explore substrate preferences of particular genera in an MMC (Albuquerque *et al.*, 2013); interestingly, the authors observed noticeable substrate uptake patterns and preferences, indicating the MMC had adapted to different substrate niches. Furthermore, differences in PHA composition were correlated to differences in the relative abundance of three particular genera including *Azoarcus*, *Thauera*, and *Paracoccus*. Together, the results of this study provided valuable insight concerning how

future SBR operating conditions may be adjusted to “fine-tune” the MMC composition, thus modulate the overall PHA process performance in the production stage. In separate study also involving fermented molasses, DGGE coupled with DNA band sequencing was applied to monitor MMC dynamics under different operating conditions (Carvalho *et al.*, 2013). The authors reported substantial MMC changes in response to increasing the OLR, which was later found to decrease the overall PHA process performance (Carvalho *et al*., 2013). The authors also observed a linear relationship between the maximum PHA content reached and the abundance of two genera, namely, *Azoarcus* and *Thauera*, further highlighting the value of investigating MMC composition. Apart from the few examples provided, gaps in knowledge regarding the role of MMC composition and physiology remain for PHA production from fermented feedstocks by MMC.

PHA production using MMC and dairy manure

Complementing the need for expanding PHA production is the need for environmentally benign waste management practices in the agricultural sector. The dairy industry is one such sector as dairy cattle generate massive quantities of manure annually; in 2007 the amount of manure generated (on a wet slurry mass basis) was estimated to be 500 billion pounds (Liebrand & Ling, 2009). Manure is valuable to the agricultural industry for its use as a fertilizer; however, in excessive, concentrated amounts, manure can pose multiple environmental risks. Not only does manure contain a number of potential environmental contaminants, its biodegradation is the second leading source of greenhouse gas emissions associated with dairy operations; an estimated 6.4 million tons of carbon dioxide equivalents are emitted per year from decomposing manure (Dairy, 2008). Furthermore, each ton of manure contains about 9.9 lbs. of nitrogen and 1.8 lbs. of phosphorus (University, 1993),

which can overwhelm the absorptive capacity of soil when manure is land applied too frequently, in excessive amounts, or when soil conditions are not conducive for absorption. Excess nitrogen and phosphorus can lead to eutrophication in surface water bodies, wreaking havoc on aquatic life (Bosch *et al.*, 2006; Hristov *et al.*, 2006; Wang *et al.*, 1999), and nutrient overload can also trigger algal blooms, which can have negative consequences on surface water systems.

Manure treatment practices besides land application, such as anaerobic digestion (AD) or lagoons, are marginally effective. AD has been advocated as a "silver bullet" with the goal of treating manure while concurrently producing biogas, although the widespread implementation is not yet sufficiently economical or reliable (EPA, 2006). Lagoons remain the most common form of manure treatment due to the ease of lagoon construction and operation; however, lagoons are a potential source of uncontrolled CO_2 and CH_4 emissions (Leytem *et al.*, 2011), and can leak or overflow, potentially releasing environmental contaminants. Ultimately, no current manure management practice fully addresses all the associated environmental and health concerns, nor captures the value of dairy manure as a resource, further reinforcing the need of developing effective manure treatment strategies. An alternative strategy involves the use of dairy manure as a feedstock for PHA production, which will be described in greater detail.

The use of dairy manure as a feedstock for PHA production is part of an integrated process centered on converting dairy manure to multiple valuable commodities. Outlined in Figure 1.12, dairy manure is first fermented to convert the organic material to VFAs. The VFA-rich fermenter liquid stream (fermented dairy manure liquor; FDML), is then used for both the enrichment stage and the fed-batch PHA production stage. The enrichment (denoted

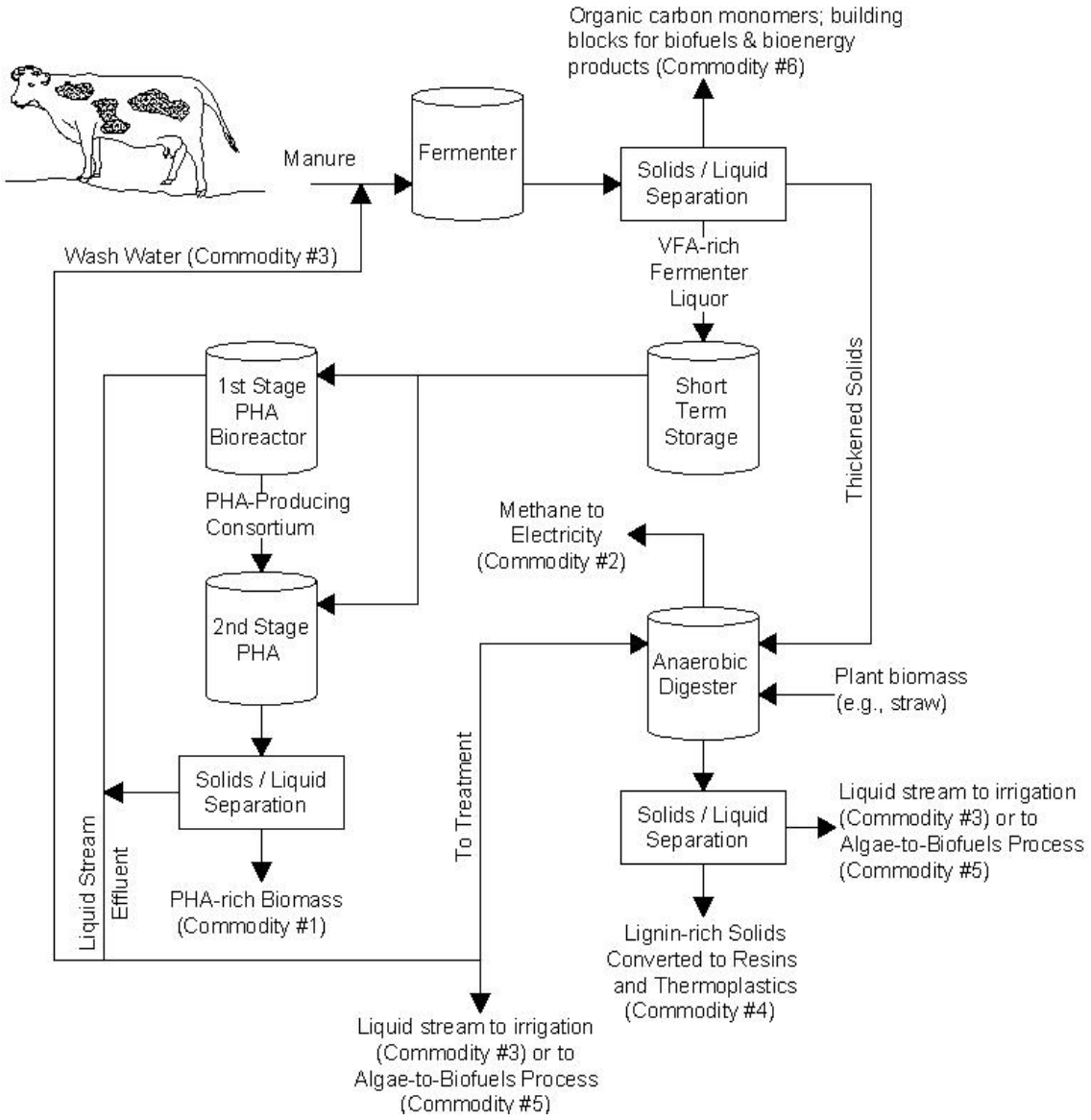

Figure 1.12. Proposed simultaneous commodity production and waste treatment process for dairy manure.

1st Stage PHA Bioreactor in Figure 1.12) of PHA-producing bacteria is carried out in an SBR operated under ADF conditions. PHA production (denoted 2nd Stage PHA in Figure 1.12) is accomplished generally in the same manner as previously described (i.e., in a fed-batch reactor using DO-based monitoring). Upon the completion of a PHA production run, the PHA-rich biomass is harvested and subjected to downstream processing to extract and purify the PHA (Wei *et al.*, 2014). Though not the focus of the research presented herein, the solids fraction from the dairy manure fermenter effluent is subjected to anaerobic digestion for the production

of methane; the effluent streams from the anaerobic digestion can then be used for other purposes. The PHA production component of this integrated dairy manure processing strategy has been investigated (Guho, 2010; Watson, 2015); the highest PHA content reached was nearly 70% of the cell dry weight – a value in line with other investigations, highlighting the potential of this process. Ultimately, to advance PHA production from fermented dairy manure, an enhanced understanding of the microbial community and functional profile must be obtained. Regarding the investigation of PHA synthesis by MMC from fermented dairy manure, strong experimental approaches include high-throughput "omics" technologies, as these culture-independent methods target the large-scale characterization of microbial community composition and physiology.

1.4 "Omics" technologies

"Omics" technologies in microbiology refer to high-throughput methods to explore the roles, relationships, and actions of single microbes to whole communities. In addition to being culture-independent, "omics" technologies permit the simultaneous examination of hundreds to thousands of desired targets, generate large datasets, and are accompanied by a vast number of different bioinformatics and statistical tools to interrogate large datasets. While a multitude of "omics" technologies exist (e.g., metagenomics, transcriptomics, proteomics, metabolomics, fluxomics, lipidomics), this section is focused on two branches of "omics" technologies, namely metagenomics and proteomics. First, the field of metagenomics is broadly overviewed, after which the discussion transitions to microbial community profiling via next-generation of the 16S rRNA gene for microbial identification. Secondly, the field of proteomics is discussed with respect to MMCs encountered in environmental biotechnology.

Metagenomics

In relation to microbial communities, metagenomics comprises the analysis of genetic material (i.e., DNA) of a number of microbes in a given environment. Metagenomics was first coined in 1998, referring to the function-based analysis of mixed environmental DNA species (Handelsman *et al.*, 1998). Since this inception, this area of research has exploded, and a large body of literature is available to highlight the success of large-scale microbial ecology investigations (Cowan *et al.*, 2005; Handelsman, 2004; Riesenfeld *et al.*, 2004; Schmeisser *et al.*, 2007; Singh *et al.*, 2009; Tringe & Rubin, 2005; Xu, 2006). Moreover, several concepts concerning the importance of microbial ecology and functionality specifically in environmental biotechnology have been reviewed (Briones & Raskin, 2003; McMahon *et al.*, 2007; Rittmann, 2006; Rittmann *et al.*, 2006). Initiatives such as the Earth Microbiome Project (Gilbert *et al.*, 2010), Human Microbiome Project (Turnbaugh *et al.*, 2007), or the Extreme Microbiome Project (http://www.extrememicrobiome.org) have been launched, and have made great progress in characterizing microbial life in both natural, built, and engineered environments. The progress in metagenomics has largely been made possible by the appreciable advancements of high-throughput DNA sequencing technology and bioinformatics tools.

A number of massively parallel DNA sequencing platforms have been introduced in the last decade as part of next-generation sequencing (NGS). The different DNA sequencing technologies and applications have been extensively reviewed (Mardis, 2008; Metzker, 2010; Morozova & Marra, 2008; Schuster, 2007; Shendure & Ji, 2008). Comprehensive microbial community profiling is now more accessible and affordable than ever with NGS of the 16S rRNA gene. Briefly, this well-established method for investigating taxonomy and phylogeny

begins with the extraction of genomic DNA from a sample, followed by PCR-based amplification of a particular region of the highly conserved eubacterial 16S rRNA gene. Amplicon library preparation varies depending on the sequencing platform used. The research presented herein used an Illumina MiSeq, therefore, included in the amplicon preparation was the attachment of universal sequence tags and sequencing-specific barcodes to enable the sequencing of multiple samples, after which samples could be assigned based on the individual barcodes. After amplicon sequencing and de-multiplexing, sequence reads are processed and taxonomically classified; a multitude of bioinformatics pipelines are readily available for data processing and interpretation. Regardless, the end result of a 16S rRNA gene sequencing workflow is a comprehensive characterization of microbial communities in a given sample.

Within environmental biotechnology, NGS of the 16S rRNA gene has great utility. Few studies related to PHA production using MMC and waste feedstocks have capitalized on the advancements of NGS and bioinformatics, although 16S rRNA gene profiling was implemented in an investigation of PHB production using wood hydrolysates and revealed major microbial community changes relative to different operational parameters (Dai *et al.*, 2015). MMC profiling has been used in various fermentation studies, including the fermentation of potato peel waste to produce lactic acid (Liang *et al.*, 2015), and waste activated sludge in an effort to reveal strategies to enhance the acidification efficiency (Li *et al.*, 2015). Studies of anaerobic digestion have benefitted through the use of 16S rRNA gene sequencing by linking microbial composition to operating conditions and the resulting performance (Briones *et al.*, 2014; Luo *et al.*, 2015; Regueiro *et al.*). 16S rRNA gene sequencing has also been used to identify and monitor fecal contamination (Cao *et al.*, 2013),

and has been shown to be effective in monitoring drinking water for potential contamination (Prest *et al.*, 2014). NGS of the 16S rRNA gene has been applied to characterize MMC in activated sludge (Guo & Zhang, 2012; Laureni *et al.*, 2015; Yadav *et al.*, 2014; Zhang *et al.*, 2015), providing valuable insight into microbial composition and changes relative to given operating conditions. Some drawbacks are associated with NGS of the 16S rRNA gene as related to MMC profiling; for example, the sequence read abundance can differ from actual abundance, as the copy number of the 16S rRNA gene can vary among bacterial species (Fogel *et al.*, 1999), PCR-based amplification can introduce sequence artefacts (Acinas *et al.*, 2005), and multiple inconsistencies mount for experimental approaches and data interpretation (Forney *et al.*, 2004). Nevertheless, the aforementioned examples of MMC profiling highlight the versatility of NGS of the 16S rRNA gene when applied to environmental biotechnology. To complement MMC characterization, the application of proteomics can provide valuable information concerning the functionality of microbial communities exposed to a given set of environmental conditions.

Proteomics

In relation to microbial communities, proteomics refers to the large scale analysis of proteins. The term proteomics originated from the "protein complement of a genome" (Wilkins *et al.*, 1996), and when proteomics is applied to MMC, the term "metaproteomics" is often used. A large body of literature is available describing various metaproteomic achievements and advancements (Dill *et al.*, 2010; Hettich *et al.*, 2013; Hettich *et al.*, 2012; Maron *et al.*, 2007; Siggins *et al.*, 2012; Wilmes & Bond, 2006b). The rapid expansion and applicability of metaproteomics has been driven largely by the substantial developments in

liquid chromatography (LC) and mass spectrometry (MS), specifically when the two are coupled, and tandem MS systems are incorporated (LC-MS/MS).

The field of proteomics has experienced considerable growth, accompanied by new and improved protocols to enhance experimental workflows starting at sample preparation and ending with data analysis. Outlined in Figure 1.13, a typical proteomic workflow includes the following stages: protein extraction, protein fractionation, protein digestion, peptide separation, peptide ionization with mass spectral analysis, protein identification, and data analysis. While many complementary and alternative methodologies can be adapted to this workflow, the basic steps remain the same. Once proteins have been extracted from an environmental sample, some type of fractionation prior to LC-MS/MS analysis is implemented.

Protein fractionation can either be "gel-based" or "gel-free." The former refers to the use of SDS PAGE (either one or two-dimensional gel electrophoresis) to separate protein mixtures based on physical properties of proteins (e.g., molecular weight or isoelectric point). Two-dimensional protein electrophoresis (2DE), which separates proteins by both isoelectric point and molecular weight (O'Farrell, 1975), provides greater protein resolving power and can provide both qualitative and quantitative information regarding proteome profiles of microbial communities (Carrette *et al.*, 2006). In fact, early metaproteomic studies relied on 2DE for comparative purposes in addition to minimizing the complexity of protein samples prior to LC-MS analysis. Though highly valuable as a pre-fractionation tool, gel-based protein separation methods have limitations. For example, 2DE is laborious with few options for automating and can be biased towards the most abundant proteins in a sample. As such, gel-free methods based on multi-dimensional chromatography were developed. A gel-free

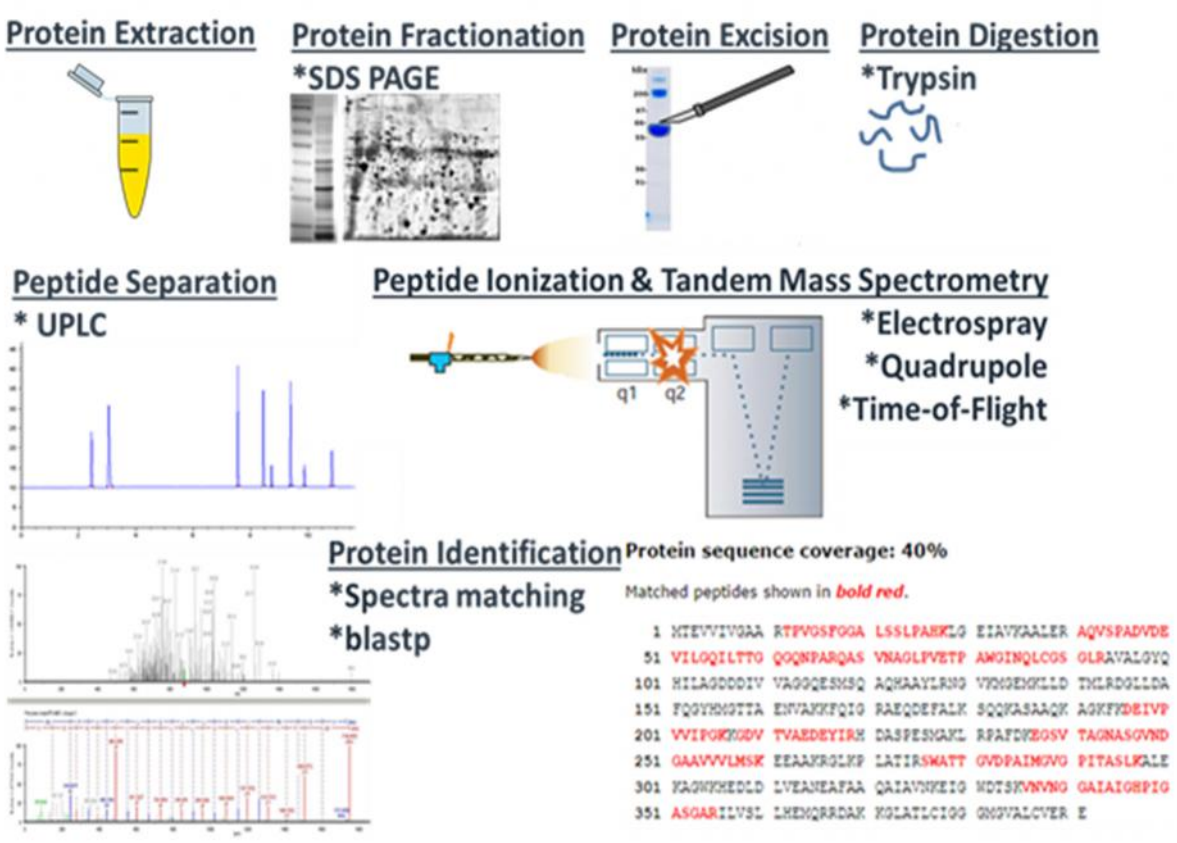

Figure 1.13. Example proteomics workflow. Adapted from Aebersold and Mann, 2003.

approach simply bypasses protein separation using gel electrophoresis, and directly applies a proteolytic enzyme (e.g., trypsin) to protein mixtures. After enzymatic digestion, the resulting peptides are separated using multi-dimensional chromatography (e.g., ion-exchange followed by reverse-phase). This particular gel-free workflow was first described as Multi-Dimensional Protein Identification Technology (MudPit) (Washburn *et al.*, 2001), and has since been implemented in metaproteomic investigations, for example in acid mine drainage (Goltsman *et al.*, 2009; Mueller *et al.*, 2010; Ram *et al.*, 2005).

Regardless of protein fractionation strategy, the cornerstone of any proteomics workflow is a tandem mass spectrometry system. In early proteomics studies, peptide mass fingerprinting was achieved through the use of matrix-assisted laser desorption/ionization-time of flight (MALDI-TOF) systems, which generated individual mass spectral peaks per

peptide (Henzel *et al.*, 1993; Yates *et al.*, 1993). However, the resolution was relatively low for complex protein mixtures, especially those arising from microbial communities. Accordingly, different ionization and MS systems were implemented, namely electrospray ionization coupled with tandem MS (ESI-MS/MS) (Fenn *et al.*, 1989; Wilm & Mann, 1994). ESI essentially creates an aerosol by applying a high voltage to a liquid (i.e., peptide sample), and in contrast to MALDI, ESI can generate multiply charged ions. By having multiply charged ions, the mass range of MS detectors is extended such that peptide fragments can be analyzed (Ho *et al.*, 2003; Pitt, 2009). Concerning tandem MS systems, configurations can vary; for example, for the research presented herein, a quadrupole-time of flight (QTOF) system was used. Another popular tandem MS configuration in proteomics workflows is a quadrupole ion trap. Irrespective of LC-MS/MS configuration used, the identification of microbial proteins present in an environmental sample provides valuable information concerning the actual functionality of bacteria.

The advantage of proteomics when applied to environmental biotechnology is the provision of direct evidence to link microbial physiology to chemical transformations observed under given conditions. Early proteomic studies on activated sludge revealed key functions related to EBPR that bolstered existing models of this highly important environmental biotechnology (Wilmes *et al.*, 2008a; Wilmes & Bond, 2006a; Wilmes & Bond, 2004; Wilmes *et al.*, 2008b). Proteomics has been applied to membrane bioreactors treating sewage sludge, highlighting both the number of extracellular proteins present in these matrices, as well as protein factors contributing to bio-fouling (Kuhn *et al.*, 2011; Zhou *et al.*, 2015). Proteomics has been applied to investigate the degradation of various environmental contaminants including benzene (Benndorf *et al.*, 2009), terephthalate (Wu *et al.*, 2013), and

toluene (Jehmlich *et al.*, 2010), with each study revealing key pathways involved in the degradation of these compounds. Proteomics has also been applied to anaerobic digestion (Abram *et al.*, 2011; D'haeseleer *et al.*, 2013; Hanreich *et al.*, 2012; Hanreich *et al.*, 2013; Lü *et al.*, 2014), providing critical insight regarding the metabolically active bacteria in complex environments that rely on syntrophic interactions to degrade cellulosic material. Together, the success of these few studies highlight both the feasibility and versatility of applying the proteomics approach to complex MMCs.

Concerning PHA synthesis in bacteria, only a few studies in pure cultures have capitalized on the power of proteomics to date. Proteomics was used to study *Cupriavidus necator* in relation to PHA synthesis in the presence of short chain organic acids (viz., acetic, propionic, and levulinic acid); proteins involved in PHA metabolism including PHA synthesis, β-oxidation, and substrate activation were found to be in increased abundance, which was strong experimental evidence to validate the central concepts related to PHA synthesis from organic acids (Lee *et al.*, 2009). In another study involving *C. necator*, growth conditions under lithoautotrophy and organoheterotrophy were interrogated using proteomics (Kohlmann *et al.*, 2011); the results provided evidence to support the great metabolic versatility of *C. necator*, reinforcing the value in using this microorganism for commercial-scale PHA production. Genetically engineered *E. coli* has been proposed as a means for large-scale PHA production, therefore, proteomics was used to study the effects of PHB synthesis (Han *et al.*, 2001). Interestingly, the authors found the synthesis and presence of PHB granules induced a stress response accompanied by a substantial increase of heat shock proteins, including molecular chaperones. Though not specifically applied to investigate PHA synthesis, in a study involving *Novosphingobium nitrogenifigens*, proteomics revealed a

unique and unexpected PHA accumulation capacity, particularly in the presence of low nitrogen, suggesting this particular bacterium may be useful for large-scale PHA production (Smit *et al.*, 2012). Though few in number, the aforementioned proteomic investigations contributed to the understanding of PHA synthesis in pure cultures, in addition to revealing new insight concerning potentially useful bacteria for the large-scale production of PHA.

1.5 Summary

PHAs can serve as functional replacements to some of the most commonly consumed petroleum-based plastic products. Despite the appealing material properties and applications of PHAs, the high cost of production using pure microbial cultures and refined feedstocks has been a barrier in the widespread production and adoption of PHA as commodity bioplastics. In an effort to decrease production costs and implement more green manufacturing technologies, the use of open MMCs enriched through ADF using waste feedstocks has received research attention. MMCs have exhibited promising capacity for PHA production from waste feedstocks, although the full potential has not been consistently actualized. As process performance is highly dependent on the microbial enrichment stage, a primary research focus has been the optimization of bioreactor operating conditions (e.g., OLR, SRT, cycle length, aeration rate, temperature, pH, etc.). In addition to the optimization of the enrichment stage, PHA production in fed-batch reactors has also garnered research attention.

Microbial community composition and physiology are recognized as being pivotal to process performance, however, few studies have extensively characterized either with respect to conventional observations. Though a conceptual basis for describing the feast-famine storage response under ADF conditions is established, a physiological description that can be

included in process design is largely deficient, as direct the characterization of microbial functions under ADF conditions or during fed-batch PHA production has not been a primary research focus. Accordingly, to advance the engineering of bioreactor environments to improve MMC enrichment and physiological adaptation using fermented waste feedstocks (including fermented dairy manure), an enhanced understanding of the microbial community and functional profile is required. By improving our fundamental understanding of the microbiology associated with conventional observations in bioreactors, process optimization can be bolstered and guided.

Considering the multi-stage PHA production approach using MMCs and fermented dairy manure as a feedstock, no microbial community or functional characterization has been performed for enrichment SBRs operated under ADF conditions. Consequently, the extent to which the microbial composition and function may relate to or influence PHA process performance using fermented dairy manure as a feedstock has not been established. With the advancements in high-throughput "omics" technologies, experimental approaches are available to investigate complex MMCs in ADF systems. High-throughput DNA sequencing provides a strong approach to characterize complex microbial communities cultivated in waste feedstocks, including fermented dairy manure. Microbial community proteomics presents an experimental approach to directly characterize microbial functions through the identification of proteins using LC-MS/MS. By applying a combination of the two approaches to bioreactors cultivated using fermented dairy manure, both microbial community composition and associated functions can be characterized, providing valuable insight that may help advance PHA production using this waste feedstock.

References

Abram, F., Enright, A. M., et al. (2011). A metaproteomic approach gives functional insights into anaerobic digestion. *J Appl Microbiol, 110*(6), 1550-1560.

Acinas, S. G., Sarma-Rupavtarm, R., et al. (2005). PCR-induced sequence artifacts and bias: insights from comparison of two 16S rRNA clone libraries constructed from the same sample. *Applied and environmental microbiology, 71*(12), 8966-8969.

Agnew, D. E., & Pfleger, B. F. (2013). Synthetic biology strategies for synthesizing polyhydroxyalkanoates from unrelated carbon sources. *Chemical Engineering Science, 103*(0), 58-67.

Akaraonye, E., Keshavarz, T., et al. (2010). Production of polyhydroxyalkanoates: the future green materials of choice. *Journal of Chemical Technology and Biotechnology, 85*(6), 732-743.

Akiyama, M., Tsuge, T., et al. (2003). Environmental life cycle comparison of polyhydroxyalkanoates produced from renewable carbon resources by bacterial fermentation. *Polymer Degradation and Stability, 80*(1), 183-194.

Albuquerque, M. G. E., Carvalho, G., et al. (2013). Link between microbial composition and carbon substrate-uptake preferences in a PHA-storing community. *Isme Journal, 7*(1), 1-12.

Albuquerque, M. G. E., Concas, S., et al. (2010a). Mixed culture polyhydroxyalkanoates production from sugar molasses: The use of a 2-stage CSTR system for culture selection. *Bioresource Technology, 101*(18), 7112-7122.

Albuquerque, M. G. E., Eiroa, M., et al. (2007). Strategies for the development of a side stream process for polyhydroxyalkanoate (PHA) production from sugar cane molasses. *Journal of Biotechnology, 130*(4), 411-421.

Albuquerque, M. G. E., Martino, V., et al. (2011). Mixed culture polyhydroxyalkanoate (PHA) production from volatile fatty acid (VFA)-rich streams: Effect of substrate composition and feeding regime on PHA productivity, composition and properties. *Journal of Biotechnology, 151*(1), 66-76.

Albuquerque MGE, T. C., Bengtsson S, Werker A, Reis MAM. (2008, 7-10 April). *Strategies for culture selection in a three-stage PHA production process from sugar cane molasses.* Paper presented at the Proceedings II of 4th IWA Specialised Conference on Sequencing Batch Reactor Technology (SBR4), Rome, Italy.

Albuquerque, M. G. E., Torres, C. A. V., et al. (2010b). Polyhydroxyalkanoate (PHA) production by a mixed microbial culture using sugar molasses: Effect of the influent substrate concentration on culture selection. *Water Research, 44*(11), 3419-3433.

Anderson, A. J., & Dawes, E. A. (1990). Occurence, metabolism, metabolic role, and industrial uses of bacterial polyhydroxyalkanoates *Microbiological Reviews, 54*(4), 450-472.

Andreeßen, B., & Steinbüchel, A. (2010). Biosynthesis and Biodegradation of 3-Hydroxypropionate- Containing Polyesters. *Applied and Environmental Microbiology, 76*(15), 4919-4925.

Anterrieu, S., Quadri, L., et al. (2014). Integration of biopolymer production with process water treatment at a sugar factory. *New Biotechnology, 31*(4), 308-323.

Avella, M., Martuscelli, E., et al. (2000). Review Properties of blends and composites based on poly (3-hydroxy) butyrate (PHB) and poly (3-hydroxybutyrate-hydroxyvalerate)(PHBV) copolymers. *Journal of Materials Science, 35*(3), 523-545.

Ayub, N. D., Pettinari, M. J., et al. (2004). A polyhydroxybutyrate-producing Pseudomonas sp. isolated from Antarctic environments with high stress resistance. *Current microbiology, 49*(3), 170-174.

Babel, W. (1992). Pecularities of methylotrophs concerning overflow metabolism, especially the synthesis of polyhydroxyalkanoates. *FEMS Microbiology Letters, 103*(2-4), 141-148.

Bachmann, B. M., & Seebach, D. (1999). Investigation of the Enzymatic Cleavage of Diastereomeric Oligo(3-hydroxybutanoates) Containing Two to Eight HB Units. A Model for the Stereoselectivity of PHB Depolymerase from Alcaligenes faecalis T1. *Macromolecules, 32*(6), 1777-1784.

Barnard, G. N., & Sanders, J. (1989). The poly-beta-hydroxybutyrate granule in vivo. A new insight based on NMR spectroscopy of whole cells. *Journal of Biological Chemistry, 264*(6), 3286-3291.

Barnes, D. K., Galgani, F., et al. (2009). Accumulation and fragmentation of plastic debris in global environments. *Philosophical Transactions of the Royal Society B: Biological Sciences, 364*(1526), 1985-1998.

Barnes, D. K. A. (2002a). Biodiversity - Invasions by marine life on plastic debris. *Nature, 416*(6883), 808-809.

Barnes, D. K. A. (2002b). Human Rubbish Assists Alien Invasions of Seas. *Directions in Science, 1*, 107-112.

Basak, B., Ince, O., et al. (2011). Effect of nitrogen limitation on enrichment of activated sludge for PHA production. *Bioprocess and Biosystems Engineering, 34*(8), 1007-1016.

Beccari, M., Bertin, L., et al. (2009). Exploiting olive oil mill effluents as a renewable resource for production of biodegradable polymers through a combined anaerobic-aerobic process. *Journal of Chemical Technology and Biotechnology, 84*(6), 901-908.

Ben, M., Mato, T., et al. (2011). Bioplastic production using wood mill effluents as feedstock. *Water Science and Technology, 63*(6), 1196-1202.

Bengtsson, S., Pisco, A. R., et al. (2010a). Molecular weight and thermal properties of polyhydroxyalkanoates produced from fermented sugar molasses by open mixed cultures. *Journal of Biotechnology, 147*(3-4), 172-179.

Bengtsson, S., Pisco, A. R., et al. (2010b). Production of polyhydroxyalkanoates from fermented sugar cane molasses by a mixed culture enriched in glycogen accumulating organisms. *Journal of Biotechnology, 145*(3), 253-263.

Bengtsson, S., Werker, A., et al. (2008a). Production of polyhydroxyalkanoates by activated sludge treating a paper mill wastewater. *Bioresource Technology, 99*(3), 509-516.

Bengtsson, S., Werker, A., et al. (2008b). Production of polyhydroxyalkanoates by glycogen accumulating organisms treating a paper mill wastewater. *Water Science and Technology, 58*(2), 323-330.

Benndorf, D., Vogt, C., et al. (2009). Improving protein extraction and separation methods for investigating the metaproteome of anaerobic benzene communities within sediments. *Biodegradation, 20*(6), 737-750.

Berger, E., Ramsay, B., et al. (1989). PHB recovery by hypochlorite digestion of non-PHB biomass. *Biotechnology Techniques, 3*(4), 227-232.

Beun, J. J., Dircks, K., et al. (2002). Poly-β-hydroxybutyrate metabolism in dynamically fed mixed microbial cultures. *Water Research, 36*(5), 1167-1180.

Beun, J. J., Paletta, F., et al. (2000). Stoichiometry and kinetics of poly-beta-hydroxybutyrate metabolism in aerobic, slow growing, activated sludge cultures. *Biotechnology and Bioengineering, 67*(4), 379-389.

Bosch, D. J., Wolfe, M. L., et al. (2006). Reducing phosphorus runoff from dairy farms. *Journal of Environmental Quality, 35*(3), 918-927.

Brämer, C. O., Vandamme, P., et al. (2001). Polyhydroxyalkanoate-accumulating bacterium isolated from soil of a sugar-cane plantation in Brazil. *International journal of systematic and evolutionary microbiology, 51*(5), 1709-1713.

Braunegg, G., Lefebvre, G., et al. (1998). Polyhydroxyalkanoates, biopolyesters from renewable resources: Physiological and engineering aspects. *Journal of Biotechnology, 65*(2-3), 127-161.

Briese, B., Schmidt, B., et al. (1994). Pseudomonas lemoignei has five poly(hydroxyalkanoic acid) (PHA) depolymerase genes: A comparative study of bacterial and eukaryotic PHA depolymerases. *Journal of environmental polymer degradation, 2*(2), 75-87.

Brigham, C. J., & Sinskey, A. J. (2012). Applications of polyhydroxyalkanoates in the medical industry. *International Journal of Biotechnology for Wellness Industries, 1*(1), 52-60.

Briones, A., Coats, E., et al. (2014). Should We Build "Obese" or "Lean" Anaerobic Digesters?

Briones, A., & Raskin, L. (2003). Diversity and dynamics of microbial communities in engineered environments and their implications for process stability. *Current Opinion in Biotechnology, 14*(3), 270-276.

Bugnicourt, E., Cinelli, P., et al. (2014). Polyhydroxyalkanoate (PHA): Review of synthesis, characteristics, processing and potential applications in packaging. *Express Polymer Letters, 8*(11).

Byrom, D. (1992). Production of Poly-Beta-Hydroxybutyrate - Poly-Beta-Hydroxyvalerate Copolymers. *Fems Microbiology Reviews, 103*(2-4), 247-250.

Byrom, D. (1994). *Plastics from microbes. Microbial synthesis of polymers and polymer precursors*: Hanser Munich.

Campanari, S., Silva, F. A. e., et al. (2014). Effect of the organic loading rate on the production of polyhydroxyalkanoates in a multi-stage process aimed at the valorization of olive oil mill wastewater. *International Journal of Biological Macromolecules, 71*, 34-41.

Cao, Y., Van De Werfhorst, L. C., et al. (2013). Evaluation of molecular community analysis methods for discerning fecal sources and human waste. *Water Research, 47*(18), 6862-6872.

Carrette, O., Burkhard, P. R., et al. (2006). State-of-the-art two-dimensional gel electrophoresis: a key tool of proteomics research. *Nature protocols, 1*(2), 812-823.

Carvalho, G., Oehmen, A., et al. (2013). The relationship between mixed microbial culture composition and PHA production performance from fermented molasses. *N Biotechnol*.

Chee, J.-Y., Yoga, S.-S., et al. (2010). Bacterially produced polyhydroxyalkanoate (PHA): converting renewable resources into bioplastics. *Current Research, Technology and education Topics in Applied microbiology and applied Biotechnology*, 1395-1404.

Chen, G.-Q., & Patel, M. K. (2011). Plastics derived from biological sources: present and future: a technical and environmental review. *Chemical reviews, 112*(4), 2082-2099.

Chen, G.-Q., & Wu, Q. (2005). The application of polyhydroxyalkanoates as tissue engineering materials. *Biomaterials, 26*(33), 6565-6578.

Chen, G. Q. (2009). A microbial polyhydroxyalkanoates (PHA) based bio- and materials industry. *Chemical Society Reviews, 38*(8), 2434-2446.

Chen, Q., & Thouas, G. (2015). *Biomaterials : a basic introduction*. Boca Raton: CRC Press, Taylor & Francis Group.

Chen, Y., Li, M., et al. (2014). Optimal poly (3-hydroxybutyrate/3-hydroxyvalerate) biosynthesis by fermentation liquid from primary and waste activated sludge. *Environmental Technology, 35*(14), 1791-1801.

Chiellini, E., Chiellini, F., et al. (2003). Biobased polymeric materials for agriculture applications *Biodegradable polymers and plastics* (pp. 185-210): Springer.

Choi, J. I., & Lee, S. Y. (1997). Process analysis and economic evaluation for poly(3-hydroxybutyrate) production by fermentation. *Bioprocess Engineering, 17*(6), 335-342.

Choi, J. i., & Lee, S. Y. (1999). Efficient and economical recovery of poly (3-hydroxybutyrate) from recombinant Escherichia coli by simple digestion with chemicals. *Biotechnology and bioengineering, 62*(5), 546-553.

Chowdhury, A. A. (1963). Poly-β-hydroxybuttersäure abbauende Bakterien und Exoenzym. *Archiv für Mikrobiologie, 47*(2), 167-200.

Chua, A. S. M., Takabatake, H., et al. (2003). Production of polyhydroxyalkanoates (PHA) by activated sludge treating municipal wastewater: effect of pH, sludge retention time (SRT), and acetate concentration in influent. *Water Research, 37*(15), 3602-3611.

Chua, H., Yu, P. F., et al. (1999). Accumulation of biopolymers in activated sludge biomass. *Applied Biochemistry and Biotechnology, 78*(1-3), 389-399.

Ciesielski, S., Cydzik-Kwiatkowska, A., et al. (2006). Molecular detection and diversity of medium-chain-length polyhydroxyalkanoates-producing bacteria enriched from activated sludge. *Journal of Applied Microbiology, 101*(1), 190-199.

Ciesielski, S., Gorniak, D., et al. (2014). The diversity of bacteria isolated from antarctic freshwater reservoirs possessing the ability to produce polyhydroxyalkanoates. *Curr Microbiol, 69*(5), 594-603.

Ciesielski, S., Pokoj, T., et al. (2008). Molecular insight into activated sludge producing polyhydroxyalkanoates under aerobic–anaerobic conditions. *Journal of industrial microbiology & biotechnology, 35*(8), 805-814.

Coats, E. R., Gregg, M., et al. (2011). Effect of organic loading and retention time on dairy manure fermentation. *Bioresource Technology, 102*(3), 2572-2577.

Coats, E. R., Loge, F. J., et al. (2007a). Functional stability of a mixed microbial consortium producing PHA from waste carbon sources. *Appl Biochem Biotechnol, 137-140*(1-12), 909-925.

Coats, E. R., Loge, F. J., et al. (2007b). Synthesis of polyhydroxyalkanoates in municipal wastewater treatment. *Water Environment Research, 79*(12), 2396-2403.

Coats, E. R., Loge, F. J., et al. (2008). Production of natural fiber reinforced thermoplastic composites through the use of polyhydroxybutyrate-rich biomass. *Bioresource technology, 99*(7), 2680-2686.

Cowan, D., Meyer, Q., et al. (2005). Metagenomic gene discovery: past, present and future. *Trends in Biotechnology, 23*(6), 321-329.

D'haeseleer, P., Gladden, J. M., et al. (2013). Proteogenomic analysis of a thermophilic bacterial consortium adapted to deconstruct switchgrass. *PLoS One, 8*(7), e68465.

Dai, J., Gliniewicz, K., et al. (2015). Influence of organic loading rate and solid retention time on polyhydroxybutyrate production from hybrid poplar hydrolysates using mixed microbial cultures. *Bioresource technology, 175*, 23-33.

Daigger, G. T. (1979). The interaction of physiological adaptation and transient response for Pseudomonas putida and its implications for dynamic modeling of microbial growth.

Daigger, G. T., & Grady, C. P. L. (1982). An assessment of the role of physiological adaptation in the transient-response of bacterial cultures *Biotechnology and Bioengineering, 24*(6), 1427-1444.

Dairy, I. C. f. U. (2008). U.S. Dairy Sustainability Initiative: A Roadmap to Reduce Greenhouse Gas Emissions and Increase Business Value. In I. C. f. U. Dairy (Ed.). U.S.

Dawes, E. A. (1983). *Environmental Regulation of Microbial Metabolism* (1st ed.).

Dawes, E. A., & Senior, P. J. (1972). The role and regulation of energy reserve polymers in micro-organisms. *Advances in microbial physiology, 10*, 135-266.

Day, M., Shaw, K., et al. (1994). Biodegradability: An assessment of commercial polymers according to the Canadian method for anaerobic conditions. *Journal of environmental polymer degradation, 2*(2), 121-127.

de Almeida, A., Catone, M. V., et al. (2011). Unexpected Stress-Reducing Effect of PhaP, a Poly(3-Hydroxybutyrate) Granule-Associated Protein, in Escherichia coli. *Applied and Environmental Microbiology, 77*(18), 6622-6629.

De Eugenio, L., García, J., et al. (2008). Comparative analysis of the physiological and structural properties of a medium chain length polyhydroxyalkanoate depolymerase from Pseudomonas putida KT2442. *Engineering in Life Sciences, 8*(3), 260-267.

de Eugenio, L. I., García, P., et al. (2007). Biochemical evidence that phaZ gene encodes a specific intracellular medium chain length polyhydroxyalkanoate depolymerase in Pseudomonas putida KT2442: Characterization of a paradigmatic enzyme *Journal of Biological Chemistry, 282*(7), 4951-4962.

Dekoning, G. (1995). Physical-properties of bacterial poly((R)-3-hydroxyalkanoates) *Canadian Journal of Microbiology, 41*, 303-309.

Derraik, J. G. B. (2002). The pollution of the marine environment by plastic debris: a review. *Marine Pollution Bulletin, 44*(9), 842-852.

Dias, J. M., Lemos, P. C., et al. (2006a). Recent advances in polyhydroxyalkanoate production by mixed aerobic cultures: from the substrate to the final product. *Macromol Biosci, 6*(11), 885-906.

Dias, J. M. L., Lemos, P. C., et al. (2006b). Recent advances in polyhydroxyalkanoate production by mixed aerobic cultures: From the substrate to the final product. *Macromolecular Bioscience, 6*(11), 885-906.

Dias, J. M. L., Oehmen, A., et al. (2008). Metabolic modelling of polyhydroxyalkanoate copolymers production by mixed microbial cultures. *Bmc Systems Biology, 2*.

Dias, J. M. L., Serafim, L. S., et al. (2005). Mathematical modelling of a mixed culture cultivation process for the production of polyhydroxybutyrate. *Biotechnology and Bioengineering, 92*(2), 209-222.

DiGregorio, B. E. (2009). Biobased Performance Bioplastic: Mirel. *Chemistry & Biology, 16*(1), 1-2.

Dill, B. D., Young, J. C., et al. (2010). Metaproteomics: techniques and applications. *Environmental Molecular Microbiology*, 37-62.

Dionisi, D., Beccari, M., et al. (2005a). Storage of biodegradable polymers by an enriched microbial community in a sequencing batch reactor operated at high organic load rate. *Journal of Chemical Technology and Biotechnology, 80*(11), 1306-1318.

Dionisi, D., Carucci, G., et al. (2005b). Olive oil mill effluents as a feedstock for production of biodegradable polymers. *Water Research, 39*(10), 2076-2084.

Dionisi, D., Majone, M., et al. (2001). Sequencing Batch Reactor: Influence of Periodic Operation on Performance of Activated Sludges in Biological Wastewater Treatment. *Industrial & Engineering Chemistry Research, 40*(23), 5110-5119.

Dionisi, D., Majone, M., et al. (2006). Effect of the applied organic load rate on biodegradable polymer production by mixed microbial cultures in a sequencing batch reactor. *Biotechnology and Bioengineering, 93*(1), 76-88.

Dionisi, D., Majone, M., et al. (2007). Effect of the length of the cycle on biodegradable polymer production and microbial community selection in a sequencing batch reactor. *Biotechnology Progress, 23*(5), 1064-1073.

Doi, Y. (1990). Microbial polyesters. *VCH Publishers*.

Doi, Y., Kawaguchi, Y., et al. (1992). Synthesis and degradation of polyhydroxyalkanoates in *Alcaligenes-eutrophus Fems Microbiology Reviews, 9*(2-4), 103-108.

Doi, Y., Tamaki, A., et al. (1988). Production of copolyesters of 3-hydroxybutyrate and 3-hydroxyvalerate by Alcaligenes eutrophus from butyric and pentanoic acids. *Applied Microbiology and Biotechnology, 28*(4-5), 330-334.

EBA. (2013). *Bioplastics market grows above average between 2012 and 2017: European Boplastics publishes market data update*. Marienstr, Berlin.

EIA, U. S. E. I. A. (2010). How much oil is used to make plastic? *Independent Statistics and Analysis.* 2014, from http://www.eia.gov/tools/faqs/faq.cfm?id=34&t=6

EIA, U. S. E. I. A. (2013). *Annual Energy Outlook 2013 Early Release Overview*. Washington, D.C.

EPA, U. S. E. P. A. (2006). Market opportunities for biogas recovery systems - improved performance at competitive costs (A. Program, Trans.) (Vol. EPA-430-8-06-004).

EPA, U. S. E. P. A. (2012). Plastics. *Wastes-Resource Conservation-Common Wastes & Materials.* 2014, from http://www.epa.gov/osw/conserve/materials/plastics.htm

Fenn, J. B., Mann, M., et al. (1989). Electrospray ionization for mass spectrometry of large biomolecules. *Science, 246*(4926), 64-71.

Findlay, R. H., & White, D. C. (1983). Polymeric beta-hydroxyalkanoates from environmental samples and Bacillus megaterium. *Applied and Environmental Microbiology, 45*(1), 71-78.

Fogel, G. B., Collins, C. R., et al. (1999). Prokaryotic Genome Size and SSU rDNA Copy Number: Estimation of Microbial Relative Abundance from a Mixed Population. *Microbial Ecology, 38*(2), 93-113.

Forney, L. J., Zhou, X., et al. (2004). Molecular microbial ecology: land of the one-eyed king. *Current Opinion in Microbiology, 7*(3), 210-220.

Frias, J. P., Sobral, P., et al. (2010). Organic pollutants in microplastics from two beaches of the Portuguese coast. *Mar Pollut Bull, 60*(11), 1988-1992.

Frigon, D., Muyzer, G., et al. (2006). rRNA and poly-beta-hydroxybutyrate dynamics in bioreactors subjected to feast and famine cycles. *Appl Environ Microbiol, 72*(4), 2322-2330.

Fukui, T., Shiomi, N., et al. (1998). Expression and Characterization of (R)-Specific Enoyl Coenzyme A Hydratase Involved in Polyhydroxyalkanoate Biosynthesis by Aeromonas caviae. *Journal of Bacteriology, 180*(3), 667-673.

Galan, B., Dinjaski, N., et al. (2011). Nucleoid-associated PhaF phasin drives intracellular location and segregation of polyhydroxyalkanoate granules in Pseudomonas putida KT2442. *Mol Microbiol, 79*(2), 402-418.

Gao, D., Maehara, A., et al. (2001). *Identification of the intracellular polyhydroxyalkanoate depolymerase gene of Paracoccus denitrificans and some properties of the gene product* (Vol. 196).

Garlotta, D. (2001). A literature review of poly (lactic acid). *Journal of Polymers and the Environment, 9*(2), 63-84.

Gasser, I., Mueller, H., et al. (2009). Ecology and characterization of polyhydroxyalkanoate-producing microorganisms on and in plants. *Fems Microbiology Ecology, 70*(1), 142-150.

Gerngross, T. U., & Slater, S. C. (2000). How green are green plastics? *Scientific American, 283*(2), 37-41.

Gerngross, T. U., Snell, K. D., et al. (1994). Overexpression and purification of the soluble polyhydroxyalkanoate synthase from Alcaligenes eutrophus: evidence for a required posttranslational modification for catalytic activity. *Biochemistry, 33*(31), 9311-9320.

Gilbert, J. A., Meyer, F., et al. (2010). The Earth Microbiome Project: Meeting report of the "1 EMP meeting on sample selection and acquisition" at Argonne National Laboratory October 6 2010. *Stand Genomic Sci, 3*(3), 249-253.

Gogolewski, S., Jovanovic, M., et al. (1993). The effect of melt-processing on the degradation of selected polyhydroxyacids: polylactides, polyhydroxybutyrate, and polyhydroxybutyrate-co-valerates. *Polymer Degradation and Stability, 40*(3), 313-322.

Goltsman, D. S. A., Denef, V. J., et al. (2009). Community genomic and proteomic analyses of chemoautotrophic iron-oxidizing “Leptospirillum rubarum”(Group II) and “Leptospirillum ferrodiazotrophum”(Group III) bacteria in acid mine drainage biofilms. *Applied and environmental microbiology, 75*(13), 4599-4615.

Gottschalk, G. (1986). *Bacterial Metabolism* (Vol. Second Edition): Springer New York.

Grage, K., Jahns, A. C., et al. (2009). Bacterial Polyhydroxyalkanoate Granules: Biogenesis, Structure, and Potential Use as Nano-/Micro-Beads in Biotechnological and Biomedical Applications. *Biomacromolecules, 10*(4), 660-669.

Gregory, M. R. (2009). Environmental implications of plastic debris in marine settings—entanglement, ingestion, smothering, hangers-on, hitch-hiking and alien invasions. *Philosophical Transactions of the Royal Society B: Biological Sciences, 364*(1526), 2013-2025.

Griebel, R., Smith, Z., et al. (1968). Metabolism of poly-beta-hydroxybutyrate. I. Purification, composition, and properties of native poly-beta-hydroxybutyrate granules from Bacillus megaterium. *Biochemistry, 7*(10), 3676-3681.

Guho, N. M. (2010). *Polyhydroxyalkanoate production coupled with waste treatment using a three-stage sequencing batch reactor system fed dairy manure.* Available from http://worldcat.org /z-wcorg/ database.

Gumel, A. M., Annuar, M. S. M., et al. (2013). Recent Advances in the Production, Recovery and Applications of Polyhydroxyalkanoates. *Journal of Polymers and the Environment, 21*(2), 580-605.

Guo, F., & Zhang, T. (2012). Profiling bulking and foaming bacteria in activated sludge by high throughput sequencing. *Water Research, 46*(8), 2772-2782.

Gurieff, N., & Lant, P. (2007). Comparative life cycle assessment and financial analysis of mixed culture polyhydroxyalkanoate production. *Bioresource technology, 98*(17), 3393-3403.

Gurieff, N. B. (2007). *Production of Biodegradable Polyhydroxyalkanoate Polymers Using Advanced Biological Wastewater Treatment Process Technology.* The University of Queensland.

Guzmán, D., Kirsebom, H., et al. (2011). Preparation of hydrophilic poly (3-hydroxybutyrate) macroporous scaffolds through enzyme-mediated modifications. *Journal of Bioactive and Compatible Polymers, 26*(5), 452-463.

Hahn, S. K., Chang, Y. K., et al. (1994). Optmiation of microbial poly(3-hydroxybutyrate) recovery using dispersions of sodium-hypochlorite solution and chloroform. *Biotechnology and Bioengineering, 44*(2), 256-261.

Han, M.-J., Yoon, S. S., et al. (2001). Proteome Analysis of Metabolically EngineeredEscherichia coli Producing Poly(3-Hydroxybutyrate). *Journal of Bacteriology, 183*(1), 301-308.

Handelsman, J. (2004). Metagenomics: application of genomics to uncultured microorganisms. *Microbiology and molecular biology reviews, 68*(4), 669-685.

Handelsman, J., Rondon, M. R., et al. (1998). Molecular biological access to the chemistry of unknown soil microbes: a new frontier for natural products. *Chemistry & biology, 5*(10), R245-R249.

Handrick, R., Reinhardt, S., et al. (2000). Mobilization of poly(3-hydroxybutyrate) in Ralstonia eutropha. *J Bacteriol, 182*(20), 5916-5918.

Handrick, R., Reinhardt, S., et al. (2004). Unraveling the function of the Rhodospirillum rubrum activator of polyhydroxybutyrate (PHB) degradation: the activator is a PHB-granule-bound protein (phasin). *J Bacteriol, 186*(8), 2466-2475.

Hanreich, A., Heyer, R., et al. (2012). Metaproteome analysis to determine the metabolically active part of a thermophilic microbial community producing biogas from agricultural biomass. *Canadian Journal of Microbiology, 58*(7), 917-922.

Hanreich, A., Schimpf, U., et al. (2013). Metagenome and metaproteome analyses of microbial communities in mesophilic biogas-producing anaerobic batch fermentations indicate concerted plant carbohydrate degradation. *Systematic and Applied Microbiology, 36*(5), 330-338.

Haywood, G., Anderson, A., et al. (1988). Characterization of two 3-ketothiolases possessing differing substrate specificities in the polyhydroxyalkanoate synthesizing organism Alcaligenes eutrophus. *FEMS microbiology letters, 52*(1-2), 91-96.

Haywood, G. W., Anderson, A. J., et al. (1989). A survey of the accumulation of novel polyhydroxyalkanoates by bacteria *Biotechnology Letters, 11*(7), 471-476.

Haywood, G. W., Anderson, A. J., et al. (1990). Accumulation of a Polyhydroxyalkanoate Containing Primarily 3-Hydroxydecanoate from Simple Carbohydrate Substrates by Pseudomonas sp. Strain NCIMB 40135. *Applied and Environmental Microbiology, 56*(11), 3354-3359.

Hein, S., Tran, H., et al. (1998). Synechocystis sp. PCC6803 possesses a two-component polyhydroxyalkanoic acid synthase similar to that of anoxygenic purple sulfur bacteria. *Archives of microbiology, 170*(3), 162-170.

Henderson, R. A., & Jones, C. W. (1997). Poly-3-hydroxybutyrate production by washed cells of Alcaligenes eutrophus; purification, characterisation and potential regulatory role of citrate synthase. *Arch Microbiol, 168*(6), 486-492.

Henzel, W. J., Billeci, T. M., et al. (1993). Identifying proteins from two-dimensional gels by molecular mass searching of peptide fragments in protein sequence databases. *Proceedings of the National Academy of Sciences of the United States of America, 90*(11), 5011-5015.

Hettich, R. L., Pan, C. L., et al. (2013). Metaproteomics: Harnessing the Power of High Performance Mass Spectrometry to Identify the Suite of Proteins That Control Metabolic Activities in Microbial Communities. *Analytical Chemistry, 85*(9), 4203-4214.

Hettich, R. L., Sharma, R., et al. (2012). Microbial metaproteomics: identifying the repertoire of proteins that microorganisms use to compete and cooperate in complex environmental communities. *Current Opinion in Microbiology, 15*(3), 373-380.

Ho, C. S., Lam, C. W. K., et al. (2003). Electrospray Ionisation Mass Spectrometry: Principles and Clinical Applications. *The Clinical Biochemist Reviews, 24*(1), 3-12.

Hoffmann, N., Amara, A. A., et al. (2002). Biochemical Characterization of the Pseudomonas putida 3-Hydroxyacyl ACP:CoA Transacylase, Which Diverts Intermediates of Fatty Acid de Novo Biosynthesis. *Journal of Biological Chemistry, 277*(45), 42926-42936.

Holbery, J., & Houston, D. (2006). Natural-fiber-reinforced polymer composites in automotive applications. *Jom, 58*(11), 80-86.

Holmes, P. (1985). Applications of PHB-a microbially produced biodegradable thermoplastic. *Physics in technology, 16*(1), 32.

Holmes, P. (1988). Biologically produced (R)-3-hydroxy-alkanoate polymers and copolymers *Developments in crystalline polymers* (pp. 1-65): Springer.

Horowitz, D. M., & Sanders, J. K. M. (1994). Amorphous, biomimetic granules of polyhydroxybutyrate: preparation, characterization, and biological implications. *Journal of the American Chemical Society, 116*(7), 2695-2702.

Hristov, A., Hazen, W., et al. (2006). Efficiency of use of imported nitrogen, phosphorus, and potassium and potential for reducing phosphorus imports on Idaho dairy farms. *Journal of dairy science, 89*(9), 3702-3712.

Huisman, G. W., Wonink, E., et al. (1991). Metabolism of poly(3-hydroxyalkanoates) (PHAs) by Pseudomonas oleovorans. Identification and sequences of genes and function of the encoded proteins in the synthesis and degradation of PHA. *J Biol Chem, 266*(4), 2191-2198.

Ince, O., Basak, B., et al. (2012). Effect of nitrogen deficiency during SBR operation on PHA storage and microbial diversity. *Environmental Technology, 33*(16), 1827-1837.

Jacquel, N., Lo, C.-W., et al. (2008). Isolation and purification of bacterial poly (3-hydroxyalkanoates). *Biochemical Engineering Journal, 39*(1), 15-27.

Jehmlich, N., Kleinsteuber, S., et al. (2010). Phylogenetic and proteomic analysis of an anaerobic toluene-degrading community. *Journal of Applied Microbiology, 109*(6), 1937-1945.

Jendrossek, D. (1998). Microbial degradation of polyesters: a review on extracellular poly(hydroxyalkanoic acid) depolymerases. *Polymer Degradation and Stability, 59*(1–3), 317-325.

Jendrossek, D. (2009). Polyhydroxyalkanoate Granules Are Complex Subcellular Organelles (Carbonosomes). *Journal of Bacteriology, 191*(10), 3195-3202.

Jendrossek, D., & Handrick, R. (2002). Microbial degradation of Polyhydroxyalkanoates*. *Annual Review of Microbiology, 56*(1), 403-432.

Jendrossek, D., Knoke, I., et al. (1993). Degradation of poly(3-hydroxybutyrate), PHB, by bacteria and purification of a novel PHB depolymerase fromComamonas sp. *Journal of environmental polymer degradation, 1*(1), 53-63.

Jendrossek, D., Selchow, O., et al. (2007). Poly(3-Hydroxybutyrate) Granules at the Early Stages of Formation Are Localized Close to the Cytoplasmic Membrane in Caryophanon latum. *Applied and Environmental Microbiology, 73*(2), 586-593.

Jeon, J. M., Brigham, C. J., et al. (2014). Biosynthesis of poly(3-hydroxybutyrate-co-3-hydroxyhexanoate) (P(HB-co-HHx)) from butyrate using engineered Ralstonia eutropha. *Appl Microbiol Biotechnol, 98*(12), 5461-5469.

Jia, Q., Xiong, H., et al. (2014). Production of polyhydroxyalkanoates (PHA) by bacterial consortium from excess sludge fermentation liquid at laboratory and pilot scales. *Bioresource Technology, 171*, 159-167.

Jiang, Y., Hebly, M., et al. (2011a). Metabolic modeling of mixed substrate uptake for polyhydroxyalkanoate (PHA) production. *Water Research, 45*(3), 1309-1321.

Jiang, Y., Marang, L., et al. (2011b). Effect of temperature and cycle length on microbial competition in PHB-producing sequencing batch reactor. *Isme Journal, 5*(5), 896-907.

Jiang, Y., Marang, L., et al. (2011c). Polyhydroxybutyrate Production From Lactate Using a Mixed Microbial Culture. *Biotechnology and Bioengineering, 108*(9), 2022-2035.

Jiang, Y., Marang, L., et al. (2012). Waste to resource: Converting paper mill wastewater to bioplastic. *Water Research, 46*(17), 5517-5530.

Jiang, Y., Sorokin, D. Y., et al. (2011d). Plasticicumulans acidivorans gen. nov., sp. nov., a polyhydroxyalkanoate-accumulating gammaproteobacterium from a sequencing-batch bioreactor. *Int J Syst Evol Microbiol, 61*(Pt 9), 2314-2319.

Johnson, K. (2010). *PHA production in aerobic mixed microbial cultures*: TU Delft, Delft University of Technology.

Johnson, K., Jiang, Y., et al. (2009a). Enrichment of a Mixed Bacterial Culture with a High Polyhydroxyalkanoate Storage Capacity. *Biomacromolecules, 10*(4), 670-676.

Johnson, K., Kleerebezem, R., et al. (2009b). Model-based data evaluation of polyhydroxybutyrate producing mixed microbial cultures in aerobic sequencing batch and fed-batch reactors. *Biotechnol Bioeng, 104*(1), 50-67.

Johnson, K., Kleerebezem, R., et al. (2010a). Influence of the C/N ratio on the performance of polyhydroxybutyrate (PHB) producing sequencing batch reactors at short SRTs. *Water Research, 44*(7), 2141-2152.

Johnson, K., van Geest, J., et al. (2010b). Short- and long-term temperature effects on aerobic polyhydroxybutyrate producing mixed cultures. *Water Research, 44*(6), 1689-1700.

Jurasek, L., & Marchessault, R. (2002). The role of phasins in the morphogenesis of poly (3-hydroxybutyrate) granules. *Biomacromolecules, 3*(2), 256-261.

Jurasek, L., & Marchessault, R. H. (2004). Polyhydroxyalkanoate (PHA) granule formation in Ralstonia eutropha cells: a computer simulation. *Applied Microbiology and Biotechnology, 64*(5), 611-617.

Kadouri, D., Jurkevitch, E., et al. (2005). Ecological and agricultural significance of bacterial polyhydroxyalkanoates. *Critical Reviews in Microbiology, 31*(2), 55-67.

Kasirajan, S., & Ngouajio, M. (2012). Polyethylene and biodegradable mulches for agricultural applications: a review. *Agronomy for Sustainable Development, 32*(2), 501-529.

Keshavarz, T., & Roy, I. (2010). Polyhydroxyalkanoates: bioplastics with a green agenda. *Current Opinion in Microbiology, 13*(3), 321-326.

Kessler, B., & Witholt, B. (2001). Factors involved in the regulatory network of polyhydroxyalkanoate metabolism. *Journal of Biotechnology, 86*(2), 97-104.

Khanna, S., & Srivastava, A. K. (2005). Recent advances in microbial polyhydroxyalkanoates. *Process Biochemistry, 40*(2), 607-619.

Kim, B. S. (2000). Production of poly(3-hydroxybutyrate) from inexpensive substrates. *Enzyme Microb Technol, 27*(10), 774-777.

Kim, D., & Rhee, Y. (2003). Biodegradation of microbial and synthetic polyesters by fungi. *Applied microbiology and biotechnology, 61*(4), 300-308.

Kleerebezem, R., & van Loosdrecht, M. C. M. (2007). Mixed culture biotechnology for bioenergy production. *Current Opinion in Biotechnology, 18*(3), 207-212.

Kleiner, M., Wentrup, C., et al. (2012). Metaproteomics of a gutless marine worm and its symbiotic microbial community reveal unusual pathways for carbon and energy use. *Proceedings of the National Academy of Sciences of the United States of America, 109*(19), E1173-E1182.

Klinke, S., de Roo, G., et al. (2000). Role of phaD in Accumulation of Medium-Chain-Length Poly(3-Hydroxyalkanoates) in Pseudomonas oleovorans. *Applied and Environmental Microbiology, 66*(9), 3705-3710.

Knoll, M., Hamm, T. M., et al. (2009). The PHA Depolymerase Engineering Database: A systematic analysis tool for the diverse family of polyhydroxyalkanoate (PHA) depolymerases. *BMC Bioinformatics, 10*, 89.

Kohlmann, Y., Pohlmann, A., et al. (2011). Analyses of soluble and membrane proteomes of Ralstonia eutropha H16 reveal major changes in the protein complement in adaptation to lithoautotrophy. *Journal of proteome research, 10*(6), 2767-2776.

Koller, M., Niebelschuetz, H., et al. (2013). Strategies for recovery and purification of poly (R)-3-hydroxyalkanoates (PHA) biopolyesters from surrounding biomass. *Engineering in Life Sciences, 13*(6), 549-562.

Krishna, C., & Van Loosdrecht, M. C. M. (1999). Effect of temperature on storage polymers and settleability of activated sludge. *Water Research, 33*(10), 2374-2382.

Kuhn, R., Benndorf, D., et al. (2011). Metaproteome analysis of sewage sludge from membrane bioreactors. *Proteomics, 11*(13), 2738-2744.

Lagaron, J. M., & Lopez-Rubio, A. (2011). Nanotechnology for bioplastics: opportunities, challenges and strategies. *Trends in Food Science & Technology, 22*(11), 611-617.

Laureni, M., Weissbrodt, D. G., et al. (2015). Activity and growth of anammox biomass on aerobically pre-treated municipal wastewater. *Water Research, 80*, 325-336.

Lee, I. Y., Kim, M. K., et al. (1995). *Regulation of poly-β-hydroxybutyrate biosynthesis by nicotinamide nucleotide in Alcaligenes eutrophus* (Vol. 131).

Lee, S.-E., Li, Q. X., et al. (2009). Diverse protein regulations on PHA formation in Ralstonia eutropha on short chain organic acids. *International journal of biological sciences, 5*(3), 215.

Lee, S. Y. (1996). Bacterial polyhydroxyalkanoates. *Biotechnology and bioengineering, 49*(1), 1-14.

Lee, S. Y. (1997). E. coli moves into the plastic age. *Nat Biotech, 15*(1), 17-18.

Lee, W. S., Chua, A. S. M., et al. (2014). Influence of temperature on the bioconversion of palm oil mill effluent into volatile fatty acids as precursor to the production of polyhydroxyalkanoates. *Journal of Chemical Technology and Biotechnology, 89*(7), 1038-1043.

Lemoigne, M. (1926). Produits de dehydration et de polymerisation de l'acide ß-oxobutyrique. *Bull Soc Chim Biol 8*, 770-782.

Lemos, P. C., Levantesi, C., et al. (2008). Microbial characterisation of polyhydroxyalkanoates storing populations selected under different operating conditions using a cell-sorting RT-PCR approach. *Applied Microbiology and Biotechnology, 78*(2), 351-360.

Lemos, P. C., Serafim, L. S., et al. (2006). Synthesis of polyhydroxyalkanoates from different short-chain fatty acids by mixed cultures submitted to aerobic dynamic feeding. *Journal of Biotechnology, 122*(2), 226-238.

Lenz, R. W., & Marchessault, R. H. (2005). Bacterial polyesters: biosynthesis, biodegradable plastics and biotechnology. *Biomacromolecules, 6*(1), 1-8.

Leytem, A. B., Dungan, R. S., et al. (2011). Emissions of Ammonia, Methane, Carbon Dioxide, and Nitrous Oxide from Dairy Cattle Housing and Manure Management Systems. *Journal of Environmental Quality, 40*(5), 1383-1394.

Li, S. Y., Dong, C. L., et al. (2011). Microbial production of polyhydroxyalkanoate block copolymer by recombinant Pseudomonas putida. *Applied microbiology and biotechnology, 90*(2), 659-669.

Li, Y., Wang, J., et al. (2015). Enhancing the quantity and quality of short-chain fatty acids production from waste activated sludge using CaO2 as an additive. *Water Research, 83*, 84-93.

Liang, S., Gliniewicz, K., et al. (2015). Comparative analysis of microbial community of novel lactic acid fermentation inoculated with different undefined mixed cultures. *Bioresource Technology, 179*, 268-274.

Liebergesell, M., & Steinbuchel, A. (1992). Cloning and nucleotide sequences of genes relevant for biosynthesis of poly(3-hydroxybutyric acid) in Chromatium vinosum strain D. *Eur J Biochem, 209*(1), 135-150.

Liebrand, C., & Ling, K. C. (2009). *Cooperative approaches for implementation of dairy manure digesters*. Washington, D.C.

Liu, H.-Y., Hall, P. V., et al. (2008). Production of polyhydroxyalkanoate during treatment of tomato cannery wastewater. *Water Environment Research, 80*(4), 367-372.

Liu, W., & Chen, G. Q. (2007). Production and characterization of medium-chain-length polyhydroxyalkanoate with high 3-hydroxytetradecanoate monomer content by fadB and fadA knockout mutant of Pseudomonas putida KT2442. *Appl Microbiol Biotechnol, 76*(5), 1153-1159.

Lopes Dias, J. M., Lemos, P., et al. (2007). Development and implementation of a non-parametric/metabolic model in the process optimisation of PHA production by mixed microbial cultures. *17th European Symposium on Computer Aided Process Engineering, 24*, 995-1000.

López-Cortés, A., Lanz-Landázuri, A., et al. (2008). Screening and isolation of PHB-producing bacteria in a polluted marine microbial mat. *Microbial ecology, 56*(1), 112-120.

Lü, F., Bize, A., et al. (2014). Metaproteomics of cellulose methanisation under thermophilic conditions reveals a surprisingly high proteolytic activity. *The ISME journal, 8*(1), 88-102.

Luengo, J. M., García, B., et al. (2003). Bioplastics from microorganisms. *Current Opinion in Microbiology, 6*(3), 251-260.

Luo, C., Lü, F., et al. (2015). Application of eco-compatible biochar in anaerobic digestion to relieve acid stress and promote the selective colonization of functional microbes. *Water Research, 68*, 710-718.

Luzier, W. D. (1992). Materials derived from biomass/biodegradable materials. *Proceedings of the National Academy of Sciences, 89*(3), 839-842.

Madbouly, S. A., Schrader, J. A., et al. (2014). Biodegradation behavior of bacterial-based polyhydroxyalkanoate (PHA) and DDGS composites. *Green Chemistry, 16*(4), 1911-1920.

Madigan, M. T., Martinko, J. M. (2006). *Brock Biology of Microorganisms* (Eleventh ed.). Upper Saddle River, NJ 07458:: Pearson Prentice Hall.

Madison, L. L., & Huisman, G. W. (1999). Metabolic engineering of poly(3-hydroxyalkanoates): from DNA to plastic. *Microbiol Mol Biol Rev, 63*(1), 21-53.

Maehara, A., Taguchi, S., et al. (2002). A repressor protein, PhaR, regulates polyhydroxyalkanoate (PHA) synthesis via its direct interaction with PHA. *J Bacteriol, 184*(14), 3992-4002.

Majone, M., Dircks, K., et al. (1999). Aerobic storage under dynamic conditions in activated sludge processes. The state of the art. *Water Science and Technology, 39*(1), 61-73.

Majone, M., Massanisso, P., et al. (1996). Influence of storage on kinetic selection to control aerobic filamentous bulking. *Water Science and Technology, 34*(5-6), 223-232.

Marang, L., Jiang, Y., et al. (2013). Butyrate as preferred substrate for polyhydroxybutyrate production. *Bioresource Technology, 142*, 232-239.

Mardis, E. R. (2008). The impact of next-generation sequencing technology on genetics. *Trends in genetics, 24*(3), 133-141.

Maron, P.-A., Ranjard, L., et al. (2007). Metaproteomics: a new approach for studying functional microbial ecology. *Microbial ecology, 53*(3), 486-493.

Matin, A., Veldhuis, C., et al. (1979). Selective advantage of a Spirillum sp. in a carbon-limited environment. Accumulation of poly-β-hydroxybutyric acid and its role in starvation. *Journal of general microbiology, 112*(2), 349-355.

Matsusaki, H., Manji, S., et al. (1998). Cloning and molecular analysis of the Poly(3-hydroxybutyrate) and Poly(3-hydroxybutyrate-co-3-hydroxyalkanoate) biosynthesis genes in Pseudomonas sp. strain 61-3. *J Bacteriol, 180*(24), 6459-6467.

McMahon, K. D., Martin, H. G., et al. (2007). Integrating ecology into biotechnology. *Current Opinion in Biotechnology, 18*(3), 287-292.

Mekonnen, T., Mussone, P., et al. (2013). Progress in bio-based plastics and plasticizing modifications. *Journal of Materials Chemistry A, 1*(43), 13379-13398.

Meng, D.-C., Shen, R., et al. (2014). Engineering the diversity of polyesters. *Current opinion in biotechnology, 29*, 24-33.

Mergaert, J., Glorieux, G., et al. (1996). Biodegradation of Poly (3-hYdroxYalkanoates in Anaerobic Sludge and Characterization of a Poly (3-hYdroxYalkanoates Degrading Anaerobic Bacterium. *Systematic and applied microbiology, 19*(3), 407-413.

Mergaert, J., Webb, A., et al. (1993). Microbial degradation of poly (3-hydroxybutyrate) and poly (3-hydroxybutyrate-co-3-hydroxyvalerate) in soils. *Applied and Environmental Microbiology, 59*(10), 3233-3238.

Mergaert, J., Wouters, A., et al. (1995). In situ biodegradation of poly (3-hydroxybutyrate) and poly (3-hydroxybutyrate-co-3-hydroxyvalerate) in natural waters. *Canadian journal of microbiology, 41*(13), 154-159.

Metzker, M. L. (2010). Sequencing technologies—the next generation. *Nature reviews genetics, 11*(1), 31-46.

Mezzina, M. P., Wetzler, D. E., et al. (2015). A phasin with extra talents: a polyhydroxyalkanoate granule-associated protein has chaperone activity. *Environmental microbiology, 17*(5), 1765-1776.

Misra, S. K., Valappil, S. P., et al. (2006). Polyhydroxyalkanoate (PHA)/inorganic phase composites for tissue engineering applications. *Biomacromolecules, 7*(8), 2249-2258.

Mizuno, K., Ohta, A., et al. (2010). Isolation of polyhydroxyalkanoate-producing bacteria from a polluted soil and characterization of the isolated strain Bacillus cereus YB-4. *Polymer Degradation and Stability, 95*(8), 1335-1339.

Moita, R., & Lemos, P. C. (2012). Biopolymers production from mixed cultures and pyrolysis by-products. *Journal of Biotechnology, 157*(4), 578-583.

Moore, C. J., Moore, S. L., et al. (2001). A Comparison of Plastic and Plankton in the North Pacific Central Gyre. *Marine Pollution Bulletin, 42*(12), 1297-1300.

Moralejo-Garate, H., Kleerebezem, R., et al. (2013a). Impact of oxygen limitation on glycerol-based biopolymer production by bacterial enrichments. *Water Research, 47*(3), 1209-1217.

Moralejo-Garate, H., Palmeiro-Sanchez, T., et al. (2013b). Influence of the Cycle Length on the Production of PHA and Polyglucose From Glycerol by Bacterial Enrichments in Sequencing Batch Reactors. *Biotechnology and Bioengineering, 110*(12), 3148-3155.

Morgan-Sagastume, F., Hjort, M., et al. (2015). Integrated production of polyhydroxyalkanoates (PHAs) with municipal wastewater and sludge treatment at pilot scale. *Bioresour Technol, 181*, 78-89.

Morgan-Sagastume, F., Karlsson, A., et al. (2010). Production of polyhydroxyalkanoates in open, mixed cultures from a waste sludge stream containing high levels of soluble organics, nitrogen and phosphorus. *Water Research, 44*(18), 5196-5211.

Morozova, O., & Marra, M. A. (2008). Applications of next-generation sequencing technologies in functional genomics. *Genomics, 92*(5), 255-264.

Mudliar, S., Vaidya, A., et al. (2008). Techno-economic evaluation of PHB production from activated sludge. *Clean Technologies and Environmental Policy, 10*(3), 255-262.

Mueller, R.-J. (2006). Biological degradation of synthetic polyesters - Enzymes as potential catalysts for polyester recycling. *Process Biochemistry, 41*(10), 2124-2128.

Mueller, R. S., Denef, V. J., et al. (2010). Ecological distribution and population physiology defined by proteomics in a natural microbial community. *Molecular systems biology, 6*(1), 374.

Müller, S., Bley, T., et al. (1999). Adaptive responses of Ralstonia eutropha to feast and famine conditions analysed by flow cytometry. *Journal of Biotechnology, 75*(2–3), 81-97.

Mumtaz, T., Yahaya, N. A., et al. (2010). Turning waste to wealth-biodegradable plastics polyhydroxyalkanoates from palm oil mill effluent - a Malaysian perspective. *Journal of Cleaner Production, 18*(14), 1393-1402.

Nakayama, K., Saito, T., et al. (1985). Purification and properties of extracellular poly(3-hydroxybutyrate) depolymerases from Pseudomonas lemoignei. *Biochimica et Biophysica Acta (BBA) - Protein Structure and Molecular Enzymology, 827*(1), 63-72.

Nelson, K., Weinel, C., et al. (2002). Complete genome sequence and comparative analysis of the metabolically versatile Pseudomonas putida KT2440. *Environmental microbiology, 4*(12), 799-808.

Neumeier, S. (1994). *Abbau thermoplastischer Biopolymere auf Poly-b-Hydroxyalkanoat-Basis durch terrestrische und marine Pilze.* (Ph.D.), Universitt Regensburg, Regensburg.

Nikodinovic-Runic, J., Guzik, M., et al. (2013). Carbon-Rich Wastes as Feedstocks for Biodegradable Polymer (Polyhydroxyalkanoate) Production Using Bacteria. In S. Sariaslani & G. M. Gadd (Eds.), *Advances in Applied Microbiology, Vol 84* (Vol. 84, pp. 139-200).

Nuti, M. P., De Bertoldi, M., et al. (1972). Influence of phenylacetic acid on poly- -hydroxybutyrate (PHB) polymerization and cell elongation in Azotobacter chroococcum Beij. *Can J Microbiol, 18*(8), 1257-1261.

O'Farrell, P. H. (1975). High resolution two-dimensional electrophoresis of proteins. *Journal of Biological Chemistry, 250*(10), 4007-4021.

Oehmen, A., Pinto, F. V., et al. (2014). The impact of pH control on the volumetric productivity of mixed culture PHA production from fermented molasses. *Engineering in Life Sciences, 14*(2), 143-152.

Östling, J., Holmquist, L., et al. (1993). Starvation and recovery of Vibrio *Starvation in bacteria* (pp. 103-127): Springer.

Ozdemir, S., Akman, D., et al. (2014). Effect of Cycle Time on Polyhydroxybutyrate (PHB) Production in Aerobic Mixed Cultures. *Applied Biochemistry and Biotechnology, 172*(5), 2390-2399.

P.J. Hocking, R. H. M. (1994). *Biopolyesters*: Blackie Academic & Professional

Page, W. J., Manchak, J., et al. (1992). Formation of poly (hydroxybutyrate-co-hydroxyvalerate) by Azotobacter vinelandii UWD. *Applied and environmental microbiology, 58*(9), 2866-2873.

Pardelha, F., Albuquerque, M. G. E., et al. (2013). Segregated flux balance analysis constrained by population structure/function data: The case of PHA production by mixed microbial cultures. *Biotechnology and Bioengineering, 110*(8), 2267-2276.

Pardelha, F., Albuquerque, M. G. E., et al. (2012). Flux balance analysis of mixed microbial cultures: Application to the production of polyhydroxyalkanoates from complex mixtures of volatile fatty acids. *Journal of Biotechnology, 162*(2-3), 336-345.

Pardelha, F., Albuquerque, M. G. E., et al. (2014). Dynamic metabolic modelling of volatile fatty acids conversion to polyhydroxyalkanoates by a mixed microbial culture. *New Biotechnology, 31*(4), 335-344.

Pederson, E. N., McChalicher, C. W., et al. (2006). Bacterial synthesis of PHA block copolymers. *Biomacromolecules, 7*(6), 1904-1911.

Peoples, O. P., & Sinskey, A. J. (1989). Poly-beta-hydroxybutyrate biosynthesis in Alcaligenes eutrophus H16. Characterization of the genes encoding beta-ketothiolase and acetoacetyl-CoA reductase. *Journal of Biological Chemistry, 264*(26), 15293-15297.

Philip, S., Keshavarz, T., et al. (2007). Polyhydroxyalkanoates: biodegradable polymers with a range of applications. *Journal of Chemical Technology and Biotechnology, 82*(3), 233-247.

Pieper-Furst, U., Madkour, M. H., et al. (1995). Identification of the region of a 14-kilodalton protein of Rhodococcus ruber that is responsible for the binding of this phasin to polyhydroxyalkanoic acid granules. *J Bacteriol, 177*(9), 2513-2523.

Pilla, S. (2011). *Handbook of bioplastics and biocomposites engineering applications* (Vol. 81): John Wiley & Sons.

Pisco, A. R., Bengtsson, S., et al. (2009). Community Structure Evolution and Enrichment of Glycogen-Accumulating Organisms Producing Polyhydroxyalkanoates from Fermented Molasses. *Applied and Environmental Microbiology, 75*(14), 4676-4686.

Pitt, J. J. (2009). Principles and Applications of Liquid Chromatography-Mass Spectrometry in Clinical Biochemistry. *The Clinical Biochemist Reviews, 30*(1), 19-34.

Pollet, E., & Avérous, L. (2011). Production, Chemistry and Properties of Polyhydroxyalkanoates *Biopolymers – New Materials for Sustainable Films and Coatings* (pp. 65-86): John Wiley & Sons, Ltd.

Potter, M., Madkour, M. H., et al. (2002). Regulation of phasin expression and polyhydroxyalkanoate (PHA) granule formation in Ralstonia eutropha H16. *Microbiology, 148*(Pt 8), 2413-2426.

Potter, M., Muller, H., et al. (2005). Influence of homologous phasins (PhaP) on PHA accumulation and regulation of their expression by the transcriptional repressor PhaR in Ralstonia eutropha H16. *Microbiology, 151*(Pt 3), 825-833.

Potter, M., & Steinbüchel, A. (2005). Poly(3-hydroxybutyrate) granule-associated proteins: Impacts on poly(3-hydroxybutyrate) synthesis and degradation. *Biomacromolecules, 6*(2), 552-560.

Pouton, C. W., & Akhtar, S. (1996). Biosynthetic polyhydroxyalkanoates and their potential in drug delivery. *Advanced Drug Delivery Reviews, 18*(2), 133-162.

Pratt, S., Werker, A., et al. (2012). Microaerophilic conditions support elevated mixed culture polyhydroxyalkanoate (PHA) yields, but result in decreased PHA production rates. *Water Science and Technology, 65*(2), 243-246.

Prest, E. I., El-Chakhtoura, J., et al. (2014). Combining flow cytometry and 16S rRNA gene pyrosequencing: A promising approach for drinking water monitoring and characterization. *Water Research, 63*, 179-189.

Prieto, M. A., Buhler, B., et al. (1999). PhaF, a polyhydroxyalkanoate-granule-associated protein of Pseudomonas oleovorans GPo1 involved in the regulatory expression system for pha genes. *J Bacteriol, 181*(3), 858-868.

Qi, Q., Steinbuchel, A., et al. (2000). In vitro synthesis of poly(3-hydroxydecanoate): purification and enzymatic characterization of type II polyhydroxyalkanoate synthases PhaC1 and PhaC2 from Pseudomonas aeruginosa. *Appl Microbiol Biotechnol, 54*(1), 37-43.

Queiros, D., Rossetti, S., et al. (2014). PHA production by mixed cultures: A way to valorize wastes from pulp industry. *Bioresource technology, 157*, 197-205.

Queiroz, A. U., & Collares-Queiroz, F. P. (2009). Innovation and industrial trends in bioplastics. *Journal of Macromolecular Science®, Part C: Polymer Reviews, 49*(2), 65-78.

Ram, R. J., VerBerkmoes, N. C., et al. (2005). Community proteomics of a natural microbial biofilm. *Science, 308*(5730), 1915-1920.

Ramsay, J., Berger, E., et al. (1990). Recovery of poly-3-hydroxyalkanoic acid granules by a surfactant-hypochlorite treatment. *Biotechnology Techniques, 4*(4), 221-226.

Reddy, C. S. K., Ghai, R., et al. (2003). Polyhydroxyalkanoates: an overview. *Bioresource Technology, 87*(2), 137-146.

Regueiro, L., Spirito, C. M., et al. Comparing the inhibitory thresholds of dairy manure co-digesters after prolonged acclimation periods: Part 2 – correlations between microbiomes and environment. *Water Research*.

Rehm, B. H. (2006). Genetics and biochemistry of polyhydroxyalkanoate granule self-assembly: The key role of polyester synthases. *Biotechnol Lett, 28*(4), 207-213.

Rehm, B. H. (2007). Biogenesis of microbial polyhydroxyalkanoate granules: a platform technology for the production of tailor-made bioparticles. *Curr Issues Mol Biol, 9*(1), 41-62.

Rehm, B. H., Kruger, N., et al. (1998). A new metabolic link between fatty acid de novo synthesis and polyhydroxyalkanoic acid synthesis. The PHAG gene from Pseudomonas putida KT2440 encodes a 3-hydroxyacyl-acyl carrier protein-coenzyme a transferase. *J Biol Chem, 273*(37), 24044-24051.

Rehm, B. H. A., Mitsky, T. A., et al. (2001). Role of Fatty Acid De Novo Biosynthesis in Polyhydroxyalkanoic Acid (PHA) and Rhamnolipid Synthesis by Pseudomonads: Establishment of the Transacylase (PhaG)-Mediated Pathway for PHA Biosynthesis inEscherichia coli. *Applied and Environmental Microbiology, 67*(7), 3102-3109.

Rehm, B. H. A., & Steinbüchel, A. (1999). Biochemical and genetic analysis of PHA synthases and other proteins required for PHA synthesis. *International Journal of Biological Macromolecules, 25*(1–3), 3-19.

Reinecke, F., & Steinbüchel, A. (2009). Ralstonia eutropha Strain H16 as Model Organism for PHA Metabolism and for Biotechnological Production of Technically Interesting Biopolymers. *Journal of Molecular Microbiology and Biotechnology, 16*(1-2), 91-108.

Reis, M., Albuquerque, M., et al. (2011). Mixed culture processes for polyhydroxyalkanoate production from agro-industrial surplus/wastes as feedstocks. *Comprehensive Biotechnology. Academic Press, Burlington*, 669-683.

Reis, M. A. M., Serafim, L. S., et al. (2003). Production of polyhydroxyalkanoates by mixed microbial cultures. *Bioprocess and Biosystems Engineering, 25*(6), 377-385.

Ren, Q., de Roo, G., et al. (2009). Simultaneous Accumulation and Degradation of Polyhydroxyalkanoates: Futile Cycle or Clever Regulation? *Biomacromolecules, 10*(4), 916-922.

Riesenfeld, C. S., Schloss, P. D., et al. (2004). Metagenomics: genomic analysis of microbial communities. *Annu. Rev. Genet., 38*, 525-552.

Rittmann, B. E. (2006). Microbial ecology to manage processes in environmental biotechnology. *TRENDS in Biotechnology, 24*(6), 261-266.

Rittmann, B. E., Hausner, M., et al. (2006). A vista for microbial ecology and environmental biotechnology. *Environmental science & technology, 40*(4), 1096-1103.

Roels, J. A. (1983). *Energetics and kinetics in biotechnology*. Amsterdam: Elsevier Biomedical Press.

Saegusa, H., Shiraki, M., et al. (2001). Cloning of an intracellular Poly[D(-)-3-Hydroxybutyrate] depolymerase gene from Ralstonia eutropha H16 and characterization of the gene product. *J Bacteriol, 183*(1), 94-100.

Saito, T., Takizawa, K., et al. (1995). Intracellular poly(3-hydroxybutyrate) depolymerase in Alcaligenes eutrophus. *Canadian Journal of Microbiology, 41*(13), 187-191.

Salehizadeh, H., & van Loosdrecht, M. C. M. (2004). Production of polyhydroxyalkanoates by mixed culture: recent trends and biotechnological importance. *Biotechnology Advances, 22*(3), 261-279.

Sang, B. I., Hori, K., et al. (2002). Fungal contribution to in situ biodegradation of poly(3-hydroxybutyrate-co-3-hydroxyvalerate) film in soil. *Appl Microbiol Biotechnol, 58*(2), 241-247.

Schembri, M. A., Bayly, R. C., et al. (1995). Phosphate concentration regulates transcription of the Acinetobacter polyhydroxyalkanoic acid biosynthetic genes. *J Bacteriol, 177*(15), 4501-4507.

Schmeisser, C., Steele, H., et al. (2007). Metagenomics, biotechnology with non-culturable microbes. *Applied microbiology and biotechnology, 75*(5), 955-962.

Schober, U., Thiel, C., et al. (2000). Poly(3-hydroxyvalerate) depolymerase of Pseudomonas lemoignei. *Appl Environ Microbiol, 66*(4), 1385-1392.

Schubert, P., Steinbüchel, A., et al. (1988). Cloning of the Alcaligenes eutrophus genes for synthesis of poly-beta-hydroxybutyric acid (PHB) and synthesis of PHB in Escherichia coli. *Journal of Bacteriology, 170*(12), 5837-5847.

Schuster, S. C. (2007). Next-generation sequencing transforms today's biology. *Nature, 200*(8), 16-18.

Serafim, L. S., Lemos, P. C., et al. (2008a). Strategies for PHA production by mixed cultures and renewable waste materials. *Applied Microbiology and Biotechnology, 81*(4), 615-628.

Serafim, L. S., Lemos, P. C., et al. (2004). Optimization of polyhydroxybutyrate production by mixed cultures submitted to aerobic dynamic feeding conditions. *Biotechnology and Bioengineering, 87*(2), 145-160.

Serafim, L. S., Lemos, P. C., et al. (2006). Microbial community analysis with a high PHA storage capacity. *Water Science and Technology, 54*(1), 183-188.

Serafim, L. S., Lemos, P. C., et al. (2008b). The influence of process parameters on the characteristics of polyhydroxyalkanoates produced by mixed cultures. *Macromolecular Bioscience, 8*(4), 355-366.

Sevastianov, V. I., Perova, N. V., et al. (2003). Production of purified polyhydroxyalkanoates (PHAs) for applications in contact with blood. *J Biomater Sci Polym Ed, 14*(10), 1029-1042.

Shah, A. A., Hasan, F., et al. (2008). Biological degradation of plastics: A comprehensive review. *Biotechnology Advances, 26*(3), 246-265.

Shahzad, K., Kettl, K.-H., et al. (2013). Comparison of ecological footprint for biobased PHA production from animal residues utilizing different energy resources. *Clean technologies and environmental policy, 15*(3), 525-536.

Shendure, J., & Ji, H. (2008). Next-generation DNA sequencing. *Nature biotechnology, 26*(10), 1135-1145.

Shishatskaya, E., Volova, T., et al. (2002). *In vivo toxicological evaluation of polyhydroxyalkanoates.* Paper presented at the Doklady Biological Sciences.

Siggins, A., Gunnigle, E., et al. (2012). Exploring mixed microbial community functioning: recent advances in metaproteomics. *FEMS Microbiol Ecol, 80*(2), 265-280.

Singh, J., Behal, A., et al. (2009). Metagenomics: Concept, methodology, ecological inference and recent advances. *Biotechnology Journal, 4*(4), 480-494.

Sivan, A. (2011). New perspectives in plastic biodegradation. *Current Opinion in Biotechnology, 22*(3), 422-426.

Slater, S. C., Voige, W. H., et al. (1988). Cloning and expression in Escherichia coli of the Alcaligenes eutrophus H16 poly-beta-hydroxybutyrate biosynthetic pathway. *Journal of Bacteriology, 170*(10), 4431-4436.

Smit, A. M., Strabala, T. J., et al. (2012). Proteomic phenotyping of Novosphingobium nitrogenifigens reveals a robust capacity for simultaneous nitrogen fixation, polyhydroxyalkanoate production, and resistance to reactive oxygen species. *Appl Environ Microbiol, 78*(14), 4802-4815.

Steinbüchel, A. (1991). *Polyhydroxyalkanoic acids*. Stockton, New York.

Steinbüchel, A. (2003). In vivo and in vitro metabolic engineering of polyhydroxyalkanoates biosynthesis pathways. In R. A. Gross & H. N. Cheng (Eds.), *Biocatalysis in Polymer Science* (Vol. 840, pp. 120-123).

Steinbüchel, A., Aerts, K., et al. (1995). Considerations on the structure and biochemistry of bacterial polyhydroxyalkanoic acid inclusions. *Can J Microbiol, 41 Suppl 1*, 94-105.

Steinbüchel, A., & Hein, S. (2001). Biochemical and molecular basis of microbial synthesis of polyhydroxyalkanoates in microorganisms. *Advances in biochemical engineering/biotechnology, 71*, 81-123.

Steinbüchel, A., Hustede, E., et al. (1992). *Molecular basis for biosynthesis and accumulation of polyhydroxyalkanoic acids in bacteria* (Vol. 9).

Steinbüchel, A., & Lütke-Eversloh, T. (2003). Metabolic engineering and pathway construction for biotechnological production of relevant polyhydroxyalkanoates in microorganisms. *Biochemical Engineering Journal, 16*(2), 81-96.

Steinbüchel, A., & Schlegel, H. G. (1991). Physiology and molecular genetics of poly(β-hydroxyalkanoic acid) synthesis in Alcaligenes eutrophus. *Molecular Microbiology, 5*(3), 535-542.

Steinbüchel, A., & Valentin, H. E. (1995). *Diversity of bacterial polyhydroxyalkanoic acids* (Vol. 128).

Stuart, E. S., Tehrani, A., et al. (1998). Protein organization on the PHA inclusion cytoplasmic boundary. *J Biotechnol, 64*(2-3), 137-144.

Stubbe, J., & Tian, J. (2003). Polyhydroxyalkanoate (PHA) homeostasis: the role of the PHA synthase. *Natural Product Reports, 20*(5), 445-457.

Sudesh, K., Abe, H., et al. (2000). Synthesis, structure and properties of polyhydroxyalkanoates: biological polyesters. *Progress in Polymer Science, 25*(10), 1503-1555.

Sudesh, K., Bhubalan, K., et al. (2011). Synthesis of polyhydroxyalkanoate from palm oil and some new applications. *Applied microbiology and biotechnology, 89*(5), 1373-1386.

Sun, J., Peng, X., et al. (2000). The ntrB and ntrC genes are involved in the regulation of poly-3-hydroxybutyrate biosynthesis by ammonia in Azospirillum brasilense Sp7. *Appl Environ Microbiol, 66*(1), 113-117.

Tabone, M. D., Cregg, J. J., et al. (2010). Sustainability metrics: life cycle assessment and green design in polymers. *Environmental science & technology, 44*(21), 8264-8269.

Tal, S., & Okon, Y. (1985). Production of the reserve material poly-β-hydroxybutyrate and its function in Azospirillum brasilense Cd. *Canadian journal of microbiology, 31*(7), 608-613.

Tal, S., Smirnoff, P., et al. (1990). The regulation of poly-β-hydroxybutyrate metabolism in Azospirillum brasilense during balanced growth and starvation. *Journal of General Microbiology, 136*(7), 1191-1196.

Tamis, J., Marang, L., et al. (2014). Modeling PHA-producing microbial enrichment cultures-towards a generalized model with predictive power. *New Biotechnology, 31*(4), 324-334.

Tanadchangsaeng, N., Kitagawa, A., et al. (2009). Identification, biosynthesis, and characterization of polyhydroxyalkanoate copolymer consisting of 3-hydroxybutyrate and 3-hydroxy-4-methylvalerate. *Biomacromolecules, 10*(10), 2866-2874.

Teuten, E. L., Saquing, J. M., et al. (2009). Transport and release of chemicals from plastics to the environment and to wildlife. *Philosophical Transactions of the Royal Society B: Biological Sciences, 364*(1526), 2027-2045.

Thellen, C., Coyne, M., et al. (2008). A processing, characterization and marine biodegradation study of melt-extruded polyhydroxyalkanoate (PHA) films. *Journal of Polymers and the Environment, 16*(1), 1-11.

Thiel, M., & Gutow, L. (2004). The ecology of rafting in the marine environment - I - The floating substrata. In R. N. Gibson, R. J. A. Atkinson & J. D. M. Gordon (Eds.), *Oceanography and Marine Biology: An Annual Review, Vol 42* (Vol. 42, pp. 181-263).

Third, K. A., Newland, M., et al. (2003). The effect of dissolved oxygen on PHB accumulation in activated sludge cultures. *Biotechnology and Bioengineering, 82*(2), 238-250.

Third, K. A., Sepramaniam, S., et al. (2004). Optimisation of storage driven denitrification by using on-line specific oxygen uptake rate monitoring during SND in a SBR. *Water Sci Technol, 50*(10), 171-180.

Thomson, N., Summers, D., et al. (2010). Synthesis, properties and uses of bacterial storage lipid granules as naturally occurring nanoparticles. *Soft Matter, 6*(17), 4045-4057.

Tian, S. J., Lai, W. J., et al. (2005). Effect of over-expression of phasin gene from Aeromonas hydrophila on biosynthesis of copolyesters of 3-hydroxybutyrate and 3-hydroxyhexanoate. *FEMS Microbiol Lett, 244*(1), 19-25.

Timm, A., & Steinbuchel, A. (1992). Cloning and molecular analysis of the poly(3-hydroxyalkanoic acid) gene locus of *Pseudomonas aeruginosa* Pao1 *European Journal of Biochemistry, 209*(1), 15-30.

Tokiwa, Y., & Calabia, B. P. (2004). Degradation of microbial polyesters. *Biotechnology Letters, 26*(15), 1181-1189.

Tringe, S. G., & Rubin, E. M. (2005). Metagenomics: DNA sequencing of environmental samples. *Nature reviews genetics, 6*(11), 805-814.

Tripathi, L., Wu, L. P., et al. (2013). Biosynthesis and characterization of diblock copolymer of p(3-hydroxypropionate)-block-p(4-hydroxybutyrate) from recombinant Escherichia coli. *Biomacromolecules, 14*(3), 862-870.

Trotsenko, Y. A., & Belova, L. L. (2000). Biosynthesis of Poly(3-Hydroxybutyrate) and Poly(3-Hydroxybutyrate-co-3-Hydroxyvalerate) and Its Regulation in Bacteria. *Microbiology, 69*(6), 635-645.

Turnbaugh, P. J., Ley, R. E., et al. (2007). The human microbiome project: exploring the microbial part of ourselves in a changing world. *Nature, 449*(7164), 804.

Uchino, K., Saito, T., et al. (2007). Isolated Poly(3-Hydroxybutyrate) (PHB) Granules Are Complex Bacterial Organelles Catalyzing Formation of PHB from Acetyl Coenzyme A (CoA) and Degradation of PHB to Acetyl-CoA. *Journal of Bacteriology, 189*(22), 8250-8256.

Ujang, S. Z., Salim, M. R., et al. (2007). Intracellular biopolymer productions using mixed microbial cultures from fermented POME. *Water Science and Technology, 56*(8), 179-185.

Umeda, F., Kitano, Y., et al. (1998). Cloning and sequence analysis of the poly (3-hydroxyalkanoic acid)-synthesis genes of Pseudomonas acidophila. *Appl Biochem Biotechnol, 70-72*, 341-352.

University, I. S. (1993). *Livestock Waste Facilities Handbook*. Ames, IA.

Urtuvia, V., Villegas, P., et al. (2014). Bacterial production of the biodegradable plastics polyhydroxyalkanoates. *International journal of biological macromolecules, 70*, 208-213.

Valappil, S. P., Boccaccini, A. R., et al. (2007). Polyhydroxyalkanoates in Gram-positive bacteria: insights from the genera Bacillus and Streptomyces. *Antonie van leeuwenhoek, 91*(1), 1-17.

Valappil, S. P., Misra, S. K., et al. (2006). Biomedical applications of polyhydroxyalkanoates, an overview of animal testing and in vivo responses. *Expert review of medical devices, 3*(6), 853-868.

Valentino, F., Beccari, M., et al. (2014). Feed frequency in a Sequencing Batch Reactor strongly affects the production of polyhydroxyalkanoates (PAHs) from volatile fatty acids. *New Biotechnology, 31*(4), 264-275.

Valentino, F., Brusca, A. A., et al. (2013). Start up of biological sequencing batch reactor (SBR) and short-term biomass acclimation for polyhydroxyalkanoates production. *Journal of Chemical Technology and Biotechnology, 88*(2), 261-270.

van Aalst-van Leeuwen, M. A., Pot, M. A., et al. (1997). Kinetic modeling of poly(β-hydroxybutyrate) production and consumption by Paracoccus pantotrophus under dynamic substrate supply. *Biotechnology and Bioengineering, 55*(5), 773-782.

Van der Walle, G., De Koning, G., et al. (2001). Properties, modifications and applications of biopolyesters *Biopolyesters* (pp. 263-291): Springer.

van Loosdrecht, M. C. M., Pot, M. A., et al. (1997). Importance of bacterial storage polymers in bioprocesses. *Water Science and Technology, 35*(1), 41-47.

Van Wegen, R. J., Ling, Y., et al. (1998). Industrial production of polyhydroxyalkanoates using Escherichia coli: An economic analysis. *Chemical Engineering Research & Design, 76*(A3), 417-426.

Vergine, P., Sousa, F., et al. (2015). Synthetic soft drink wastewater suitability for the production of volatile fatty acids. *Process Biochemistry, 50*(8), 1308-1312.

Verlinden, R. A. J., Hill, D. J., et al. (2007). Bacterial synthesis of biodegradable polyhydroxyalkanoates. *Journal of Applied Microbiology, 102*(6), 1437-1449.

Villano, M., Beccari, M., et al. (2010a). Effect of pH on the production of bacterial polyhydroxyalkanoates by mixed cultures enriched under periodic feeding. *Process Biochemistry, 45*(5), 714-723.

Villano, M., Lampis, S., et al. (2010b). Effect of hydraulic and organic loads in Sequencing Batch Reactor on microbial ecology of activated sludge and storage of polyhydroxyalkanoates. In E. Bardone & A. Viglia (Eds.), *Ibic2010: 2nd International Conference on Industrial Biotechnology* (Vol. 20, pp. 187-192).

Volova, T. G., Boyandin, A. N., et al. (2011). Biodegradation of polyhydroxyalkanoates (PHAs) in the South China Sea and identification of PHA-degrading bacteria. *Microbiology, 80*(2), 252-260.

Wallen, L. L., & Rohwedder, W. K. (1974). Poly-.beta.-hydroxyalkanoate from activated sludge. *Environmental Science & Technology, 8*(6), 576-579.

Waller, J. L., Green, P. G., et al. (2012). Mixed-culture polyhydroxyalkanoate production from olive oil mill pomace. *Bioresource Technology, 120*, 285-289.

Wang, F., & Lee, S. Y. (1998). High cell density culture of metabolically engineered Escherichia coli for the production of poly(3-hydroxybutyrate) in a defined medium. *Biotechnol Bioeng, 58*(2-3), 325-328.

Wang, S., Fox, D., et al. (1999). Impact of dairy farming on well water nitrate level and soil content of phosphorus and potassium. *Journal of dairy science, 82*(10), 2164-2169.

Wang, Z., Itoh, Y., et al. (2003). Novel transdermal drug delivery system with polyhydroxyalkanoate and starburst polyamidoamine dendrimer. *Journal of bioscience and bioengineering, 95*(5), 541-543.

Ward, A. C., Rowley, B. I., et al. (1977). Effect of oxygen and nitrogen limitation on poly-β-hydroxybutyrate biosynthesis in ammonium-grown Azotobacter beijerinckii. *Journal of General Microbiology, 102*(1), 61-68.

Washburn, M. P., Wolters, D., et al. (2001). Large-scale analysis of the yeast proteome by multidimensional protein identification technology. *Nature biotechnology, 19*(3), 242-247.

Watson, B. (2015). *Optimization of Dairy Manure Based Polyhydroxyalkanoate Production through Reduced Aeration on Enrichment Cultures.* (Masters of Science), University of Idaho, Moscow, ID.

Wei, L., Guho, N. M., et al. (2014). Characterization of Poly(3-hydroxybutyrate- co-3-hydroxyvalerate) Biosynthesized by Mixed Microbial Consortia Fed Fermented Dairy Manure. *Journal of Applied Polymer Science, 131*(11).

White, D. (2007). *The Physiology and Biochemistry of Prokaryotes* (Vol. Third Edition): Oxford University Press.

Wilkins, M. R., Sanchez, J. C., et al. (1996). Progress with proteome projects: Why all proteins expressed by a genome should be identified and how to do it. *Biotechnology and Genetic Engineering Reviews, Vol 13, 13*, 19-50.

Williams, S. F., & Martin, D. P. (2005). Applications of polyhydroxyalkanoates (PHA) in medicine and pharmacy. *Biopolymers Online*.

Wilm, M. S., & Mann, M. (1994). Electrospray and Taylor-Cone theory, Dole's beam of macromolecules at last? *International Journal of Mass Spectrometry and Ion Processes, 136*(2), 167-180.

Wilmes, P., Andersson, A. F., et al. (2008a). Community proteogenomics highlights microbial strain-variant protein expression within activated sludge performing enhanced biological phosphorus removal. *ISME J, 2*(8), 853-864.

Wilmes, P., & Bond, P. (2006a). Towards exposure of elusive metabolic mixed-culture processes: the application of metaproteomic analyses to activated sludge. *Water Science & Technology, 54*(1), 217-226.

Wilmes, P., & Bond, P. L. (2004). The application of two-dimensional polyacrylamide gel electrophoresis and downstream analyses to a mixed community of prokaryotic microorganisms. *Environ Microbiol, 6*(9), 911-920.

Wilmes, P., & Bond, P. L. (2006b). Metaproteomics: studying functional gene expression in microbial ecosystems. *Trends Microbiol, 14*(2), 92-97.

Wilmes, P., Wexler, M., et al. (2008b). Metaproteomics provides functional insight into activated sludge wastewater treatment. *PLoS One, 3*(3), e1778.

Wu, J. H., Wu, F. Y., et al. (2013). Community and proteomic analysis of methanogenic consortia degrading terephthalate. *Appl Environ Microbiol, 79*(1), 105-112.

Xu, J. (2006). Invited review: microbial ecology in the age of genomics and metagenomics: concepts, tools, and recent advances. *Molecular ecology, 15*(7), 1713-1731.

Yadav, T. C., Khardenavis, A. A., et al. (2014). Shifts in microbial community in response to dissolved oxygen levels in activated sludge. *Bioresource Technology, 165*, 257-264.

Yates, J. R., 3rd, Speicher, S., et al. (1993). Peptide mass maps: a highly informative approach to protein identification. *Anal Biochem, 214*(2), 397-408.

York, G. M., Junker, B. H., et al. (2001a). Accumulation of the PhaP phasin of Ralstonia eutropha is dependent on production of polyhydroxybutyrate in cells. *Journal of bacteriology, 183*(14), 4217-4226.

York, G. M., Lupberger, J., et al. (2003). Ralstonia eutropha H16 Encodes Two and Possibly Three Intracellular Poly[d-(−)-3-Hydroxybutyrate] Depolymerase Genes. *Journal of Bacteriology, 185*(13), 3788-3794.

York, G. M., Stubbe, J., et al. (2001b). New insight into the role of the PhaP phasin of Ralstonia eutropha in promoting synthesis of polyhydroxybutyrate. *Journal of bacteriology, 183*(7), 2394-2397.

York, G. M., Stubbe, J., et al. (2002). The Ralstonia eutropha PhaR protein couples synthesis of the PhaP phasin to the presence of polyhydroxybutyrate in cells and promotes polyhydroxybutyrate production. *Journal of bacteriology, 184*(1), 59-66.

Yu, H., Shi, Y., et al. (2003). Genetic strategy for solving chemical engineering problems in biochemical engineering. *Journal of Chemical Technology & Biotechnology, 78*(2-3), 283-286.

Zhang, P., Guo, J.-S., et al. (2015). Microbial communities, extracellular proteomics and polysaccharides: A comparative investigation on biofilm and suspended sludge. *Bioresource Technology, 190*, 21-28.

Zhou, Z., Meng, F., et al. (2015). Metaproteomic analysis of biocake proteins to understand membrane fouling in a submerged membrane bioreactor. *Environ Sci Technol, 49*(2), 1068-1077.

Zinn, M., Witholt, B., et al. (2001). Occurrence, synthesis and medical application of bacterial polyhydroxyalkanoate. *Advanced Drug Delivery Reviews, 53*(1), 5-21.

Chapter 2. Proteomic profiling of an undefined microbial consortium cultivated in fermented dairy manure: methods development

(Andrea J. Hanson, Andrzej J. Paszczynski, and Erik R. Coats[1])

2.1 Abstract

The production of polyhydroxyalkanoates (PHA; bioplastics) from waste or surplus feedstocks using mixed microbial consortia (MMC) and aerobic dynamic feeding (ADF) is a growing field within mixed culture biotechnology. This study aimed to optimize a 2DE workflow to investigate the proteome dynamics of an MMC synthesizing PHA from fermented dairy manure. To mitigate the challenges posed to effective 2DE by this complex sample matrix, the bacterial biomass was purified using Accudenz gradient centrifugation (AGC) before protein extraction. The optimized 2DE method yielded high-quality gels suitable for quantitative comparative analysis and subsequent protein identification by LC-MS/MS. The optimized 2DE method could be adapted to other proteomic investigations involving MMC in complex organic or environmental matrices.

[1] This chapter is currently in revision as "Proteomic profiling of an undefined microbial consortium cultured in fermented dairy manure: methods development" in the journal *Electrophoresis*.

2.2 Introduction

The production of PHA using MMC and fermented waste/surplus feedstocks has attracted attention as an inexpensive alternative to current commercial production which relies on pure cultures and refined substrates (Dias *et al.*, 2006). To be successful, the MMC must be highly enriched for PHA-producing bacteria. This is commonly achieved through ADF (Majone *et al.*, 1996), which imposes transient exogenous carbon availability (i.e., feast-famine conditions). However, advancement of this process has been impeded by an incomplete understanding of the physiology and biochemistry of the MMC response to ADF conditions. 2DE-based proteomics offers a powerful approach to elucidate functional responses; however, optimal 2DE procedures have not been established for MMC cultured in fermented waste feedstocks. To address this need, the research herein focused on the application of 2DE to an MMC subjected to ADF conditions and cultured on fermented dairy manure.

Like other 2DE-based investigations involving mixed culture biotechnology (e.g., activated sludge processes and anaerobic digestion), the fermented dairy manure sample matrix added to the inherent complexity of MMC protein mixtures. Direct protein extraction from MMC biomass and subsequent electrophoretic separation is challenging due to the abundance of non-bacterial protein impurities and non-bacterial solids (including volatile fatty acids, salts, crude fat, non-structural carbohydrates, inert particulates, lignocellulose degradation products, and pigmented compounds).

To combat similar interferences, indirect protein extraction approaches utilizing gradient centrifugation that first isolate/purify bacterial cells from complex matrices have been applied in MMC proteome studies of soil and freshwater samples using 1D SDS PAGE (Pierre-Alain

et al., 2007; Williams *et al.*, 2010). Drawing from these investigations, the aim of this study was to optimize an MMC sample processing procedure using AGC and sequential protein extraction to improve the recovery of bacterial proteins from reactor biomass and ensure effective protein separation by 2DE.

2.3 Materials and methods

Sample source: MMC biomass samples were obtained from a sequencing batch reactor operated under ADF conditions conducive for PHA synthesis. Briefly, the reactor was fully aerobic, constantly mixed, had a volume of 1.8 L, solids and hydraulic retention time of 4 d, and cycle length of 24 h. The fermented dairy manure used for substrate was prepared in the following manner: effluent from a lab-scale manure fermenter was screened to remove large solids, centrifuged at 8,000 rpm for 5 min to remove fine solids, autoclaved, and diluted with tap water prior to addition to the reactor. The suspended solids concentration (including microbial biomass) in the reactor was maintained above 2,000 mg/L.

Optimized "AGC 2DE" method: The following procedures are outlined in Figure 2.1. All reagents used were of electrophoresis-grade. Initial biomass collection and washing was adapted from Wilmes and Bond (Wilmes & Bond, 2004) with minor modifications. Briefly, 80 mL MMC sample was centrifuged at 5,000 rpm for 15 min at 4°C in an SS-34 rotor (Sorvall, Waltham, MA). The supernatant was discarded; the pellet was resuspended in 40 mL of 0.9% NaCl and washed by centrifugation at 5,000 rpm for 15 min at 4°C. After discarding the wash, the pellet was resuspended in 25 mL of 25 mM Tris, pH 7.4.

The AGC procedures were adapted from published protocols (Courtois *et al.*, 2001; Williams *et al.*, 2010) with modifications. Briefly, to the 25 mL washed biomass suspension,

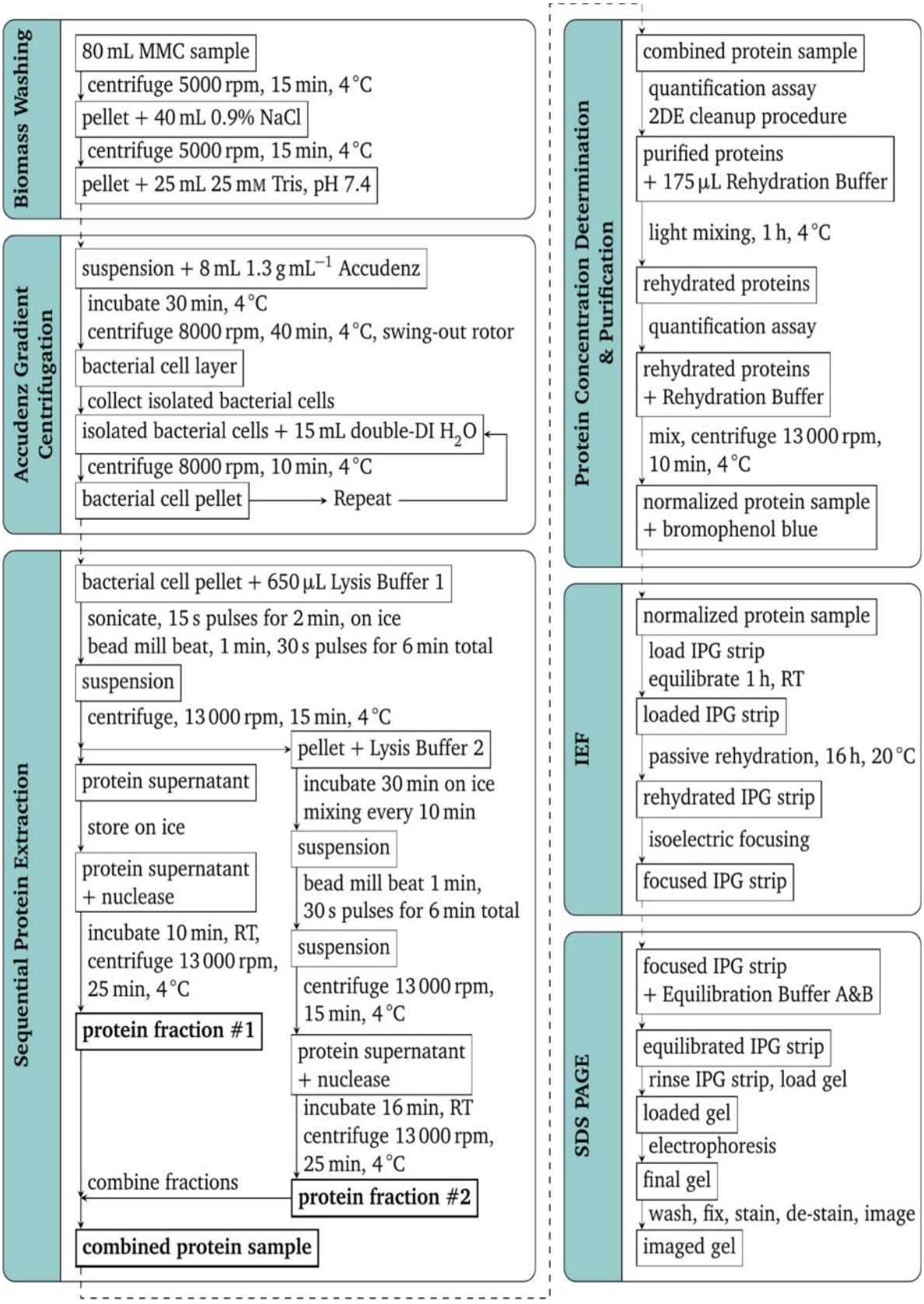

Figure 2.1. Outline of the optimized "AGC 2DE" workflow. See text for additional details.

8 mL of 1.3 g/mL Accudenz (Accurate Chemical Company, Westbury, NY) solution was added beneath the sample and incubated for 30 min at 4°C. The sample was centrifuged at 8,000 rpm for 40 min at 4°C in a JS13.1 swing-out rotor (Beckman Coulter, Pasadena, CA). Separated bacterial cells at the gradient interface (a visible turbid layer) were collected with a 5-mL syringe fitted with an 18-gauge needle bent at 90° (this size permits bacterial cell flow). Collected cells were washed twice in 15 mL of double-DI H_2O by centrifugation at 8,000 rpm for 10 min at 4°C using the same rotor; washes were discarded and the bacterial cell pellet was subjected to sequential protein extraction.

For sequential protein extraction, the bacterial cell pellet was resuspended in 650 µL Lysis Buffer 1 (25 mM Tris pH 7.4, 0.1 mM EDTA, and 0.5 mM 4-(2-aminoethyl)benzenesulfonyl fluoride hydrochloride (AEBSF)), vigorously mixed, and transferred to a 1.5-mL self-standing screw cap tube. The bacterial cell suspension was sonicated using a Model 100 Sonic Dismembrator (Thermo Fisher, Waltham, MA) on ice with 15 s pulses up to 2 min with the power setting at 3, after which 0.1 mm zirconia/silica beads (Biospec Products Inc., Bartlesville, OK) were added to the suspension to approximately half the sample volume. The suspension was homogenized in a bead mill beater (Biospec Products Inc.) for 1 min, followed by 30 sec pulses for 6 min, and then centrifuged at 13,000 rpm for 15 min at 4°C, and the supernatant (protein fraction #1) was stored on ice. The pellet was resuspended in 600 µL Lysis Buffer 2 (7M urea, 2M thiourea, 4% w/v CHAPS, 10mM Tris-1mM EDTA, 50 mM DTT, and 0.5 mM AEBSF; DTT, CHAPS and AEBSF were added immediately before use), then incubated on ice for 30 min with vigorous mixing every 10 min. The aforementioned bead mill beating procedure was repeated, along with centrifugation and supernatant retention (protein fraction #2). A nuclease treatment was performed separately

on each protein fraction by adding 50U of Benzonase nuclease (Sigma-Aldrich, St. Louis, MO) and incubating at room temperature for 10 min with light mixing every 2 min. Suspensions were centrifuged at 13,000 rpm for 25 min at 4°C; the supernatants were combined into one sample and vigorously mixed. When required, protein samples were stored at -80°C.

Protein concentration of the combined fractions was determined by the RCDC Protein Assay (Bio-Rad, Hercules, CA) following the manufacturer's instructions and using BSA as the protein standard. Protein precipitation and clean-up procedures were performed using a ReadyPrep 2-D Cleanup Kit (Bio-Rad) following the manufacturer's instructions. The protein pellet was resuspended in 175 µL Rehydration Buffer (7M urea, 2M thiourea, 3% w/v CHAPS, 50 mM DTT, and 0.2% w/v Bio-Lyte 3/10 ampholytes; DTT, CHAPS, and ampholytes were added immediately before use). The sample was mixed for 1 h at 4°C. Protein concentration in the rehydration solution was determined using the RCDC Assay, and the sample was diluted in Rehydration Buffer to normalize the concentration to 3.2 mg/mL; a trace amount of bromophenol blue was added, followed by vigorous mixing and centrifugation at 13,000 rpm for 10 min at 4°C prior to IPG strip loading.

For IEF, 400 µg protein in 125 µL was loaded onto a 7-cm ReadyStrip IPG Strip pH 4-7 (Bio-Rad), equilibrated for 1 h at room temperature, covered with mineral oil, and passively rehydrated for 16 h at 20°C. The IPG strip was focused in a PROTEAN IEF Cell (Bio-Rad) at 250 V for 15 min, followed by linear ramping to 4,000 V in 2.5 h, and 4,000 V for 13,000 V-hr. Immediately following IEF, the IPG strip was equilibrated twice for 20 min each in Equilibration Buffer A (6 M urea, 30% (w/v) glycerol, 2% (w/v) SDS in 0.05 M Tris pH 8.8, and 20 mg/mL DTT) and Equilibration Buffer B (same as A only DTT was replaced

by 25 mg/mL iodoacedamide) with gentle shaking; for each equilibration, fresh buffer was exchanged after 10 min.

For SDS PAGE separation, the IPG strip was rinsed in Tris-Glycine-SDS buffer (25 mM Tris, 192 mM glycine, 0.1% SDS), loaded onto an 8x10 cm 12% Mini-PROTEAN TGX pre-cast gel (Bio-Rad), sealed with overlay agarose, and electrophoresed at 70 V for 40 min, followed by 150 V until the tracking dye reached the bottom of the gel; molecular weight markers were applied to an electrode wick and inserted into the gel before the application of overlay agarose. The gel was washed twice in double-DI H_2O for 5 min, fixed in ethanol/acetic acid/water (40:10:50, v/v) for 30 min, stained with pre-made Coomassie Brilliant Blue G-250 (CBB; Bio-Rad) for 20 h, and de-stained with double-DI H_2O for several hours. The gel was scanned using an Odyssey Imaging System (Li-COR Biosciences, Lincoln, NE) with the following settings which generated 16 bit, 600 DPI TIFF files: resolution, 42 µm; quality, medium; focus offset, 0.5; detection channel, 700 nm. REDFIN 3 Gel Image Analysis Software (Ludesi, Malmö, Sweden) was used for gel image analysis following the manufacturer's recommendations related to image quality control, gel warping, spot matching, spot intensity measurement, background correction, and spot volume normalization.

2.4 Results and discussion

The primary objective during the development of the "AGC 2DE" workflow (Figure 2.1) was to increase the reliability and reproducibility of 2DE for investigating MMC operated under ADF conditions. Initial 2DE attempts indicated significant interference from the sample matrix and biased protein recovery, in addition to poor-quality gels (data not shown). AGC

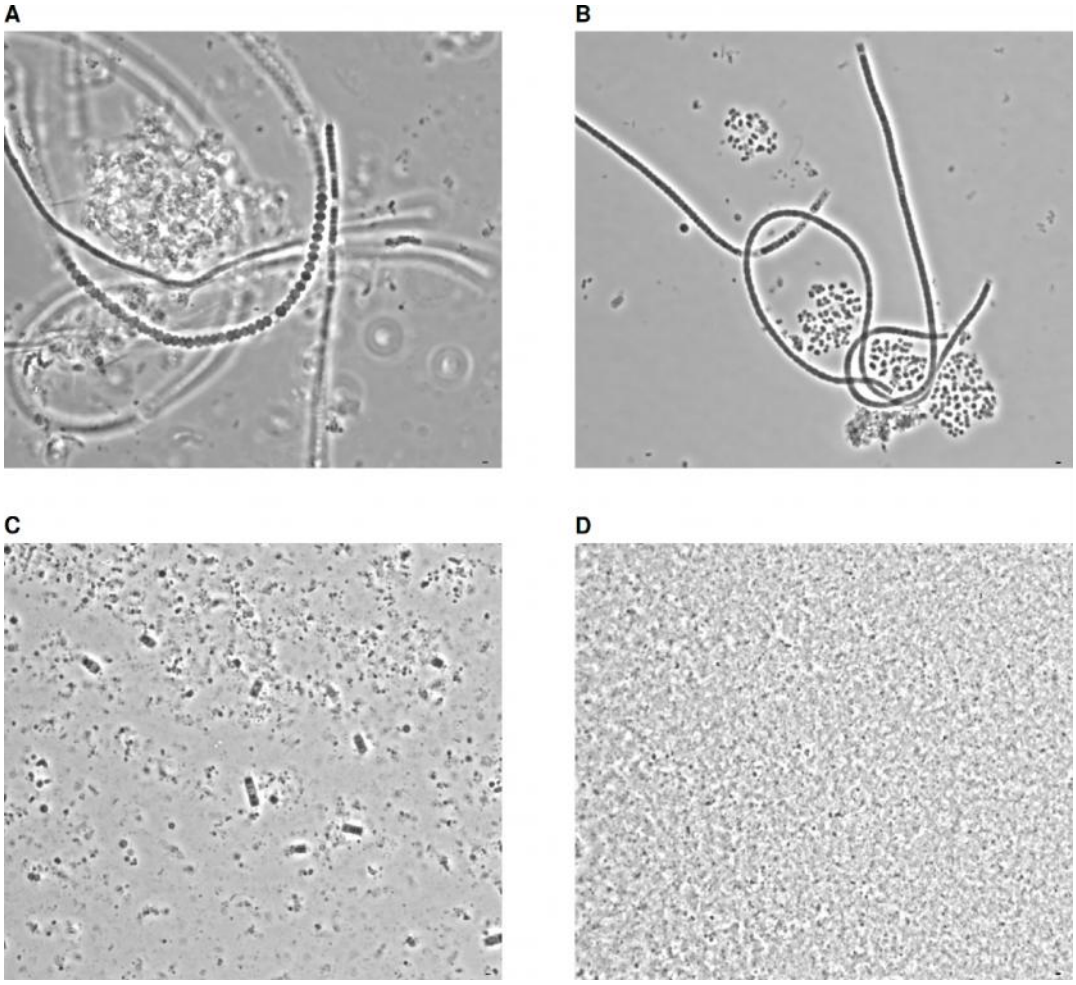

Figure 2.2. Bacterial cell separation and disruption. Phase contrast images (1000x) showing representative images of A) biomass directly from the MMC reactor, B) bacterial cells isolated using AGC, C) bacterial suspension after brief sonication and 1st bead mill beating in Lysis Buffer 1, and D) bacterial suspension after 30 min incubation and 2nd bead mill beating in Lysis Buffer 2. Images were acquired using a Nikon Eclipse 55i phase contrast microscope with NIS-147 Elements Br. 3.0. Bars in the bottom right corner represent 1 µm.

and sequential protein extraction were incorporated into the method to address these shortcomings.

AGC was used to mitigate the interference from the fermented dairy manure matrix on the bacterial protein extraction by separating the bacterial cells from the non-bacterial solids. While AGC may introduce bias into the bacterial recovery (Holmsgaard *et al.*, 2011), priority was given to achieving successful 2DE. To that end, AGC removed the non-bacterial solids from the sample, reducing the potential for the co-extraction of impurities and partitioning of proteins during extraction. The suspended solids concentration in the MMC

reactor was 2394 ± 736 mg/L, and as shown in Figure 2.2A and 2.2B, AGC effectively isolated bacterial cells from other solids. The bacterial cell pellet was typically 1/3 of the initial biomass pellet wet mass, reinforcing the value of AGC as a purification tool to separate bacterial cells from matrix debris.

Sequential protein extraction was adopted in an effort to maximize bacterial protein recovery while reducing extraction bias. As shown in Figure 2.2B, cell morphology was diverse in the MMC; the brief sonication, coupled with two rounds of bead mill beating applied in the "AGC 2DE" method aided cell disruption (Figure 2.2C and 2.2D) to help maximize protein recovery. No protein loss was observed following protein fraction combination, allaying concerns that protein precipitation might occur due to buffer dissimilarity. Throughout "AGC 2DE" development, the protein concentration in the combined protein sample was 12.8 mg/mL ± 5.5, which was sufficiently high for the 2DE clean-up and purification procedures. Together with the identification of both cytoplasmic and hydrophobic membrane-bound proteins (excised from the 2DE gel and identified by LC-MS/MS using the procedures adapted from Checinska et al. (Checinska *et al.*, 2012); data not shown), the effectiveness of the sequential protein extraction was reinforced.

The "AGC 2DE" method was repeated multiple times and consistently yielded gels with spot patterns similar to that shown in Figure 2.3. Throughout "AGC 2DE" optimization, the number of detected protein spots ranged from 585 to 639, with an average of 608 ± 26; spot numbers for the "AGC 2DE" method were higher compared to 2DE attempts involving direct extraction (data not shown). Other positive results of the "AGC 2DE" method included well-resolved spots, minimal horizontal streaking, reduced vertical stacking, and nominal background interference (Figure 2.3). Proteins from the "AGC 2DE" method exhibited an

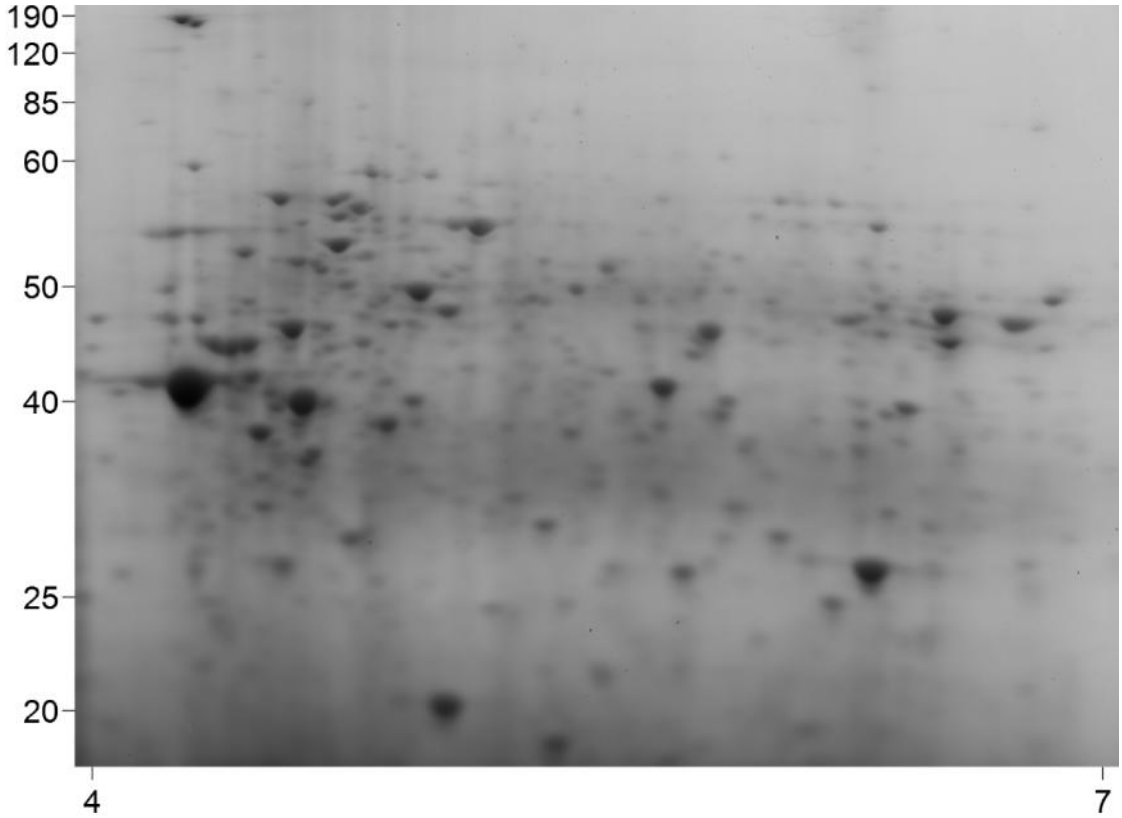

Figure 2.3. Representative 2DE gel image for the optimized "AGC 2DE" method. Molecular weight markers (in kDa) are listed to the left of the image, and the pH range of the IPG strip is depicted below the image.

array of isoelectric points across the pH 4 to 7 range, and an apparent molecular weight range spanning from less than 15 kDa up to 190 kDa. IPG strips with pH 3-10 and 7-10 ranges were evaluated, in addition to active IPG strip rehydration; however, protein resolution was not improved (data not shown). CBB G-250 was ultimately chosen over other evaluated stains (CBB R-250, Silver Stain for MS, and SYPRO Ruby) for its low background interference, reproducibility, sensitivity when used in combination with infrared scanning, and compatibility with LC-MS/MS.

The high-quality 2DE gels resulting from the "AGC 2DE" method enabled protein spot identification via LC-MS/MS which complimented the quantitative comparative assessments. As an example, LC-MS/MS analysis of one protein spot and subsequent MS/MS ion search using Mascot resulted in the assignment of four proteins to *Meganema*

perideroedes (the Mascot search criteria used and corresponding protein identification information is provided in Appendix A, Table A.1). The highest scoring protein was an amino acid ABC transporter substrate-binding protein with 17 peptide matches representing 74% protein sequence coverage. The other candidate proteins associated with the excised protein spot included two hypothetical proteins and LacI transcriptional regulator, each assigned to *Meganema perideroedes*. The mass spectrometry proteomics data have been deposited to the ProteomeXchange Consortium (Vizcaino *et al*., 2014) via the PRIDE partner repository with the dataset identifier PXD003004 and 10.6019/PXD003004; the Mascot result file, peak list file, and all raw LC-MS/MS data can be accessed through the PRIDE repository.

The optimized "AGC 2DE" procedures presented herein were effective as a biomass processing method for MMC protein profiling in an engineered system laden with 2DE-interfering impurities and non-bacterial solids. The "AGC 2DE" method yielded reproducible, high quality 2DE gels from which protein spots have been excised and identified via LC-MS/MS. Notably, the presented workflow could be modified based on available laboratory equipment; for example, a similar make or model of swing-out rotor could be substituted, different cell disruption methods could be implemented, or alternative gel imaging systems could be used in place of an infrared scanner. As such, the "AGC 2DE" workflow could be adapted to other MMC in the complex matrices often encountered in mixed culture biotechnology studies as part of a gel-based or gel-free proteomics approach.

2.5 Acknowledgements

The authors acknowledge Nicholas M. Guho at the University of Idaho for assistance with gel image processing and figure editing. This material is based upon work supported by the

National Science Foundation under Grant Number CBET-0950498, and Environmental Protection Agency Science to Achieve Results Fellowship. Any opinions, findings, and conclusions or recommendations expressed in this material are those of the authors and do not necessarily reflect the views of the funding agency. The authors declare no conflicts of interest.

References

Checinska, A., Burbank, M., et al. (2012). Protection of Bacillus pumilus Spores by Catalases. *Applied and Environmental Microbiology, 78*(18), 6413-6422.

Courtois, S., Frostegard, A., et al. (2001). Quantification of bacterial subgroups in soil: comparison of DNA extracted directly from soil or from cells previously released by density gradient centrifugation. *Environmental Microbiology, 3*(7), 431-439.

Dias, J. M. L., Lemos, P. C., et al. (2006). Recent advances in polyhydroxyalkanoate production by mixed aerobic cultures: From the substrate to the final product. *Macromolecular Bioscience, 6*(11), 885-906.

Holmsgaard, P. N., Norman, A., et al. (2011). Bias in bacterial diversity as a result of Nycodenz extraction from bulk soil. *Soil Biology and Biochemistry, 43*(10), 2152-2159.

Majone, M., Massanisso, P., et al. (1996). Influence of storage on kinetic selection to control aerobic filamentous bulking. *Water Science and Technology, 34*(5-6), 223-232.

Pierre-Alain, M., Christophe, M., et al. (2007). Protein extraction and fingerprinting optimization of bacterial communities in natural environment. *Microbial ecology, 53*(3), 426-434.

Vizcaino, J. A., Deutsch, E. W., et al. (2014). ProteomeXchange provides globally coordinated proteomics data submission and dissemination. *Nat Biotech, 32*(3), 223-226.

Williams, M. A., Taylor, E. B., et al. (2010). Metaproteomic characterization of a soil microbial community following carbon amendment. *Soil Biology & Biochemistry, 42*(7), 1148-1156.

Wilmes, P., & Bond, P. L. (2004). The application of two-dimensional polyacrylamide gel electrophoresis and downstream analyses to a mixed community of prokaryotic microorganisms. *Environ Microbiol, 6*(9), 911-920.

Chapter 3. Community Proteomics Reveals Insight into Polyhydroxyalkanoate Production from Fermented Dairy Manure Using a Mixed Microbial Culture

(Andrea J. Hanson, Nicholas M. Guho, Andrzej J. Paszczynski, and Erik R. Coats[1])

3.1 Abstract

Polyhydroxyalkanoates (PHAs) are bio-based, biodegradable polyesters that can be produced from organic-rich waste streams using mixed microbial cultures (MMCs). To maximize PHA production, MMCs are enriched for PHA-producing bacteria with a high polymer storage capacity through the application of aerobic dynamic feeding (ADF) which entails the cyclic imposition of feast-famine conditions in a sequencing batch reactor (SBR). The objective of this study was to investigate the microbial community composition and proteome profile of an MMC enriched under ADF conditions in an SBR cultivated on fermented dairy manure. Bulk solution process parameters were evaluated, and 16S rRNA gene sequencing was used to characterize the microbial community composition. Two-dimensional electrophoresis was used to compare protein abundance during an SBR cycle and fed-batch PHA accumulation tests, and 83 protein spots of interest were identified using LC-MS/MS. The MMC exhibited an appropriate feast-famine response and was dominated by the *Meganema* genus. During the feast phase, proteins involved in PHA and protein synthesis, as well as enzymes involved in energy generation, exhibited increased abundance. During the famine phase, proteins in increased abundance included multiple ABC transport proteins, enzymes involved in acyl-CoA metabolism, and proteins performing housekeeping functions. Collectively, the results provided insight regarding the functional response of MMC to ADF conditions, which may help to improve PHA production from waste feedstocks using MMCs.

[1]This chapter will be submitted to *Applied Microbiology and Biotechnology*.

3.2 Introduction

Polyhydroxyalkanoates (PHAs) have gained appeal as bioplastics given their breadth of material properties, utility as functional replacements to some conventional petroleum-based plastics, and positive life cycle assessments (Gurieff & Lant, 2007; Keshavarz & Roy, 2010). To expand commercial PHA production, the use of mixed microbial cultures (MMCs) and inexpensive waste feedstocks of agricultural or industrial origin has been proposed as a means to reduce production costs while simultaneously achieving waste management (Dias *et al.*, 2006a; Serafim *et al.*, 2008). For this approach to be successful, MMCs must first be enriched for PHA-producing bacteria with high PHA storage capacity that are physiologically conditioned for polymer accumulation prior to inoculating separate fed-batch reactors to produce commercial quantities of PHA. When waste feedstocks are used, a fermentation step is incorporated upstream to convert the complex organic material therein (e.g., carbohydrates, proteins, and lipids) to volatile fatty acids (VFAs), which are the preferred precursors for PHA synthesis in these MMCs (Reis *et al.*, 2003). This three-stage PHA production approach has been successfully evaluated using multiple waste feedstocks, including paper mill effluent (Jiang *et al.*, 2012), olive oil mill effluent (Dionisi *et al.*, 2005), and molasses (Albuquerque *et al.*, 2007).

The enrichment of MMCs for PHA production is most effectively accomplished through the imposition of feast-famine conditions (specifically referred to as aerobic dynamic feeding, ADF in a sequencing batch reactor (SBR) (Dias *et al.*, 2006b; Majone *et al.*, 1996; Serafim *et al.*, 2008). For a typical SBR cycle, substrate is added at the beginning of the cycle creating an excess of PHA precursors in solution (i.e., feast phase); during the feast phase, bacteria able to produce PHA simultaneously synthesize PHA (storage) and new biomass (growth),

whereas bacteria lacking the PHA synthesis capacity simply grow (Dias *et al.*, 2006b; Reis *et al.*, 2003; van Loosdrecht *et al.*, 1997). For the remainder the cycle following exogenous substrate depletion (i.e., famine phase), bacteria with PHA mobilize their endogenous stores for carbon and energy to support continued growth and cellular maintenance, while bacteria lacking PHA stores decay (van Loosdrecht *et al.*, 1997). Accordingly, PHA-producing bacteria can be enriched by combining short periods of exogenous substrate availability with long periods of exogenous substrate dearth (Johnson *et al.*, 2009; Reis *et al.*, 2003; van Loosdrecht *et al.*, 1997).

While the overall success of the three-stage PHA production process hinges on the enrichment of PHA-producing bacteria in the MMC, research to date has primarily concentrated on the empirical determination of optimal operating conditions. Efforts to analyze the microbial composition of MMCs in enrichment SBRs have relied on the application of classical molecular methods including fluorescence *in situ* hybridization (FISH) coupled with PHA staining (Oehmen *et al.*, 2014), clone library construction (Albuquerque *et al.*, 2013), or denaturing gradient gel electrophoresis (Carvalho *et al.*, 2013). Though these methods have been useful in identifying dominant populations within MMCs and visualizing the relative abundance of PHA-producing bacteria in clean (synthetic or filtered) feedstocks, their utility in characterizing diverse consortia cultured in raw, waste feedstocks has limitations (Muyzer et al., 2004). Though links between MMC composition and process performance have been established in some investigations (Albuquerque *et al.*, 2013; Carvalho *et al.*, 2013), microbial functional changes associated with a feast-famine response during an SBR cycle are still largely inferred from bulk solution variables.

To ultimately advance MMC PHA production using waste feedstocks, knowledge of community-level functionality during an ADF SBR cycle is required. The microbial physiology driving the feast-famine PHA storage response is widely attributed to an internal limitation of protein synthesis machinery as a result of withstanding the famine phase. This reduced anabolic capacity renders bacteria unable to grow at a rate commensurate with the substrate availability in the subsequent feast phase, thereby inducing the storage of excess substrate as PHA (Dias *et al.*, 2006b; Serafim *et al.*, 2008; van Loosdrecht *et al.*, 1997). Despite this theoretical proposition concerning the feast-famine response in MMC, little molecular-level evidence is available to corroborate the observed feast-famine response in MMC at a bulk solution-level. To directly characterize microbial community-level functions, proteomics can be applied, as successfully demonstrated in other studies involving activated sludge (Wilmes *et al.*, 2008) or anaerobic digestion (Abram *et al.*, 2011).

In the present study, genomic and proteomic tools were employed to investigate the microbial composition and function of an MMC in an enrichment SBR operated under ADF conditions using fermented dairy manure as the feedstock. 16S rRNA gene sequencing was performed using an Illumina MiSeq to characterize the microbial composition of the MMC. Two-dimensional electrophoresis (2DE) was used to resolve MMC protein mixtures, allowing for the visualization and quantitative comparison of proteome dynamics during the SBR cycle as well as fed-batch PHA accumulation assessments. Proteins of interest were excised from the 2DE gels and identified by nano-LC followed by QTOF mass spectrometry. By integrating the microbial community molecular-level data with bulk solution variables, a closer examination of the MMC was made possible. To the authors' knowledge, this study is

the first microbial community and proteomic profiling of an MMC enriched under ADF conditions as part of a multi-stage PHA production system.

3.3 Materials and methods

3.3.1 Waste feedstock preparation

The fermented dairy manure liquor (FDML) feedstock for the PHA enrichment SBR was obtained from a 20 L dairy manure fermenter operated under conditions as previously described (Stowe *et al.*, 2015). Briefly, manure was supplied from lactating Holstein cows at the University of Idaho Dairy, Moscow, ID. Effluent from the fermenter was poured through a mesh screen to remove large solids. After screening, the liquid was centrifuged at 8,000 rpm for 5 min to remove fine solids. The supernatant (i.e., the FDML feedstock), was then sterilized by autoclaving. To compensate for phosphate precipitation during autoclaving, equimolar KH_2PO_4 and K_2HPO_4 were added aseptically after cooling. The range of soluble VFA, ammonia, and phosphate concentrations in the final FDML feedstock are provided in Table 3.1.

3.3.2 Enrichment SBR operation

The enrichment SBR was operated under ADF conditions and at an operating volume of 1.8 L, a solids retention time (SRT) of 4 d, a hydraulic retention time (HRT) of 4 d, and a cycle length (CL) of 24 h. The cycle consisted of a fill phase (2 min), a react phase (1433 min), and a draw phase (5 min). Mixing was maintained throughout the cycle by a magnetic stir bar. House air was introduced into the SBR at a rate of approximately 1 L min^{-1} through a stainless steel diffusor to achieve aeration during the fill and react phases. FDML and autoclaved tap water were added to the reactor simultaneously during the fill phase, at a volumetric ratio of

40:60, respectively. The pumps and aeration were controlled by a programmable logic controller. The enrichment SBR was operated in a temperature-controlled room (20-26°C), and the pH was monitored, but not controlled. When necessary, foaming was controlled with the addition of Antifoam A Concentrate (Sigma Aldrich, St. Louis, MO, USA). The enrichment SBR was inoculated from a 20 L SBR (same SRT, HRT, and CL but fed non-sterilize FDML) that had been stably operated for 4 years (and inoculated with an MMC from the Moscow, ID wastewater treatment facility). After inoculation the enrichment SBR was operated for approximately 2.5 months (equivalent to 18+ SRTs) to ensure the SBR had reached an equilibrated state, during which preliminary assessments of bulk solution changes (viz. VFA consumption, oxygen consumption, PHA accumulation, and biomass generation) were completed to confirm the enrichment SBR was exhibiting a typical response relative to PHA synthesis under ADF conditions. Once a feast-famine response (i.e., for the feast phase: rapid VFA uptake, rapid decrease in dissolved oxygen (DO) concentration, and PHA synthesis; for the famine phase: steady increase in DO, depletion of PHA stores (Beun *et al.*, 2002; Dionisi *et al.*, 2004; Serafim *et al.*, 2004)) was established, three independent sampling events (Sampling #1, Sampling #2, and Sampling #3; sampling events were spaced two SRTs apart) spanning an operational cycle (24 h) were completed.

3.3.3 Fed-batch PHA accumulation tests

During each of the three enrichment SBR sampling events, the culture was subjected to fed-batch PHA accumulation capacity tests. Using the 450 mL of effluent from the enrichment SBR, the fed-batch tests were conducted in a separate 1 L beaker under fully aerobic and completely mixed conditions with the same FDML and tap water fed to the enrichment SBR. A total of three pulse-additions of FDML feedstock (112 mL, 140 mL, and 175 mL,

respectively) were applied; the pulse-addition time was determined by manually monitoring dissolved oxygen (DO) concentration and adding the next feedstock pulse when the DO began to rise (Dias *et al.*, 2006a). The fed-batch tests were carried out in the same temperature-controlled room (20-26°C) and the pH was monitored, but not controlled.

3.3.4 Analytical procedures

DO, pH, and temperature were monitored using a Hach HQ40 meter with LDO101 and PHC101 probes (Hach, Loveland, CO). Volatile suspended solids (VSS) was determined in accordance with Standard Methods (Rice, 2005). Soluble VFAs (viz. acetic, propionic, butyric, valeric, caproic, iso-butyric, and iso-valeric acids) were quantified as previously described (Coats *et al.*, 2011). Chemical oxygen demand (COD), phosphate (PO_4^{3-} -P), ammonia (NH_3-N), nitrite (NO_2^- -N), and nitrate (NO_3^- -N) concentrations were determined after sample filtration through a sterile 0.22 µm syringe filter (Millipore Corp., Billerica, MA) in accordance with Standard Methods (Rice, 2005). The active biomass, X, was determined as the difference between the VSS and PHA (X=VSS-PHA) and was assumed to the stoichiometric formula $C_5H_7O_2N$ (Grady *et al*., 2011).

Biomass PHA content was determined as methyl esters using gas chromatography-mass spectrometry (GC-MS) as previously described (Dobroth *et al.*, 2011) with minor modifications. Briefly, 400 µL of 6.25% sodium hypochlorite was added to lyse cells and halt metabolic activity. Biomass was then harvested by centrifugation at 10,000 rpm for 10 min, rinsed twice with deionized water, and oven-dried at 103-105°C for 24 h. Dried biomass was then digested in 2 mL each of acidified methanol (3% v/v sulfuric acid) and chloroform (containing 0.25 mg mL^{-1} benzoic acid as internal standard) at 100°C for 4 h. Once cooled, samples were vigorously mixed for 30 s following the addition of 1 mL deionized water. The

organic phase was recovered using a Pasteur pipette and dehydrated with anhydrous sodium sulfate prior to GC-MS analysis. PHA analysis was performed using a PolarisQ iontrap GC-MS instrument (Thermo Electron Corporation, San Jose, CA) in positive EI mode. Hydroxybutyrate (HB) and hydroxyvalerate (HV) methyl esters were identified by retention time and mass spectra matching with commercially available standards (Lancaster Synthesis, Ward Hill, MA); quantification of each monomer was determined using standard curves prepared from the same standards. The maximum PHA content was calculated on a cell dry weight basis and expressed as a percent (i.e., (mg PHA/mg total suspended solids)*100). PHA yield was expressed as Cmmol PHA Cmmol VFA^{-1}.

3.3.5 Microbial community analysis

Microbial genomic DNA was isolated from biomass samples using the PowerSoil DNA Isolation Kit (MOBIO, Carlsbad, CA) following the manufacturer's instructions. Genomic DNA yield and purity was quantified using a Synergy H1 Multi-Mode Reader (BioTek, Winooski, VT). Bacterial 16S rRNA gene fragments were amplified and sequenced following previously described methods (Dai *et al.*, 2015; Liang *et al.*, 2015) with minor modifications. Briefly, sample amplicons were generated using two rounds of PCR: PCR1 amplified the targeted V1-V3 regions (*Escherichia coli* positions 27F-533R of the 16S rRNA gene), and PCR2 attached sequencing adapters and sample barcodes. PCR1 used the following primer sets listed according to position and direction:

27F-1:ACACTGACGACATGGTTCTACAGT**AGAGTTTGATCCTGGCTCAG**;

27F-2:ACACTGACGACATGGTTCTACA*C*GT**AGAGTTTGATCATGGCTCAG**;

27F-3:ACACTGACGACATGGTTCTACA*AC*GT**AGAGTTTGATTCTGGCTCAG**;

27F-4:ACACTGACGACATGGTTCTACA*TAC*GT**AGAGTTTGATTCTGGCTCAG**;

533R-1:TACGGTAGCAGAGACTTGGTCT**TTACCGCGGCTGCTGGCAC**;

533R-2:TACGGTAGCAGAGACTTGGTCT*G***TTACCGCGGCTGCTGGCAC;**

533R-3:TACGGTAGCAGAGACTTGGTCT*TG***TTACCGCGGCTGCTGGCAC;**

533R-4:TACGGTAGCAGAGACTTGGTCT*ATG***TTACCGCGGCTGCTGGCAC.**

The underlined sequences denote universal tag sequences CS1 (ACACTGACGACATGGTTCTACA; tag on the forward primer) and CS2 (TACGGTAGCAGAGACTTGGTCT; tag on the reverse primer), bold sequences denote the universal 16S rRNA primers 27F and 533R, and the italicized bases denote the added bases to the template-specific primers in order to introduce variability of base calls during Illumina sequencing. For PCR2, the adapter primers included the Illumina-specific sequences P7 and P5 for dual indexing:

P7-CS2:

CAAGCAGAAGACGGCATACGAGAT*NNNNNNNN*TACGGTAGCAGAGACTTGGTCT

and

P5-CS1:

AATGATACGGCGACCACCGAGATCTACAC*NNNNNNNN*ACACTGACGACATGGTTCTACA, where the unique sequence barcodes were denoted by the 8 italicized N's, and the underlined sequences denote the universal sequences CS1 and CS2.

Amplicon concentrations were determined using the PicoGreen assay (Molecular Probes Inc., USA) and a fluorometer (SpectraMax Gemini XPS 96-well plate reader, Molecular Devices, Sunnyvale, CA). The amplicons were then pooled into a single tube in approximately equal amounts (~100 ng). The amplicon pool was then cleaned to remove short, undesirable fragments following the procedures previously reported (Dai *et al.*, 2015;

Liang *et al.*, 2015). Finally, sequences were obtained using an Illumina MiSeq paired-end 300 bp protocol (Illumina, Inc., San Diego, CA).

For sequence analysis and taxonomic classification, raw DNA sequence reads from the Illumina MiSeq were demultiplexed and subsequently processed to identify and assign reads by both expected barcode and primer sequences using the python application *dbcAmplicons* (https://github.com/msettles/dbcAmplicons). Briefly, barcodes were allowed to have at most one mismatch and primers were allowed to have at most 4 mismatches (as long as the final four bases of the primer matched the target sequence perfectly). Reads were then trimmed of their primer sequence and joined into a single amplicon sequence using the application *FLASH* (Magoč & Salzberg, 2011). Finally, the Ribosomal Database Project (RDP) Bayesian classifier was used to assign sequences to phylotypes (Wang *et al.*, 2007); reads were assigned to the first RDP taxonomic level with a bootstrap score ≥50. The relative abundance of individual phylotypes in each sampling event was determined as the percentage of the corresponding sequence reads among all sequence reads. The raw 16S rRNA gene sequencing data is available through the National Center for Biotechnology Information Short Reads Archive (http://www.ncbi.nlm.nih.gov/sra) accession number SRP065770. Microbial community data analysis was performed using *R v3.0.3* software (http://www.r-project.org/) using the *vegan* package.

3.3.6 Protein extraction, purification, and 2DE

To profile protein abundance during the SBR cycle, samples for 2DE analysis were collected at 1 h, 4.5 h, 11.5 h, 17.5 h, and 23.5 h from the start of the cycle (Figure 3.1). The 1 h sample represented activity within the feast phase of the SBR cycle, and the remaining samples represented activity within the famine phase of the SBR cycle. For the fed-batch proteome

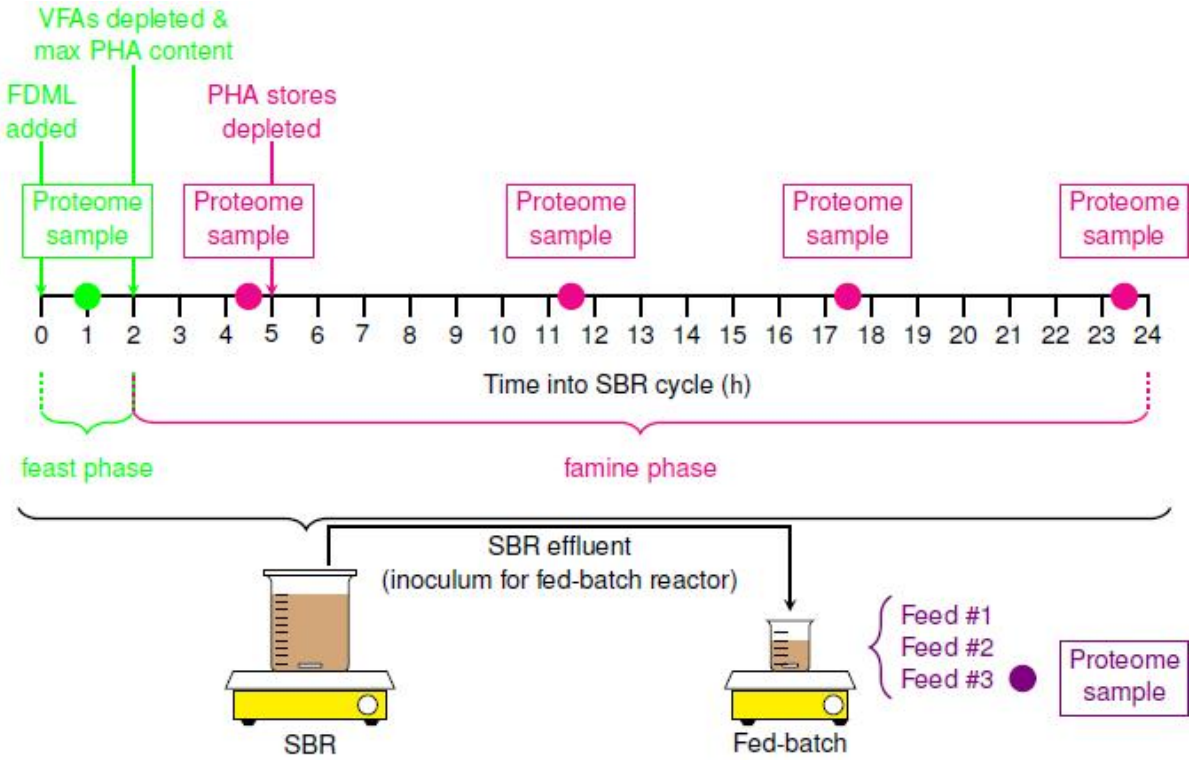

Figure 3.1. Proteomic sampling scheme for enrichment SBR and fed-batch reactor. Approximate times are shown for VFA depletion, maximum PHA content reached, and PHA stores depletion. The times at which proteome samples were taken during the SBR cycle are indicated by the solid circles. The proteome samples for the fed-batch PHA production assessment were taken approximately 1 h after the 3rd feedstock addition.

profiling, a sample was collected approximately 1 h after the third feedstock addition. The three sampling events therefore constitute three biological replicates for each time point.

Bacterial protein extraction from the biomass, purification, and 2DE were performed following methods previously described (Chapter 2). Briefly, bacterial cells were first separated from MMC biomass samples by Accudenz gradient centrifugation. Bacterial cell disruption and sequential protein extraction was performed by sonication and bead mill beating. Protein concentrations were determined using the RCDC Protein Assay (Bio-Rad, Hercules, CA) following the manufacturer's instructions using bovine serum albumin as the protein standard. Protein purification for 2DE was performed using the ReadyPrep 2DE Clean-Up Kit (Bio-Rad), and 400 µg of purified protein was loaded onto 7 cm immobilized pH gradient (IPG) strips with a pH range of 4-7 (Bio-Rad), which were passively rehydrated

for 16 h at 22°C. IPG strips were focused in a PROTEAN IEF Cell (Bio-Rad) at 250 V for 15 min, followed by linear ramping to 4,000 V in 2.5 h, after which 4,000 V was held for approximately 3.25 h (total of 13,000 V-h). Immediately following IEF, IPG strips were equilibrated and subjected to SDS PAGE for protein separation by molecular weight. After SDS PAGE, gels were washed twice in double-deionized H_2O for 5 min, fixed in ethanol/acetic acid/water (40:10:50, v/v) for 30 min, stained with Coomassie Brilliant Blue G-250 (Bio-Rad) for 20 h, and de-stained with double-deionized H_2O for several hours prior to imaging.

3.3.7 2DE gel image acquisition and statistical analysis

2DE gels were scanned using an Odyssey Imaging System (Li-COR Biosciences, Lincoln, NE) with the following settings: resolution, 42 µm; quality, medium; channel, 700 nm; and focus offset, 0.5. These settings generated 16 bit, 600 DPI images which were saved as TIFF files. Gel images were analyzed using *REDFIN 3 Solo* Software (Ludesi, Malmö, Sweden, http://www.ludesi.com). After image quality control checks were passed, anchor points were manually set on features shared by all gel images. The software was used to warp each of the gel images to a reference based on the shared anchor points, creating a composite image. Protein spot intensities were calculated with background correction and normalization to correct for systematic differences in gel intensity; replicate gel variability was assessed by constructing a correlation matrix based on the spot intensities using Pearson's product moment correlation coefficient (Wilmes & Bond, 2004). Using Figure 3.1 as a reference, the feast phase (1 h) was compared to the individual time points of the famine phase (4.5 h, 11.5 h, 17.5 h, and 23.5 h), and protein samples from the fed-batch PHA accumulation tests were compared to protein samples from the enrichment SBR; ANOVA was applied to determine

protein spots exhibiting statistically significant differential abundance (taken to be at least a 2-fold change in protein spot intensity with an accompanying p-value <0.05).

3.3.8 In-gel trypsin digestion, LC-MS/MS, and proteomic data analysis

Protein spots of interest were picked manually from gels using a 1.5 mm OneTouch Plus Spotpicker (The Gel Company, San Francisco, CA) with disposable tips and transferred to microfuge tubes. In-gel trypsin digestion was performed following procedures described (Shevchenko *et al.*, 2006) with modifications. Gel pieces were de-stained overnight with light shaking in approximately 500 µL 50% acetonitrile (v/v in H_2O) and 25 mM ammonium bicarbonate. The extract was discarded and 50 µL 100% acetonitrile was added to completely dehydrate the gel pieces. After the gel pieces became opaque, they were washed with 25 mM ammonium bicarbonate and dehydrated again by adding 50 µL acetonitrile; the acetonitrile was then evaporated. The dried gel pieces were rehydrated in an excess volume of 12.5 ng μL^{-1} sequencing grade trypsin (Promega, Madison, WI) solution for 1.5 h at 4°C. Excess trypsin solution was removed and a small volume (~25 µL) of 25 mM ammonium bicarbonate was added to cover the gel pieces to ensure no evaporation occurred for the duration of the enzymatic digestion. Gel pieces were then incubated for 16 h at 37°C. The water extracts were retained in LoBind 0.5 mL microcentrifuge tubes (Eppendorf, Hauppauge, NY), after which peptides were eluted from the gel pieces using 50% acetonitrile in water containing 0.1% formic acid with light vortexing for 15 min. Samples were centrifuged briefly and the extracts were retained. This step was repeated and extracts were concentrated using a SpeedVac until approximately 10 µL remained. Prior to analysis by liquid chromatography-tandem mass spectrometry (LC-MS/MS), approximately 10 µL of 5% acetonitrile with 0.1%

formic acid was added to the sample, which was then clarified by centrifugation at 16,000 × g for 10 min.

LC-MS/MS analysis followed previously reported methods (Bansal *et al.*, 2009; Checinska *et al.*, 2012) with minor modifications. Peptides were separated using reverse-phase LC on a nano-ACQUITY Ultra Performance Liquid Chromatograph (Waters Corporation, Milford, MA) prior to analysis using a QTOF Premier tandem mass spectrometry system equipped with a nano-electrospray ionization (ESI) source. A 2 µL sample was first loaded onto a Symmetry C18 trap column (0.18 by 20 mm) before separation using a BEH 130 C18 analytical column (0.075 by 200 mm; Waters Corporation). Two solvents were used: A, 0.1% formic acid in water; and B, 0.1% formic acid in acetonitrile. Peptides were trapped by 100% solvent A for 3 min with a flow rate of 10 µL min^{-1}. Separation was performed at 35°C at a flow rate of 0.4 µL min^{-1} with the following conditions: (i) isocratic, 1 min, 95% solvent A and 5% solvent B; (ii) gradient, 44 min, solvent A concentration gradually decreased from 95% to 50% and solvent B concentration increased from 5% to 50%; (iii) gradient, 5 min, solvent A concentration decreased to 10% and solvent B concentration increased to 90%; (iv) isocratic, 5 min, 10% solvent A and 90% solvent B; and (v) gradient, 5 min, solvent A concentration increased to 80% and solvent B concentration decreased to 20%. The nano-ESI source was operated with the following settings: capillary voltage, 3.7 kV; cone voltage, 30 V; source temperature, 120 °C; nebulizing gas pressure, 0.45 × 105 Pa; collision energy, 5.0 V; detector voltage, 1,825 V. The data acquisition was performed using MS survey mode with the following parameters: mass range, 300 to 2,000 Da; scan time, 1s; and interscan delay, 0.1 s. The threshold of MS/MS acquisition was 20 counts per second with the following settings: mass range, 50 to 2,000 Da; 3 ions selected from a single MS survey scan; scan time,

2 s; and interscan delay, 0.05 s. [Glu1]-fibrinopeptide B (Sigma-Aldrich, St. Louis, MO) was used for dynamic calibration (lockmass) with a 30 s frequency.

The raw data files from the peptide sequencing were converted to peak lists files by *ProteinLynx Global Server 2.3* software (Waters Corporation) using the following parameters: (i) smooth channels, 4; number of smooths, 2; smooth mode, Savitzy Golay; (ii) peak height to calculate the centroid spectra, 80%; (iii) baseline subtraction, none allowed; and (iv) peptide tolerance, 100 ppm. Mascot (v2.5, Matrix Science, London, United Kingdom) was used for MS/MS ions matching and protein identification. The peak list files were searched against the NCBInr database (October 2015; 73,055,898 protein sequences) with no species restriction and the following search parameters: (i) specific enzyme, trypsin; (ii) peptide window tolerance, ±0.4 Da; (iii) fragment mass tolerance, ±0.4 Da; (iv) missed cleavage sites, 1; and (v) variable modifications, carbamidomethyl C, deamidated NQ, and oxidized M. The decoy option was included for each search to determine the false discovery rate. For protein identification, protein hits with at least two peptide matches and individual protein scores above the significance score calculated by Mascot ($p < 0.05$; the individual ion score is $-10 \times \log(p)$, where p is the probability that the observed match is the random match) were accepted. In instances when more than one protein was assigned from a single protein spot (a well-established occurrence for 2DE (Thiede *et al.*, 2013)), the highest scoring protein was accepted. When a "hypothetical protein" was the highest scoring Mascot result, the corresponding protein accession number was searched using Blastp for homology based protein identification; the protein match with the highest percent similarity based on the number of identical amino acids to a known bacterial protein was considered for identification. The mass spectrometry proteomics data have been deposited to the ProteomeXchange

Consortium (http://proteomecentral.proteomexchange.org) via the PRIDE partner repository (Vizcaino *et al.*, 2013) with the dataset identifier PXD003126 and 10.6019/PXD003126.

3.4 Results

3.4.1 Enrichment SBR and fed-batch PHA performance

To induce a feast-famine response in the MMC, ADF conditions were applied to an enrichment SBR using fermented dairy manure as the feedstock. Shortly after SBR start-up (9 d), the DO began to exhibit the characteristic feast-famine profile (Beun *et al.*, 2002; Dionisi *et al.*, 2004; Serafim *et al.*, 2004). During the 2.5 month SBR stabilization period, VFA exhaustion from solution typically occurred within 2 h, and the maximum PHA content ranged from 4-14% (wt. basis; data not shown). The composition of the FDML during sampling is summarized in Table 3.1. Seven different VFAs were consistently identified in the FDML, with acetate and propionate dominating at 50% and 23%, respectively, of the total VFA content. In total, VFAs accounted for approximately 70% of the soluble COD (sCOD). The ammonia and phosphate concentrations were 24.2 mM ± 4.5, and 0.07 mM ± 0.03, respectively.

Representative profiles of select bulk solution parameters are depicted in Figure 3.2 (all sampling data is provided in Appendix B, Figures B.1-B.6). During the feast phase, VFA consumption was zero-order (Figure 3.2A), with acetate being consumed at the highest rate (average uptake rate for all three sampling events was 0.042 Cmmol HAc Cmmol X^{-1} h^{-1}) followed by propionate (average uptake rate for all three sampling events was 0.032 Cmmol

Table 3.1. Characterization of fermented dairy manure liquor.

Constituent[a]	Concentration[b]
HAc	43.2 mM ± 3.6
HPro	16.0 mM ± 1.1
HBu	9.7 mM ± 1.5
HiBu	1.6 mM ± 0.2
HVa	1.8 mM ± 0.2
HiVa	1.4 mM ± 0.2
HCa	0.6 mM ± 0.2
NH_3-N	24.2 mM ± 4.5
PO_4^{3-} -P	0.07 mM ± 0.03
COD	10,066 mg L^{-1} ± 1,287

[a] Abbreviations: HAc (acetic acid), HPro (propionic acid), HBu (butyric acid), HiBu (iso-butyric acid), HVa (valeric acid), HiVa (iso-valeric acid), and HCa (caproic acid)
[b] The concentration and standard deviation are listed; n=9 for all samples

HPro Cmmol X^{-1} h^{-1}). All measured VFAs were depleted within 2.5 h (which corresponded with the initial reduction of sCOD; Appendix B, Figure B.1), at which point the DO exhibited the first notable increase (Figure 3.2C). Shortly after VFA depletion, the maximum PHA content was observed (wt. basis; 8-16%; shown in Figure 3.2B as Cmmol PHA L^{-1}) the PHA yield ranged from 0.36-0.88 Cmmol PHA Cmmol VFA^{-1}) among the three sampling events. A copolymer of HB and HV was consistently synthesized with molar fractions (HB:HV) of 36:64, 38:62, and 34:66, observed at the maximum PHA content for Sampling #1, Sampling #2, and Sampling #3, respectively. Ammonia, nitrite, and nitrate consumption was also observed during the feast phase (Appendix B, Figure B.2), and the VSS concentrations remained approximately constant (Appendix B, Figure B.3). The pH decreased slightly with substrate addition to approximately 8.6, before increasing to approximately 9.1, and the temperature increased slightly (Appendix B, Figures B.4 and B.5, respectively).

The famine phase commenced with the exhaustion of VFAs and first notable increase in DO concentration. Within the famine phase, PHA stores were depleted 3-12 h after VFA exhaustion. The depletion of PHA corresponded to the next notable increase in DO

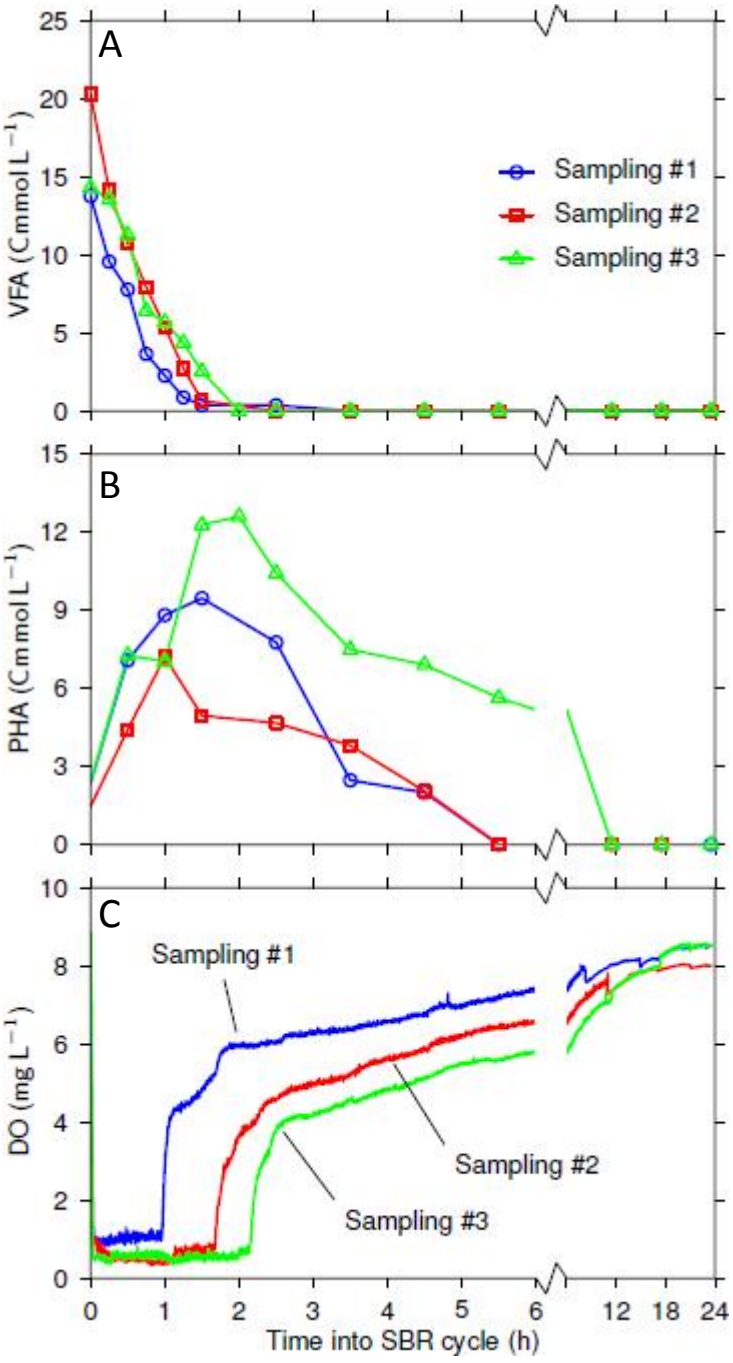

Figure 3.2. Concentration profiles of select bulk solution variables during SBR cycle. A) total VFAs; B) total PHA; and C) dissolved oxygen. Note the break and scale change in the abscissa at 6 h.

concentration (Figure 3.2C). Near-complete ammonia removal was realized by the end of the SBR cycle (Appendix B, Figure B.2; final concentrations ranged from 0.017-0.28 mM). Both nitrite and nitrate gradually increased during the famine phase (Appendix B, Figure B.2; final concentrations ranged from 1.04-4.36 mM and 0.41-1.01 mM for nitrite and nitrate,

respectively). Continuing from the end of the feast phase, sCOD and VSS remained approximately constant (Appendix B, Figures B.1 and B.3, respectively; final concentrations ranged from 875-1,242 mg L^{-1} for sCOD and 1,267-2,700 mg L^{-1} for VSS). After decreasing to approximately 8.5, the pH gradually increased to approximately 8.8, whereas the temperature slightly decreased (Appendix B, Figures B.4 and B.5, respectively).

For each of the enrichment SBR sampling events, a parallel fed-batch test was completed to assess the PHA production capacity of the enriched MMC. The maximum PHA content measured during the fed-batch tests ranged from 22-40% (wt. basis; shown as Cmmol PHA Cmmol VFA^{-1} in Appendix B, Figure B.6); the highest PHA content was achieved on Sampling #1 (40%). The PHA yield ranged from 0.55-1.14 Cmmol PHA Cmmol VFA^{-1}. Similar to the enrichment SBR, the copolymer PHBV was produced with molar fractions (HB:HV) of 23:77, 28:72, and 39:61 for Sampling #1, Sampling #2, and Sampling #3, respectively.

3.4.2 Microbial community analysis

To characterize the microbial composition of the MMC in the enrichment SBR, amplicons of the V1-V3 region of the 16S rRNA gene were sequenced and assigned to phylotypes. A total of 70,004 high quality sequences from the three sampling events (average of 23,334 reads per sample) were obtained from the raw data after Illumina sequencing; sequencing depth was considered sufficient for each sample based on rarefaction analysis (Appendix B, Figure B.7). An overview of the microbial community composition (from Sampling #1) is shown in Figure 3.3A (the other sampling events are displayed in Appendix B, Figures B.8 and B.9), and the best classification of phylotypes from all sampling events is

shown Figure 3.3B. A total of 24 bacterial phyla were identified in the MMC (Appendix B, Table B.1). *Proteobacteria* was the most abundant phylum (73-75%) for each sampling event, followed by *Bacteroidetes* (15-18%). Less abundant phyla included *Verrucomicrobia* (0.6-3%) and *Planctomycetes* (0.5-3%), *Actinobacteria* (1.2-1.8%), and *Chloroflexi* (0.7-1%). Eighteen minor (<1% of the abundance) bacterial phyla accounted for the approximately 1.5% remaining of the total abundance. At the class level, members of *Proteobacteria* were most abundant with *Alphaproteobacteria* (43-68%), *Betaproteobacteria* (5-21%), *Deltaroteobacteria* (1.5-9%), and *Gammaproteobacteria* (1-7%). Within *Bacterioidetes*, *Sphingobacteriia* was the most abundant class (10-11%), followed by *Flavobacteriia* (3-6%). Forty-one minor (<1% of the abundance) classes comprised the approximately remaining 3% of the abundance (Appendix B, Table B.2).

The number of phylotypes classified by the RDP was 217, 298, and 342 for Sampling #1, Sampling #2, and Sampling #3, respectively. The Shannon index (selected for its value as a general diversity measure considering both richness and evenness (Hill *et al.*, 2003)), values were 2.20, 3.31, and 3.00 for Sampling #1, Sampling #2, and Sampling #3, respectively. As shown in Figure 3.3B, *Meganema* was most abundant genus in all samples (31-61%). For Sampling #1, other genera included *Terrimonas* (4.6%) and *Thauera* (2.2%); minor phylotypes (< 1% of the abundance) comprised 15% of the abundance. For Sampling #2, other genera included *Thauera* (8%), *Nannocystis* (6%), *Flavitalea* (6%), *Hyphomonas* (2.7%), and *Terrimonas* (2.6%); minor phylotypes comprised 22% of the abundance. For Sampling #3, other genera included *Thauera* (12%), a member of *Flavobacteriales* (4.6 %), *Terrimonas* (3%), *Flavitalea* (2.7%), and *Nannocystis* (2%); minor phylotypes comprised 18% of the abundance.

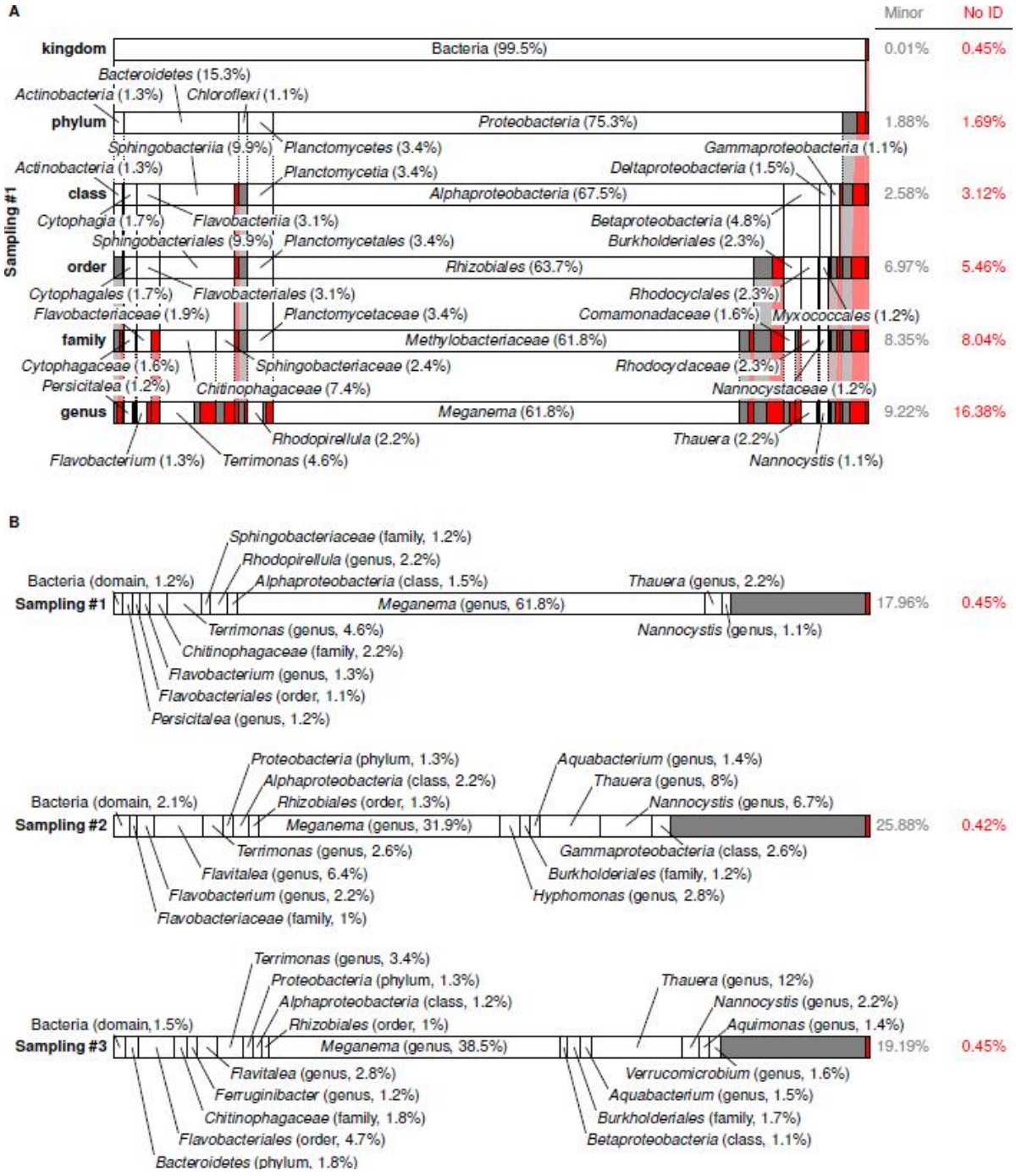

Figure 3.3. Relative abundance and taxonomic classification of the 16S rRNA gene sequencing results using the RDP. Relative abundance and taxonomic classification of the 16S rRNA gene sequencing results using the RDP. A) overview of taxonomic hierarchy (from Sampling #1); and B) the best classification of phylotypes for Sampling #1, Sampling #2, and Sampling #3. In both A and B, phylotypes which were not identified by the RDP or those whose identification at a specific taxonomic level was not statistically significant were aggregated, denoted "No ID", and depicted in red. Identified phylotypes with less than 1% of the total relative abundance were aggregated, denoted "Minor", and depicted in gray. Phylotypes with at least 1% relative abundance are labeled.

3.4.3 2DE analysis and proteomic profiling

To visualize and quantify changes in protein abundance under ADF conditions using FDML as a feedstock, 2DE was used to resolve protein mixtures from the MMC in the enrichment SBR at five time points during an operational cycle, as well as a single time point during the accompanying fed-batch PHA accumulation tests (Figure 3.1). The average protein concentrations in whole cell lysates ranged from 9.6-15.2 mg mL^{-1} (Appendix B, Figure B.10). An example set of 2DE gels (from Sampling #3; identified protein spots are shown in color) is shown in Figure 3.4; all other gels are shown in Appendix B, Figures B.11 and B.12. The resulting 2DE spot patterns for replicate gels exhibited strong correlation with coefficients ranging from 0.71-0.95 (Appendix B, Table B.3). As shown in Figure 3.4, protein spots were well-resolved, and horizontal streaking and diffuse background interference on the gels was minimal. The composite image of all 18 gels created using *REDFIN 3 Solo* software resulted in the detection of 712 protein spots. Protein spots exhibited a range of apparent molecular weights (~10-190 kDa) and isoelectric points in the pH 4-7 range.

In total, 90 protein spots were selected for LC-MS/MS proteomic analysis, 83 of which were successfully identified. Protein spot selection priority was given to protein spots that displayed high abundance across all gels and protein spots that exhibited large, statistically-significant abundance changes between the feast and famine phases, or between the SBR samples and fed-batch samples. In total, 157 proteins met the search criteria for acceptable protein identification from the 83 successfully analyzed protein spots (some spots had more than one identified protein). Of those, the 74 corresponding proteins corresponding to the prioritized protein spots are presented in Tables 3.2-3.5. Of all 157 proteins, 149 proteins

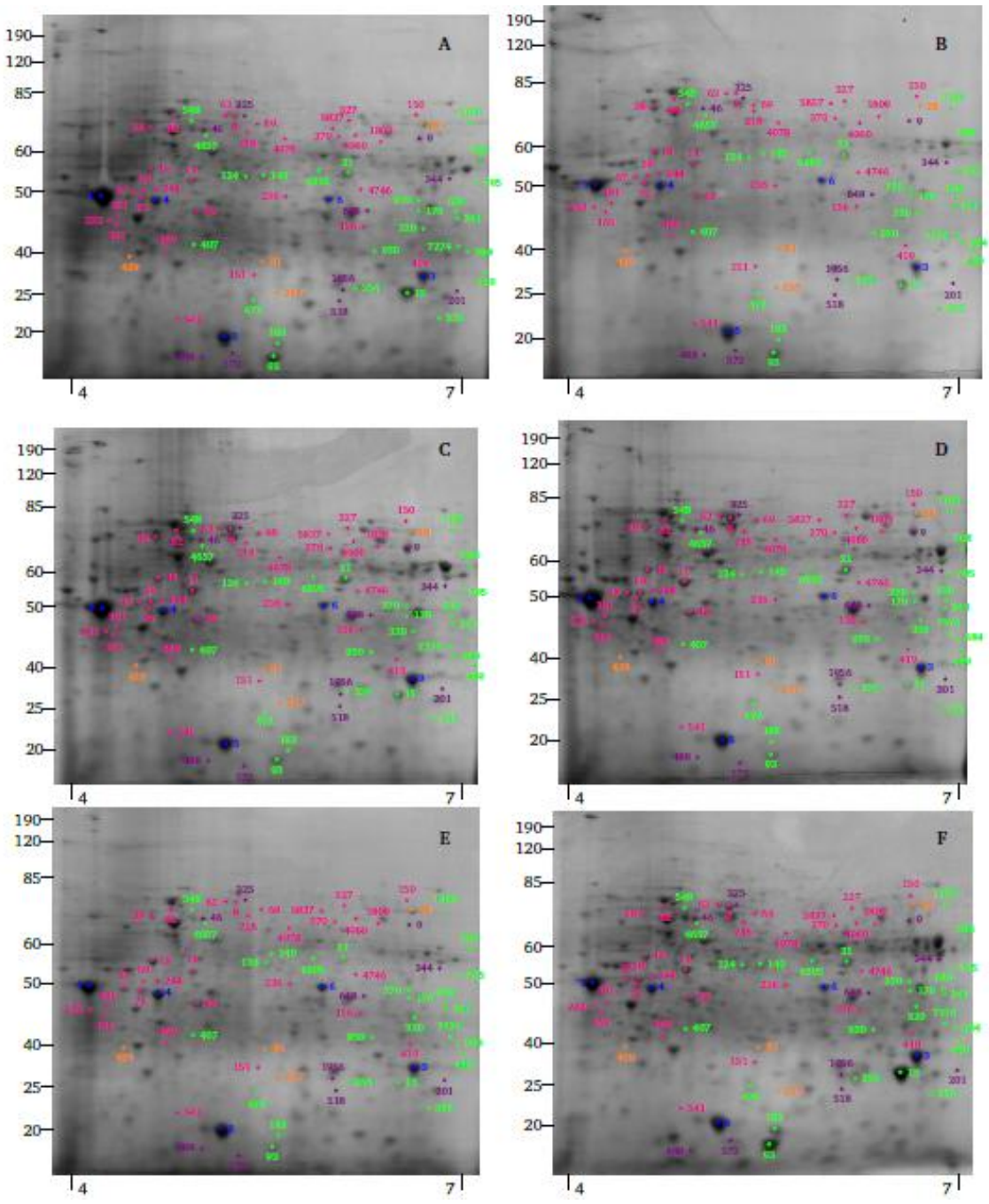

Figure 3.4. Representative 2DE gel images for SBR and fed-batch proteome profiling. Representative colloidal Coomassie-stained 2DE gel images for SBR and fed-batch MMC proteins. Gel images are from Sampling #3. A, B, C, D, and E represent the samples taken throughout the SBR cycle at 1 h, 4.5 h, 11.5 h 17.5 h, and 23.5 h, respectively; F represents the sample taken during the fed-batch PHA production assessment. The contrast for the 2DE gel images has been uniformly adjusted across all images. The molecular weight markers (kDa) and pH ranges are depicted on each 2DE gel image. The colored numbers highlight protein spots that were identified with the most abundant protein spots in blue, proteins exhibiting increased abundance during the feast phase in green, proteins exhibiting increased abundance during the famine phase in magenta, proteins exhibiting increased abundance in the fed-batch in violet, and proteins exhibiting increased abundance in the SBR in orange (respective proteins are listed in Tables 2-5 and the abundances are in Appendix B).

Table 3.2. Identification and functional characterization of the most abundant proteins observed on all 2DE gels. Spot numbers refer to those in Figure 3.4 that were excised from 2DE-gels, analyzed by LC-MS/MS, and identified by MS/MS ions searching using Mascot. When a "hypothetical protein" was the highest scoring protein result using Mascot, the protein accession number was searched using Blastp for homology based protein identification. Abbreviations: MW, the calculated molecular weight of the identified protein; pI, the calculated isoelectric point.

Spot	Protein name	Accession	Mascot score	No. peptides matched	MW	pI	General function
1	Porin*	WP_018631314	227	4	36221	4.53	Nutrient transport
3	Superoxide dismutase*	WP_018632695	209	4	21878	5.89	Reactive oxygen species destruction
4	Amino acid ABC transporter substrate-binding protein*	WP_018632268	722	8	37781	4.89	Nutrient transport
5	Bacterioferritin	WP_026310284	227	4	18528	4.95	Iron homeostasis
6	ABC transporter substrate-binding protein*	WP_018631899	614	9	39576	6.36	Nutrient transport

*Indicates a homology based protein identification of a hypothetical protein Mascot result made using Blastp (See Appendix B, Table B.6 for Blastp details)

Table 3.3. Identification and functional characterization of proteins exhibiting at least a 2-fold change increase in abundance during the feast phase relative to the famine phase. Spot numbers refer to those in Figure 3.4 that were excised from 2DE-gels, analyzed by LC-MS/MS, and identified by MS/MS ions searching using Mascot. The time during the SBR cycle at which the given spot number exhibited the fold-change listed is indicated. When a "hypothetical protein" was the highest scoring protein result using Mascot, the protein accession number was searched using Blastp for homology based protein identification. Abbreviations: MW, the calculated molecular weight of the identified protein; pI, calculated isoelectric point.

Spot	Fold-change	Time (h)	Protein name	Accession	Mascot Score	No. peptides matched	MW	pI	General function
341	3.3	23.5	Isocitrate dehydrogenase	WP_018631946	237	4	44956	6.04	Energy generation and conversion
407	3.8	23.5	Aldehyde dehydrogenase	WP_018633284	302	4	55302	6.14	Energy generation and conversion
584	8.5	23.5	Malate dehydrogenase	WP_018631935	82	2	33324	5.49	Energy generation and conversion
636	3.0	17.5	Isocitrate dehydrogenase§	WP_003813356	145	2	45249	5.24	Energy generation and conversion
950	5.3	11.5	Methylmalonate-semialdehyde dehydrogenase*	WP_018632449	142	2	54008	5.94	Energy generation and conversion
1196	3.9	17.5	Aldehyde dehydrogenase	WP_018633284	433	7	55302	6.14	Energy generation and conversion
7274	3.2	4.5	Malate dehydrogenase§	WP_020951282	189	3	33433	5.34	Energy generation and conversion
21	3.1	23.5	Acetyl-CoA acetyltransferase	WP_018631634	711	9	40685	5.97	PHA synthesis
15	6.7	23.5	Phasin*	WP_018634051	493	7	18623	5.80	PHA synthesis
93	4.2	17.5	Phasin*	WP_018634051	468	7	18623	5.80	PHA synthesis
183	5.4	23.5	Phasin*	WP_018634051	348	6	18623	5.80	PHA synthesis
354	6.3	23.5	Phasin*	WP_018634051	520	7	18623	5.80	PHA synthesis
472	4.5	23.5	Phasin*	WP_018634051	213	4	18623	5.80	PHA synthesis
568	4.1	23.5	Acetyl-CoA acetyltransferase	WP_018631634	545	8	40685	5.97	PHA synthesis
124	4.3	17.5	Elongation factor Tu	WP_018631570	627	11	43422	5.42	Translation
140	2.8	4.5	Elongation factor Tu	WP_018631570	369	7	43422	5.42	Translation
449	17.6	23.5	50S ribosomal protein L6	WP_018631584	138	2	21182	9.21	Translation
6395	3.5	11.5	Elongation factor Tu	WP_018631570	286	5	43422	5.42	Translation

*Indicates a homology based protein identification of a hypothetical protein Mascot result made using Blastp (See Appendix B, Table B.6 for Blastp details)
§Indicates Mascot taxonomy other than *Meganema perideroedes* (See Appendix B, Table B.5 for taxonomy)

Table 3.3 continued. Identification and functional characterization of proteins exhibiting at least a 2-fold change increase in abundance during the feast phase relative to the famine phase.

Spot	Fold-change	Time (h)	Protein name	Accession	Mascot Score	No. peptides matched	MW	pI	General function
548	3.3	17.5	Molecular chaperone GroEL	WP_018633070	184	4	57962	5.05	Posttranslation protein modification
4657	3.4	23.5	Molecular chaperone GroEL	WP_018633070	214	5	57962	5.05	Posttranslation protein modification
270	2.2	17.5	Malyl-CoA lyase*	WP_018632386	137	3	34755	5.82	Carbohydrate metabolism
170	3.2	23.5	Translocation protein TolB	WP_026310348	182	4	47660	9.4	Intracellular trafficking
320	4.1	4.5	2,5-didehydrogluconate reductase*	WP_018633267	566	7	30332	5.81	Ketogluconate metabolism
552	5.8	11.5	Pentapeptide repeat-containing protein*	WP_018634194	116	3	21188	5.86	Uncharacterized
795	9.7	23.5	Membrane protein	WP_018634320	126	3	35466	6.05	Uncharacterized

* Indicates a homology based protein identification of a hypothetical protein Mascot result made using Blastp (See Appendix B, Table B.6 for Blastp details)

were assigned to *Meganema perideroedes*, 69 of which were hypothetical proteins; upon using Blastp for homology-based identification, 49 of the hypothetical proteins were matched with >50% amino acid identity to known bacterial proteins (the 20 remaining proteins were matched with 31-49% amino acid identity). Generally, the observed molecular weight and isoelectric points of the selected protein spots were in agreement with calculated values. Five highly-abundant protein spots, each observed with an individual average normalized volume >1% of the total spot volume on all 18 gels were first selected for identification. In order of average abundance of each protein spot on all gels, these proteins were identified as a porin, manganese superoxide dismutase, bacterioferritin, and two ABC amino acid transporters (Table 3.2).

Considering the feast phase, 28, 30, 44, and 33 proteins exhibited statistically-significant abundance increases relative to the famine phase samples at 4.5 h, 11.5 h, 17.5 h, and 23.5 h, respectively. In total, 25 protein spots from the feast phase were identified (Table 3.3). Of particular interest, PHA synthesis-related proteins, namely, acetyl-CoA acetyltransferase and a phasin protein were identified. Other identified proteins in increased abundance during the feast phase included three associated with protein synthesis, two TCA cycle enzymes, two uncharacterized membrane proteins, aldehyde dehydrogenase, methylmalonate-semialdehyde dehydrogenase, malyl-CoA lyase, 2,5-didehydrogluconate reductase, and translocation protein TolB. Evaluating functionally related feast phase proteins over the SBR cycle (Appendix B, Figures B.19-B.38), acetyl-CoA acetyltransferase and phasin proteins generally decreased in abundance until the end of the cycle (23.5 h). Both TCA cycle enzymes appeared to decrease at 4.5 h and then remain approximately constant until the end of the cycle. Translation proteins (elongation factor Tu and 50S ribosomal

protein L6) appeared to decrease at 4.5 h and then remain approximately constant for the rest of the cycle; molecular chaperone GroEL appeared to steadily decrease until the end of the cycle. Other PHA synthesis-related proteins (i.e., NADPH-dependent acetoacetyl-CoA reductase and PHA synthase) were detected (Appendix B, Table B.5); however, the abundance and temporal characteristics were not immediately determined.

For the famine phase, 24, 19, 25, and 13 proteins exhibited increased abundance at 4.5 h, 11.5 h, 17.5 h, and 23.5 h compared to the feast phase (1 h), respectively. In total, 30 protein spots arising from the famine phase were identified (Table 3.4). Identified proteins included ten ABC transporters, four enzymes associated with acyl-CoA metabolism, three proteins associated with nucleotide metabolism, two subunits of the ATP synthase complex, Fis family transcriptional regulator, quinone oxidoreductase, aldehyde dehydrogenase, quinohemoprotein amine dehydrogenase, glycerol kinase, fumarate hydratase, molecular chaperone GroEL, and an uncharacterized membrane protein. Evaluating the abundance of functionally related famine phase proteins over the SBR cycle (Appendix B, Figures B.44-B.71), most of the ABC transport proteins appeared to steadily increase as the famine progressed, with the highest abundance occurring at 23.5 h. Other protein groups (e.g., proteins involved in acyl-CoA metabolism, housekeeping functions, and energy production) did not necessarily appear to exhibit a common trend similar to the ABC transporters.

Table 3.4. Identification and functional characterization of proteins exhibiting at least a 2-fold change increase in abundance during the famine phase relative to the feast phase. Spot numbers refer to those in Figure 3.4 that were excised from 2DE-gels, analyzed by LC-MS/MS, and identified by MS/MS ions searching using Mascot. The time during the SBR cycle at which the given spot number exhibited the fold-change listed is indicated. When a "hypothetical protein" was the highest scoring protein result using Mascot, the protein accession number was searched using Blastp for homology based protein identification. Abbreviations: MW, the calculated molecular weight of the identified protein; pI, calculated isoelectric point.

Spot	Fold-change	Time (h)	Protein name	Accession	Mascot Score	No. peptides matched	MW	pI	General function
38	5.0	11.5	Quinohemoprotein amine dehydrogenase*	WP_018634151	170	4	55372	4.81	Energy production and conversion
69	3.3	11.5	Glycerol kinase*	WP_018632171	265	6	54320	5.29	Energy production and conversion
469	2.3	23.5	F0F1 ATP synthase subunit beta	WP_018631700	313	7	50791	4.79	Energy production and conversion
1809	3.3	11.5	Fumarate hydratase	WP_018633280	211	4	49297	5.74	Energy generation and conversion
4746	3.4	11.5	Quinone oxidoreductase	WP_018632319	220	4	35673	5.53	Energy production and conversion
4960	2.6	4.5	F0F1 ATP synthase subunit alpha§	WP_004261865	288	5	55268	5.59	Energy production and conversion
150	2.4	4.5	Acetyl-CoA synthetase	WP_018631372	169	3	70657	5.88	Lipid transport and metabolism
151	2.3	11.5	Acetyl-CoA acetyltransferase	WP_018631634	328	2	40685	5.97	Lipid transport and metabolism
327	2.5	11.5	Propionyl-CoA synthetase	WP_018632631	178	4	68489	5.73	Lipid transport and metabolism
541	9.4	11.5	Succinyl-CoA:3-ketoacid-CoA transferase	WP_018634294	100	2	22360	4.69	Lipid transport and metabolism
11	3.4	17.5	Sulfate transporter subunit*	WP_018634284	672	7	36835	4.91	Nutrient transport
13	2.3	23.5	ABC transporter permease	WP_018632451	533	7	42583	4.83	Nutrient transport
37	4.6	23.5	ABC transporter substrate-binding protein*	WP_018633424	896	11	38323	4.72	Nutrient transport
59	5.8	17.5	ABC transporter substrate-binding protein*	WP_018633424	577	9	38323	4.72	Nutrient transport

* Indicates a homology based protein identification of a hypothetical protein Mascot result made using Blastp (See Appendix B, Table B.6 for Blastp details)
§Indicates taxonomy other than *Meganema perideroedes* (See Appendix B, Table B.5 for taxonomy)

Table 3.4 continued. Identification and functional characterization of proteins exhibiting at least a 2-fold change increase in abundance during the famine phase relative to the feast phase.

Spot	Fold-change	Time (h)	Protein name	Accession	Mascot Score	No. peptides matched	Mr	pI	General function
82	3.4	23.5	ABC transporter substrate-binding protein	WP_040789902	406	7	57296	4.8	Nutrient transport
156	2.5	23.5	ABC transporter substrate-binding protein*	WP_018631899	180	3	39576	6.36	Nutrient transport
165	2.6	17.5	Amino acid ABC transporter*	WP_018632269	258	4	37330	4.69	Nutrient transport
181	4.1	17.5	Amino acid ABC transporter*	WP_018632269	408	7	37330	4.69	Nutrient transport
232	6.2	23.5	ABC transporter substrate-binding protein*	WP_018633993	339	6	33128	4.53	Nutrient transport
236	2.8	23.5	ABC transporter substrate-binding protein*	WP_018631899	117	3	39576	6.36	Nutrient transport
244	2.6	4.5	Amino acid ABC transporter*	WP_018632268	481	8	37781	4.89	Nutrient transport
370	4.2	11.5	TelA*	WP_018632854	296	6	45037	5.48	Inorganic ion transport and metabolism
75	2.8	23.5	Multifunctional 2'3'-cyclic-nucleotide 2'phosphodiesterase	WP_018631853	801	10	58603	4.72	Nucleotide transport and metabolism
8	6.3	17.5	Molecular chaperone GroEL	WP_018633070	1441	19	57962	5.05	Posttranslation protein modification
63	4.4	11.5	Molecular chaperone GroEL	WP_018633070	909	15	57962	5.05	Posttranslation protein modification
218	3.4	17.5	Molecular chaperone GroEL	WP_018633070	574	8	57962	5.05	Posttranslation protein modification
4978	5.4	11.5	Molecular chaperone GroEL	WP_018633070	265	5	57962	5.05	Posttranslation protein modification
5837	3.9	17.5	Sigma-54-dependent Fis family transcriptional regulator	WP_018633103	80	2	53526	5.41	Signal transduction
419	2.0	23.5	Elongation factor Tu	WP_018631570	154	2	43422	5.42	Translation
42	2.0	23.5	Membrane protein*	WP_018633522	623	9	34894	5.00	Uncharacterized

* Indicates a homology based protein identification of a hypothetical protein Mascot result made using Blastp (See Appendix B, Table B.6 for Blastp details)

Table 3.5. Identification and functional characterization of proteins exhibiting at least a 2-fold increase in abundance in the fed-batch PHA production reactor or in the SBR. Spot numbers refer to those in Figure 3.4 that were excised from 2DE gels, analyzed by LC-MS/MS, and identified by MS/MS ions searching using Mascot. Proteins in increased abundance during fed-batch PHA production relative to all SBR samples are in the top panel of the table; proteins in increased abundance in all SBR samples relative to the fed-batch PHA production are in the bottom panel of the table.

Spot	Fold-change	Protein name	Accession	Mascot Score	No. peptides matched	MW	pI	General function
Fed-batch								
9	2.2	F0F1 ATP synthase subunit alpha	WP_018631697	139	3	55571	5.7	Energy production and conversion
488	6.4	ATP synthase epsilon chain*	WP_018631701	177	2	13935	4.89	Energy production and conversion
518	2.9	Methylmalonate-semialdehyde dehydrogenase*	WP_018632449	151	2	54008	5.94	Energy production and conversion
648	5.2	Malate dehydrogenase	WP_018631935	131	2	33324	5.49	Energy production and conversion
201	9.1	Phasin*	WP_018634051	196	3	18623	5.80	PHA synthesis
344	2.3	Phasin*	WP_018634051	311	6	18623	5.80	PHA synthesis
572	2.1	Phasin*	WP_018634051	334	6	18623	5.80	PHA synthesis
1956	3.2	Phasin*	WP_018634051	486	8	18623	5.80	PHA synthesis
46	2.0	ABC transporter substrate-binding protein*	WP_018633957	344	7	54148	4.96	Nutrient transport
325	2.3	Molecular chaperone GroEL	WP_018633070	981	14	57962	5.05	Posttranslation protein modification
SBR								
28	2.4	Dihydrolipoamide dehydrogenase*	WP_018632931	537	8	48291	5.79	Energy production and conversion
81	2.8	Adenylate kinase	WP_018631593	240	4	22738	5.46	Energy production and conversion
429	23.5	Amino acid ABC transporter substrate-binding protein	WP_018632268	366	5	37781	4.89	Nutrient transport
257	2.1	Transcription termination/antitermination factor NusG	WP_018631560	126	3	20049	5.16	Transcription

* Indicates a homology based protein identification of a hypothetical protein Mascot result made using Blastp (See Appendix B, Table B.6 for Blastp details)

Finally, comparing the fed-batch to the SBR samples, 19 protein spots exhibited statistically significant increases in abundance the fed-batch compared to the SBR; of these proteins spots, 10 were selected for LC-MS/MS analysis, resulting in the identification of seven unique proteins (Table 3.5). Identified proteins included a phasin, an ABC transporter, two subunits of ATP synthase, malate dehydrogenase, methylmalonate-semialdehyde dehydrogenase, and molecular chaperone GroEL. Inverting the comparison (i.e., the SBR samples relative to the fed-batch reactor samples), six proteins were in higher abundance in all of the SBR samples compared to the fed-batch PHA production reactor. Of those, four were selected for LC-MS/MS analysis and identified (Table 3.5) as adenylate kinase, dihydrolipoamide dehydrogenase, an amino acid transporter, and a protein involved in transcription.

3.5 Discussion

3.5.1 Enrichment SBR and fed-batch performance

The primary purpose of this research was to investigate proteome dynamics of an MMC exhibiting a feast-famine PHA synthesis response when cultivated on a fermented waste feedstock. In this regard, fermented dairy manure represents a novel feedstock for multi-stage PHA production using MMC. Indeed, the establishment of a feast-famine response using this feedstock and the applied ADF conditions was validated through the observed bulk solution changes (e.g., VFA uptake, DO profile, PHA synthesis and mobilization). Bulk solution parameters including VFA consumption rates, maximum PHA content, and PHA production yields in the enrichment SBR were in line with other studies using fermented waste feedstocks (Morgan-Sagastume *et al.*, 2010; Oehmen *et al.*, 2014)

(0.25-0.35 Cmmol VFA Cmmol X^{-1} h^{-1}, 4-25% PHA, and 0.43-0.79 Cmmol PHA Cmmol VFA^{-1}, respectively). Consistent with VFA uptake, sCOD was consumed during the feast phase; however, sCOD remained approximately constant during the famine phase, suggesting the residual sCOD was either recalcitrant, or too slowly biodegradable to be consumed within the SBR cycle. Thus, even though non-VFA carbon sources were not monitored, the results suggested the FDML substrate was VFA-dominated.

PHA accumulation in a fed-batch reactor was evaluated to assess the overall PHA production capacity of the enriched MMC. The maximum PHA content reached in this study (40% wt. basis) was in range of other studies using waste feedstocks, including tomato cannery wastewater (~20%) (Liu *et al.*, 2008) and fermented paper mill effluent (~48%) (Bengtsson *et al.*, 2008), although lower compared to other fermented feedstocks such as molasses (~60%) (Albuquerque *et al.*, 2013) or paper mill wastewater (~77%) (Jiang *et al.*, 2012). The PHA yield in the fed-batch tests was generally lower compared to previous studies using fermented waste feedstocks (0.62-0.80) (Albuquerque *et al*., 2013; Jiang *et al*., 2013), although the PHA yield observed for Sampling #1 (1.14) indicated non-VFA substrates contributed to PHA accumulation. Comparing the aforementioned intracellular PHA content and production yield values reported in the literature to this research suggests further optimization of the enrichment SBR operated herein is possible. Nevertheless, PHA accumulation in the fed-batch reactor exceeded that in the enrichment SBR in all three sampling events, which, combined with the observed feast-famine response, indicated that the enriched MMC was an appropriate candidate for microbial community and proteomic profiling.

3.5.2 Microbial community profile

The value of high-throughput 16S rRNA gene sequencing applied to an MMC cultivated on a waste feedstock was demonstrated in this study, as a comprehensive characterization of the microbial community was obtained. Overall, the microbial composition of the MMC at the genus level differed from other ADF enrichment investigations. The most abundant genus identified (*Meganema*), has been observed in another ADF enrichment SBR (Majone *et al.*, 2006); however, the high abundance of *Meganema* in this study was in contrast to more commonly reported dominant genera including *Thauera* (Albuquerque *et al.*, 2013; Carvalho *et al.*, 2013; Lemos *et al.*, 2008), *Azoarcus* (Bengtsson *et al.*, 2010a; Bengtsson *et al.*, 2010b; Waller *et al.*, 2012), or *Plasticicumulans* (Jiang *et al.*, 2011; Jiang *et al.*, 2012; Marang *et al.*, 2013). Furthermore, some of the PHA-producing genera identified in this study such as *Nannocystis, Hyphomonas,* and *Rhodopirellula* have not been reported in other ADF investigations involving waste feedstocks. The number of taxa identified in this study was also higher compared to previous studies, and the microbial diversity (based on the Shannon index) was higher than that reported for an ADF enrichment SBR cultivated on fermented molasses (≤ 1.0) (Carvalho *et al.*, 2013). High-throughput sequencing may have revealed a more diverse MMC in this study, but additional possible explanations for the dissimilarity in microbial composition include different inoculum sources, feedstock composition, and applied operating conditions. Interestingly, despite the marked differences in microbial composition in this study relative to others, a similar feast-famine response was observed in the SBR. This observation suggests the microbial composition may not be the strongest determinant in eliciting a feast-famine response, but rather the functional capabilities of the taxa present is more pertinent.

To explore potential implications of the microbial composition with respect to functional observations, the major phylotypes comprising at least 1% of the relative abundance during the sampling events were further scrutinized. Though not all phylotypes were assigned to a species level, the physiological capabilities of subordinate taxa may be used to corroborate the observed bulk solution changes and attribute activities to different populations within the MMC. More than half of the major phylotypes have at least one member known to possess either one, a combination of, or all of the following capabilities: VFA assimilation, PHA synthesis, or denitrification (at least one step). This assessment indicates that bulk solution changes were likely catalyzed collectively by several individual populations. Specifically, the capabilities of the most abundant genus identified (*Meganema*) may be evaluated by considering one species in the RDP database, namely *M. perideroedes*, as a proxy. *M. perideroedes* is a filamentous organism that was identified in activated sludge (Thomsen *et al.*, 2006) and was shown to exhibit rapid substrate uptake (including acetate, propionate, and butyrate) using various electron acceptors (oxygen, nitrite, and nitrate) in addition to a high PHA-accumulation capacity (Kragelund *et al.*, 2005; Thomsen *et al.*, 2006). These metabolic characteristics of *M. perideroedes*, coupled with the presence of *Thauera* (a genus also known for its metabolic versatility) align with the observed bulk solution changes.

The impact of the microbial composition of the enriched MMC on fed-batch PHA production is of particular importance for overall process success. The maximum PHA content and PHA yield achieved in the fed-batch tests corresponded to the MMC composition with the lowest species richness and diversity (Sampling #1), whereas the lowest maximum PHA content and PHA yield corresponded to the MMC with the highest species richness (Sampling #3). Indeed, some of the highest maximum PHA contents achieved (75% - 80%

PHA for waste feedstocks (Albuquerque *et al.*, 2010; Carvalho *et al.*, 2013) and upwards of 90% PHB for synthetic substrates (Jiang *et al.*, 2011; Johnson *et al.*, 2009)) have involved MMC enrichments with low microbial diversity. These observations suggest lower microbial diversity in enriched MMCs is favorable for fed-batch PHA production. A common explanation for this correlation may be the additional populations in more diverse MMCs do not significantly contribute to PHA production, thereby reducing the maximal PHA content and PHA yield (Jiang *et al.*, 2012; Queiros *et al.*, 2014; Tamis *et al.*, 2014). If this explanation holds, the use of high-throughput 16S rRNA gene sequencing may provide a useful means of assessing overall PHA process performance given the superior microbial community characterization.

3.5.3 Proteome profile

The high resolving power of 2DE coupled with LC-MS/MS can provide useful information concerning the functionality of MMCs in engineered systems. Overall, the quality of the 2DE gels and number of protein spots resolved in this study were comparable to other studies involving processes with complex MMCs, such as enhanced biological phosphorus removal (Wilmes *et al.*, 2008) and anaerobic digestion (Hanreich *et al.*, 2013). The high number of protein assignments to *Meganema perideroedes* substantiated the abundance of the genus as revealed by the 16S rRNA gene sequencing. However, the detection of proteins from other taxa may have been impeded by the lack of genome sequences available for many of the genera identified, coupled with potential biases related to the protein extraction procedure or 2DE towards proteins arising from the most abundant species

(Holmsgaard *et al.*, 2011; Jehmlich *et al.*, 2010). Nevertheless, proteins of physiological relevance to the functional response of the MMC to ADF conditions were identified.

3.5.3.1 Highly abundant proteins

Proteins in high abundance were expected to have principal physiological roles in the MMC and were therefore of interest for identification. The consistently high abundance of porin proteins may be explained by the necessity to sustain nutrient (small molecules <1000 Da; e.g., ions, carbohydrates, peptides, signaling molecules, etc.) diffusion and transport into the cell (Koch, 1990; Koch, 1997; Konopka, 2000), which was further supported by the high abundance of two amino acid transporters. The high abundance of superoxide dismutase throughout the SBR cycle was consistent with the need to destroy superoxide anion radicals generated under fully aerobic conditions (White, 2007). The high abundance of bacterioferritin may have contributed to the destruction of the hydrogen peroxide produced by superoxide dismutase, since these iron storage proteins exhibit ferroxidation chemistry, in addition to contributing to iron homeostasis (Chiancone *et al.*, 2004).

3.5.3.2 Feast phase proteins

The identification of proteins integral to PHA synthesis during the feast phase corroborated central concepts concerning VFA uptake and PHA synthesis under ADF conditions. The increased abundance of acetyl-CoA acetyltransferase (also referred to as β-ketothiolase) was logical, as this enzyme catalyzes the first step of polyhydroxybutyrate synthesis via the condensation of two acetyl-CoA moieties to yield acetoacetyl-CoA (the precursor to HB) (Steinbüchel & Schlegel, 1991). This enzyme may have also been involved in the condensation of acetyl-CoA and propionyl-CoA to yield 3-ketovaleryl-CoA (the precursor to HV). The presence of this enzyme for the entire SBR cycle (Appendix B, Figure

B.20 and B.25) was in accordance with pure culture studies reporting the enzyme's constitutive expression (Brigham *et al.*, 2012; Lawrence *et al.*, 2005) and known involvement in other metabolic pathways. In fact, a basal level of acetyl-CoA acetyltransferase at the end of the SBR cycle may be advantageous to PHA-producing bacteria, as PHA synthesis could be initiated quickly upon the start of the next feast phase. Coupled with the detection of peptides from NADPH-dependent acetoacetyl-CoA reductase and PHA synthase (Appendix B, Table B.5), experimental evidence to support the PHA biosynthetic capability in MMC cultivated under ADF conditions was obtained.

Also aligning with the observed PHA synthesis was the detection of multiple phasin proteins - structural proteins that envelope the surface of PHA granules (Potter & Steinbüchel, 2005). Distinct phasin proteins (Potter *et al.*, 2004; Wieczorek *et al.*, 1995) and phasin isoforms (Smit *et al.*, 2012) have been identified in pure cultures. Furthermore, phasins have been shown to perform diverse functions including preventing PHA granule coalescence upon contact with the cytoplasm (Wieczorek *et al.*, 1995), regulating of the size and number of PHA granules (Kuchta *et al.*, 2007), and displaying chaperone-like protection from heat and superoxide stress (Mezzina *et al.*, 2015). Considering some of the phasin protein spots displayed markedly different isoelectric points (up to approximately one pH unit), the possibility arises that some of the phasin proteins identified were unique, exhibiting differential functionality in catabolic or anabolic processes. Apart from roles in PHA synthesis, phasin proteins have been shown to be involved in PHA degradation (Kuchta *et al.*, 2007). Accordingly, phasin iso-forms in the MMC may have functioned in modulating the trafficking of PHA monomers or oligomers across the PHA granule surface, making them available for other metabolic processes. Finally, given the high abundance of the phasin

proteins but gradual decrease throughout the SBR cycle, phasins may have also served as an endogenous source of amino acids during the famine phase, suggesting the ecological importance of PHA in MMC cultivated under ADF conditions may extend beyond a storage medium for carbon and reducing equivalents.

The proteomic investigation reinforced additional functional responses observed and often inferred during the feast phase. Specifically, enzymes supporting simultaneous respiration of carbon substrates concurrent with PHA synthesis were detected (i.e., isocitrate dehydrogenase, malate dehydrogenase, malyl-CoA lyase, and aldehyde dehydrogenase). Related to cellular respiration and PHA synthesis, the generation of anabolic reducing equivalents during the feast phase was expected. Indeed, NADPH, the electron carrier supplying reducing equivalents to PHA, could have been generated by the reaction catalyzed by isocitrate dehydrogenase (isocitrate + $NADP^+$ <=> α-ketoglutarate + CO_2 + NADPH + H^+) (White, 2007) as well as by the activity of 2,5-didehydrogluconate reductase (2-keto-D-gluconic acid + $NADP^+$ <=> 2,5-didehydro-D-gluconate + NADPH + H^+) (Khurana *et al.*, 2000), among other pathways. Additionally, the detection of proteins involved in protein synthesis (50S ribosomal protein L6, elongation factor Tu, chaperone GroEL) in increased abundance during the feast phase supported simultaneous growth occurring with PHA synthesis.

Finally, the detection of methylmalonate-semialdehyde dehydrogenase during the feast phase was intriguing, as this enzyme can generate acetyl-CoA and propionyl-CoA (PHBV precursors) from malonate semialdehyde and methylmalonate semialdehyde, respectively, which are intermediates of valine degradation (Bannerjee *et al.*, 1970). PHBV synthesis in a pure culture has been reported wherein a mutant overproduced valine in the presence of

sufficient ammonia (Steinbüchel & Pieper, 1992), suggesting valine may be a suitable precursor for PHBV synthesis in MMCs. Though the presence of valine in the FDML was undetermined, supplementing waste feedstocks with valine may offer a strategy to increase the HV content of PHA, and thus improve polymer material properties (Dekoning, 1995). Regarding the remaining proteins in increased abundance during the feast (translocation protein TolB, pentapeptide repeat, and an uncharacterized membrane protein), possible relevance of these proteins in the feast is difficult to deduce although TolB may have played a role in maintaining outer membrane integrity or possibly in the assembly of porin proteins (Lazzaroni *et al.*, 1999).

3.5.3.3 Famine phase proteins

The ability to sequester nutrients and use stored substrates to support growth and cellular maintenance during the famine phase is a critical aspect of the MMC functional response to ADF conditions. In this regard, the detection of ABC transporters in 10 discrete protein spots, many of which increased in abundance as the SBR cycle progressed (Appendix B, Figures B.44-B.54), supported the importance of nutrient scavenging during the famine phase. Exogenous amino acids may have been scarce since four of the assigned ABC transporters were specific for amino acids, and an enzyme involved in serine biosynthesis (D-3-phosphoglycerate dehydrogenase) was detected. Extending to ADF systems in general, apart from the value of obtaining nutrients to support growth and cellular maintenance during the famine phase, the presence of many solute transporters in high abundance at the end of an SBR cycle provides an additional explanation for the rapid substrate uptake in the subsequent feast phase. Previous descriptions concerning the feast phase have noted PHA storage facilitates rapid substrate uptake (Johnson *et al.*, 2009; Reis *et al.*, 2003; van Loosdrecht *et*

al., 1997). However, the results presented herein suggest transport proteins may be important in facilitating rapid substrate uptake.

Another central concept concerning the functional response to ADF conditions includes the mobilization of PHA stores to support growth and cellular maintenance that occur during the famine phase. The increased abundance of acetyl-CoA synthetase, propionyl-CoA synthetase, and succinyl-CoA:3-ketoacid-CoA transferase corresponded with the observed PHA depletion. As PHA was hydrolyzed, liberated PHA monomers could have been activated by the aforementioned acyl-CoA synthetases to metabolites suitable for oxidation, likely through the TCA cycle as evidenced by the detection of fumarate hydratase in increased abundance (coupled with the presence of TCA cycle enzymes identified from the feast phase). Resulting acetyl-CoA could immediately enter the TCA cycle, whereas propionyl-CoA could enter the TCA cycle as succinyl-CoA (via methylmalonyl-CoA), or be converted to pyruvate via the methylcitrate pathway (Textor *et al.*, 1997). The detection of succinyl-CoA:3-ketoacid-CoA transferase further supported PHA monomer oxidation via the TCA cycle, as this enzyme is involved in the reversible condensation of succinyl-CoA and acetoacetate to yield acetoacetyl-CoA and succinate.

Because MMCs must respond to diminishing nutrients in ADF SBRs, energy generation and substrate scavenging are anticipated to be critical functions during the famine phase. The necessity of generating energy during the famine phase was supported by the detection of two ATP synthase subunits, quinone oxidoreductase, and aldehyde dehydrogenase in increased abundance. The increased abundance of quinohemoportein amine dehydrogenase, an enzyme that deaminates primary aliphatic and aromatic amines, suggested the utilization of other substrates, as amines can be used as a source of carbon, nitrogen, and energy (Takagi *et al.*,

2001). Though the detection of glycerol kinase in increased abundance was not expected, as glycerol was not anticipated to be present in the FDML, the enzyme can phosphorylate other substrates including dihydroxyacetone, D-glyceraldehyde, and L-glyceraldehyde (Hayashi & Lin, 1967), which could contribute to the generation of biomass precursors, thus supporting growth.

Cellular maintenance and housekeeping functions are expected to occur during the famine phase. The detection of chaperone GroEL in increased abundance (Appendix B, Figures B.65-B.68) may have been partly attributed to new protein synthesis that occurred during the famine phase. Additionally, an increase in chaperone GroEL may have been in response to potential protein misfolding caused by the stress of the famine conditions, in accordance with other studies reporting the upregulation of GroEL in response to starvation (Patrauchan *et al.*, 2012), and in a similarly complex activated sludge system that was exposed to toxic chemicals (Bott & Love, 2001). Lastly, the identification of proteins involved in other housekeeping functions (e.g., transcription or DNA processing) in increased abundance supported existing descriptions of maintenance functions occurring in the famine.

3.5.3.4 Fed-batch proteins

The proteome profile for the fed-batch PHA accumulation assessments supported increased PHA synthesis. Indeed, many of the proteins in increased abundance during the SBR feast phase were also in increased abundance in the fed-batch tests, including acetyl-CoA acetyltransferase and multiple phasins, which was in agreement with the higher PHA content achieved in the fed-batch tests. The detection of methylmalonate-semialdehyde dehydrogenase in increased abundance during fed-batch PHA production supported the idea

in that valine may be a potentially useful substrate to increase PHA content and the HV fraction.

3.6 Conclusions

The results of this study present an exploration of microbial community composition and functionality in a multi-stage PHA production system cultivated on a waste feedstock, and the following conclusions can be drawn:

- An MMC capable of producing up to 40% PHA from fermented dairy manure was enriched through the application of ADF.
- The microbial composition of the MMC supported the observed bulk solution variable changes and was dominated by the *Meganema* genus (reflected in both 16S data and protein assignments).
- During the feast phase, PHA synthesis and energy generation are prominent functions.
- PHA granule-bound phasin proteins may play important roles in PHA metabolism of MMC cultivated under ADF conditions.
- During the famine phase, nutrient transport and cellular maintenance are prominent functions.
- This study highlights the power of combining microbial community profiling through the use of high-throughput 16S rRNA gene sequencing with mass spectrometry-based proteomics for exploring microbial community dynamics in engineered systems.

3.7 Acknowledgements

The authors acknowledge Dr. Armando McDonald at the University of Idaho for the use of GC-MS. The authors acknowledge Mr. Dan New and Dr. Alida Gerritsen of the Institute for Bioinformatics and Evolutionary Studies Genomics Resources Core at the University of Idaho, and Dr. Matt Settles of the Bioinformatics Core at the Genome Center at the University of California-Davis for technical assistance related to the 16S rRNA gene sequencing and bioinformatics analysis. The authors acknowledge Dr. Lee Deobald of the Mass Spectrometry Core at the University of Idaho for technical assistance related to the identification of proteins via LC-MS/MS. This material is based on work supported by the National Science Foundation under Grant Number CBET-0950498, the Environmental Protection Agency Science to Achieve Results Fellowship, and the National Institute of General Medical Sciences from the National Institutes of Health, P30 GM103324. Any opinions, findings, and conclusions or recommendations expressed in this material are those of the authors and do not necessarily reflect the views of the funding agency. The authors declare no conflicts of interest.

References

Abram, F., Enright, A. M., et al. (2011). A metaproteomic approach gives functional insights into anaerobic digestion. *J Appl Microbiol, 110*(6), 1550-1560.

Albuquerque, M. G. E., Carvalho, G., et al. (2013). Link between microbial composition and carbon substrate-uptake preferences in a PHA-storing community. *Isme Journal, 7*(1), 1-12.

Albuquerque, M. G. E., Eiroa, M., et al. (2007). Strategies for the development of a side stream process for polyhydroxyalkanoate (PHA) production from sugar cane molasses. *Journal of Biotechnology, 130*(4), 411-421.

Bannerjee, D., Sanders, L. E., et al. (1970). Properties of purified methylmalonate semialdehyde dehydrogenase of Pseudomonas aeruginosa. *Journal of Biological Chemistry, 245*(7), 1828-1835.

Bansal, R., Deobald, L. A., et al. (2009). Proteomic detection of proteins involved in perchlorate and chlorate metabolism. *Biodegradation, 20*(5), 603-620.

Bengtsson, S., Pisco, A. R., et al. (2010a). Molecular weight and thermal properties of polyhydroxyalkanoates produced from fermented sugar molasses by open mixed cultures. *Journal of Biotechnology, 147*(3-4), 172-179.

Bengtsson, S., Pisco, A. R., et al. (2010b). Production of polyhydroxyalkanoates from fermented sugar cane molasses by a mixed culture enriched in glycogen accumulating organisms. *Journal of Biotechnology, 145*(3), 253-263.

Bengtsson, S., Werker, A., et al. (2008). Production of polyhydroxyalkanoates by activated sludge treating a paper mill wastewater. *Bioresource Technology, 99*(3), 509-516.

Beun, J. J., Dircks, K., et al. (2002). Poly-β-hydroxybutyrate metabolism in dynamically fed mixed microbial cultures. *Water Research, 36*(5), 1167-1180.

Bott, C. B., & Love, N. G. (2001). The immunochemical detection of stress proteins in activated sludge exposed to toxic chemicals. *Water Research, 35*(1), 91-100.

Brigham, C. J., Speth, D. R., et al. (2012). Whole-genome microarray and gene deletion studies reveal regulation of the polyhydroxyalkanoate production cycle by the stringent response in Ralstonia eutropha H16. *Applied and environmental microbiology, 78*(22), 8033-8044.

Carvalho, G., Oehmen, A., et al. (2013). The relationship between mixed microbial culture composition and PHA production performance from fermented molasses. *N Biotechnol*.

Checinska, A., Burbank, M., et al. (2012). Protection of Bacillus pumilus Spores by Catalases. *Applied and Environmental Microbiology, 78*(18), 6413-6422.

Chiancone, E., Ceci, P., et al. (2004). Iron and proteins for iron storage and detoxification. *Biometals, 17*(3), 197-202.

Coats, E. R., Gregg, M., et al. (2011). Effect of organic loading and retention time on dairy manure fermentation. *Bioresource Technology, 102*(3), 2572-2577.

Dai, J., Gliniewicz, K., et al. (2015). Influence of organic loading rate and solid retention time on polyhydroxybutyrate production from hybrid poplar hydrolysates using mixed microbial cultures. *Bioresource technology, 175*, 23-33.

Dekoning, G. (1995). Physical-properties of bacterial poly((R)-3-hydroxyalkanoates) *Canadian Journal of Microbiology, 41*, 303-309.

Dias, J. M., Lemos, P. C., et al. (2006a). Recent advances in polyhydroxyalkanoate production by mixed aerobic cultures: from the substrate to the final product. *Macromol Biosci, 6*(11), 885-906.

Dias, J. M. L., Lemos, P. C., et al. (2006b). Recent advances in polyhydroxyalkanoate production by mixed aerobic cultures: From the substrate to the final product. *Macromolecular Bioscience, 6*(11), 885-906.

Dionisi, D., Carucci, G., et al. (2005). Olive oil mill effluents as a feedstock for production of biodegradable polymers. *Water Research, 39*(10), 2076-2084.

Dionisi, D., Majone, M., et al. (2004). Biodegradable polymers from organic acids by using activated sludge enriched by aerobic periodic feeding. *Biotechnology and Bioengineering, 85*(6), 569-579.

Dobroth, Z. T., Hu, S., et al. (2011). Polyhydroxybutyrate synthesis on biodiesel wastewater using mixed microbial consortia. *Bioresource Technology, 102*(3), 3352-3359.

Grady, C., Daigger, G., et al. (2011). Biological wastewater treatment: CRC Press.

Gurieff, N., & Lant, P. (2007). Comparative life cycle assessment and financial analysis of mixed culture polyhydroxyalkanoate production. *Bioresource technology, 98*(17), 3393-3403.

Hanreich, A., Schimpf, U., et al. (2013). Metagenome and metaproteome analyses of microbial communities in mesophilic biogas-producing anaerobic batch fermentations indicate concerted plant carbohydrate degradation. *Systematic and Applied Microbiology, 36*(5), 330-338.

Hayashi, S.-I., & Lin, E. C. C. (1967). Purification and Properties of Glycerol Kinase from Escherichia coli. *Journal of Biological Chemistry, 242*(5), 1030-1035.

Hill, T. C. J., Walsh, K. A., et al. (2003). *Using ecological diversity measures with bacterial communities* (Vol. 43).

Holmsgaard, P. N., Norman, A., et al. (2011). Bias in bacterial diversity as a result of Nycodenz extraction from bulk soil. *Soil Biology and Biochemistry, 43*(10), 2152-2159.

Jehmlich, N., Kleinsteuber, S., et al. (2010). Phylogenetic and proteomic analysis of an anaerobic toluene-degrading community. *Journal of Applied Microbiology, 109*(6), 1937-1945.

Jiang, Y., Marang, L., et al. (2011). Polyhydroxybutyrate Production From Lactate Using a Mixed Microbial Culture. *Biotechnology and Bioengineering, 108*(9), 2022-2035.

Jiang, Y., Marang, L., et al. (2012). Waste to resource: Converting paper mill wastewater to bioplastic. *Water Research, 46*(17), 5517-5530.

Johnson, K., Jiang, Y., et al. (2009). Enrichment of a Mixed Bacterial Culture with a High Polyhydroxyalkanoate Storage Capacity. *Biomacromolecules, 10*(4), 670-676.

Keshavarz, T., & Roy, I. (2010). Polyhydroxyalkanoates: bioplastics with a green agenda. *Current Opinion in Microbiology, 13*(3), 321-326.

Khurana, S., Sanli, G., et al. (2000). Molecular modeling of substrate binding in wild-type and mutant Corynebacteria 2,5-diketo-D-gluconate reductases. *Proteins, 39*(1), 68-75.

Koch, A. (1990). Diffusion The Crucial Process in Many Aspects of the Biology of Bacteria. In K. C. Marshall (Ed.), *Advances in Microbial Ecology* (Vol. 11, pp. 37-70): Springer US.

Koch, A. L. (1997). Microbial physiology and ecology of slow growth. *Microbiology and Molecular Biology Reviews, 61*(3), 305-318.

Konopka, A. (2000). Microbial physiological state at low growth rate in natural and engineered ecosystems. *Curr Opin Microbiol, 3*(3), 244-247.

Kragelund, C., Nielsen, J. L., et al. (2005). Ecophysiology of the filamentous Alphaproteobaeterium Meganema perideroedes in activated sludge. *Fems Microbiology Ecology, 54*(1), 111-122.

Kuchta, K., Chi, L., et al. (2007). Studies on the influence of phasins on accumulation and degradation of PHB and nanostructure of PHB granules in Ralstonia eutropha H16. *Biomacromolecules, 8*(2), 657-662.

Lawrence, A. G., Schoenheit, J., et al. (2005). Transcriptional analysis of Ralstonia eutropha genes related to poly-(R)-3-hydroxybutyrate homeostasis during batch fermentation. *Applied microbiology and biotechnology, 68*(5), 663-672.

Lazzaroni, J. C., Germon, P., et al. (1999). The Tol proteins of Escherichia coli and their involvement in the uptake of biomolecules and outer membrane stability. *FEMS microbiology letters, 177*(2), 191-197.

Lemos, P. C., Levantesi, C., et al. (2008). Microbial characterisation of polyhydroxyalkanoates storing populations selected under different operating conditions using a cell-sorting RT-PCR approach. *Applied Microbiology and Biotechnology*, *78*(2), 351-360.

Liang, S., Gliniewicz, K., et al. (2015). Comparative analysis of microbial community of novel lactic acid fermentation inoculated with different undefined mixed cultures. *Bioresource Technology, 179*, 268-274.

Liu, H.-Y., Hall, P. V., et al. (2008). Production of polyhydroxyalkanoate during treatment of tomato cannery wastewater. *Water Environment Research, 80*(4), 367-372.

Magoč, T., & Salzberg, S. L. (2011). FLASH: fast length adjustment of short reads to improve genome assemblies. *Bioinformatics, 27*(21), 2957-2963.

Majone, M., Beccari, M., et al. (2006). Enrichment of activated sludge in a sequencing batch reactor for polyhydroxyalkanoate production. *Water Sci Technol, 54*(1), 119-128.

Majone, M., Massanisso, P., et al. (1996). Influence of storage on kinetic selection to control aerobic filamentous bulking. *Water Science and Technology, 34*(5-6), 223-232.

Marang, L., Jiang, Y., et al. (2013). Butyrate as preferred substrate for polyhydroxybutyrate production. *Bioresource Technology, 142*, 232-239.

Mezzina, M. P., Wetzler, D. E., et al. (2015). A phasin with extra talents: a polyhydroxyalkanoate granule-associated protein has chaperone activity. *Environmental microbiology, 17*(5), 1765-1776.

Morgan-Sagastume, F., Karlsson, A., et al. (2010). Production of polyhydroxyalkanoates in open, mixed cultures from a waste sludge stream containing high levels of soluble organics, nitrogen and phosphorus. *Water Research, 44*(18), 5196-5211.

Muyzer, G., Brinkhoff, T., et al. (2004). Denaturing gradient gel electrophoresis (DGGE) in microbial ecology. *Molecular microbial ecology manual.* Volumes 1 and 2 Ed. 2: 743-769.

Oehmen, A., Pinto, F. V., et al. (2014). The impact of pH control on the volumetric productivity of mixed culture PHA production from fermented molasses. *Engineering in Life Sciences, 14*(2), 143-152.

Patrauchan, M. A., Miyazawa, D., et al. (2012). Proteomic Analysis of Survival of Rhodococcus jostii RHA1 during Carbon Starvation. *Applied and Environmental Microbiology, 78*(18), 6714-6725.

Potter, M., Muller, H., et al. (2004). The complex structure of polyhydroxybutyrate (PHB) granules: four orthologous and paralogous phasins occur in Ralstonia eutropha. *Microbiology, 150*(Pt 7), 2301-2311.

Potter, M., & Steinbüchel, A. (2005). Poly(3-hydroxybutyrate) granule-associated proteins: Impacts on poly(3-hydroxybutyrate) synthesis and degradation. *Biomacromolecules, 6*(2), 552-560.

Queiros, D., Rossetti, S., et al. (2014). PHA production by mixed cultures: A way to valorize wastes from pulp industry. *Bioresource technology, 157*, 197-205.

Reis, M. A. M., Serafim, L. S., et al. (2003). Production of polyhydroxyalkanoates by mixed microbial cultures. *Bioprocess and Biosystems Engineering, 25*(6), 377-385.

Rice, E. W., et al. (2005). *Standard Methods for the Examination of Water & Wastewater. 21st ed.*

Serafim, L. S., Lemos, P. C., et al. (2008). Strategies for PHA production by mixed cultures and renewable waste materials. *Applied Microbiology and Biotechnology, 81*(4), 615-628.

Serafim, L. S., Lemos, P. C., et al. (2004). Optimization of polyhydroxybutyrate production by mixed cultures submitted to aerobic dynamic feeding conditions. *Biotechnology and Bioengineering, 87*(2), 145-160.

Shevchenko, A., Tomas, H., et al. (2006). In-gel digestion for mass spectrometric characterization of proteins and proteomes. *Nature Protocols, 1*(6), 2856-2860.

Smit, A. M., Strabala, T. J., et al. (2012). Proteomic phenotyping of Novosphingobium nitrogenifigens reveals a robust capacity for simultaneous nitrogen fixation, polyhydroxyalkanoate production, and resistance to reactive oxygen species. *Appl Environ Microbiol, 78*(14), 4802-4815.

Steinbüchel, A., & Pieper, U. (1992). Production of a copolyester of 3-hydroxybutyric acid and 3-hydroxyvaleric acid from single unrelated carbon sources by a mutant of Alcaligenes eutrophus. *Applied Microbiology and Biotechnology, 37*(1), 1-6.

Steinbüchel, A., & Schlegel, H. G. (1991). Physiology and molecular genetics of poly(β-hydroxyalkanoic acid) synthesis in Alcaligenes eutrophus. *Molecular Microbiology, 5*(3), 535-542.

Stowe, E. J., Coats, E. R., et al. (2015). Dairy manure resource recovery utilizing two-stage anaerobic digestion – Implications of solids fractionation. *Bioresource Technology, 198*, 237-245.

Takagi, K., Yamamoto, K., et al. (2001). New pathway of amine oxidation respiratory chain of Paracoccus denitrificans IFO 12442. *European Journal of Biochemistry, 268*(2), 470-476.

Tamis, J., Lužkov, K., et al. (2014). Enrichment of Plasticicumulans acidivorans at pilot-scale for PHA production on industrial wastewater. *Journal of biotechnology, 192*, 161-169.

Textor, S., Wendisch, V. F., et al. (1997). Propionate oxidation in Escherichia coli: evidence for operation of a methylcitrate cycle in bacteria. *Arch Microbiol, 168*(5), 428-436.

Thiede, B., Koehler, C. J., et al. (2013). High resolution quantitative proteomics of HeLa cells protein species using stable isotope labeling with amino acids in cell culture(SILAC), two-dimensional gel electrophoresis(2DE) and nano-liquid chromatograpohy coupled to an LTQ-OrbitrapMass spectrometer. *Mol Cell Proteomics, 12*(2), 529-538.

Thomsen, T. R., Blackall, L. L., et al. (2006). Meganema perideroedes gen. nov., sp nov., a filamentous alphaproteobacterium from activated sludge. *International Journal of Systematic and Evolutionary Microbiology, 56*, 1865-1868.

van Loosdrecht, M. C. M., Pot, M. A., et al. (1997). Importance of bacterial storage polymers in bioprocesses. *Water Science and Technology, 35*(1), 41-47.

Vizcaino, J. A., Cote, R. G., et al. (2013). The PRoteomics IDEntifications (PRIDE) database and associated tools: status in 2013. *Nucleic Acids Res, 41*(Database issue), D1063-1069.

Waller, J. L., Green, P. G., et al. (2012). Mixed-culture polyhydroxyalkanoate production from olive oil mill pomace. *Bioresource Technology, 120*, 285-289.

Wang, Q., Garrity, G. M., et al. (2007). Naïve Bayesian Classifier for Rapid Assignment of rRNA Sequences into the New Bacterial Taxonomy. *Applied and Environmental Microbiology, 73*(16), 5261-5267.

White, D. (2007). *The Physiology and Biochemistry of Prokaryotes* (Vol. Third Edition): Oxford University Press.

Wieczorek, R., Pries, A., et al. (1995). Analysis of a 24-kilodalton protein associated with the polyhydroxyalkanoic acid granules in Alcaligenes eutrophus. *J Bacteriol, 177*(9), 2425-2435.

Wilmes, P., & Bond, P. L. (2004). The application of two-dimensional polyacrylamide gel electrophoresis and downstream analyses to a mixed community of prokaryotic microorganisms. *Environmental Microbiology, 6*(9), 911-920.

Wilmes, P., Wexler, M., et al. (2008). Metaproteomics provides functional insight into activated sludge wastewater treatment. *PLoS One, 3*(3), e1778.

Chapter 4. Microbial Community Dynamics in a Sequencing Batch Reactor Operated Under Aerobic Dynamic Feeding Conditions for the Synthesis of Polyhydroxyalkanoates from Fermented Dairy Manure

(Andrea J. Hanson and Erik R. Coats[1])

4.1 Abstract

In this study, microbial community dynamics in a sequencing batch reactor (SBR) operated under aerobic dynamic feeding (ADF) conditions for the synthesis of polyhydroxyalkanoates (PHAs) from fermented dairy manure were investigated. To characterize the microbial community composition, 16S rRNA gene sequencing was performed on biomass samples collected from the SBR approximately every four days over an operational period of 120 days. At the genus level, *Ohtaekwangia*, *Meganema*, and *Thauera* were among the most abundant phylotypes identified, but overall the microbial community composition fluctuated for the duration for SBR monitoring. To explore prospective relationships between the microbial community composition and observed SBR performance, the microbial community profile was examined with respect to select bulk solution variables including the feast-to-famine ratio, substrate utilization, and maximum PHA content realized. Consistent correlations were not observed between the microbial community composition and these performance parameters, although lower microbial diversity appeared to more favorable for enhanced PHA production in a fed-batch mode. Together the findings of this study provide insight regarding the extent to which microbial community dynamics may influence PHA process performance using fermented dairy manure as a feedstock.

[1] This chapter will be revised and submitted to *Bioresource Technology*.

4.2 Introduction

Polyhydroxyalkanoates (PHAs) are a class of biologically-produced polyesters that have drawn increasing attention as functional replacements to conventional petroleum-based thermoplastics. PHAs exhibit appealing material properties and have positive life cycle assessments (Gurieff & Lant, 2007), but the adoption of the polymer as commodity bioplastics has been limited mostly due to the production costs associated with the use of pure cultures and refined substrates (Chen & Patel, 2011; Choi & Lee, 1997). To address the cost limitations, alternative PHA production strategies have been sought, including the use of mixed microbial cultures (MMCs) and waste or surplus feedstocks. Distinct from conventional pure culture-based PHA production methodologies, MMC PHA production typically comprises three stages: i) acidogenic fermentation, wherein the organic content of the feedstock is converted to volatile fatty acids (VFAs); ii) MMC enrichment, wherein a sequencing batch reactor (SBR) is operated using aerobic dynamic feeding (ADF) conditions to selectively enrich MMC for PHA-producing bacteria exhibiting a desired feast-famine metabolic response; and iii) PHA production, wherein the PHA accumulation capacity is maximized in bacterial cells harvested from the enrichment SBR. This three-stage PHA production strategy has been evaluated with a number of waste feedstocks, including fermented molasses (Albuquerque *et al.*, 2007; Albuquerque *et al.*, 2010), fermented olive mill effluents (Beccari *et al.*, 2009; Dionisi *et al.*, 2005b), fermented paper mill effluents (Bengtsson *et al.*, 2008; Jiang *et al.*, 2012), and domestic or industrial wastewaters (Morgan-Sagastume *et al.*, 2015; Queiros *et al.*, 2014) . For many of these studies, the microbial composition of the enriched MMC has been implicated in overall PHA process performance.

The microbial composition of MMCs enriched through ADF is influenced by the applied operating conditions. For a typical SBR cycle operated under ADF conditions, excess substrate is provided at the start of the cycle, creating a substrate surplus (i.e., feast), after which follows a prolonged period devoid of exogenous substrate (i.e., famine). With ADF inducing a feast-famine metabolic response, the ecological role of PHA contributes to the favorable enrichment of PHA-producing bacteria over non-PHA producing bacteria (Dias *et al.*, 2006b; Majone *et al.*, 1996; Reis *et al.*, 2003; van Loosdrecht *et al.*, 1997). To investigate MMC composition and monitor MMC dynamics associated with the imposition of ADF, a suite of classical molecular techniques including fluorescence *in situ* hybridization (FISH) coupled with PHA staining (Oehmen *et al.*, 2014; Serafim *et al.*, 2006), clone library construction (Albuquerque *et al.*, 2013; Dionisi *et al.*, 2006), or denaturing gradient gel electrophoresis (Beccari *et al.*, 2009; Dionisi *et al.*, 2005a) have been applied to MMC in enrichment SBRs. These techniques have provided awareness regarding the prevalence of particular PHA-producing genera (e.g., *Thauera*, *Azoarcus*, and *Paracoccus*) in ADF systems, and a basis to examine potential relationships with observed process performance.

Previous studies have indicated the relative abundance of specific MMC constituents (e.g., *Thauera*, *Azoarcus*, *Paracoccus*, and *Plasticicumulans*) can exert a strong effect on particular feast phase parameters including the specific VFA uptake rate, specific PHA synthesis rate, maximum PHA content achieved, and PHA composition (Albuquerque *et al.*, 2013; Carvalho *et al.*, 2013; Jiang *et al.*, 2012). Studies have also associated MMC composition with the feast-to-famine (F:F) ratio (Beccari *et al.*, 1998; Dionisi *et al.*, 2006; Wen *et al.*, 2012), a value calculated by comparing the feast phase length to the entire SBR cycle and considered to be important regarding whether a PHA storage response dominates

during the feast phase (Reis *et al.*, 2011). Microbial diversity and functional redundancy are also important components in linking MMC dynamics to process performance and stability (Briones & Raskin, 2003), however, neither aspect has been extensively interrogated for many enrichment SBRs. As such, exploring the microbial composition and diversity in MMCs as related to conventional observations is a critical component of enrichment SBR operation, especially when utilizing novel feedstocks.

One such novel feedstock that exhibits potential for use in ADF PHA production is dairy manure. Fermented dairy manure has been used for both the MMC enrichment and PHA production stages (Guho, 2010; Watson, 2015), with the highest PHA production capacity reaching nearly 70% (w/w) of the total biomass content (Guho, 2010). However, no microbial community characterization has been performed for enrichment SBRs operated under ADF conditions using this feedstock. As such, potentially relevant relationships between microbial composition and process performance parameters have not been examined. Consequently, the extent to which the microbial composition may influence PHA process performance using fermented dairy manure as a feedstock has not been established. Extrapolating MMC composition and possible contribution to process performance from other enrichment SBRs cultivated on fermented waste substrates is unfeasible, as different operating conditions are imposed, and the chemical composition of fermented dairy manure is unlike other waste feedstocks (e.g., molasses or paper mill effluent). Furthermore, the methods that have most commonly been applied to characterize MMC in enrichment SBRs (e.g., FISH or DGGE) are not easily applicable because of the fermented dairy manure matrix and are limited in resolving complex MMC compositions. In contrast, next-generation sequencing of the bacterial 16S rRNA gene provides a powerful alternative molecular tool.

Obtaining a comprehensive profile of the microbial community present in an enrichment SBR cultivated on fermented dairy manure is important to more fully understand how the applied ADF conditions influence the microbial composition and dynamics, as well as the extent to which the microbial composition may impact process performance. As such, the aim of this study was to characterize and monitor microbial composition and diversity in an enrichment SBR in conjunction with conventional bulk solution observations. During SBR start-up, equilibration, and stable operation (a total of 120 days), biomass samples were collected approximately every equivalent solids retention time (SRT) for microbial community profiling based on the bacterial 16S rRNA gene. The microbial composition and diversity were evaluated and examined with respect to select bulk solution parameters including the F:F ratio, VFA uptake, and maximum PHA content realized.

4.3 Materials and methods

4.3.1 Waste feedstock preparation

The fermented dairy manure feedstock for the enrichment SBR was obtained from a 20-L dairy manure fermenter operated under conditions as previously described (Stowe *et al.*, 2015). Briefly, manure for the fermenter was obtained from lactating Holstein cows from the University of Idaho Dairy, Moscow, ID. Effluent from the fermenter was poured through a mesh screen to remove large solids. After screening, the liquid was centrifuged at 8,000 rpm for 5 min to remove fine solids. The supernatant (i.e., the FDML feedstock), was then sterilized by autoclaving. To compensate for phosphate precipitation during autoclaving, equimolar KH_2PO_4 and K_2HPO_4 were added aseptically after cooling. The range of soluble

VFAs, ammonia, and phosphate concentrations in the final FDML feedstock are provided in Table 4.1.

4.3.2 Enrichment SBR operation

The enrichment sequencing batch reactor (SBR) was operated under aerobic dynamic feeding (ADF) conditions. The enrichment SBR had an operating volume of 1.8 L, solids retention time (SRT) of 4 d, hydraulic retention time (HRT) of 4 d, and cycle length (CL) of 24 h. The cycle consisted of a fill phase (2 min), a react phase (1433 min), and a draw phase (5 min). Mixing was maintained throughout the cycle by a magnetic stir bar and stir plate. House air was introduced into the reactor at a rate of approximately 1 L min^{-1} through a stainless steel diffusor to achieve aeration during the fill and react phases. FDML and autoclaved tap water were added to the reactor simultaneously during the fill phase, at a volumetric ratio of 40:60, respectively. The pumps and aeration were controlled by a programmable logic controller. The enrichment SBR was operated in a temperature-controlled room (20-26°C), and the pH monitored, but not controlled. When necessary, foaming was controlled with Antifoam A Concentrate (Sigma Aldrich, St. Louis, MO, USA). The enrichment SBR was inoculated from a 20 L SBR (same SRT, HRT, and CL but fed unsterilized FDML) that had been operated stably for 4 years.

4.3.3 Fed-batch PHA accumulation tests

The MMC in the enrichment SBR was subjected to fed-batch PHA accumulation capacity tests in a separate reactor. Using the 450 mL effluent from the enrichment SBR, the fed-batch tests were conducted in a 1 L beaker under fully aerobic and completely mixed conditions with the same FDML and tap water fed to the enrichment SBR. A total of 3 pulse-additions of FDML feedstock (112 mL, 140 mL, and 175 mL, respectively) were applied; the

frequency of which was determined by manual monitoring of the dissolved oxygen (DO) concentration and adding the next feedstock pulse when the DO began to rise (Dias *et al.*, 2006a). The fed-batch tests were carried out in the same temperature-controlled room (20-26°C) and the pH was monitored, but not controlled.

4.3.4 Analytical procedures

DO, pH, and temperature were monitored using a Hach HQ40 meter with LDO101 and PHC101 probes DO (Hach, Loveland, CO). Volatile suspended solids (VSS) concentration was determined according to Standard Methods (Rice, 2005). Soluble VFAs (viz. acetic, propionic, butyric, valeric, caproic, iso-butyric, and iso-valeric acids) concentrations were quantified using a gas chromatograph equipped with a flame ionization detector as previously described (Coats *et al.*, 2011). The specific VFA uptake rate was estimated as follows: total mass of VFAs consumed (mg)/mass of VSS (mg)/feast length (h). Chemical oxygen demand (COD), phosphate (PO_4^{3-} -P), and ammonia (NH_3-N) concentrations were determined after sample filtration through a sterile 0.22 µm syringe filter (Millipore Corp., Billerica, MA) according to Standard Methods (Rice, 2005).

Biomass PHA content was determined as methyl esters using gas chromatography-mass spectrometry (GC-MS) as previously described (Dobroth *et al.*, 2011) with minor modifications. Briefly, 400 µL of 6.25% sodium hypochlorite was added to lyse cells and halt metabolic activity. Biomass was then harvested by centrifugation at 10,000 rpm for 10 min, rinsed twice with deionized water, and oven-dried at 103-105°C for 24 hr. Dried biomass was then digested in 2 mL each of acidified methanol (3% v/v sulfuric acid) and chloroform (containing 0.25 mg mL^{-1} benzoic acid as internal standard) at 100°C for 4 h. Once cooled, 1 mL deionized water was added to the samples and vigorously mixed for 30 s. The organic

phase was recovered using a Pasteur pipette and dehydrated with anhydrous sodium sulfate prior to GC-MS analysis. PHA analysis was performed using a PolarisQ iontrap GC-MS instrument (Thermo Electron, San Jose, CA) in positive EI mode. Hydroxybutyrate (HB) and hydroxyvalerate (HV) methyl esters were identified by retention time and mass spectra matching with commercially available standards (Lancaster Synthesis, Ward Hill, MA); quantification of each monomer was determined using standard curves prepared from the same standards. Total intracellular PHA content was calculated on a dry weight basis (mg PHA mg total solids^{-1}) and expressed as a percent.

4.3.5 Microbial community analysis

Microbial genomic DNA was isolated from biomass using a PowerSoil DNA Isolation Kit (MOBIO, Carlsbad, CA) following the manufacturer's instructions. Genomic DNA yield and purity was quantified using a Synergy H1 Multi-Mode Reader (BioTek, Winooski, VT). Bacterial 16S rRNA gene fragments were amplified and sequenced following previously described methods (Dai *et al.*, 2015; Liang *et al.*, 2015) with minor modifications. Briefly, sample amplicons were generated using two rounds of PCR: PCR1 amplified the targeted V1-V3 regions (*Escherichia coli* positions 27F-533R of the 16S rRNA gene), and PCR2 attached sequencing adapters and sample barcodes. PCR1 used the following primer sets listed according to position and direction:

27F-1:ACACTGACGACATGGTTCTACAGT**AGAGTTTGATCCTGGCTCAG**;

27F-2:ACACTGACGACATGGTTCTACA*C*GT**AGAGTTTGATCATGGCTCAG**;

27F-3:ACACTGACGACATGGTTCTACA*AC*GT**AGAGTTTGATTCTGGCTCAG**;

27F-4:ACACTGACGACATGGTTCTACA*TAC*GT**AGAGTTTGATTCTGGCTCAG**;

533R-1:TACGGTAGCAGAGACTTGGTCT**TTACCGCGGCTGCTGGCAC**;

533R-2:TACGGTAGCAGAGACTTGGTCT*G***TTACCGCGGCTGCTGGCAC;**

533R-3:TACGGTAGCAGAGACTTGGTCT*TG***TTACCGCGGCTGCTGGCAC;**

533R-4:TACGGTAGCAGAGACTTGGTCT*ATG***TTACCGCGGCTGCTGGCAC.**

The underlined sequences denote universal tag sequences CS1 (ACACTGACGACATGGTTCTACA; tag on the forward primer) and CS2 (TACGGTAGCAGAGACTTGGTCT; tag on the reverse primer), bold sequences denote the universal 16S rRNA primers 27F and 533R, and the italicized bases denote the added bases to the template-specific primers in order to introduce variability of base calls during Illumina sequencing. For PCR2, the adapter primers included the Illumina-specific sequences P7 and P5 for dual indexing:

P7-CS2:

CAAGCAGAAGACGGCATACGAGAT*NNNNNNNN*TACGGTAGCAGAGACTTGGTCT

and

P5-CS1:

AATGATACGGCGACCACCGAGATCTACAC*NNNNNNNN*ACACTGACGACATGGTTCTACA, where the unique sequence barcodes were denoted by the 8 italicized N's, and the underlined sequences denote the universal sequences CS1 and CS2. This permitted sequencing of amplicons from many samples simultaneously, while using relatively few barcoded adapter primers, and afterwards assign each sequence to the original sample.

Amplicon concentrations were determined using the PicoGreen assay (Molecular Probes Inc., USA) and a fluorometer (SpectraMax Gemini XPS 96-well plate reader, Molecular Devices, Sunnyvale, CA) and then pooled into approximately equal amounts (~100 ng) in a single tube. The amplicon pool was then cleaned to remove short, undesirable

fragments following the procedures previously reported (Dai *et al.*, 2015; Liang *et al.*, 2015). Finally, sequences were obtained using an Illumina MiSeq paired-end 300 bp protocol (Illumina, Inc., San Diego, CA).

For sequence analysis and taxonomic classification, raw DNA sequence reads from the Illumina MiSeq were demultiplexed and subsequently processed using the custom python application *dbcAmplicons* (https://github.com/msettles/dbcAmplicons) to identify and assign reads by both expected barcode and primer sequences. Briefly, barcodes were allowed to have at most 1 mismatch and primers were allowed to have at most 4 mismatches (as long as the final 4 bases of the primer matched the target sequence exactly). Reads were then trimmed of their primer sequence and joined into a single amplicon sequence using the application *FLASH* (Magoč & Salzberg, 2011). Finally, the Ribosomal Database Project (RDP) Bayesian classifier was used to assign sequences to phylotypes (Wang *et al.*, 2007); reads were assigned to the first RDP taxonomic level with a bootstrap score ≥50. The relative abundance of individual phylotypes was based on the percentage of sequences obtained for each MMC biomass sample. The raw 16S rRNA gene sequencing data is available through the National Center for Biotechnology Information Short Reads Archive (http://www.ncbi.nlm.nih.gov/sra) accession number SRP065770. Microbial community data analysis was performed using *R* v3.0.3 software (http://www.r-project.org/) and *MEGAN* (Huson *et al.*, 2007). Regression analysis was performed to examine prospective relationships between the microbial community (viz. Shannon index and some of the most abundant phylotypes) and select process performance parameters (viz. F:F ratio, estimated specific VFA uptake rate, SBR PHA content, and fed-batch PHA content); the F-test was applied to test for significance of regression.

4.4 Results and discussion

4.4.1 Substrate characteristics

To monitor nutritional aspects of the fermented dairy manure liquor (FDML) composition, select constituents were measured throughout the SBR evaluation period. The VFA content was of particular interest given the VFA loading and distribution has been shown to influence PHA process performance (Albuquerque *et al.*, 2010) and could thus affect MMC dynamics. Acetate was always present in the highest concentration, followed by propionate, and butyrate; additional VFAs present in the FDML influent, albeit in decreased concentration, included iso-butyrate, valerate, iso-valerate, and caproate (Table 4.1). Though the total VFA content varied, the relative distribution was fairly constant (Appendix C, Figures C.1 and C.2). Overall, the VFA profile (concerning both the total VFA content and speciation) was in the range of other studies using fermented waste substrates including molasses (1,681 mg L^{-1} and 444 mg L^{-1} HAc and HPro, respectively) (Albuquerque *et al.*, 2007), paper mill wastewater (2,942 mg L^{-1} and 1,259 mg L^{-1} /L HAc and HPro, respectively) (Jiang *et al.*, 2012), and waste activated sludge (5,046 mg L^{-1} and 2251 mg L^{-1} HAc and HPro, respectively) (Morgan-Sagastume *et al.*, 2010). Furthermore, the distribution of acetate and propionate, as well as the other even and odd-chain VFAs, ensured the potential for the synthesis of the desirable copolymer poly(3-hydroxybutyrate-co-3-hydroxyvalerate) (PHBV) (Dekoning, 1995). VFAs represented approximately 70% of the soluble COD (sCOD), indicating a large fraction of the potential soluble substrates were readily biodegradable; however, the remaining 30% of the sCOD was not identified, most of which may not have been biodegradable. Consequently, the extent to which this unidentified sCOD may have impacted the process was largely unknown, as often encountered using fermented waste

Table 4.1. Characterization of fermented dairy manure liquor.

FDML constituent	concentration, mg L^{-1}
HAc	2,027 ± 328 (n=133)
HPro	1,021 ± 199 (n=133)
HBu	727 ± 162 (n=133)
HiBu	135 ± 18 (n=133)
HVa	131 ± 37 (n=133)
HiVa	148 ± 21 (n=133)
HCa	30 ± 30 (n=133)
NH_3	488 ± 129 (n=12)
PO_4^{3-}	5 ± 1 (n=12)

Abbreviations: HAc (acetic acid), HPro (propionic acid), HBu (butyric acid), HiBu (iso-butyric acid), HVa (valeric acid), HiVa (iso-valeric acid), HCa (caproic acid), NH_3 (ammonia, measured as NH_3-N), and PO_4^{3-} (phosphate, measured as PO_4-P).

substrates (Albuquerque *et al.*, 2007; Albuquerque *et al.*, 2010; Jiang *et al.*, 2012; Morgan-Sagastume *et al.*, 2010). The ammonia and phosphate concentrations were 488 mg L^{-1} ± 129 and 5 mg L^{-1} ± 1, respectively (Table 4.1).

4.4.2 Process performance

To characterize and assess stabilization of the feast-famine response of the enrichment SBR upon initial start-up, the dissolved oxygen (DO) concentration was monitored, as this parameter has been generally regarded as a stability marker (Dias *et al.*, 2006b). During SBR start-up, the DO profiles were not immediately indicative of a feast-famine response (Figure 4.1, dotted lines); specifically, a typical feast-famine response is characterized by a drastic reduction in DO concentration upon the addition of substrate at the start of an SBR cycle, followed by a notable increase in DO concentration upon VFA exhaustion from solution (Albuquerque *et al.*, 2007; Dias *et al.*, 2006a; Johnson *et al.*, 2009; Morgan-Sagastume *et al.*, 2010). By day 9 (Figure 4.1, solid black line), however, the enrichment SBR began to exhibit a more stable, typical feast-famine response. After Day 9, similar DO profiles (Figure 4.1, solid lines) were consistently observed for the duration of SBR monitoring (120 days),

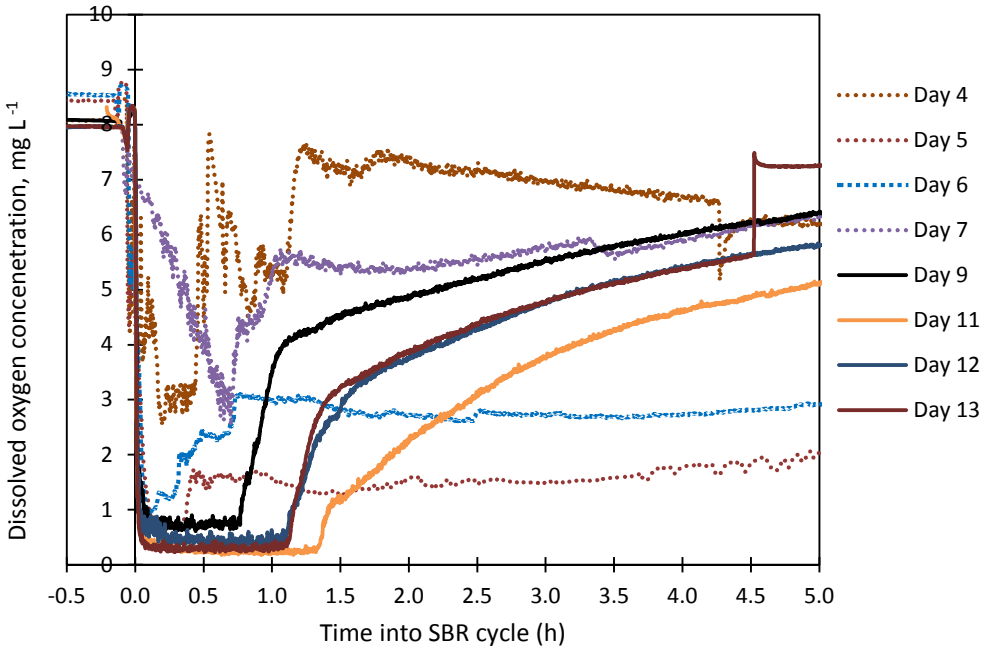

Figure 4.1. DO profiles during initial SBR start-up. The SBR cycle starts at time 0.0 when the FDML is added to the SBR. Dashed lines indicate an unstable feast-famine response. Solid lines indicate a typical feast-famine response.

indicating a typical feast-famine response was elicited and maintained through the applied ADF conditions. The VSS concentrations (used as a surrogate for the biomass concentration), measured at the end of the SBR cycle were variable during the initial SBR start-up; this variability persisted throughout SBR sampling (data not shown). Nevertheless, the VSS concentration was maintained above 1,000 mg L^{-1}, and at its highest reached approximately 3,700 mg L^{-1}.

The F:F ratio was calculated and monitored to assess the feast-famine conditions during SBR operation. The F:F ratios (calculated by comparing the feast length, based on the DO concentration, to the entire cycle length), ranged from 0.02 to 0.2 (Appendix C, Figure C.3), with an average of 0.06 ± 0.03 (n=64). The measured F:F ratios were in line with other investigations using waste substrates such as fermented molasses (F:F ratio range of 0.2-1.2) (Albuquerque *et al.*, 2010), and below the recommended maximum value of 0.2, which has been suggested as an indicator for the enrichment of PHA-producing (Johnson *et al.*, 2009).

For the duration of SBR operation, the F:F ratios fluctuated, but this was not unexpected as the specific VFA uptake rates were variable as well, given the VFA content and VSS varied. Furthermore, soluble, non-VFA COD was known to be present in the FDML, which could have affected the feast length and subsequent F:F ratio, as the possible catabolism of these substrates would exhibit an oxygen demand. Finally, because no nitrification inhibitor was added to the SBR, the consumption of residual DO by nitrifying bacteria may have been another factor contributing to the feast length variability, as nitrification activity would exhibit

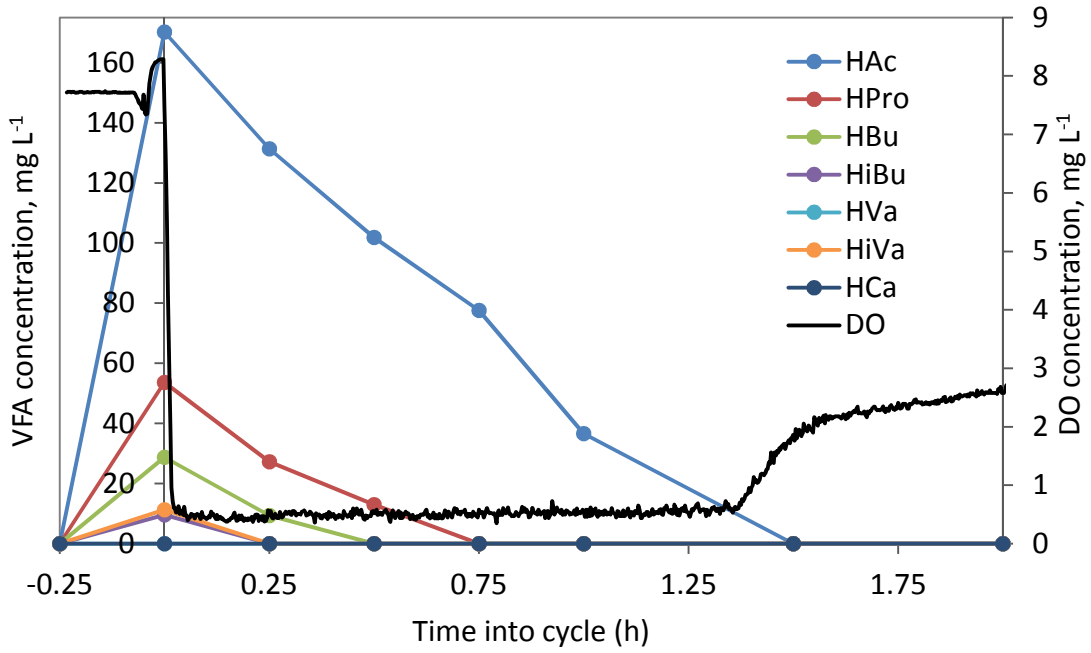

Figure 4.2. Representative VFA and DO consumption during the feast phase of an SBR cycle. Colored lines indicate distinct VFA species measured (VFA abbreviations are the same as listed in Table 1); the solid black line indicates the DO concentration.

a significant oxygen demand. In conclusion, the feast-famine conditions appeared to be suitable for the enrichment of PHA-producing bacteria.

To characterize SBR performance concerning VFA consumption and PHA synthesis, bulk solution parameter assessments were completed once the enrichment SBR began exhibiting consistent DO profiles. A representative profile of VFA and DO consumption

during the feast phase is shown in Figure 4.2. As shown, upon FDML addition (0 h) VFAs were immediately consumed in a zero-order manner (approximately linear with time). As expected, VFA consumption was accompanied by a rapid decrease in DO concentration, followed by a period of low DO concentration (less than 1 mg L^{-1}; Figure 4.2, solid black line); upon VFA exhaustion, a notable increase in DO concentration was observed (Figure 4.2, solid black line). The estimated specific gross VFA uptake rates during SBR operation ranged from approximately 0.05-0.2 mg VFA mg VSS^{-1} h^{-1} and were variable throughout SBR monitoring (Appendix C, Figure C.4). Shortly after VFA depletion, PHA content reached its maximum, ranging from approximately 5-16% of the dried biomass weight (Appendix C, Figure C.4). The PHA yield (Cmmol PHA Cmmol VFA^{-1}) ranged from 0.31-0.88, in line with other literature values for fermented feedstocks; for example waste activated sludge exhibited yields ranging from 0.2-0.43 (Morgan-Sagastume *et al.*, 2010). The copolymer PHBV was consistently synthesized, which consisted of 34-66 mol% HB and 34-66 mol% HV. Together the results substantiated a feast-famine response was established in the enrichment SBR operated under the applied ADF conditions using FDML as a substrate, providing evidence to support the MMC was functionally stable.

The PHA accumulation capacity of the enriched MMC was assessed using fed-batch PHA production tests. Notably, fed-batch PHA production strategies had not been previously optimized for this particular ADF system and were not the focus of this study; rather the fed-batch tests were focused on evaluating the PHA production potential of the enriched MMC. Maximum PHA content reached during the fed-batch tests ranged from 21-40% of the dried biomass weight; the maximum PHA content was in range of other studies using waste feedstocks, including tomato cannery wastewater (20% PHA) (Liu *et al.*, 2008), fermented

olive oil mill pomace (39% PHA) (Waller *et al.*, 2012), and fermented paper mill effluent (48% PHA) (Bengtsson *et al.*, 2008), although lower compared to other fermented feedstocks such as molasses (60% and 74.6% PHA) (Albuquerque *et al.*, 2013; Albuquerque *et al.*, 2010), hardwood spent sulfite liquor (67.6% PHA) (Queiros *et al.*, 2014), or paper mill wastewater (77% PHA) (Jiang *et al.*, 2012). The PHA yield (Cmmol PHA Cmmol VFA^{-1}) ranged from 0.14-0.88, and were comparable to other studies using waste feedstocks (yields ranging from 0.25-0.81) (Albuquerque *et al.*, 2010; Bengtsson *et al.*, 2008). The copolymer PHBV was synthesized and consisted of 23-71 mol% HB and 29-77 mol% HV; the HV content in this study was generally higher compared to previous studies wherein PHBV was synthesized from FDML using MMCs (Guho, 2010; Wei *et al.*, 2014), suggesting residual substrates may have present in this study that yielded additional propionyl-CoA that was incorporated into PHBV. Given the maximum PHA content and yield were lower compared to other studies, the results indicated further process optimization of reactors operated herein is possible. Nevertheless, the maximum PHA content reached in the fed-batch tests was in excess of the enrichment SBR, which was the primary consideration for the microbial community profiling.

4.4.3 Microbial community characterization

4.4.3.1 Overview of 16S rRNA gene sequencing

To characterize and monitor the microbial composition during SBR evaluation, 16S rRNA gene sequencing was performed on biomass samples that had been collected approximately every SRT following SBR start-up (a total of 30 samples were collected for analysis). The amount of nucleic acids extracted from biomass ranged from 95.7 to 290.2 ng

Table 4.2. 16S rRNA gene sequencing results and microbial diversity indices. All samples were collected from the enrichment SBR, denoted by the operational day. The percentage in brackets indicates the relative abundance.

Operational Day	No. reads	No. phylotypes	No. major phylotypes (>1%)	No. minor phylotypes (<1%)	Shannon index	Simpson index
Day 1	10,390	263	17	246	3.00	0.861
Day 8	9,403	263	12	251	3.19	0.880
Day 11	10,294	259	16	243	3.15	0.867
Day 14	9,278	241	15	226	2.87	0.824
Day 18	10,951	240	12	228	2.83	0.824
Day 26	7,339	230	11	219	2.95	0.851
Day 29	7,020	225	13	212	3.01	0.865
Day 34	8,444	220	13	207	2.73	0.842
Day 38	11,852	221	11	210	2.62	0.845
Day 42	13,465	261	13	248	3.07	0.884
Day 50	12,109	272	16	256	3.29	0.904
Day 54	13,890	267	18	249	3.21	0.892
Day 59	8,618	234	11	223	2.85	0.817
Day 66	9,762	227	12	215	2.56	0.754
Day 70	11,481	217	11	206	2.37	0.708
Day 74	9,471	213	12	201	2.22	0.618
Day 77	11,886	217	13	204	2.20	0.613
Day 79	16,870	253	12	241	2.61	0.763
Day 86	16,991	298	17	281	3.31	0.858
Day 88	15,201	257	18	239	3.07	0.878
Day 91	12,458	293	18	275	3.26	0.863
Day 93	13,756	281	18	263	3.06	0.879
Day 95	13,085	296	21	275	3.38	0.887
Day 99	11,692	250	19	231	3.18	0.872
Day 103	87,127	392	22	370	3.29	0.883
Day 104	41,127	342	18	324	3.00	0.830
Day 107	93,539	380	19	361	3.17	0.868
Day 111	78,850	393	20	373	3.28	0.868
Day 115	94,431	432	20	412	3.36	0.892
Day 119	40,357	340	19	321	3.09	0.858

μL^{-1} (Appendix C, Table C.1), which was sufficient for PCR-based amplification of the V1-V3 region of the 16S rRNA gene. The quality of nucleic acids (based on the ratio of absorbance at 260 nm and 280 nm) ranged from 1.869 to 1.983 (Appendix C, Table C.1), indicating DNA was extracted from MMC biomass with high purity (Yeates *et al.*, 1998). The dual-PCR yielded amplicons of sufficient quality and quantity for amplification of the V1-V3 region (data not shown). After sequencing of the dual-barcoded 16S rRNA gene amplicons for all 30 samples and de-multiplexing, a total of 828,463 high quality reads were obtained. The number of reads per sample ranged from 7,020 to 94,431 (Table 4.2; average of 25,889 reads per sample). Rarefaction analysis (Appendix C, Figure C.5) indicated the sequencing depth appeared to be adequate for most samples, although samples with <10,000 reads per sample may not have been amply represented. This variation in the number of reads per sample was likely attributed to systematic variation during sequencing.

4.4.3.2 MMC diversity, composition, and temporal characteristics

To characterize MMC dynamics during the SBR operational period, the phylotypes present and associated microbial diversity were examined. The total number of phylotypes in the MMC ranged from 213 to 432 (Table 4.2 and further visualized in Appendix C, Figure C.6), which was far greater than similar enrichment SBR investigations involving fermented waste substrates (non-sterile) that characterized MMC using fluorescence *in situ* hybridization (Albuquerque *et al.*, 2010; Oehmen *et al.*, 2014; Tamis *et al.*, 2014), denaturing gradient gel electrophoresis coupled with DNA band sequencing (Carvalho *et al.*, 2013; Morgan-Sagastume *et al.*, 2015), or clone library construction (Albuquerque *et al.*, 2013), wherein the total number of taxa reported ranged from 1-28; collectively, these results highlight the power of high-throughput sequencing applied to MMCs in enrichment SBRs. The total number of

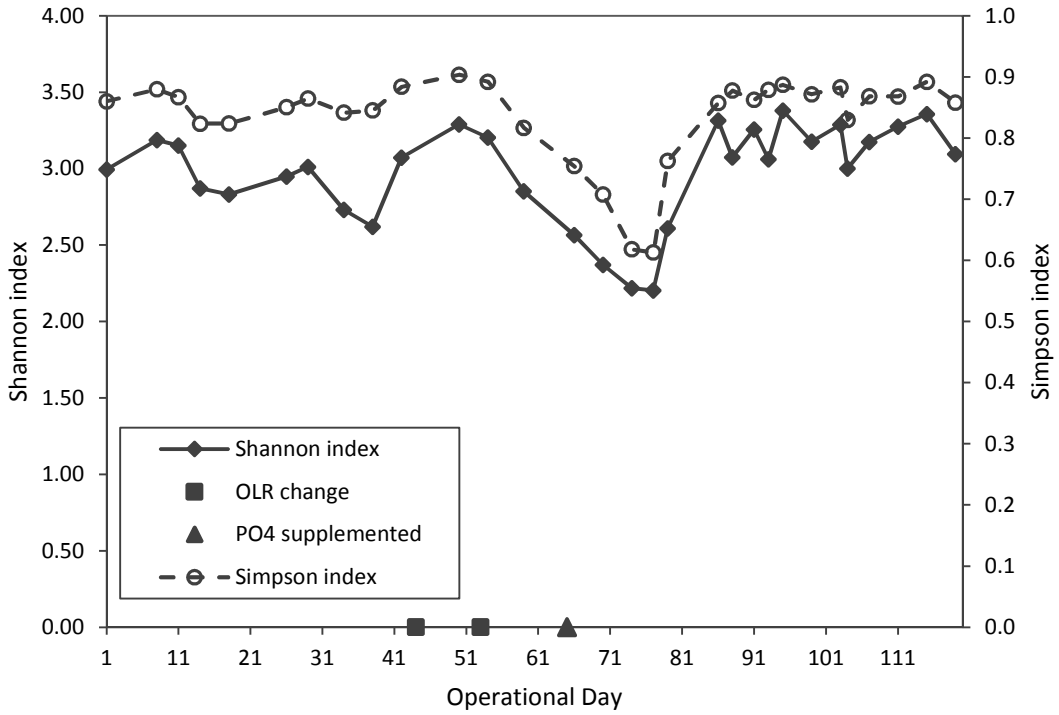

Figure 4.3. Microbial diversity indices during SBR operation. The selected microbial diversity indices are denoted. Operational changes are also indicated. On Day 44 the OLR was adjusted from 40% (v/v) to 50% (v/v); on Day 53, the OLR was adjusted back to 40% (v/v). From Day 65 and onward, equimolar amounts of KH_2PO_4 and K_2HPO_4 were added to the feedstock (indicated by PO4 supplemented).

phylotypes in the MMC varied for the duration of SBR monitoring (Appendix C, Figure C.6); however, the number of major phylotypes (i.e., greater than 1% of the relative abundance) was fairly stable, typically ranging from 10-20, indicating major phylotypes were well-established and consistently maintained in the MMC, in accordance with similar SBRs cultivated on fermented waste substrate noting the persistence of dominant taxa (Albuquerque *et al.*, 2013; Carvalho *et al.*, 2013).

In evaluating the microbial diversity for the entire SBR monitoring period, the Shannon diversity index was selected for its usefulness as a general diversity index, accounting for both species richness and evenness, while the Simpson index was chosen as it is more heavily weighted by dominant taxa (Hill *et al.*, 2003). The calculated diversity indices for all MMC samples are listed in Table 4.2 and further visualized with respect to the SBR operational

period in Figure 4.3. Overall, the microbial diversity (based on the Shannon index) for all samples was higher compared to the one other PHA enrichment SBR investigation wherein the index was reported (≤1.00) (Carvalho *et al.*, 2013), but lower than similarly complex MMC in other engineered systems such as activated sludge (Shannon indices ranging from 4.00-7.36) (Hai *et al.*, 2014; Hu *et al.*, 2012; Kapley *et al.*, 2007). The apparent fluctuation observed in microbial diversity (Figure 4.3) was in agreement with the apparent changes in microbial composition as later discussed and shown in Figure 4.4; this variation was not unexpected, given the inherent variability of the ADF system. The microbial diversity appeared to decrease from Day 50 until Day 77, which may have been partly attributed to three operational changes that were made as shown in Figure 4.3, although definitively determining potential impacts of these operational changes on the microbial diversity was difficult, as only one SBR was being evaluated. Further assessing the temporal characteristics of the microbial composition supported the observations concerning the microbial diversity.

At the phylum level, for the first 54 days of SBR operation, *Proteobacteria* and *Bacteroidetes* appeared to be approximately in equal abundance, ranging from 32-59% and 31-58% of the relative abundance, respectively (Appendix C, Figure C.7). Phyla in less abundance during the first 54 days included *Verrucomicrobia* (1-4%) and *Planctomycetes* (1-4%); 27 other phyla comprised the approximately remaining 2% of the abundance. After Day 54, *Proteobacteria* appeared to be the most abundant phylum (68-79%), followed by *Bacteroidetes* (15-25%), *Verrucomicrobia* (0.4-4%), *Planctomycetes* (0.3-3.4%), and *Actinobacteria* (0.2-2.1%). The high abundance of *Proteobacteria* was in accordance with other PHA enrichment SBR investigations (Lee *et al.*, 2015; Queiros *et al.*, 2014). Though *Bacteroidetes* has not typically been reported for PHA enrichment SBRs, the phylum does

have PHA-producing members (Liu *et al.*, 2013b). At the class level for the entire duration of SBR monitoring (Appendix C, Figure C.8), within in *Proteobacteria*, *Alphaproteobacteria* appeared to the most abundant class (18-68%), followed by *Betaproteobacteria* (4-24%), *Gammaproteobacteria* (1-10%), and *Deltaproteobacteria* (0.3-10%). Within *Bacteroidetes*, an unknown class appeared to be the most abundant (0.2-39%), followed by *Sphingobacteriia* (1-12%) and *Flavobacteriia* (2-10%). *Alphaproteobacteria* has been reported as the dominant class in another PHA enrichment SBR (Serafim *et al.*, 2006), although *Betaproteobacteria* has more commonly been observed in higher abundance (Albuquerque *et al.*, 2013; Carvalho *et al.*, 2013; Lee *et al.*, 2015).

The temporal characteristics of the MMC composition at the highest classification level were also evaluated. For nearly the first two months of SBR operation, *Ohtaekwangia* appeared to be the most abundant genus in the MMC (24-39%), followed by *Meganema* (9-27%), and *Thauera* (2-21%) (Figure 4.4). For the remainder of SBR monitoring, *Meganema* appeared to be the most abundant genus (28-62%), followed by *Thauera* (1-16%), *Ohtaekwangia* (0.2-13%), *Nannocystis* (1-9%), and *Flavitalea* (0.02-8%). Just four MMC constituents, namely, *Meganema* (genus), *Thauera* (genus), an unclassified bacterium, and a member of the *Alphaproteobacteria* class, appeared to be present at a minimum of 1% of the abundance for the entirety of SBR monitoring. Given the changing influent characteristics and dynamic conditions imposed on the MMC, the apparent persistent variability in the relative abundance of major phylotypes was not surprising, although the fluctuation may have also been partly attributed to the inconsistency in the number of sequence reads for each sample.

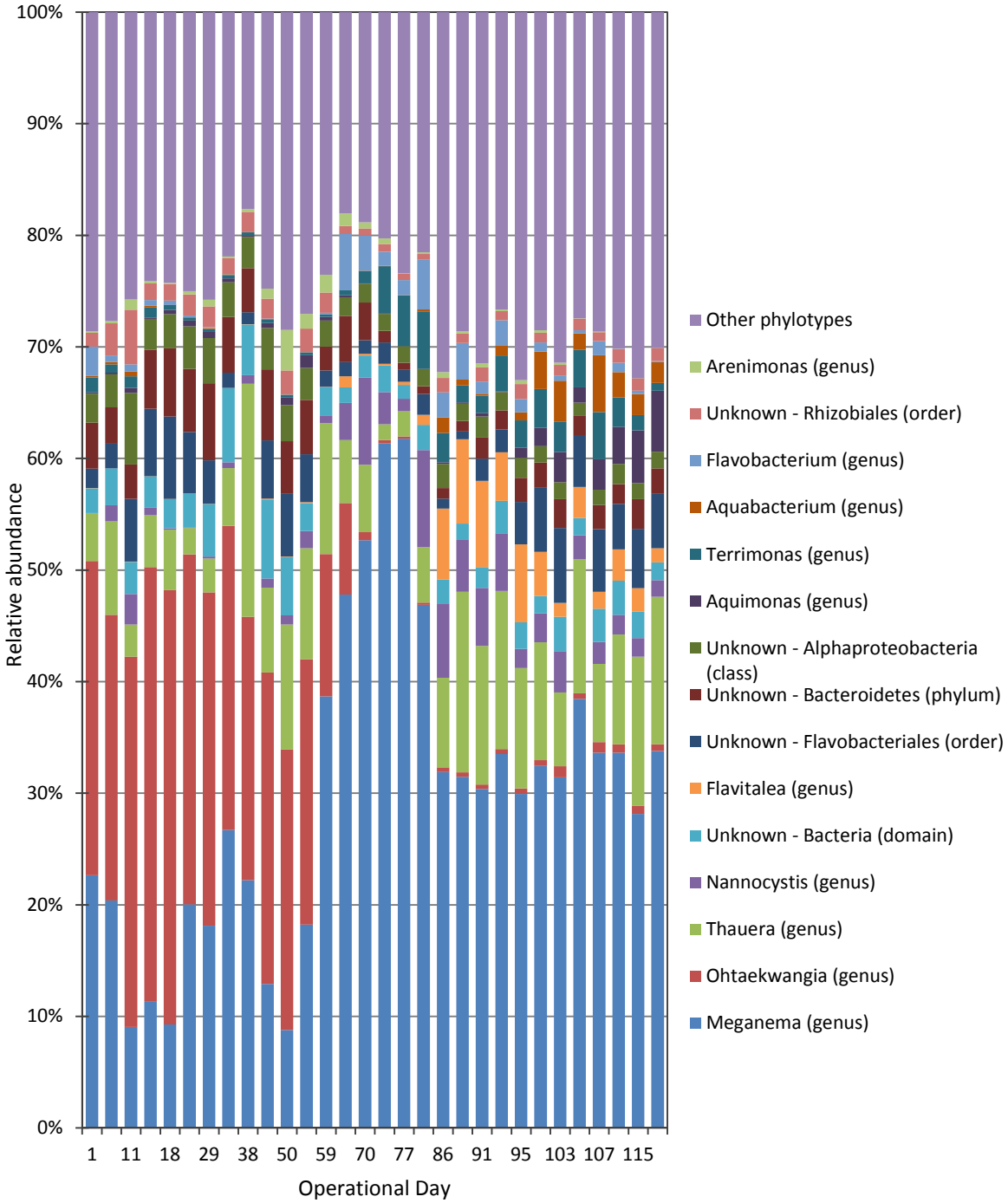

Figure 4.4. Highest classification of phylotypes present in the MMC for the duration of SBR monitoring. For phylotypes not classified to the genus level, the phylotype is denoted as "unknown" and accompanied by best classification level. For viewing simplicity, the top 15 major phylotypes are shown.

The changes in relative abundance of the three most abundant genera beginning on Day 59 (Figure 4.4) indicated a potentially important change in SBR operation. Principal coordinate analysis and cluster analysis supported this apparent MMC composition shift (Appendix C, Figures C.9 and C.10), but identifying the exact reasons was difficult to conclusively determine. The only operating conditions modified intentionally included a brief change in OLR in which the concentration of FDML was adjusted (increased to 50% v/v on Day 44 and then decreased back to 40% v/v on Day 53) and phosphate supplementation (Day 65). An increase in OLR has been reported to increase microbial diversity of an MMC in an enrichment SBR cultivated on fermented molasses (Carvalho *et al.*, 2013). A potential explanation for these observations may be that a higher substrate concentration may sustain more bacteria; however, since only one SBR was evaluated in this study, attributing the change in OLR was met with hesitancy. Additionally, the abundance of *Meganema* appeared to be increasing at the time additional phosphate was supplemented, and appeared to further increase after the phosphate supplementation; the increase in *Meganema* coincided with the decrease of both *Ohtaekwangia* and *Thauera*, suggesting the added phosphate may have been advantageous for *Meganema*. Indeed, the accumulation of polyphosphate has been observed in the *Meganema* genus (Kragelund *et al.*, 2005; Thomsen *et al.*, 2006), suggesting the availability and utilization of phosphorus may contribute to the competitiveness of *Meganema* under dynamic conditions. However, the phosphorus concentration was not closely monitored in the SBR bulk solution or biomass prior to the supplementation, therefore, ascribing the increase in phosphorus to this MMC compositional shift is speculative.

Related to other PHA enrichment SBR investigations, the MMC composition in this study was quite different compared to others. Apart from *Meganema* being reported in another

ADF enrichment SBR (Majone *et al.*, 2006), and the presence of *Thauera*, many genera identified in this study including *Ohtaekwangia*, *Nannocystis*, *Flavitalea*, *Aquimonas*, and *Terrimonas* (four of which are known PHA-producing genera) have not been reported for other PHA enrichment SBRs. Furthermore, dominant genera in MMC often reported for enrichment SBRs including *Azoarcus* (Albuquerque *et al.*, 2013; Albuquerque *et al.*, 2010; Carvalho *et al.*, 2013; Lemos *et al.*, 2008; Oehmen *et al.*, 2014), *Paracoccus* (Albuquerque *et al.*, 2013; Carvalho *et al.*, 2013; Queiros *et al.*, 2014), or *Plasticiculumans* (Jiang *et al.*, 2011; Jiang *et al.*, 2012; Marang *et al.*, 2013) were not identified as highly abundant phylotypes in this MMC. The ADF conditions applied (e.g., SRT, HRT, cycle length, OLR) and particular feedstock used in this study were likely strong determinants influencing the differences in microbial composition, and these results highlight the inherent diversity of PHA enrichment SBRs cultivated on fermented waste substrates.

4.4.3.3 Linking MMC composition and process performance

To investigate possible relationships between MMC composition and PHA process performance, the MMC composition was explored in relation to select process performance parameters. To begin, the physiological characteristics of three of the most abundant genera (*Ohtaekwangia*, *Meganema*, and *Thauera*) were scrutinized, after which the Shannon index values along with the relative abundances of the three genera above were examined with respect to the F:F ratio, estimated specific VFA uptake rate, and the maximum PHA content observed in the both the SBR and fed-batch tests.

The *Ohtaekwangia* genus has two species that have been phenotypically characterized in greater detail, namely, *O. koreensis* and *O. kribbensis*, isolated from marine sand (Yoon *et al.*, 2011). Considering these are the only two documented species in the RDP, both were

considered as proxies in an effort to explore potential implications in the enrichment stage. Neither species was reported to consume acetate or propionate (VFAs that were in the greatest abundance in the FDML) nor synthesize PHA. One species was shown to assimilate various saccharides, including cellobiose, a disaccharide generated from the hydrolysis of cellulose. Given the source of the FDML (dairy manure) and the fact that hydrolysis/fermentation of complex carbohydrates occurred upstream of the SBR, residual saccharides may well have been present in the FDML; thus bacteria with non-VFA substrate requirements or preferences (with no PHA synthesis capacity) may have been able to sustain growth and establishment in the SBR, despite the feast-famine conditions. The persistence of this genus in the SBR would not likely be beneficial for overall PHA process performance. Even though this individual population may not have diverted VFAs away from PHA-producing bacteria, a non-PHA storing fraction of the MMC would be detrimental to PHA yield and likely increase the costs of PHA extraction.

The *Meganema* genus has one species that has been characterized in greater detail, namely, *M. perideroides*, a filamentous organism isolated from activated sludge (Kragelund *et al.*, 2005; Thomsen *et al.*, 2006). Since *M. perideroides* is the only documented species in the RDP, this species was also considered as a proxy. In contrast to *O. koreensis* and *O. kribbensis*, *M. perideroides* was reported to rapidly consume a range of substrates (e.g., glucose, acetate, propionate, and butyrate) under different electron acceptor conditions (viz., oxygen, nitrite, and nitrate) and accumulate large amounts of PHA (Kragelund *et al.*, 2005). The final genus that was in high abundance during SBR monitoring, *Thauera*, has been described in greater detail, with many phenotypic descriptions and sequenced genomes available. Some members of the *Thauera* genus have been shown to possess or exhibit

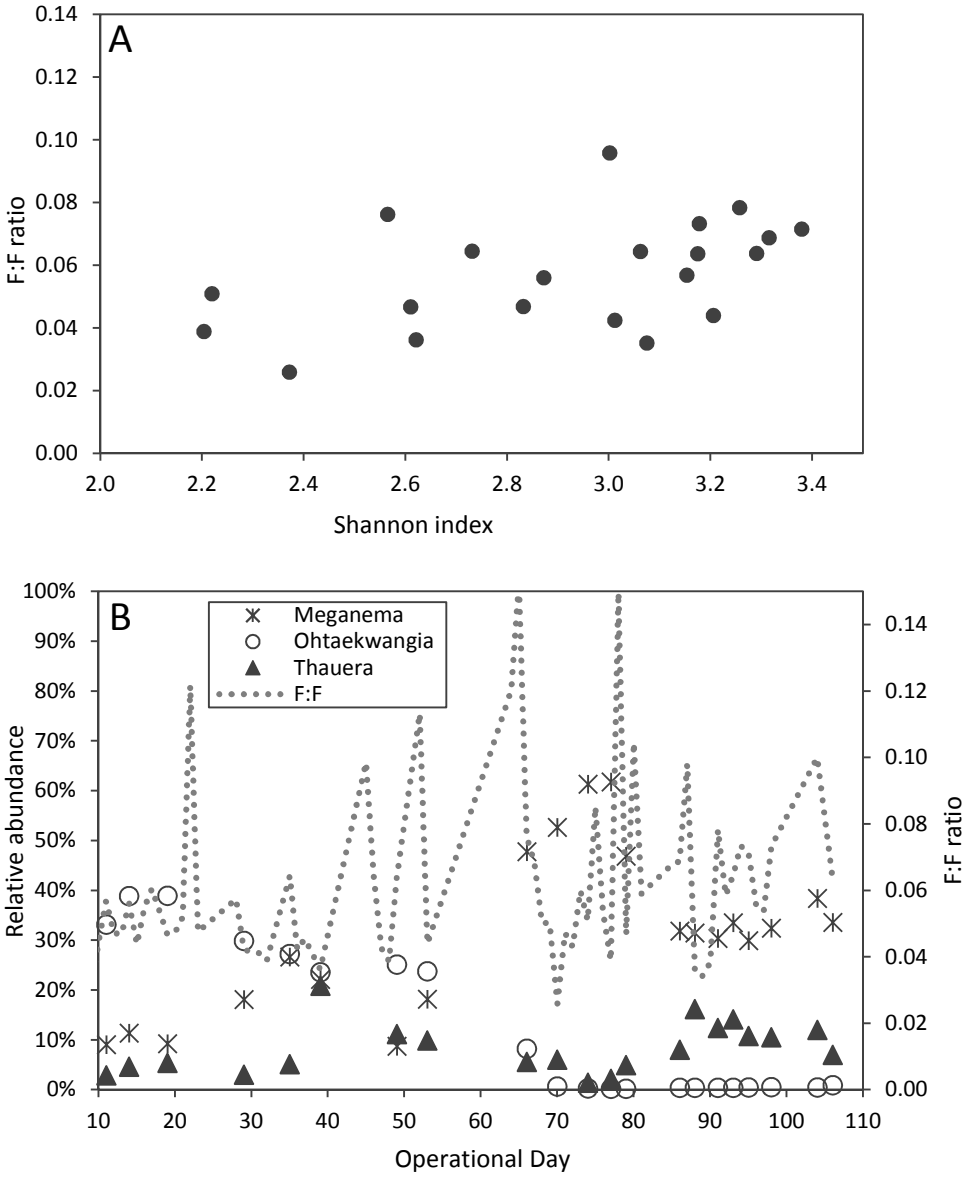

Figure 4.5. Relationships between the measured F:F ratio and MMC profile. A) F:F ratios with respect to Shannon index values; B) Relative abundance of specific genera with respect to F:F ratio and SBR operational day. For panel A, a linear relationship between the F:F ratio and microbial diversity (based on the Shannon index) was not found to be statistically significant (R^2=0.224, p=0.06) at a 95% confidence interval.

metabolic versatility in their ability to assimilate a variety of substrates (e.g., glucose, VFAs, and aromatic hydrocarbons) under different electron acceptor conditions and synthesize large amounts of PHA (Dubbels *et al.*, 2009; Liu *et al.*, 2013a; Scholten *et al.*, 1999). Given the physiological characteristics of both *Meganema* and *Thauera* within the context of the environmental focus of this research, these genera would appear to be well-suited for

persistence in an enrichment SBR. In fact, *Thauera* has been widely reported as a dominant genus in enrichment SBRs (Albuquerque *et al.*, 2013; Carvalho *et al.*, 2013; Chen *et al.*, 2014). Both genera would likely be beneficial for PHA process performance, although the filamentous *Meganema* may not be ideal for MMC biomass processing (e.g., poor settling characteristics (Levantesi *et al.*, 2004)).

Potential relationships between the MMC composition and the F:F ratio were first questioned. The lowest F:F ratio corresponded to a Shannon index of 2.37 (a lower value), although no correlation between the F:F ratio and MMC diversity was observed (Figure 4.5A). The lowest F:F also corresponded to a MMC composition wherein the abundance of *Meganema* was about 52%, but a consistent relationship between the abundance of *Meganema* (along with *Ohtaekwangia* and *Thauera*) and the F:F ratio was not observed (Figure 4.5B), suggesting the F:F ratio may not be highly sensitive to single MMC constituents; however, such a relationship may have been partly masked by the inconsistency of the feast lengths (and resulting F:F ratios). Although these findings provided limited insight regarding potential relationships of specific microbial constituents and an important operational parameter, the results did provide evidence to support the overall feast-famine response of the MMC was maintained despite the fluctuation of individual phylotypes.

Considering the specific VFA uptake rate is a critical functional response associated with PHA synthesis in MMC, prospective relationships with MMC composition and the estimated VFA uptake rates were explored. The highest estimated specific VFA uptake rate corresponded to a Shannon index of 3.19 (a higher value), but no consistent correlation was observed between the two parameters (Figure 4.6A). The highest estimated VFA uptake rate corresponded to the highest abundance of *Meganema* (approximately 60%, Figure 4.6B),

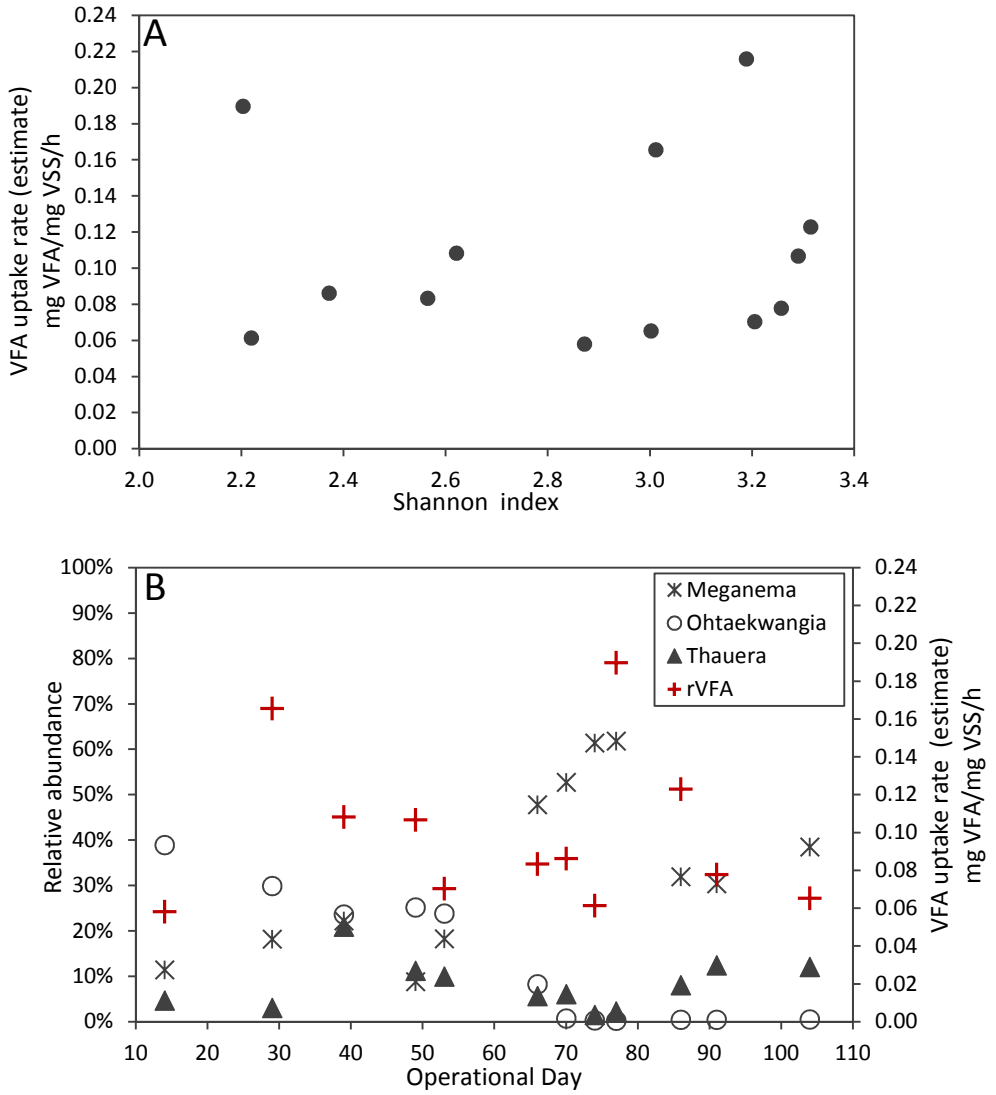

Figure 4.6. Relationships between estimated specific VFA uptake rates and MMC profile. A) estimated specific VFA uptake rates and microbial diversity; and B) estimated specific VFA uptake rate and select genera (rVFA indicates the estimated specific VFA uptake rate). For panel A, a linear relationship between the estimated specific VFA uptake rate and microbial diversity (based on the Shannon index) was not found to be statistically significant (R^2=0.003, p=0.87) at a 95% confidence interval.

which was in agreement with the substrate uptake characteristics previously reported for *M. perideroides* (Kragelund *et al.*, 2005), but a correlation was not observed. In contrast, in a previous investigation using fermented molasses as a substrate, the relative abundance and apparent VFA preference of specific genera were reported to influence specific VFA uptake rates (Albuquerque *et al.*, 2013). In a separate study also using fermented molasses as a substrate, the relative abundance of two genera (*Azoarcus* and *Thauera*) was clearly correlated

to the maximum specific VFA uptake rates (Carvalho *et al.*, 2013), suggesting relationships between particular MMC constituents and VFA uptake may affect this performance parameter. The lowest estimated specific VFA uptake rate in this study corresponded to the MMC composition soon after SBR start up when *Ohtaekwangia* represented nearly 40% of the abundance. This observation may be explained by the fact the SBR had only been in operation for 14 days and the feast-famine response (at a bulk solutions-level) was still equilibrating. Alternatively, the estimated specific VFA uptake rate may have been low if, in fact, the member of *Ohtaekwangia* that was present did not assimilate VFAs, as previously reported for two species of this genus (Yoon *et al.*, 2011). Overall, the estimated VFA uptake rates were fairly similar, indicating this parameter may not have been highly sensitive to the fluctuation of specific MMC constituents. However, further investigation of multiple SBR configurations is warranted to explore prospective relationships. By better defining prospective relationships between microbial composition and VFA uptake in enrichment SBRs, particular operating conditions may be implemented to target the enrichment of specific bacteria that exhibit preferable VFA uptake. In turn, process performance in the fed-batch PHA production may be improved.

As PHA process performance was expected to be influenced the most by the MMC composition, microbial diversity and specific constituents were examined with respect to the PHA content in both the enrichment SBR and fed-batch PHA products tests. The highest PHA content reached in the enrichment SBR corresponded to a Shannon index of 2.85 (a mid-range value), but no correlation was observed for the two parameters (Figure 4.7), suggesting the MMC diversity did not greatly influence the maximum PHA content in the SBR. Furthermore, no apparent association was observed considering the relative abundance of

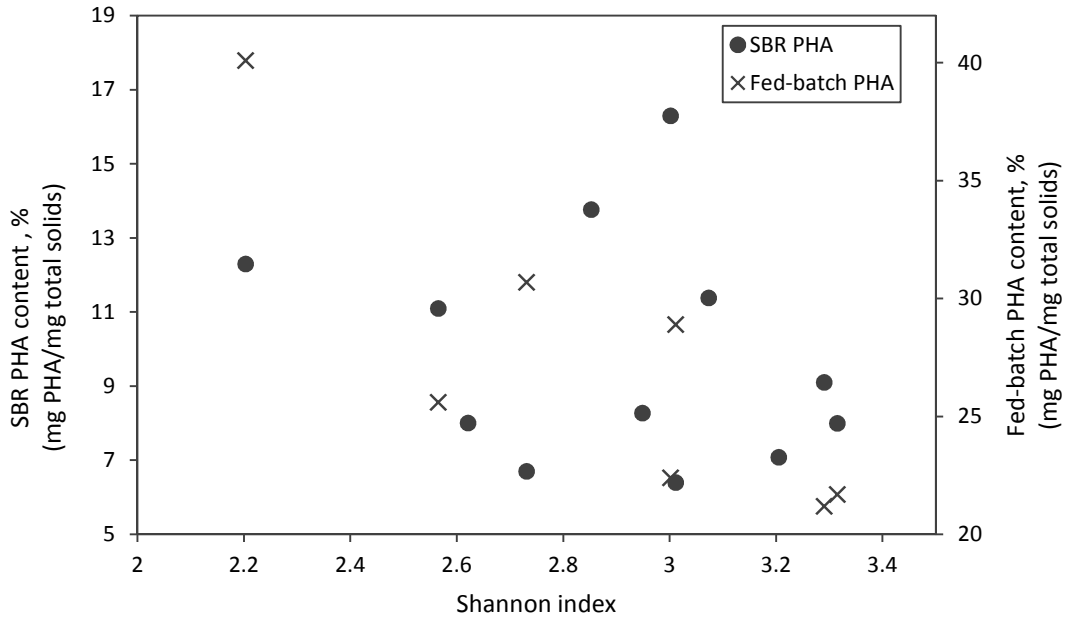

Figure 4.7. Relationships between maximum PHA content achieved in the SBR or fed-batch reactor and microbial diversity. For SBR PHA, a linear relationship between the SBR PHA content and microbial diversity (based on the Shannon index) was not found to be statistically significant (R^2=0.059, p=0.87) at a 95% confidence interval. For fed-batch PHA, a linear relationship between the fed-batch PHA and the microbial diversity (based on the Shannon index) was found to be statistically significant (R^2=0.736, p=0.01) at a 95% confidence interval.

Meganema, *Ohtaekwangia*, and *Thauera* with respect to maximum PHA content reached (Figure 4.8A). Concerning the overall PHA synthesis capacity of the MMC, at least 28 of the 52 identified major phylotypes identified during the entire SBR evaluation period have at least one member known to synthesize PHA. Potential implications of other phylotypes on PHA accumulation including a non-PHA storing "flanking population" were difficult to determine because the quantification of PHA-producing bacteria was limited, as many phylotypes were not assigned to the genus level.

In contrast to the SBR operations, results indicate the MMC diversity may have had a greater impact on PHA production in the fed-batch tests, as the highest PHA content reached corresponded to the lowest Shannon index (2.20) (Figure 4.7). Furthermore, the maximum PHA content in the fed-batch tests appeared to decrease as the MMC diversity increased

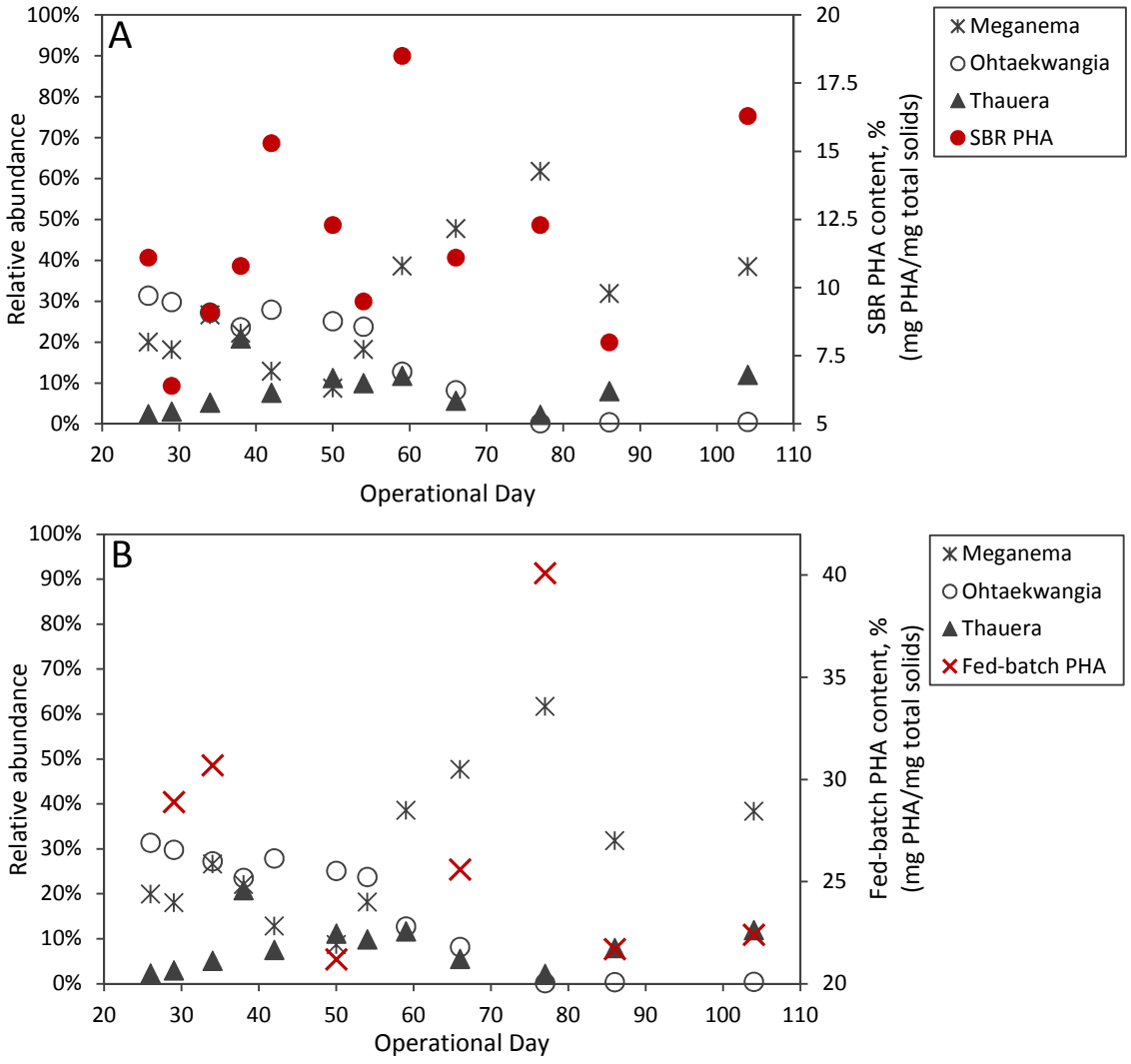

Figure 4.8. Relationships between maximum PHA content achieved in SBR or fed-batch reactor and select genera. A) SBR PHA content and select genera; and B) fed-batch PHA content and select genera.

(Figure 4.7), suggesting lower diversity may have favored higher PHA accumulation in the fed-batch mode. This observation paralleled previous investigations using fermented molasses wherein the maximum PHA accumulation (nearly 75% and 80% PHA) was realized when just two or three genera comprised over 80% of the bacterial abundance in the MMC (Albuquerque *et al.*, 2010; Carvalho *et al.*, 2013). The highest PHA content reached in the fed-batch tests corresponded to the MMC composition in which *Meganema* was in the greatest abundance (approximately 62%), further suggesting PHA process performance may be

favored when a fewer number of taxa comprise the MMC. A possible explanation for this observation is with fewer taxa present, the competition for resources (e.g., VFAs) will be less, and therefore, more VFAs will be converted to PHA. Considering the number of minor phylotypes (i.e., phylotypes comprising less than 1% of the relative abundance) present in the MMC, the decreased process performance may have been partly attributed to the presence of a "flanking population" that diverted VFAs away from PHA-storing bacteria while adding to the total biomass content, thus reducing the maximum PHA content and overall PHA yield (Albuquerque *et al.*, 2013; Jiang *et al.*, 2012). Interestingly, the maximum PHA content reached in the fed-batch tests also corresponded to a decreased abundance of *Thauera* (approximately 2%) (Figure 4.8B), which was in contrast to a previous study that reported a direct relationship between high PHA content and *Thauera* abundance (Carvalho *et al.*, 2013), further highlighting the diversity in multi-stage PHA production implementations.

4.5 Conclusions and future perspectives

Given the interdependent nature of enrichment SBRs and fed-batch PHA production reactors, exploring potential relationships between microbial composition and process performance is essential. Generally for biological systems, functional stability has often been correlated to species richness and evenness (Cardinale *et al.*, 2002; McCann, 2000; Stirling & Wilsey, 2001), whereas in engineered biological systems (e.g., an enrichment SBR), functional stability has been better correlated to functional redundancy (Briones & Raskin, 2003). In the context of the research presented herein, functional redundancy may be considered as the ability to synthesize PHA under imposed ADF conditions, therefore, the enrichment of as many PHA-producing bacteria as possible in SBRs may be preferable for the

functional stability of SBRs. However, in contrast, studies reporting some of the highest PHA contents to date have been achieved using enriched MMCs with very few taxa, although these studies were performed using synthetic feedstocks (Jiang *et al.*, 2011; Johnson *et al.*, 2009). Nevertheless, the enrichment SBRs were functionally stable (i.e., exhibited a consistent feast-famine response), suggesting functional redundancy may not be an absolute requirement for stable SBR operation. In contrast, given the inherent variability of fermented waste feedstocks, functional redundancy may be more critical for the stable operation of enrichment SBRs, although an undesirable trade-off may be decreased PHA process performance in the production stage if microbial diversity is high. Though the limitations in the quantification of PHA-producing bacteria restricted the assessment of functional redundancy in relation to functional stability, the results of this study were significant as a first exploration of microbial composition and dynamics in an enrichment SBR operated under ADF conditions using FDML as a substrate. In evaluating the microbial community profile with respect to conventional bulk solution observations, the following conclusions were drawn:

- A feast-famine response was effectively established in the enrichment SBR, and PHA production up to 40% PHA was achieved in a fed-batch mode.
- Individual bacterial populations of the MMC appeared to fluctuate within a functionally stable SBR.
- Consistent correlations were not observed between microbial composition with respect to SBR performance parameters including the F:F ratio, estimated specific VFA uptake rates, and maximum PHA content.
- Lower microbial diversity may favor higher PHA accumulation the in the PHA production stage.

Concerning future work involving enrichment SBRs cultivated on FDML, methods to improve the quantification of PHA-producing bacteria must be further developed. With enhanced quantification of PHA-producing bacteria, MMC profiling may be applied to multiple SBR configurations in order to more fully examine potential relationships between microbial composition and overall PHA process performance. The inclusion of multivariate and network analyses may reveal other process variables that may contribute to conventional observations and process performance. Furthermore, these analyses may provide greater insight concerning process parameters that influence the selective enrichment of PHA-producing bacteria, which may in turn facilitate the implementation of improved reactor configurations.

4.6 Acknowledgements

The authors acknowledge Dr. Armando McDonald at the University of Idaho for the use of GC-MS for PHA analysis. The authors acknowledge Mr. Dan New and Dr. Alida Gerritsen of the Institute for Bioinformatics and Evolutionary Studies Genomics Resources Core at the University of Idaho, and Dr. Matt Settles of the Bioinformatics Core at the Genome Center at the University of California-Davis for technical assistance related to the 16S rRNA gene sequencing and bioinformatics analysis. This material is based on work supported by the National Science Foundation under Grant Number CBET-0950498, the Environmental Protection Agency Science to Achieve Results Fellowship, and the National Institute of General Medical Sciences from the National Institutes of Health P30 GM103324. Any opinions, findings, and conclusions or recommendations expressed in this material are those

of the authors and do not necessarily reflect the views of the funding agency. The authors declare no conflicts of interest.

References

Albuquerque, M. G. E., Carvalho, G., et al. (2013). Link between microbial composition and carbon substrate-uptake preferences in a PHA-storing community. *Isme Journal, 7*(1), 1-12.

Albuquerque, M. G. E., Eiroa, M., et al. (2007). Strategies for the development of a side stream process for polyhydroxyalkanoate (PHA) production from sugar cane molasses. *Journal of Biotechnology, 130*(4), 411-421.

Albuquerque, M. G. E., Torres, C. A. V., et al. (2010). Polyhydroxyalkanoate (PHA) production by a mixed microbial culture using sugar molasses: Effect of the influent substrate concentration on culture selection. *Water Research, 44*(11), 3419-3433.

Beccari, M., Bertin, L., et al. (2009). Exploiting olive oil mill effluents as a renewable resource for production of biodegradable polymers through a combined anaerobic-aerobic process. *Journal of Chemical Technology and Biotechnology, 84*(6), 901-908.

Beccari, M., Majone, M., et al. (1998). A bulking sludge with high storage response selected under intermittent feeding. *Water Research, 32*(11), 3403-3413.

Bengtsson, S., Werker, A., et al. (2008). Production of polyhydroxyalkanoates by activated sludge treating a paper mill wastewater. *Bioresource Technology, 99*(3), 509-516.

Briones, A., & Raskin, L. (2003). Diversity and dynamics of microbial communities in engineered environments and their implications for process stability. *Current Opinion in Biotechnology, 14*(3), 270-276.

Cardinale, B. J., Palmer, M. A., et al. (2002). Species diversity enhances ecosystem functioning through interspecific facilitation. *Nature, 415*(6870), 426-429.

Carvalho, G., Oehmen, A., et al. (2013). The relationship between mixed microbial culture composition and PHA production performance from fermented molasses. *N Biotechnol*.

Chen, G.-Q., & Patel, M. K. (2011). Plastics derived from biological sources: present and future: a technical and environmental review. *Chemical reviews, 112*(4), 2082-2099.

Chen, Y., Li, M., et al. (2014). Optimal poly (3-hydroxybutyrate/3-hydroxyvalerate) biosynthesis by fermentation liquid from primary and waste activated sludge. *Environmental Technology, 35*(14), 1791-1801.

Choi, J. I., & Lee, S. Y. (1997). Process analysis and economic evaluation for poly(3-hydroxybutyrate) production by fermentation. *Bioprocess Engineering, 17*(6), 335-342.

Coats, E. R., Gregg, M., et al. (2011). Effect of organic loading and retention time on dairy manure fermentation. *Bioresource Technology, 102*(3), 2572-2577.

Dai, J., Gliniewicz, K., et al. (2015). Influence of organic loading rate and solid retention time on polyhydroxybutyrate production from hybrid poplar hydrolysates using mixed microbial cultures. *Bioresource technology, 175*, 23-33.

Dekoning, G. (1995). Physical-properties of bacterial poly((R)-3-hydroxyalkanoates) *Canadian Journal of Microbiology, 41*, 303-309.

Dias, J. M., Lemos, P. C., et al. (2006a). Recent advances in polyhydroxyalkanoate production by mixed aerobic cultures: from the substrate to the final product. *Macromol Biosci, 6*(11), 885-906.

Dias, J. M. L., Lemos, P. C., et al. (2006b). Recent advances in polyhydroxyalkanoate production by mixed aerobic cultures: From the substrate to the final product. *Macromolecular Bioscience, 6*(11), 885-906.

Dionisi, D., Beccari, M., et al. (2005a). Storage of biodegradable polymers by an enriched microbial community in a sequencing batch reactor operated at high organic load rate. *Journal of Chemical Technology and Biotechnology, 80*(11), 1306-1318.

Dionisi, D., Carucci, G., et al. (2005b). Olive oil mill effluents as a feedstock for production of biodegradable polymers. *Water Research, 39*(10), 2076-2084.

Dionisi, D., Majone, M., et al. (2006). Effect of the applied organic load rate on biodegradable polymer production by mixed microbial cultures in a sequencing batch reactor. *Biotechnology and Bioengineering, 93*(1), 76-88.

Dobroth, Z. T., Hu, S., et al. (2011). Polyhydroxybutyrate synthesis on biodiesel wastewater using mixed microbial consortia. *Bioresource Technology, 102*(3), 3352-3359.

Dubbels, B. L., Sayavedra-Soto, L. A., et al. (2009). Thauera butanivorans sp. nov., a C(2)–C(9) alkane-oxidizing bacterium previously referred to as 'Pseudomonas butanovora'. *International Journal of Systematic and Evolutionary Microbiology, 59*(Pt 7), 1576-1578.

Guho, N. M. (2010). *Polyhydroxyalkanoate production coupled with waste treatment using a three-stage sequencing batch reactor system fed dairy manure.* Available from http://worldcat.org /z-wcorg/ database.

Gurieff, N., & Lant, P. (2007). Comparative life cycle assessment and financial analysis of mixed culture polyhydroxyalkanoate production. *Bioresource technology, 98*(17), 3393-3403.

Hai, R., Wang, Y., et al. (2014). Impacts of Multiwalled Carbon Nanotubes on Nutrient Removal from Wastewater and Bacterial Community Structure in Activated Sludge. *PLoS ONE, 9*(9), e107345.

Hill, T. C. J., Walsh, K. A., et al. (2003). *Using ecological diversity measures with bacterial communities* (Vol. 43).

Hu, M., Wang, X., et al. (2012). Microbial community structures in different wastewater treatment plants as revealed by 454-pyrosequencing analysis. *Bioresource Technology, 117*, 72-79.

Huson, D. H., Auch, A. F., et al. (2007). MEGAN analysis of metagenomic data. *Genome Research, 17*(3), 377-386.

Jiang, Y., Marang, L., et al. (2011). Polyhydroxybutyrate Production From Lactate Using a Mixed Microbial Culture. *Biotechnology and Bioengineering, 108*(9), 2022-2035.

Jiang, Y., Marang, L., et al. (2012). Waste to resource: Converting paper mill wastewater to bioplastic. *Water Research, 46*(17), 5517-5530.

Johnson, K., Jiang, Y., et al. (2009). Enrichment of a Mixed Bacterial Culture with a High Polyhydroxyalkanoate Storage Capacity. *Biomacromolecules, 10*(4), 670-676.

Kapley, A., De Baere, T., et al. (2007). Eubacterial diversity of activated biomass from a common effluent treatment plant. *Research in Microbiology, 158*(6), 494-500.

Kragelund, C., Nielsen, J. L., et al. (2005). Ecophysiology of the filamentous Alphaproteobaeterium Meganema perideroedes in activated sludge. *Fems Microbiology Ecology, 54*(1), 111-122.

Lee, W. S., Chua, A. S. M., et al. (2015). Strategy for the biotransformation of fermented palm oil mill effluent into biodegradable polyhydroxyalkanoates by activated sludge. *Chemical Engineering Journal, 269*, 288-297.

Lemos, P. C., Levantesi, C., et al. (2008). Microbial characterisation of polyhydroxyalkanoates storing populations selected under different operating conditions using a cell-sorting RT-PCR approach. *Applied Microbiology and Biotechnology, 78*(2), 351-360.

Levantesi, C., Beimfohr, C., et al. (2004). Filamentous Alphaproteobacteria associated with bulking in industrial wastewater treatment plants. *Syst Appl Microbiol, 27*(6), 716-727.

Liang, S., Gliniewicz, K., et al. (2015). Comparative analysis of microbial community of novel lactic acid fermentation inoculated with different undefined mixed cultures. *Bioresource Technology, 179*, 268-274.

Liu, B., Frostegård, Å., et al. (2013a). Draft Genome Sequences of Five Strains in the Genus Thauera. *Genome Announcements, 1*(1).

Liu, C., Wang, H., et al. (2013b). Composition diversity and nutrition conditions for accumulation of polyhydroxyalkanoate (PHA) in a bacterial community from activated sludge. *Appl Microbiol Biotechnol, 97*(21), 9377-9387.

Liu, H.-Y., Hall, P. V., et al. (2008). Production of polyhydroxyalkanoate during treatment of tomato cannery wastewater. *Water Environment Research, 80*(4), 367-372.

Magoč, T., & Salzberg, S. L. (2011). FLASH: fast length adjustment of short reads to improve genome assemblies. *Bioinformatics, 27*(21), 2957-2963.

Majone, M., Beccari, M., et al. (2006). Enrichment of activated sludge in a sequencing batch reactor for polyhydroxyalkanoate production. *Water Sci Technol, 54*(1), 119-128.

Majone, M., Massanisso, P., et al. (1996). Influence of storage on kinetic selection to control aerobic filamentous bulking. *Water Science and Technology, 34*(5-6), 223-232.

Marang, L., Jiang, Y., et al. (2013). Butyrate as preferred substrate for polyhydroxybutyrate production. *Bioresource Technology, 142*, 232-239.

McCann, K. S. (2000). The diversity-stability debate. *Nature, 405*(6783), 228-233.

Morgan-Sagastume, F., Hjort, M., et al. (2015). Integrated production of polyhydroxyalkanoates (PHAs) with municipal wastewater and sludge treatment at pilot scale. *Bioresour Technol, 181*, 78-89.

Morgan-Sagastume, F., Karlsson, A., et al. (2010). Production of polyhydroxyalkanoates in open, mixed cultures from a waste sludge stream containing high levels of soluble organics, nitrogen and phosphorus. *Water Research, 44*(18), 5196-5211.

Oehmen, A., Pinto, F. V., et al. (2014). The impact of pH control on the volumetric productivity of mixed culture PHA production from fermented molasses. *Engineering in Life Sciences, 14*(2), 143-152.

Queiros, D., Rossetti, S., et al. (2014). PHA production by mixed cultures: A way to valorize wastes from pulp industry. *Bioresource technology, 157*, 197-205.

Reis, M., Albuquerque, M., et al. (2011). Mixed culture processes for polyhydroxyalkanoate production from agro-industrial surplus/wastes as feedstocks. *Comprehensive Biotechnology. Academic Press, Burlington*, 669-683.

Reis, M. A. M., Serafim, L. S., et al. (2003). Production of polyhydroxyalkanoates by mixed microbial cultures. *Bioprocess and Biosystems Engineering, 25*(6), 377-385.

Rice, E. W., et al. (2005). *Standard Methods for the Examination of Water & Wastewater. 21st ed.*

Scholten, E., Lukow, T., et al. (1999). Thauera mechernichensis sp. nov., an aerobic denitrifier from a leachate treatment plant. *Int J Syst Bacteriol, 49 Pt 3*, 1045-1051.

Serafim, L. S., Lemos, P. C., et al. (2006). Microbial community analysis with a high PHA storage capacity. *Water Science and Technology, 54*(1), 183-188.

Stirling, G., & Wilsey, B. (2001). Empirical Relationships between Species Richness, Evenness, and Proportional Diversity. *Am Nat, 158*(3), 286-299.

Stowe, E. J., Coats, E. R., et al. (2015). Dairy manure resource recovery utilizing two-stage anaerobic digestion – Implications of solids fractionation. *Bioresource Technology, 198*, 237-245.

Tamis, J., Lužkov, K., et al. (2014). Enrichment of Plasticicumulans acidivorans at pilot-scale for PHA production on industrial wastewater. *Journal of biotechnology, 192*, 161-169.

Thomsen, T. R., Blackall, L. L., et al. (2006). Meganema perideroedes gen. nov., sp nov., a filamentous alphaproteobacterium from activated sludge. *International Journal of Systematic and Evolutionary Microbiology, 56*, 1865-1868.

van Loosdrecht, M. C. M., Pot, M. A., et al. (1997). Importance of bacterial storage polymers in bioprocesses. *Water Science and Technology, 35*(1), 41-47.

Waller, J. L., Green, P. G., et al. (2012). Mixed-culture polyhydroxyalkanoate production from olive oil mill pomace. *Bioresource Technology, 120*, 285-289.

Wang, Q., Garrity, G. M., et al. (2007). Naïve Bayesian Classifier for Rapid Assignment of rRNA Sequences into the New Bacterial Taxonomy. *Applied and Environmental Microbiology, 73*(16), 5261-5267.

Watson, B. (2015). *Optimization of Dairy Manure Based Polyhydroxyalkanoate Production through Reduced Aeration on Enrichment Cultures.* (Masters of Science), University of Idaho, Moscow, ID.

Wen, Q., Chen, Z., et al. (2012). Bulking sludge for PHA production: Energy saving and comparative storage capacity with well-settled sludge. *Journal of Environmental Sciences-China, 24*(10), 1744-1752.

Wei, L., Guho, N.M., et al. (2014) Characterization of poly(3-hydroxybutyrate-co-3-hydroxyvalerate) biosyntheiszed by mixed microbial consoria fed fermented dairy manure. *Journal of Applied Polymer Science, 131*(11), 40333-40344.

Yeates, C., Gillings, M., et al. (1998). Methods for microbial DNA extraction from soil for PCR amplification. *Biological procedures online, 1*(1), 40-47.

Yoon, J.-H., Kang, S.-J., et al. (2011). Ohtaekwangia koreensis gen. nov., sp. nov. and Ohtaekwangia kribbensis sp. nov., isolated from marine sand, deep-branching members of the phylum Bacteroidetes. *International Journal of Systematic and Evolutionary Microbiology, 61*(5), 1066-1072.

Chapter 5. Conclusions and Future Work

5.1 Summary and conclusions

The research presented herein centered on profiling the microbial community and proteome dynamics of an MMC synthesizing PHA from fermented dairy manure under ADF conditions. Given the heretofore limited characterization of both the microbial composition and functionality of an MMC in an enrichment SBR cultivated on fermented dairy manure, archetypal questions in mixed culture biotechnology, namely, "who is there" and "what are they doing" were used as a guide in implementing experimental approaches. Before commencing proteomic profiling, a technical objective, namely, the optimization of proteomic methods including 2DE (Chapter 2), first had to be completed, as the success of the proteomic investigations was contingent upon effective 2DE protein resolution. Once optimal 2DE methods were established, microbial community and proteome profiling were completed on an enrichment SBR in conjunction with conventional bulk solution variable sampling (Chapter 3). Lastly, the MMC composition and dynamics of the enrichment SBR were evaluated over an operational period of 120 days with respect to select process performance parameters (Chapter 4).

Upon completing the optimization of proteomic methods in Chapter 2, it can be concluded that 2DE still holds value in community-level proteomics within mixed culture biotechnology. The technique has been criticized for its labor-intensive nature and susceptibility to poor reproducibility when applied to complex samples; however, the biomass purification and sequential protein extraction procedures developed in Chapter 2 were robust and reliable. Though the inclusion of separation media may bias bacterial recovery, the

improved gel quality and reproducibility were considered superior advantages. The resulting 2DE gels were high quality and suitable for comparative, quantitative analysis. Due to the utility of the biomass purification and sequential protein extraction procedures and resultant high quality 2DE gels, the workflow presented in Chapter 2 could be adapted to other MMCs cultivated in complex environmental matrices as part of a proteomics approach to investigate microbial functionality.

The material presented in Chapter 3 represented the first microbial community and proteomic profiling of an MMC enriched under ADF conditions for the production of PHA. The identification of phylotypes known to have members with the capacity for VFA assimilation, PHA synthesis, and denitrification provided a basis for the associated bulk solution variable observations, and the identification of proteins of functional relevance to the feast-famine response provided biological explanations for the observed bulk solution changes. In evaluating the proteome profile of the MMC in the enrichment SBR, several conclusions can be made. Given the abundance of porin proteins and ABC transporters, nutrient transport is likely a critical aspect of microbial physiology in ADF systems. Substrate transporters may facilitate rapid substrate uptake in the feast phase and nutrient scavenging during the famine phase – both roles may contribute to the persistence of bacteria in MMCs cultivated under ADF conditions. Related to PHA synthesis under ADF conditions, maintaining a basal abundance of acetyl-CoA acetyltransferase and phasin proteins over a complete SBR cycle may be critical for the rapid initiation of PHA synthesis upon substrate addition in the feast phase. Furthermore, since acetyl-CoA acetyltransferase and phasin proteins were among the proteins that exhibited the largest fold-change in the feast phase, PHA synthesis appeared to be a predominant response.

On the topic of phasins, it can be speculated that phasin proteins may play a key (and heretofore largely unacknowledged role) in PHA metabolism in MMC cultivated under ADF conditions. Considering the role of phasin proteins in PHA synthesis, the abundance of phasin proteins may exert an influence on the kinetics of PHA synthesis during the feast phase, which would be a direct implication of microbial physiology on an important performance parameter. Alternatively, if phasin proteins impart a regulatory role on the maximum PHA content achieved, the abundance of phasins may directly influence process performance. Transitioning to the famine phase of the SBR cycle, given the observed gradual decrease of phasin proteins in relation to the depletion of PHA stores, phasin proteins may play a role in modulating the mobilization of PHA stores. If so, the abundance of phasin proteins may be a principal physiological factor in governing the overall PHA metabolism under ADF conditions. Furthermore, given the high abundance of phasin proteins, PHA-producing bacteria in ADF SBRs may gain more than carbon and reducing equivalents storage through the synthesis of PHA, but also amino acid storage in the form of PHA granule-associated phasins. This potential amino acid storage medium may further contribute to the competitiveness of PHA-producing bacteria in enrichment SBRs.

Moving to the famine phase, the proteome profile provided insight concerning the physiological condition of the MMC. The increased abundance of ABC transporters and molecular chaperone GroEL suggested the MMC was in a stressed state; this stress may have been instigated in more than one way. For example, the limited availability of exogenous substrate or other nutrients may have invoked stress, or oxidative stress may have been more marked given the steady increase in DO during the famine phase. However, determining the extent to which this stress may have been detrimental to overall performance is challenging.

Indeed, for ADF systems physiological stress is ultimately needed to induce PHA synthesis. The increases in abundance of ABC transporters and housekeeping proteins highlighted the apparent physiological shift from PHA synthesis and energy generation in the feast phase to more cellular maintenance-related functions during the famine. More broadly related to physiological stress in MMC, the proteomic evidence was ultimately insufficient to definitively conclude a reduction in anabolic capacity (i.e., a reduction in the number of proteins/enzymes, or the impetus for PHA synthesis under feast-famine conditions) had resulted from the applied ADF conditions. Given these results (with a cycle length of 24 h), it is difficult to anticipate a reduction in anabolic capacity at a protein-level would occur in other enrichment SBRs that have shorter cycle lengths (e.g., 12 h) for a given SRT. Nevertheless, valuable proteome-level evidence was obtained in this research to support principal metabolic concepts pertaining to feast-famine PHA synthesis in ADF systems and provide physiological explanations for conventional observations.

The material presented in Chapter 4 describes the first characterization of microbial composition and dynamics on an MMC in an enrichment SBR cultivated under ADF conditions using fermented dairy manure as a feedstock. Considering the temporal microbial community profile, the microbial composition in enrichment SBRs is likely not static, but rather in a constant state of fluctuation. The continual imposition of "selective pressure" in enrichment SBRs will likely always cause changes in the relative abundance of individual populations within MMCs. Furthermore, the observation of a stable bulk solution profile does not necessarily guarantee a stable microbial community profile. Overall, the functional stability of enrichment SBRs (i.e., the consistent observation of a characteristic bulk solution profile) may not be highly sensitive to microbial community-level changes, but the

performance in the fed-batch PHA production stage may be markedly impacted by fluctuation in the microbial community. As such, the MMC profile in enrichment SBRs should be closely monitored and examined with respect to the performance in the fed-batch PHA production stage.

Additional conclusions were drawn upon integrating the bulk solution, MMC proteome, and microbial community profiles. The applied ADF conditions appeared to be appropriate for eliciting and maintaining a feast-famine response in the enrichment SBR. The collective results in Chapters 3 and 4 would indicate bacteria that can assimilate VFAs and synthesize PHA under different electron acceptor conditions may be the best-suited microorganisms for this particular ADF system, but this may be true for other ADF systems as well, given the commonly observed low DO concentrations in the presence of VFAs. In considering the "selective pressure" of the applied operating conditions, the microbial composition of the MMC was likely influenced beyond solely a PHA synthesis capacity. For example, the lack of a settling phase in the SBR operational cycle likely contributed to the proliferation of a filamentous microorganism in the MMC, and the microaerophilic conditions during the feast phase may have contributed to the enrichment of denitrifying bacteria. Furthermore, the use of an autoclaved feedstock may have influenced the microbial composition. For instance, autoclaving the fermented dairy manure liquor may have caused secondary breakdown of slowly-biodegradable carbon sources such that potential non-VFA assimilating bacteria (e.g., *Ohtaekwangia*) could more readily persist in the SBR, despite the ADF conditions. The findings obtained illustrate the potential for multiple factors to influence (albeit inadvertently) microbial competition in enrichment SBRs, thus possibly affecting the community composition and resultant productivity of enriched MMCs.

Many of the bulk solution variables measured in the SBR (e.g., VFA uptake and PHA yield) were in line with other investigations, and the proteomic results supported aspects concerning the functional response to feast-famine conditions. However, the results obtained from the fed-batch PHA accumulation tests indicated the PHA production stage was not fully optimized. Many potential reasons for this sub-optimal performance may exist. For example, the food-to-microorganism ratio (i.e., the proportion of available substrate to bacteria present) may not have been optimal, leading to substrate over-loading. The pulse-feeding strategy may not have been ideal, therefore, VFA consumption and PHA synthesis may not have been favorable. Additionally, the enriched MMC in this research may not have possessed a high PHA accumulation capacity. This decreased PHA storage may have partly been attributed to the abundance of the filamentous *Meganema* genus. Historically, the PHA storage capacity of filamentous bacteria has been considered to be lower compared to floc-forming bacteria (Krishna & Van Loosdrecht, 1999; Majone *et al.*, 1996). Furthermore, when the substrate concentration is high (e.g., in a fed-batch PHA production reactor) floc-forming bacteria can grow faster than filamentous bacteria (Grady *et al.*, 2011). In other words, an MMC dominated by filamentous bacteria may not be ideal for fed-batch PHA production given their growth kinetics may not be as fast, thus biomass and PHA production rates (and PHA accumulation capacity) may be inherently low. Lastly, given filamentous bacteria can cause issues with biomass handling (e.g., excessive foaming or poor settling), this MMC biomass would not likely be ideal for fed-batch PHA production, as biomass collection may be challenging. Considering these disadvantages, it may be prudent to implement a settling phase in the enrichment SBR cycle prior to the draw phase in an effort to “wash out” filamentous bacteria.

Bearing in mind the proteome profile for the enrichment SBR did not appear to exhibit a drastic reduction in the number of proteins during the famine, implementing a longer cycle length may improve the PHA storage response. A longer cycle length may further deplete intracellular components (e.g., proteins, enzymes, and metabolite pools) such that growth in the feast phase may be more markedly impaired, thus enhancing the PHA storage response. Additionally, with a longer cycle length and famine phase, it may be anticipated that a greater amount of PHA would be stored in the feast phase (as more PHA would be required to withstand a longer famine phase), further enhancing the storage response. Notably, extending the cycle length would likely require a re-formulation of the OLR to ensure enough substrate is provided at the start of the SBR cycle. Lastly, a longer cycle length may enhance the microbial composition of enrichment MMCs, as a longer cycle length (especially a longer famine phase) would be anticipated to minimize the growth and persistence of non-PHA producing bacteria. Ultimately, devising and implementing alternative ways to further modulate or minimize the heterogeneity of the growth rates of bacteria present in enrichment SBRs may result in improved fed-batch PHA production.

Given the apparent stressed physiological state of the MMC during the famine phase (Chapter 3), it may be tempting to increase the substrate concentration at the start of the SBR cycle. However, given the observations presented and discussed in Chapter 4, this may be counterproductive, as a higher substrate concentration may sustain a more diverse microbial community (possibly non-PHA storing bacteria), which may be detrimental to the fed-batch PHA production stage. Given the observation of soluble non-VFA COD during the famine phase of the SBR cycle coupled with the microbial community profile, it may be beneficial to implement a settling and draw phase upon the end the feast phase to remove residual soluble

non-VFA COD in an effort to minimize possible growth of non-PHA storing bacteria; however, a draw phase may remove ammonia, which could negatively impact PHA-producing bacteria, as an ammonia limitation could limit growth on PHA stores during the famine.

By exploring fundamental aspects of the microbial community and proteome profile in an enrichment SBR, the research presented herein permitted a more meaningful evaluation of the applied operating conditions employed for the purpose of obtaining an enriched MMC for PHA production, highlighting the integration of molecular-based sciences with engineering. The application of next-generation DNA sequencing coupled with mass spectrometry-based proteomics to MMC PHA production was novel, as these systems have historically been studied from a "black box" perspective by extrapolating molecular-level functions based on macro-level bulk solution measurements. Not only did this research contribute to the fundamental knowledge base regarding feast-famine PHA synthesis in MMC, useful information was obtained that can be translated into engineering terms to guide future studies aiming to improve PHA production strategies.

5.2 Future work

The production of a valuable commodity from an otherwise undesirable waste, while simultaneously achieving enhanced waste management is a desirable objective within environmental biotechnology. PHA process optimization is obviously important, but engineering alone will not suffice in advancing the technology. Apart from the assessment of different SBR configurations in conjunction with fed-batch PHA production tests, increased attention regarding waste feedstock composition, microbial community composition, and the

physiological component underpinning observed PHA process performance should accompany all empirical optimization efforts.

As alluded to previously, based on the results obtained in Chapters 3 and 4, future SBR investigations may include altered parameters. The same operating conditions (i.e., OLR, SRT, and HRT) used in Chapters 3 and 4 may be re-evaluated with the implementation of a settling phase prior to the draw phase, in addition to a longer cycle length. As noted previously, the inclusion of a settling phase for the SBR may minimize the enrichment of filamentous bacteria, and a longer cycle length may improve the PHA storage response. These two operational changes may positively influence the enriched MMC composition and functional response such that PHA accumulation in the fed-batch production stage is enhanced. Another potential operational change may include the reduction of aeration during the famine phase in the event higher DO concentrations evoke more pronounced oxidative stress on the MMC. By potentially lessening the oxidative stress on the MMC, biomass growth during the famine may be enhanced. Reducing the aeration during the famine phase would also save on energy costs, which would be beneficial as well.

Operational adjustments may be evaluated in the fed-batch PHA production stage. For instance, the supplementation of fermented dairy manure with valine could be assessed to determine if the HV content could be increased. The inclusion of a short settling phase followed by a draw phase at the end of each feed (immediately prior to the next feedstock addition) may remove residual soluble COD and ammonia, ideally minimizing the possibility for growth to become dominant to PHA storage, especially for any non-PHA producing bacteria that may be present. In turn, the volumetric productivity of the MMCs may be increased in the fed-batch PHA production stage. Given the proteome profile observed at the

end of the SBR cycle, imposing an extended famine condition on the MMC prior to PHA production may improve the PHA storage response. As such, the effluent from the SBR (that will be used in the fed-batch PHA production) may be maintained under aerobic conditions for an extended length of time prior to commencing PHA production.

To bolster investigations of different SBR and fed-batch operating parameters, the incomplete characterization of nutrients in fermented dairy manure (along with other waste feedstocks) must be addressed. Apart from the quantification of VFAs, ammonia, and phosphate, other potential carbon and inorganic nutrient sources in waste fermentates (e.g., carbohydrates, lipids, cationic, anionic, or metallic constituents), have received less attention for quantification, therefore, any potential roles are largely unknown – this is especially true for fermented dairy manure. For example, if a particular nutrient(s) is limiting, it calls into question whether or not enrichment SBRs are operated strictly under carbon-limited conditions. Under one set of nutrient conditions, competing bacteria may coexist in a stable manner, however, under a different set of nutrient conditions (which may be likely for fermented dairy manure), specific taxa may be "outcompeted" as a result of a given nutrient limitation. Considering enrichment SBRs are operated for long periods (i.e., years) under dynamic conditions, nutrient availability may well influence microbial competition in these systems (Cherif & Loreau, 2007; Hibbing *et al.*, 2010; Smith, 2002). Lastly, little research has examined the types and survival of microorganisms present in waste fermentates. It has been assumed microorganisms from an anaerobic fermenter would not survive in the aerobic feast-famine conditions, however, this has not been verified. In conclusion, possible matrix effects influencing the microbial composition and physiology are largely underdetermined for

enrichment SBRs cultivated on fermented dairy manure, as well as many other waste feedstocks and warrant further investigation.

Considering the relatively small fraction of proteins that were identified in Chapter 3, additional protein spots that were processed should be identified using LC-MS/MS. The identification of as many proteins as possible, especially those protein spots that consistently exhibited high or differential abundance, would supplement the results presented in Chapter 3 concerning microbial functional dynamics over an SBR cycle. An improved MMC proteome profile for the SBR operating conditions applied in Chapter 3 may in turn direct future proteomic investigations (e.g., studies quantifying the turnover of all PHA-metabolism related enzymes or phasin proteins). Additionally, the identification of more proteins from Chapter 3 may provide further insight regarding how future SBR configurations may be implemented and evaluated. For example, if remaining PHA synthesis-related enzymes (i.e., NADPH-dependent acetoacetyl-CoA reductase, PHA synthase, and PHA depolymerase) could be identified and the turnover established for one set of operating conditions, a reference could be ascertained for future investigations.

With proteomic methods established for this particular system, proteomics could be applied in factorial analyses of different SBR configurations (including a non-PHA enrichment SBR control) and associated fed-batch PHA production tests. Proteome profiles could be investigated with respect to differences in process performance, potentially revealing key distinctions in community-level functionality as related to improved or decreased process performance. Alternatively, identifying similarities of proteome dynamics of MMC in different SBR configurations and fed-batch PHA production reactors may reveal commonalities in community-level function (regardless of operating conditions), providing

insight concerning the extent to which MMC may be "conditioned" for a particular functional response under different ADF conditions. As in Chapter 3, the microbial composition should be evaluated in conjunction with proteomic investigations to determine if potential differences in proteome profiles is due to different MMC compositions.

More generally applied to enrichment SBRs, the microbial physiology driving the induction of PHA synthesis under feast-famine conditions must be re-visited. Though this area has received some research attention as discussed in Chapter 1, the results of these studies were ultimately inconclusive and limited to pure cultures. Of many possible experimental approaches to assess the physiology of MMC cultivated under feast-famine conditions (Guho, 2014), one valuable evaluation would include comparing proteome profiles of a microbial culture maintained in an ADF enrichment SBR, as well as a chemostat operated under conventional conditions for PHA production (induction of PHA synthesis via external nutrient limitation). In comparing proteome profiles of these different cultures, additional explanations concerning feast-famine PHA synthesis may be obtained. With an improved understanding of physiological mechanisms triggered by feast-famine conditions, devising reactor operating conditions may be better guided.

Due to the interdependence of enrichment SBRs and fed-batch PHA production reactors, greater attention should be given to exploring microbial diversity and composition with respect to functional stability and overall performance in these systems. A great deal of literature discussing relationships between species diversity and stability in a variety of ecosystems is available (Bell *et al.*, 2005; Briones & Raskin, 2003; Cardinale *et al.*, 2002; McCann, 2000; Naeem, 1998; Naeem & Li, 1997; Wittebolle *et al.*, 2009), and such ecological concepts are often adapted to microbial communities. Generally, species diversity is

correlated with functional stability, and with this in mind questions pertaining to enrichment SBRs arise. For instance, will a microbial community in an enrichment SBR with more pathways towards PHA production (as many PHA-producing bacteria possible) be functionally more stable compared to one in which is less diverse? Will this type of enriched MMC generate a more desirable product in a fed-batch mode (e.g., greater amounts of PHA and higher HV content)? Will this type of MMC exhibit enhanced PHA yields and specific synthesis rates? Though the results presented in Chapter 4 established a foundation for which future work could expand, to begin answering such questions and exploring possible correlations between microbial diversity and process performance, quantifying the abundance of viable PHA-producing bacteria in enrichment SBRs relative to all bacteria present needs improvement. This enhanced quantification may require greater 16S rRNA gene sequencing depth to identify phylotypes to a species level or additional bioinformatics to search 16S sequences using other tools such as Blast. Alternatively, quantitative PCR targeting the PHA synthase gene may be useful in determining the relative abundance of PHA-producing bacterial relative to all bacteria. Ideally, the viability of bacteria present in enrichment SBRs would also be evaluated in conjunction with the quantification of PHA-producers, but this may be challenging as the dairy manure matrix may interfere with viability assessments. Nevertheless, a more accurate quantification and taxonomic assignment of PHA-producing bacteria in MMCs would be helpful in better defining possible correlations between microbial diversity and PHA production performance.

As with future work in applying proteomics, microbial community profiling could be applied to future factorial analyses of different SBR configurations and corresponding fed-batch PHA production assessments. With comprehensive bulk solution-level data for both

SBRs and fed-batch reactors (e.g., specific VFA uptake rate, specific PHA synthesis rate, PHA yield, and biomass production) and associated microbial community profiles, multivariate analyses may reveal key correlations between microbial diversity and system performance. Arguably, in order to accomplish the goal of optimizing enrichment SBR operating conditions, an improved understanding concerning the relationships between applied operating conditions and the resulting microbial community composition is required. However, linking microbial community dynamics to process stability and performance will involve basic ecological issues, therefore, a collaborative effort between engineers and microbial ecologists would be beneficial.

Additionally, metagenome-guided investigations may facilitate obtaining an enhanced metabolic blueprint for MMC cultivated under different SBR operating conditions. Metagenome information related to the overall PHA metabolism (e.g., PHA biosynthetic genes, PHA depolymerase, and regulators), may provide clues related to PHA turnover in an ADF cycle. For example, if more was known about potential PHA regulatory mechanisms, such knowledge may be factored into designing and implementing different SBR configurations to improve the enrichment stage. Independent of PHA synthesis, an improved awareness of other metabolic potential may facilitate enhanced nutrient recovery. For instance, if a repertoire of genes related to nitrogen metabolism (e.g., nitrification and denitrification) are consistently identified, strategies may be implemented to possibly exploit a particular metabolism and in turn, perhaps improve the quality of PHA process effluent. Taken further, obtaining an enhanced understanding of the global metabolic potential may bolster existing metabolic models that are necessary for process optimization.

Further interrogation of metabolic activity of MMC cultivated under ADF conditions in the presence of mixed substrates is also warranted. Historically, the extent to which PHA storage and growth occur simultaneously during the feast phase has typically been estimated by carbon and nitrogen mass balancing, with activity through central metabolic pathways (e.g., glycolysis, Enter-Doudoroff pathway, TCA cycle, and the pentose phosphate pathway) only being considered implicitly through assumed stoichiometry. Surprisingly, the metabolic activity during the famine phase has received little attention, despite its importance to the culture's "history" that strongly dictates the PHA storage response in the subsequent feast phase. PHA degradation during the famine phase has been observed in many studies, but limited evidence (apart from that described in Chapter 3) is available to describe how or through which pathways liberated PHA monomers are utilized for growth and energy generation during the famine. Furthermore, given a drastic reduction in protein abundance at the end of the SBR cycle for the operating conditions applied was not observed, a reduction in anabolic capacity may arise from decreased metabolite pools. As such, the quantification of metabolic intermediates would be useful.

As visible in Figure 5.1, microbial metabolism involving mixed substrates is complex. Inferring intracellular metabolite changes to ADF conditions based on bulk solution variables or even the mathematical models discussed in Chapter 1 is challenging, especially in the presence of mixed substrates given the complexity of possible metabolic routes in Figure 5.1. With the advancements in gas and liquid chromatography coupled to mass spectrometry systems, the high-throughput, simultaneous analysis of hundreds of metabolites (including those in Figure 5.1) is feasible, although this type of experimental approach should first be applied to MMC cultivated using a synthetic feedstock. Though inherently complex,

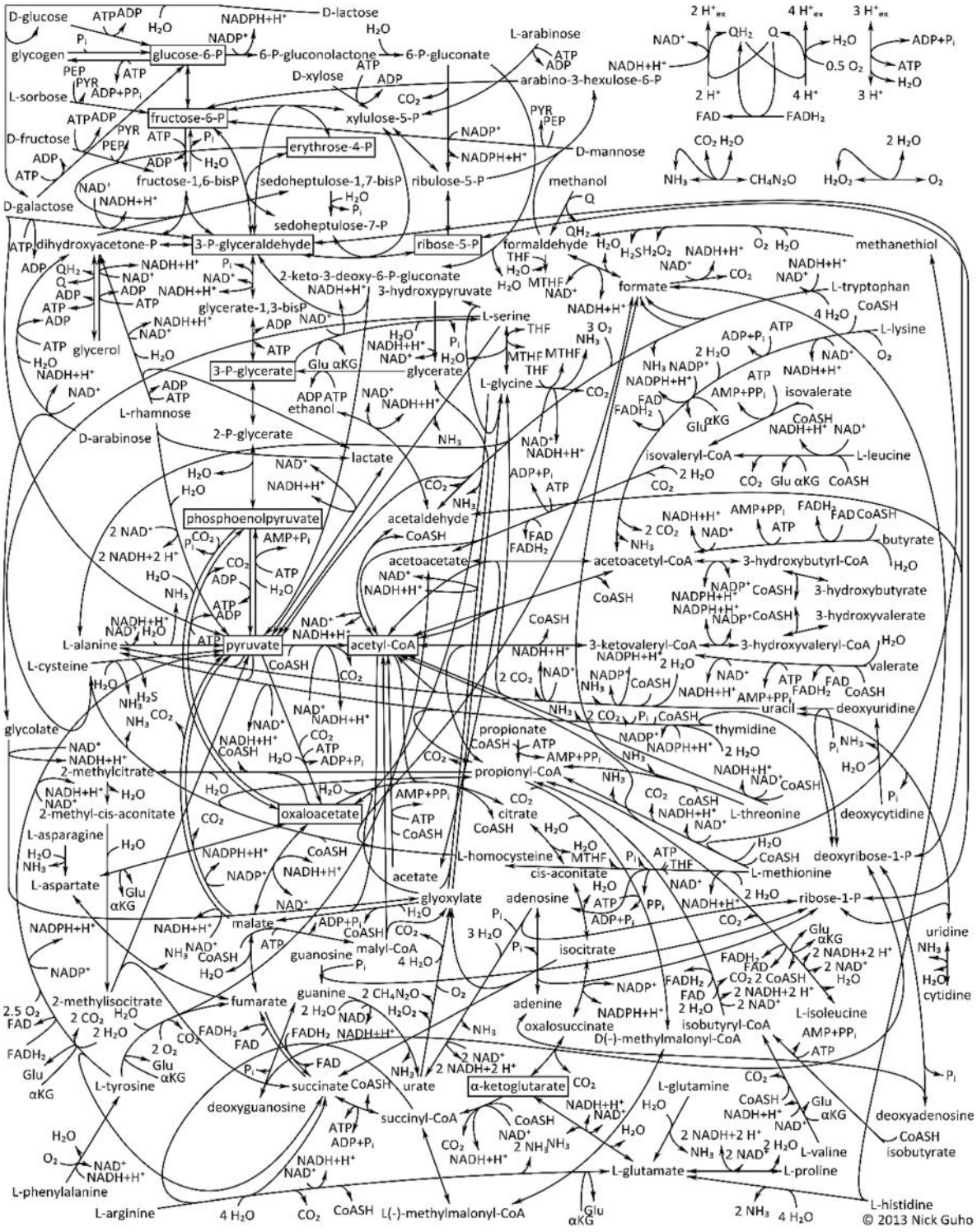

Figure 5.1. Prospective metabolism of mixed substrates in MMCs. Boxed metabolites indicate direct biomass precursors. (Figure courtesy of Nicholas M. Guho)

ascertaining points of reference regarding intracellular metabolite pool dynamics over a complete SBR cycle is necessary to more fully understand the functional responses exhibited by MMC in relation to process performance. Monitoring the activity associated with the central metabolic pathways (i.e., pathways that generate precursors for other pathways, such as glycolysis, Entner-Doudoroff pathway, pentose phosphate pathway, and the TCA cycle) in relation to PHA synthesis over an ADF operational cycle may be the most quantitative assessment of MMC metabolism. During the feast phase, the direct quantification of intermediate metabolites of carbohydrate and organic acid catabolism, including the generation of acyl-CoA thioester PHBV precursors (Figure 5.1), may yield a more representative description of biomass growth relative to PHA storage in the feast phase as opposed to carbon and nitrogen mass balancing. Furthermore, the direct quantification of metabolites in fed-batch PHA production reactors may reveal rate-limiting steps or metabolic bottlenecks during fed-batch PHA synthesis.

Concerning the famine phase of an SBR cycle, monitoring intermediates of the aforementioned central metabolic pathways may provide greater details concerning how stored PHA is used for anabolic purposes under ADF conditions. The quantification of metabolic intermediates during the famine phase may also reveal the extent of an internal limitation caused by the absence of exogenous substrate (i.e., which metabolite pools are the most depleted). For both the feast and the famine phases, by directly measuring metabolites, the MMC metabolic activity along with associated stoichiometry and kinetics may be better defined. With an enhanced understanding of the "global" metabolism, both SBR and fed-batch reactor configurations may be improved. Whether such changes are in the form of for example, adjusting specific combinations of operational parameters (e.g., OLR, SRT, CL) in

SBRs or fed-batch reactors, selectively timed feedstock supplementations, or imposing physical means of segregating bioreactor constituents, implementing macro-level alterations with a microbiological rationale will likely bolster future empirical optimization. In conclusion, an integrated approach capitalizing on the advancements in high-throughput "omics" technologies coupled with conventional bulk solution variable evaluations offers great potential to advance this technology.

References

Bell, T., Newman, J. A., et al. (2005). The contribution of species richness and composition to bacterial services. *Nature, 436*(7054), 1157-1160.

Briones, A., & Raskin, L. (2003). Diversity and dynamics of microbial communities in engineered environments and their implications for process stability. *Current Opinion in Biotechnology, 14*(3), 270-276.

Cardinale, B. J., Palmer, M. A., et al. (2002). Species diversity enhances ecosystem functioning through interspecific facilitation. *Nature, 415*(6870), 426-429.

Cherif, M., & Loreau, M. (2007). Stoichiometric constraints on resource use, competitive interactions, and elemental cycling in microbial decomposers. *Am Nat, 169*(6), 709-724.

Grady, C., Daigger, G., et al. (2011). *Biological wastewater treatment*: CRC Press.

Guho, N. M. (2014). [Advancing Bioplastic Production from Waste Feedstocks using Mixed Microbial Consortia by Reconsidering the Underlying Biochemical Basis: One Step Back, Two Steps Forward].

Hibbing, M. E., Fuqua, C., et al. (2010). Bacterial competition: surviving and thriving in the microbial jungle. *Nat Rev Microbiol, 8*(1), 15-25.

Krishna, C., & Van Loosdrecht, M. C. M. (1999). Effect of temperature on storage polymers and settleability of activated sludge. *Water Research, 33*(10), 2374-2382.

Majone, M., Massanisso, P., et al. (1996). Influence of storage on kinetic selection to control aerobic filamentous bulking. *Water Science and Technology, 34*(5-6), 223-232.

McCann, K. S. (2000). The diversity-stability debate. *Nature, 405*(6783), 228-233.

Naeem, S. (1998). Species redundancy and ecosystem reliability. *Conservation Biology, 12*(1), 39-45.

Naeem, S., & Li, S. (1997). Biodiversity enhances ecosystem reliability. *Nature, 390*(6659), 507-509.

Smith, V. H. (2002). Effects of resource supplies on the structure and function of microbial communities. *Antonie Van Leeuwenhoek, 81*(1-4), 99-106.

Wittebolle, L., Marzorati, M., et al. (2009). Initial community evenness favours functionality under selective stress. *Nature, 458*(7238), 623-626.

Appendix A

Supplementary material for:

Chapter 2. Proteomic profiling of an undefined microbial consortium cultured in fermented dairy manure: methods development

Table A.1. Identification of proteins arising from a single 2DE protein spot. The raw data files from the peptide sequencing were converted to a peak list file by ProteinLynx Global Server (PLGS) 2.3 software (Waters Corporation). The peak list file was searched against the NCBInr database (October 2015, 73,055,898 protein sequences) with a bacterial species restriction and the following search parameters: (i) specific enzyme, trypsin; (ii) peptide window tolerance, ±0.4 Da; (iii) fragment mass tolerance, ±0.4 Da; (iv) missed cleavage sites, 1; and (v) variable modifications, carbamidomethyl C, deamidated NQ, and oxidized M. The decoy option was included for each search to include the false discovery rate. For protein identification, only protein hits with at least two peptide matches and individual protein scores above the significance score calculated by Mascot ($p < 0.05$; the individual ion score is $-10 \times \log(p)$, where p is the probability that the observed match is the random match) were accepted.

Protein Accession	Protein Name	Taxonomy	Mascot Score	MW[a]	pI[b]	No. Peptides Matched	Protein Sequence Coverage (%)
WP_026310202	Amino acid ABC transporter substrate-binding protein	*Meganema perideroedes*	1576	36687	4.77	17	74
WP_018634075	Hypothetical protein	*Meganema perideroedes*	322	91904	5.54	5	11
WP_018634183	LacI family transcriptional regulator	*Meganema perideroedes*	220	33205	4.90	2	18
WP_018632502	Hypothetical protein	*Meganema perideroedes*	162	53170	4.77	3	10

[a] The calculated molecular weight of the protein.
[b] The calculated isoelectric point of the protein.

Appendix B

Supplementary material for:

Chapter 3. Community Proteomics Reveals Insight into Polyhydroxyalkanoate Production from Fermented Dairy Manure Using a Mixed Microbial Culture

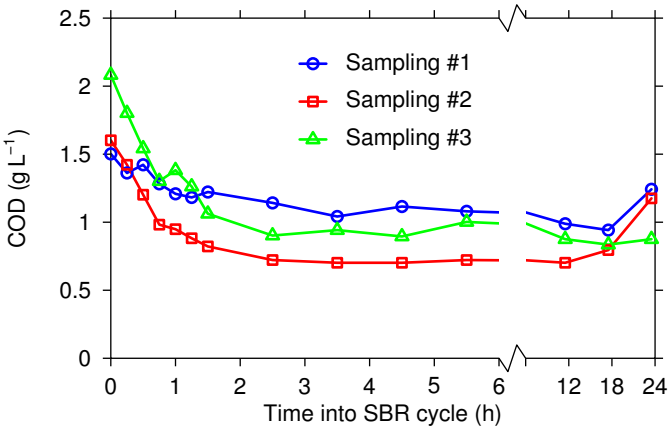

Figure B.1. Soluble COD vs. time into SBR cycle for the three sampling events. Note the break and scale change in the abscissa at 6 h into the SBR cycle.

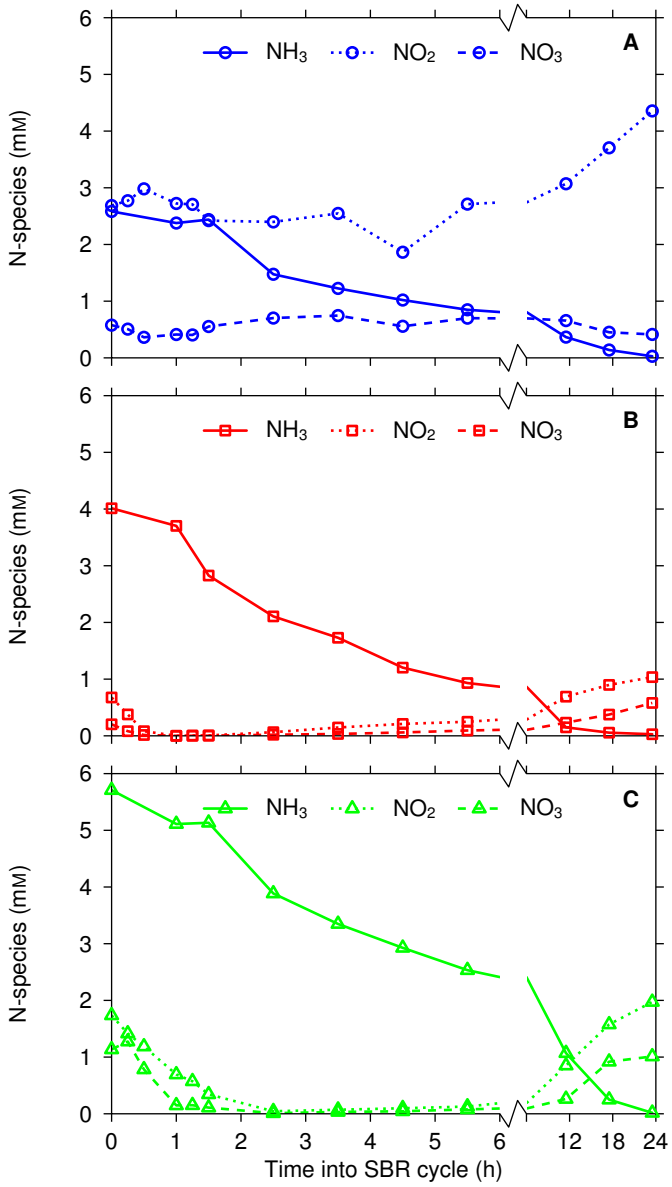

Figure B.2. Nitrogen species vs. time into SBR cycle for the three sampling events. **A**, **B**, and **C** correspond to Sampling events #1, #2, and #3, respectively. Note the break and scale change in the abscissa at 6 h into the SBR cycle.

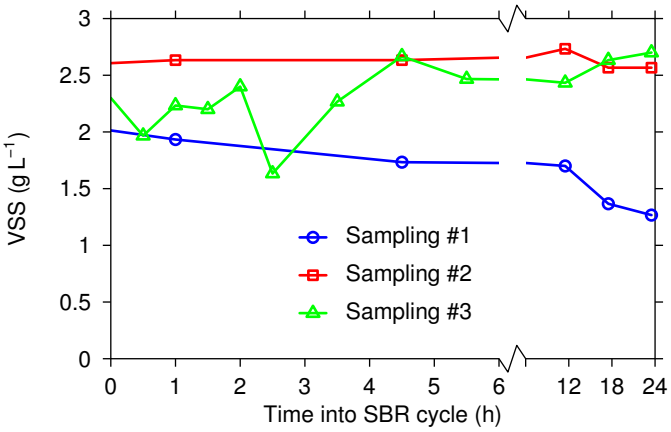

Figure B.3. Volatile suspended solids vs. time into SBR cycle for the three sampling events. Note the break and scale change in the abscissa at 6 h into the SBR cycle.

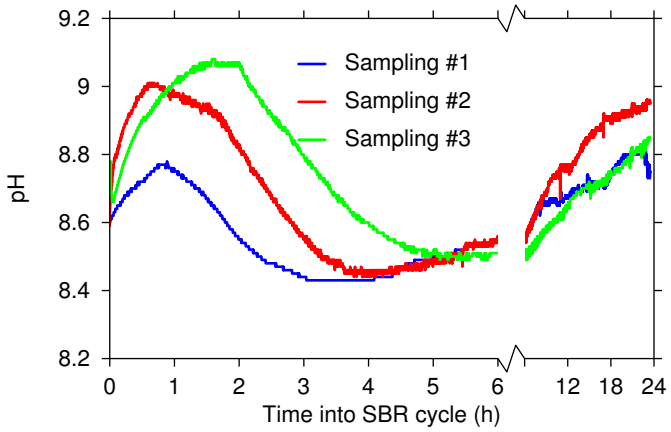

Figure B.4. pH vs. time into SBR cycle for the three sampling events. Note the break and scale change in the abscissa at 6 h into the SBR cycle.

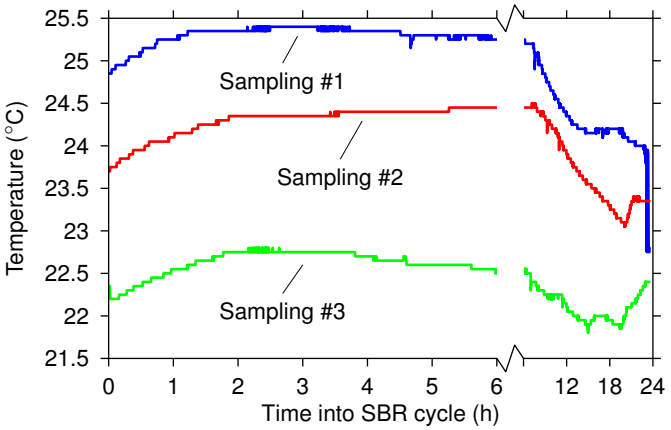

Figure B.5. Temperature vs. time into SBR cycle for the three sampling events. Note the break and scale change in the abscissa at 6 h into the SBR cycle.

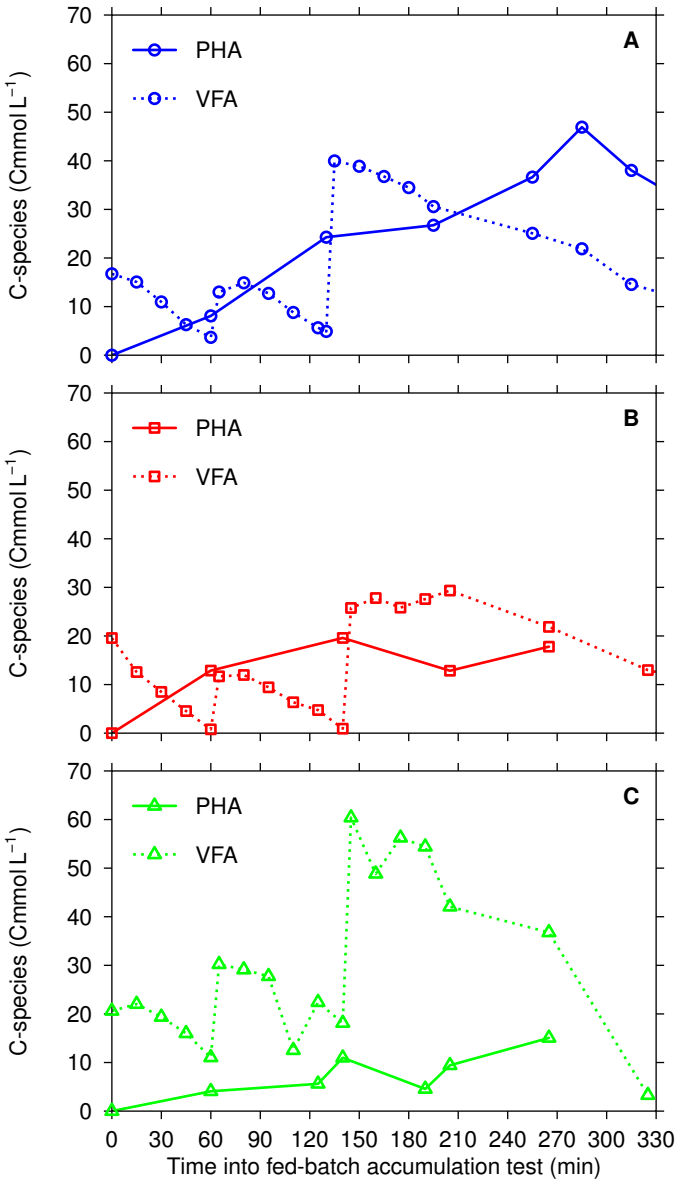

Figure B.6. Total VFA and PHA vs. time into fed-batch accumulation tests for the three sampling events. **A**, **B**, and **C** correspond to the fed-batch accumulation tests performed during Sampling events #1, #2, and #3, respectively.

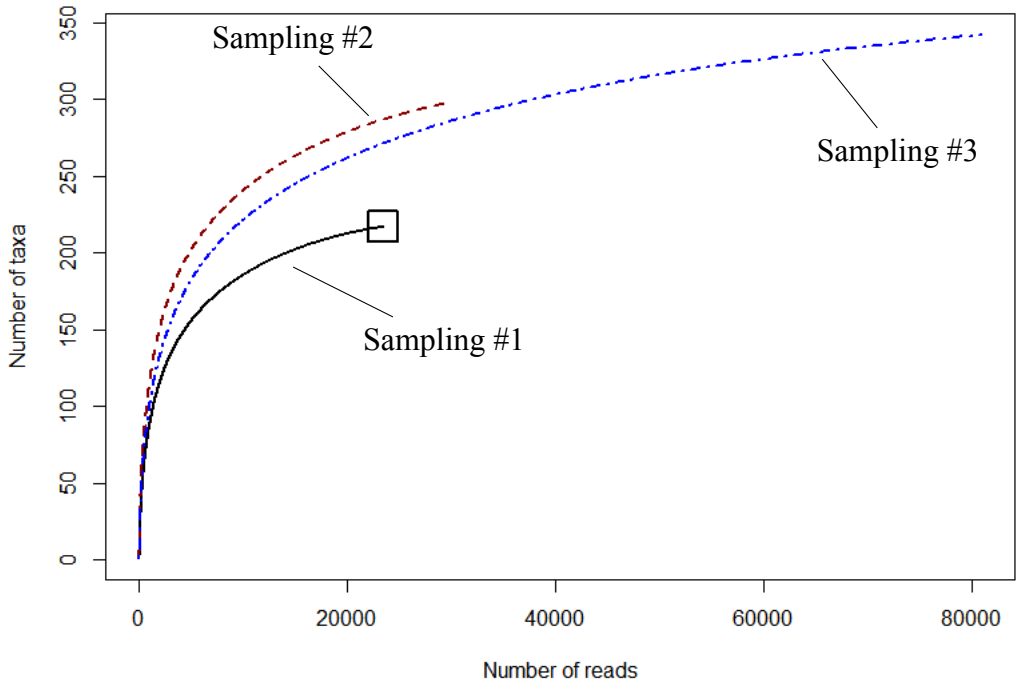

Figure B.7. Rarefaction analysis for the three sampling events. The rarefaction curves were generated using the `vegan` package in `R`. The open box indicates the sample with the lowest number of reads.

Table B.1. Phylum-level relative abundance.

Phylum	Sampling #1 (%)[a]	Sampling #2 (%)[a]	Sampling #3 (%)[a]
Proteobacteria	75.3	74.7	73.3
Bacteroidetes	15.3	17.0	18.1
Verrucomicrobia	0.896	0.588	3.38
Planctomycetes	3.37	0.972	0.548
Bacteria	1.25	2.13	1.54
Actinobacteria	1.33	1.86	1.25
Chloroflexi	1.09	0.815	0.701
Firmicutes	8.96×10^{-2}	0.674	0.365
Acidobacteria	0.474	0.514	0.408
Gemmatimonadetes	0.363	0.270	0.159
SR1	0.354	N. D.	N. D.
Chlamydiae	2.99×10^{-2}	0.207	5.07×10^{-2}
Candidatus Saccharibacteria	4.27×10^{-3}	0.120	3.21×10^{-2}
Unknown	7.25×10^{-2}	6.34×10^{-2}	4.57×10^{-2}
Hydrogenedentes	N. D.	7.01×10^{-2}	1.24×10^{-2}
Armatimonadetes	8.53×10^{-3}	N. D.	4.94×10^{-3}
Crenarchaeota	8.53×10^{-3}	3.34×10^{-3}	3.71×10^{-3}
Deinococcus-Thermus	8.53×10^{-3}	6.68×10^{-3}	3.71×10^{-3}
Tenericutes	8.53×10^{-3}	6.68×10^{-3}	N. D.
Candidate division WPS-2	N. D.	N. D.	7.42×10^{-3}
Archaea	N. D.	6.68×10^{-3}	N. D.
Spirochaetes	N. D.	6.68×10^{-3}	2.47×10^{-3}
Candidate division WPS-1	N. D.	N. D.	6.18×10^{-3}
Aquificae	4.27×10^{-3}	N. D.	N. D.
Elusimicrobia	4.27×10^{-3}	3.34×10^{-3}	3.71×10^{-3}
BRC1	N. D.	N. D.	3.71×10^{-3}
Fusobacteria	N. D.	N. D.	3.71×10^{-3}

[a] N. D. = Not detected.

Table B.2. Class-level relative abundance.

Class	Sampling #1 (%)[a]	Sampling #2 (%)[a]	Sampling #3 (%)[a]
Alphaproteobacteria	67.5	42.8	44.1
Betaproteobacteria	4.76	14.8	20.8
Sphingobacteriia	9.93	11.0	9.89
Deltaproteobacteria	1.54	8.87	3.02
Gammaproteobacteria	1.14	6.91	4.13
Flavobacteriia	3.06	4.18	5.71
Planctomycetia	3.37	0.958	0.545
Verrucomicrobiae	0.653	0.300	2.67
Actinobacteria	1.33	1.86	1.25
Bacteroidetes	0.623	0.952	1.76
Cytophagia	1.50	0.411	0.295
Proteobacteria	0.337	1.32	1.26
Bacteria	1.25	2.13	1.54
Caldilineae	0.973	0.414	0.465
Clostridia	7.68×10^{-2}	0.624	0.309
Bacteroidetes incertae sedis	0.205	0.421	0.488
Opitutae	2.13×10^{-2}	0.180	0.424
Thermomicrobia	0.102	0.367	0.198
Gemmatimonadetes	0.363	0.270	0.159
SR1 genera incertae sedis	0.354	N. D.	N. D.
Acidobacteria Gp4	0.290	0.127	8.41×10^{-2}
Acidobacteria Gp3	9.81×10^{-2}	0.194	0.248
Chlamydiia	2.99×10^{-2}	0.207	5.07×10^{-2}
Spartobacteria	0.145	6.68×10^{-2}	4.45×10^{-2}
Subdivision3	8.53×10^{-3}	1.34×10^{-2}	0.140
Acidobacteria Gp6	6.40×10^{-2}	0.127	4.57×10^{-2}
Saccharibacteria genera incertae sedis	4.27×10^{-3}	0.120	3.21×10^{-2}
Verrucomicrobia	6.83×10^{-2}	2.67×10^{-2}	0.104
Unknown	7.25×10^{-2}	6.34×10^{-2}	4.57×10^{-2}
Candidatus Hydrogenedens	N. D.	7.01×10^{-2}	1.24×10^{-2}
Acidobacteria	2.13×10^{-2}	6.34×10^{-2}	2.97×10^{-2}
Bacilli	8.53×10^{-3}	4.34×10^{-2}	5.19×10^{-2}
Chloroflexi	1.71×10^{-2}	2.67×10^{-2}	3.83×10^{-2}

Table B.2. Class-level relative abundance continued.

Class	Sampling #1 (%)[a]	Sampling #2 (%)[a]	Sampling #3 (%)[a]
Epsilonproteobacteria	1.71×10^{-2}	6.68×10^{-3}	N. D.
Planctomycetes	N. D.	1.34×10^{-2}	N. D.
Bacteroidia	8.53×10^{-3}	1.00×10^{-2}	7.42×10^{-3}
Deinococci	8.53×10^{-3}	6.68×10^{-3}	3.71×10^{-3}
Fimbriimonadia	8.53×10^{-3}	N. D.	4.94×10^{-3}
Mollicutes	8.53×10^{-3}	6.68×10^{-3}	N. D.
Thermoprotei	8.53×10^{-3}	3.34×10^{-3}	3.71×10^{-3}
WPS-2 genera incertae sedis	N. D.	N. D.	7.42×10^{-3}
Anaerolineae	N. D.	6.68×10^{-3}	N. D.
Archaea	N. D.	6.68×10^{-3}	N. D.
Erysipelotrichia	N. D.	6.68×10^{-3}	2.47×10^{-3}
Spirochaetia	N. D.	6.68×10^{-3}	2.47×10^{-3}
WPS-1 genera incertae sedis	N. D.	N. D.	6.18×10^{-3}
Aquificae	4.27×10^{-3}	N. D.	N. D.
Elusimicrobia	4.27×10^{-3}	3.34×10^{-3}	3.71×10^{-3}
Firmicutes	4.27×10^{-3}	N. D.	1.24×10^{-3}
BRC1 genera incertae sedis	N. D.	N. D.	3.71×10^{-3}
Fusobacteriia	N. D.	N. D.	3.71×10^{-3}
Acidobacteria Gp1	N. D.	3.34×10^{-3}	N. D.
Actinobacteria	N. D.	N. D.	2.47×10^{-3}
Phycisphaerae	N. D.	N. D.	2.47×10^{-3}

[a] N. D. = Not detected.

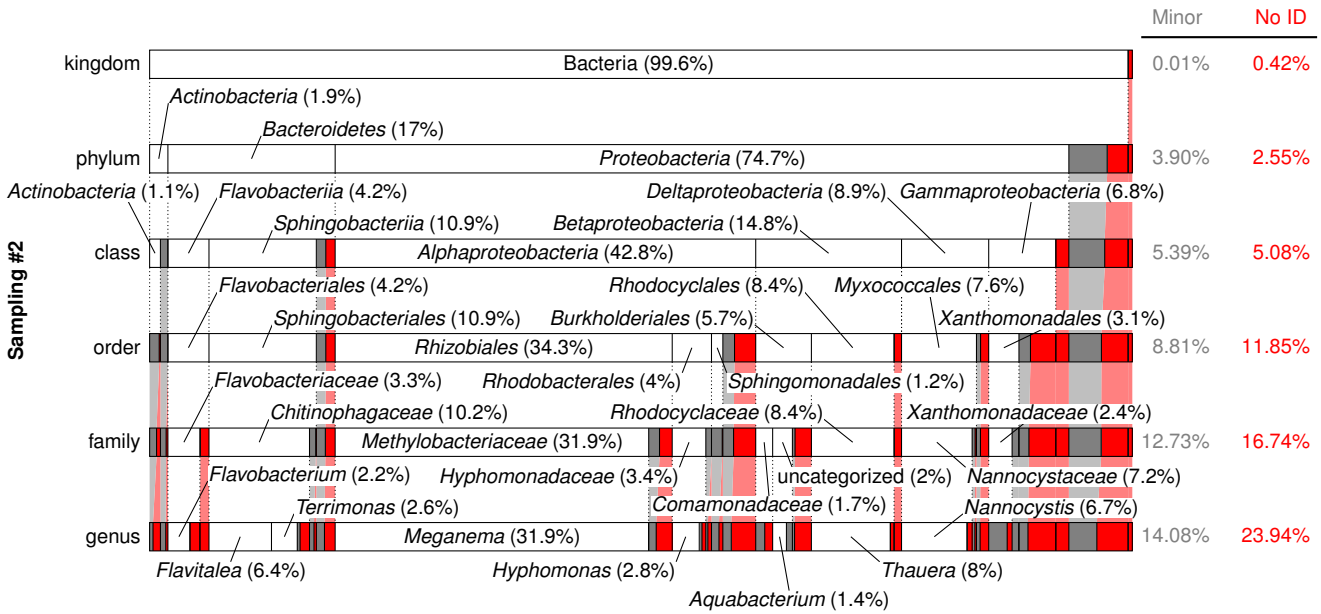

Figure B.8. Relative abundance and taxonomic classification of the 16S rRNA gene sequencing results using the RDP from Sampling #2. The classified phylotypes are depicted in terms of the taxonomic hierarchy, as obtained from NCBI. Phylotypes which were not identified by the RDP or those whose identification at a specific taxonomic level was not statistically significant were aggregated, denoted ``No ID'', and depicted in red. Identified phylotypes with less than 1% of the total relative abundance were aggregated, denoted ``Minor'', and depicted in gray. Phylotypes with at least 1% relative abundance are labeled. See the supplementary material for the tabulated results.

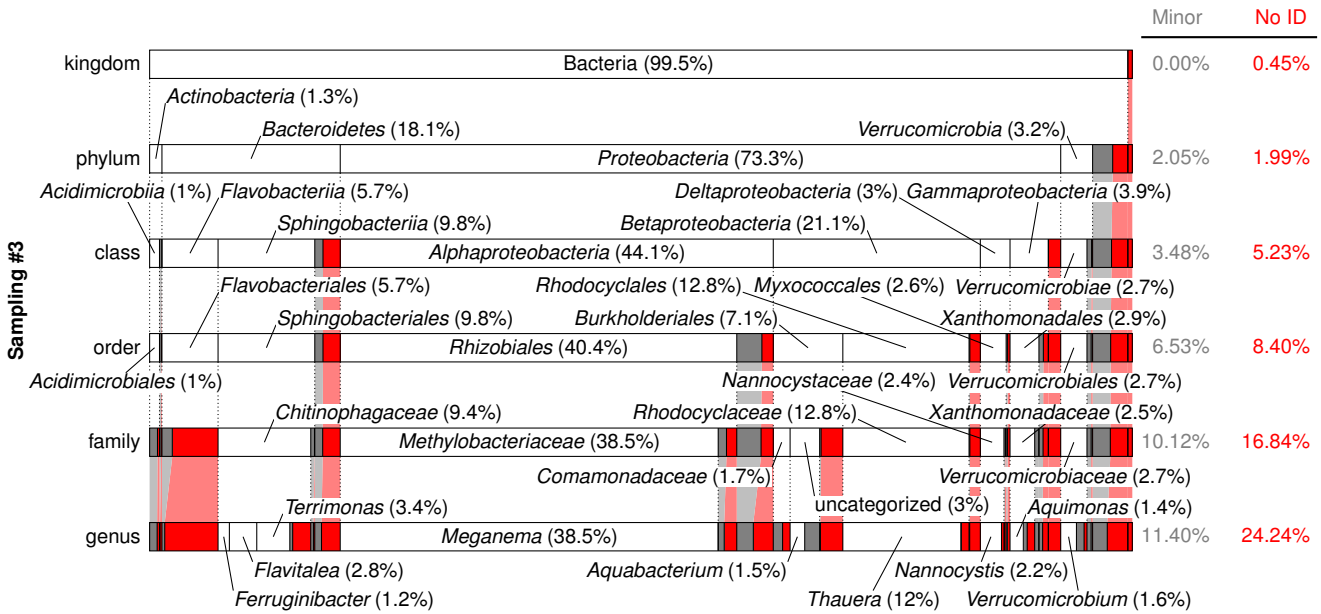

Figure B.9. Relative abundance and taxonomic classification of the 16S rRNA gene sequencing results using the RDP from Sampling #3. The classified phylotypes are depicted in terms of the taxonomic hierarchy, as obtained from NCBI. Phylotypes which were not identified by the RDP or those whose identification at a specific taxonomic level was not statistically significant were aggregated, denoted ``No ID'', and depicted in red. Identified phylotypes with less than 1% of the total relative abundance were aggregated, denoted ``Minor'', and depicted in gray. Phylotypes with at least 1% relative abundance are labeled. See the supplementary material for the tabulated results.

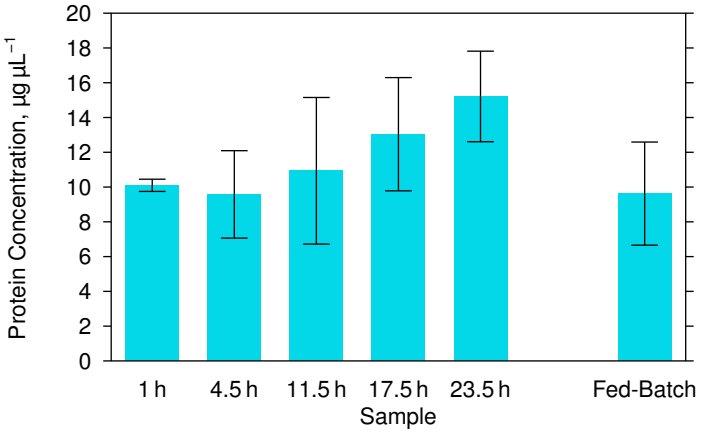

Figure B.10. Mean protein concentration for each of the sample times. Error bars depict the standard deviation ($n = 9$ for 1 h, 4.5 h, 11.5 h, 17.5 h, and 23.5 h; $n = 8$ for Fed-Batch).

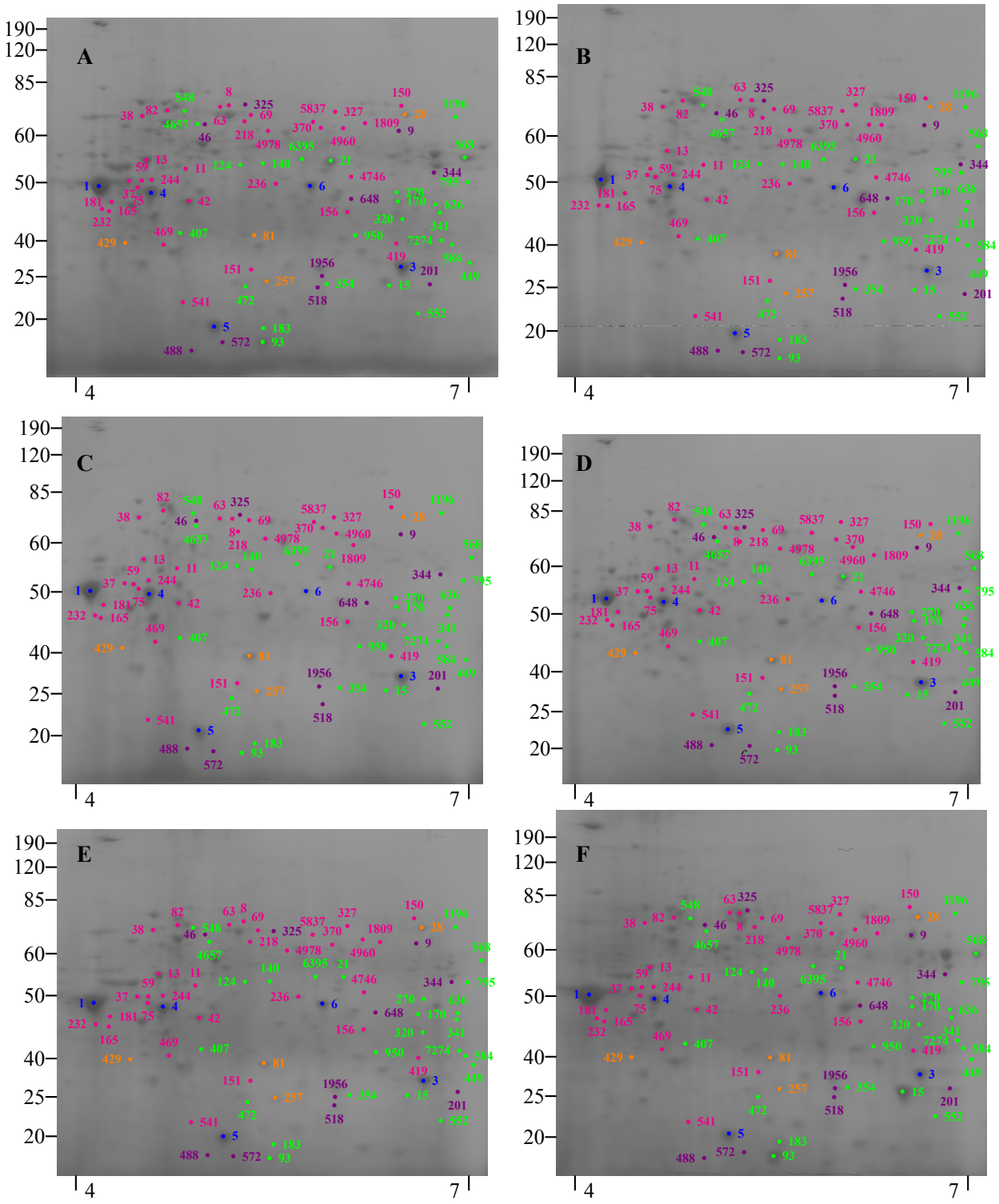

Figure B.11. Gel set from Sampling #1. **A**, **B**, **C**, **D**, and **E** correspond to samples taken at SBR cycle times of 1 h, 4.5 h, 11.5 h, 17.5 h, and 23.5 h, respectively. **F** is the gel corresponding to the fed-batch assessment. The raw cropped gel images used in the REDFIN 3 Solo Software analysis are depicted. Note that the spacing and alignment of the molecular weight markers (kDa) and pH ranges are approximate. Spots are grouped according to Table B.4, with most abundant proteins in blue, feast phase proteins in green, famine phase proteins in magenta, fed-batch proteins in violet, and SBR proteins in orange.

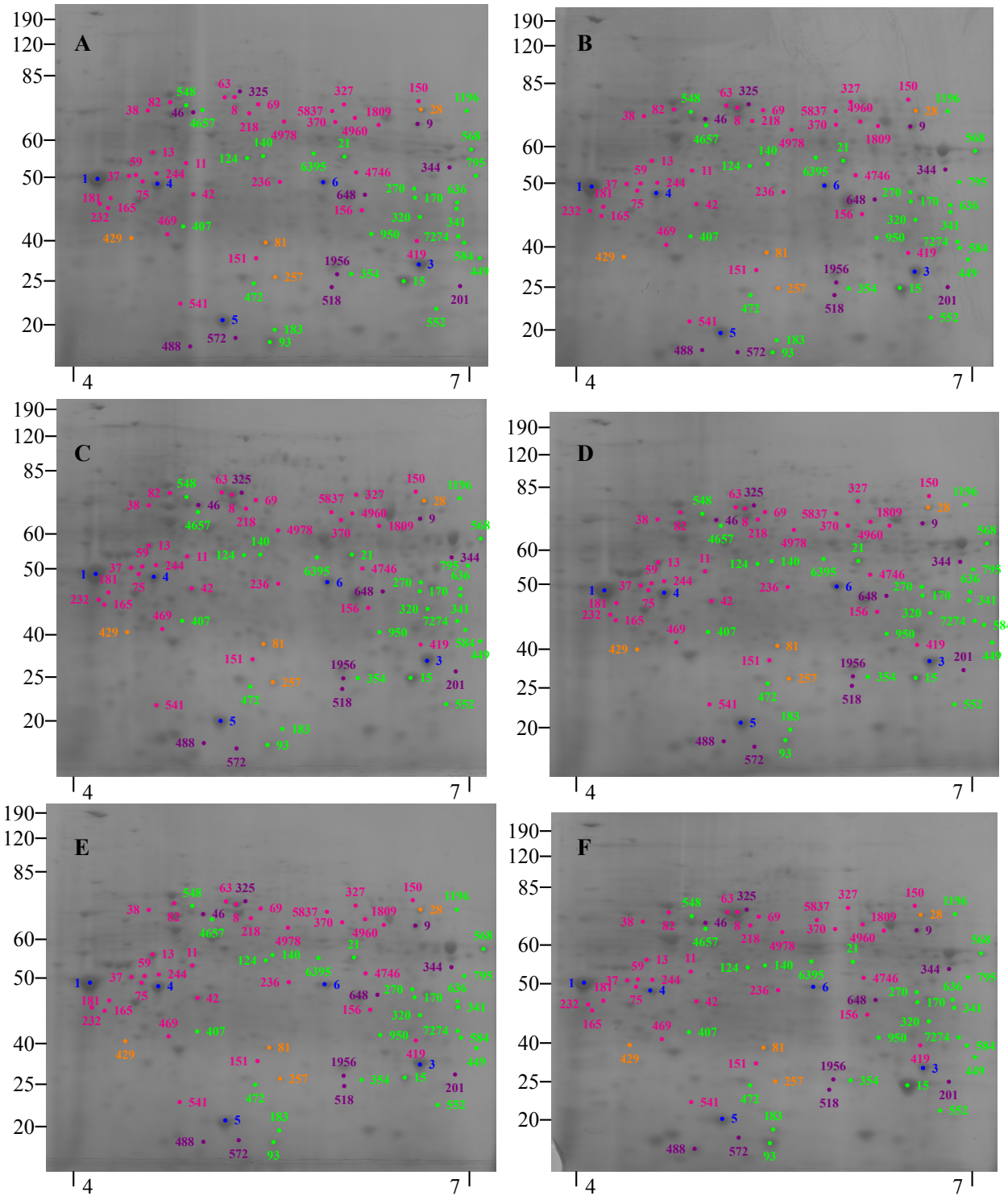

Figure B.12. Gel set from Sampling #2. **A**, **B**, **C**, **D**, and **E** correspond to samples taken at SBR cycle times of 1 h, 4.5 h, 11.5 h, 17.5 h, and 23.5 h, respectively. **F** is the gel corresponding to the fed-batch assessment. The raw cropped gel images used in the REDFIN 3 Solo Software analysis are depicted. Note that the spacing and alignment of the molecular weight markers (kDa) and pH ranges are approximate. Spots are grouped according to Table B.4, with most abundant proteins in blue, feast phase proteins in green, famine phase proteins in magenta, fed-batch proteins in violet, and SBR proteins in orange.

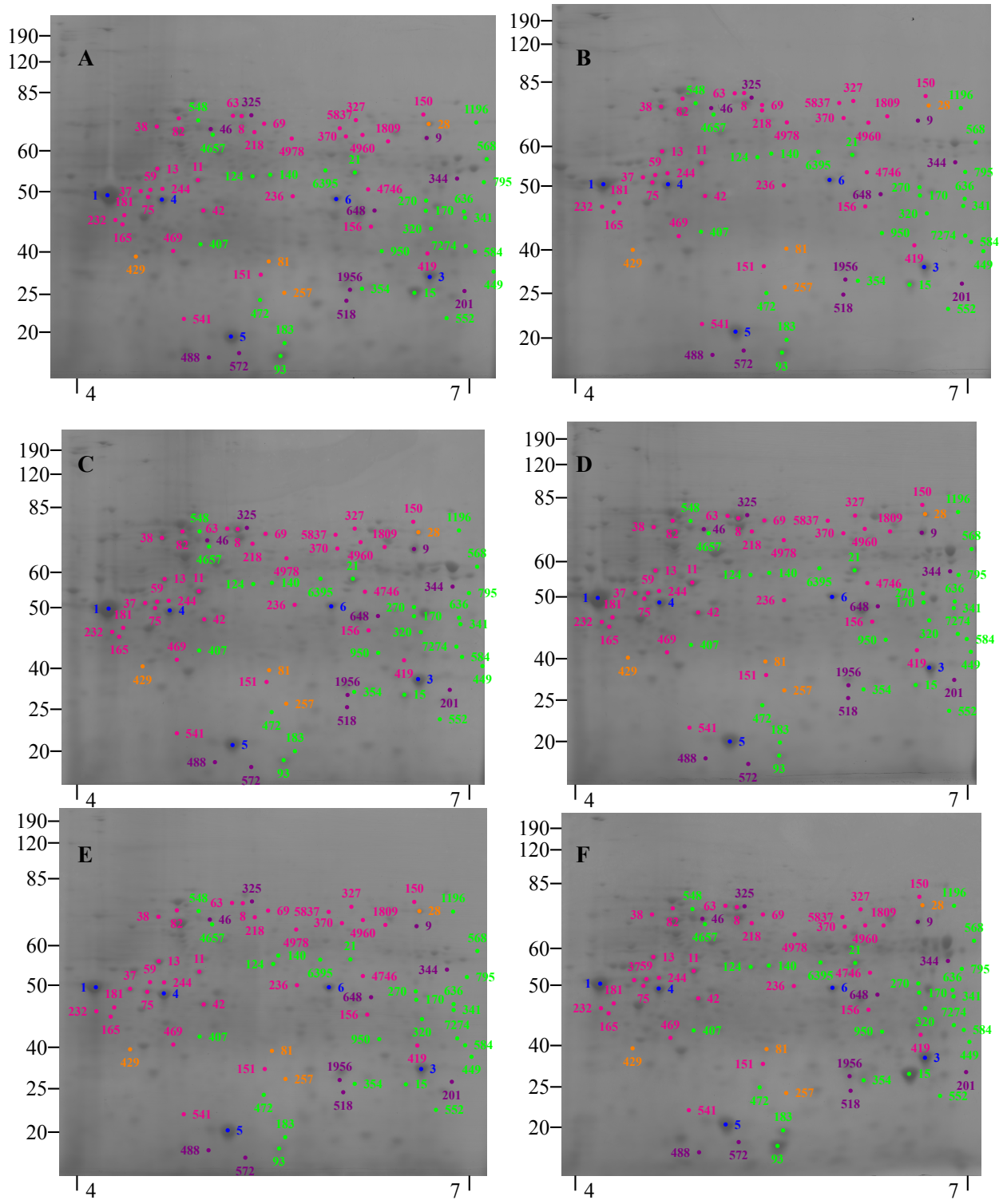

Figure B.13. Gel set from Sampling #3. **A**, **B**, **C**, **D**, and **E** correspond to samples taken at SBR cycle times of 1 h, 4.5 h, 11.5 h, 17.5 h, and 23.5 h, respectively. **F** is the gel corresponding to the fed-batch assessment. The raw cropped gel images used in the REDFIN 3 Solo Software analysis are depicted. Note that the spacing and alignment of the molecular weight markers (kDa) and pH ranges are approximate. Spots are grouped according to Table B.4, with most abundant proteins in blue, feast phase proteins in green, famine phase proteins in magenta, fed-batch proteins in violet, and SBR proteins in orange.

Table B.3. Replicate gel correlation coefficients based on normalized protein spot intensities. The correlation matrix was constructed based on normalized protein spot intensities using Pearson's product moment correlation coefficient.

Time		1 h			4.5 h			11.5 h			17.5 h			23.5 h			Fed-batch		
	Sampling #	1	2	3	1	2	3	1	2	3	1	2	3	1	2	3	1	2	3
1 h	1	1																	
	2	0.90	1																
	3	0.89	0.94	1															
4.5 h	1	0.84	0.77	0.80	1														
	2	0.82	0.88	0.87	0.83	1													
	3	0.88	0.85	0.88	0.86	0.87	1												
11.5 h	1	0.77	0.71	0.72	0.85	0.70	0.77	1											
	2	0.81	0.86	0.84	0.80	0.91	0.83	0.72	1										
	3	0.85	0.84	0.87	0.84	0.89	0.91	0.75	0.90	1									
17.5 h	1	0.81	0.73	0.76	0.86	0.76	0.82	0.84	0.77	0.82	1								
	2	0.83	0.85	0.85	0.80	0.91	0.86	0.70	0.92	0.91	0.82	1							
	3	0.83	0.80	0.84	0.85	0.88	0.89	0.74	0.88	0.94	0.85	0.92	1						
23.5 h	1	0.88	0.83	0.82	0.80	0.79	0.87	0.77	0.81	0.84	0.81	0.85	0.84	1					
	2	0.88	0.87	0.86	0.83	0.86	0.89	0.75	0.89	0.91	0.82	0.91	0.90	0.94	1				
	3	0.86	0.84	0.87	0.80	0.80	0.88	0.76	0.83	0.88	0.79	0.85	0.86	0.94	0.95	1			
Fed-batch	1	0.81	0.87	0.82	0.72	0.86	0.78	0.64	0.79	0.77	0.66	0.81	0.77	0.73	0.77	0.71	1		
	2	0.74	0.87	0.83	0.69	0.86	0.74	0.60	0.80	0.74	0.59	0.78	0.72	0.66	0.74	0.68	0.92	1	
	3	0.80	0.88	0.86	0.70	0.85	0.79	0.61	0.79	0.78	0.63	0.81	0.75	0.70	0.76	0.72	0.93	0.92	1

Table B.4. Protein spot categorization.

[a] These proteins exhibited the greatest abundance in all of the gels assessed, each constituting more than 1% of the average normalized spot volume.

[b] These proteins each exhibited large, statistically-significant fold changes in the feast phase relative to the famine phase in the SBR cycle (i.e., they were more abundant in the feast than in the famine).

[c] These proteins each exhibited large, statistically-significant fold changes in the famine phase relative to the feast phase in the SBR cycle (i.e., they were more abundant in the famine than in the feast).

[d] These proteins each exhibited large, statistically-significant fold changes in the fed-batch relative to the SBR (i.e., they were more abundant in the fed-batch than in the SBR).

[e] These proteins each exhibited large, statistically-significant fold changes in the SBR relative to the fed-batch (i.e., they were more abundant in the SBR than in the fed-batch).

[f] An * following the protein name indicates protein identification made using Blastp.

B.1 Most abundant proteins

These proteins exhibited the greatest abundance in all of the gels assessed, each constituting more than 1% of the average normalized spot volume.

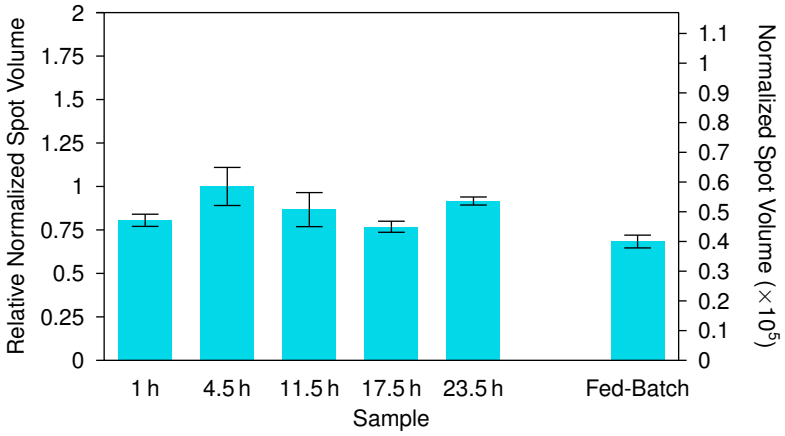

Figure B.14. Spot number 1 identified as Porin*. Error bars depict the standard error of the mean normalized spot volume ($n = 3$).

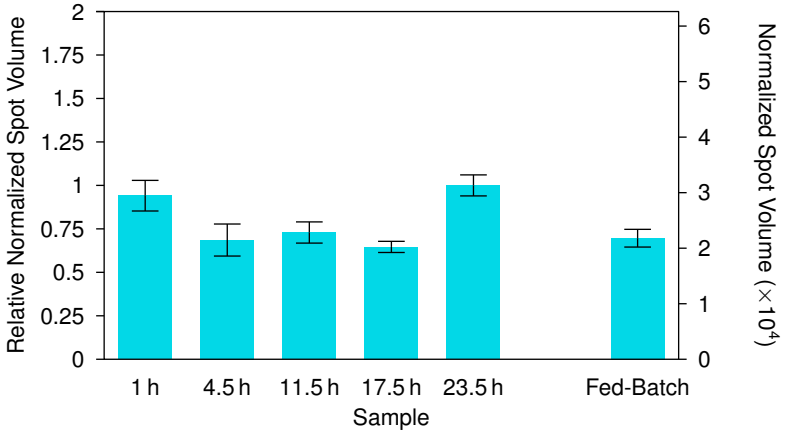

Figure B.15. Spot number 3 identified as Superoxide dismutase*. Error bars depict the standard error of the mean normalized spot volume ($n = 3$).

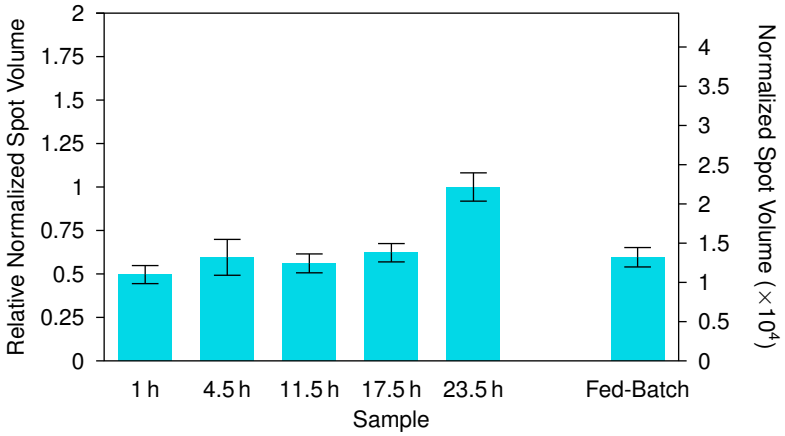

Figure B.16. Spot number 4 identified as Amino acid ABC transporter substrate-binding protein*. Error bars depict the standard error of the mean normalized spot volume ($n = 3$).

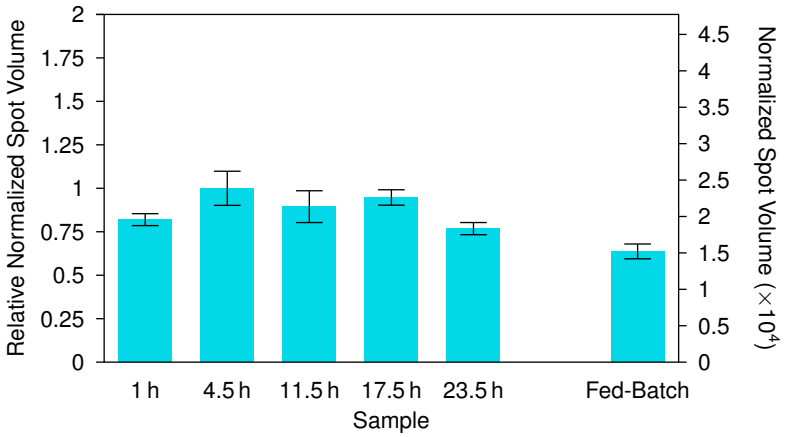

Figure B.17. Spot number 5 identified as Bacterioferritin. Error bars depict the standard error of the mean normalized spot volume ($n = 3$).

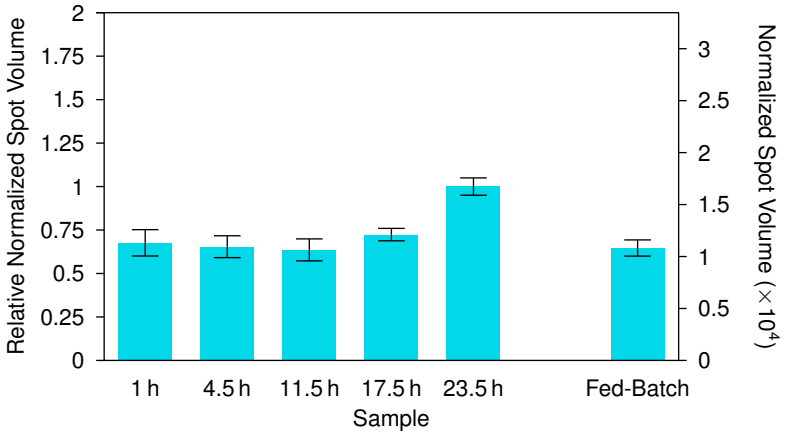

Figure B.18. Spot number 6 identified as ABC transporter substrate-binding protein*. Error bars depict the standard error of the mean normalized spot volume ($n = 3$).

B.2 Feast phase proteins

These proteins each exhibited large, statistically-significant fold changes in the feast phase relative to the famine phase in the SBR cycle (i.e., they were more abundant in the feast than in the famine).

B.2.1 PHA synthesis

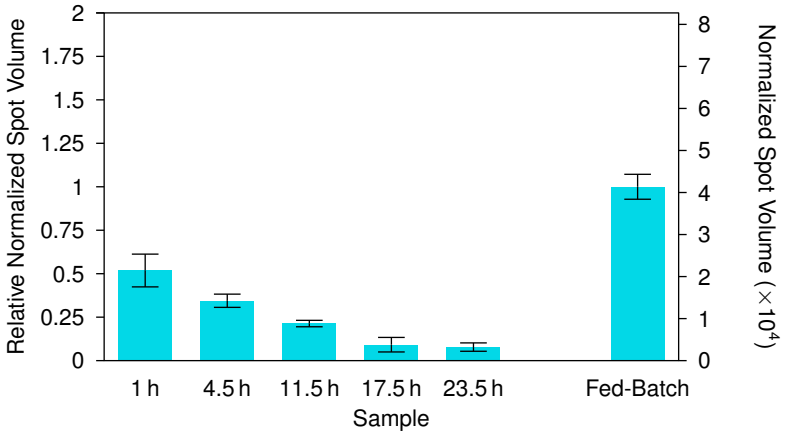

Figure B.19. Spot number 15 identified as Phasin*. Error bars depict the standard error of the mean normalized spot volume ($n = 3$).

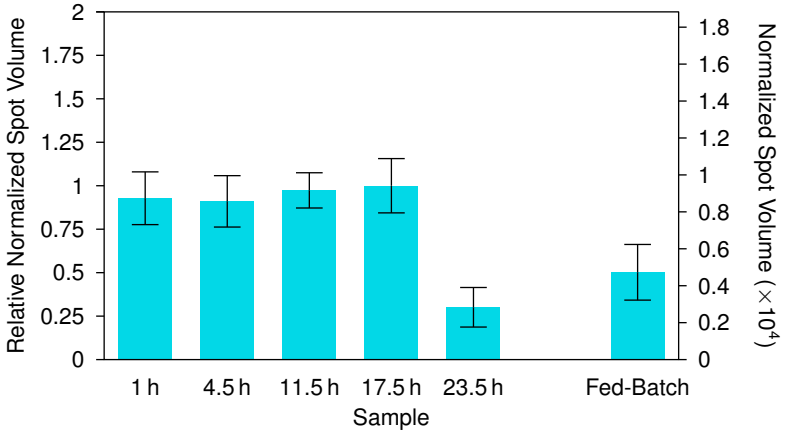

Figure B.20. Spot number 21 identified as Acetyl-CoA acetyltransferase. Error bars depict the standard error of the mean normalized spot volume ($n = 3$).

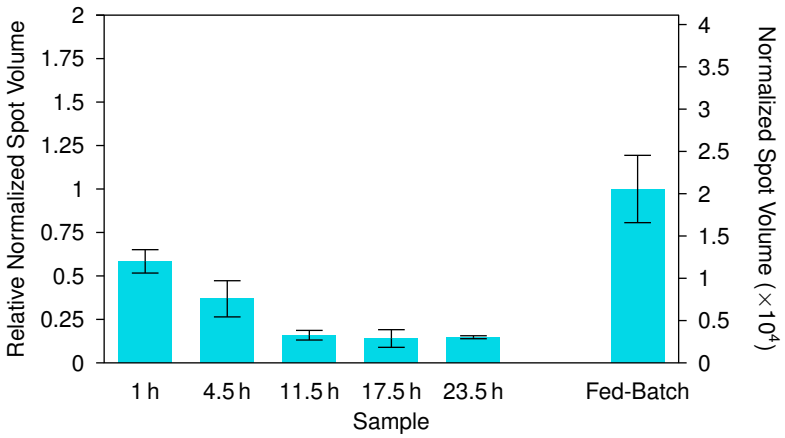

Figure B.21. Spot number 93 identified as Phasin*. Error bars depict the standard error of the mean normalized spot volume ($n = 3$).

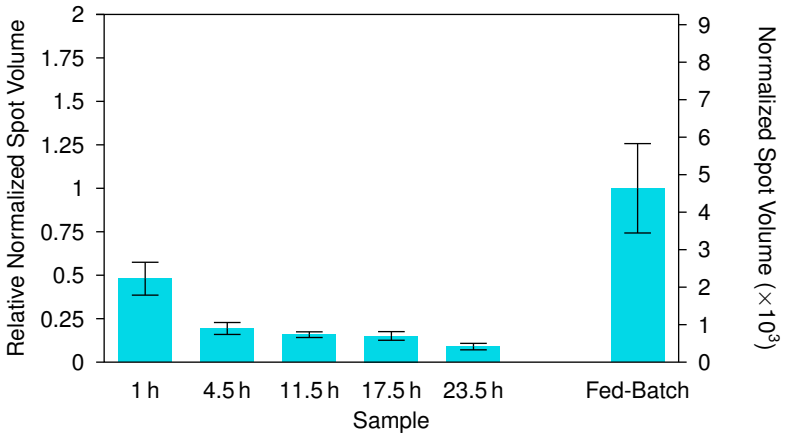

Figure B.22. Spot number 183 identified as Phasin*. Error bars depict the standard error of the mean normalized spot volume ($n = 3$).

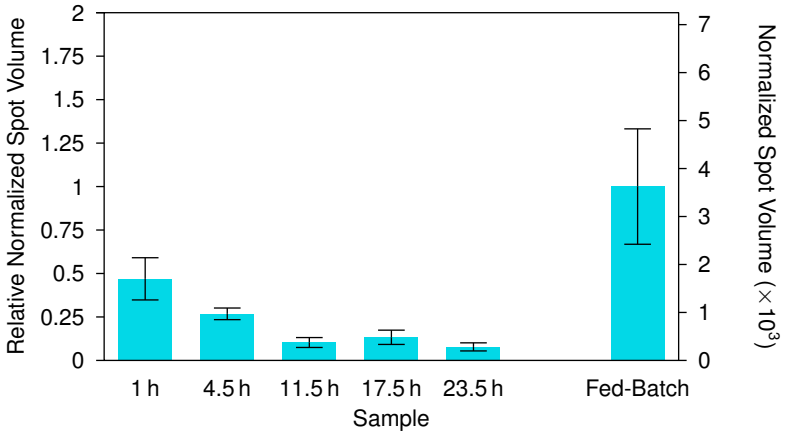

Figure B.23. Spot number 354 identified as Phasin*. Error bars depict the standard error of the mean normalized spot volume ($n = 3$).

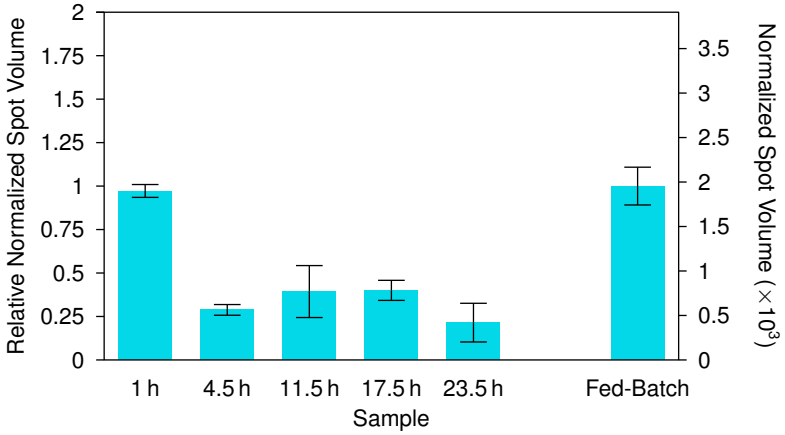

Figure B.24. Spot number 472 identified as Phasin*. Error bars depict the standard error of the mean normalized spot volume ($n = 3$).

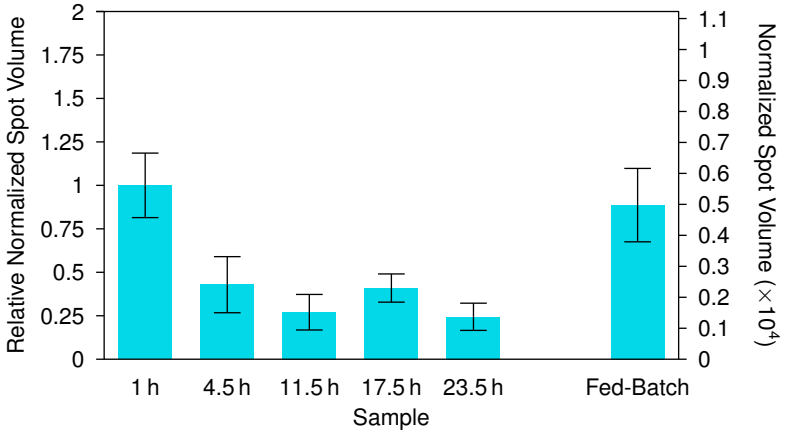

Figure B.25. Spot number 568 identified as Acetyl-CoA acetyltransferase. Error bars depict the standard error of the mean normalized spot volume ($n = 3$).

B.2.2 Energy generation/conversion

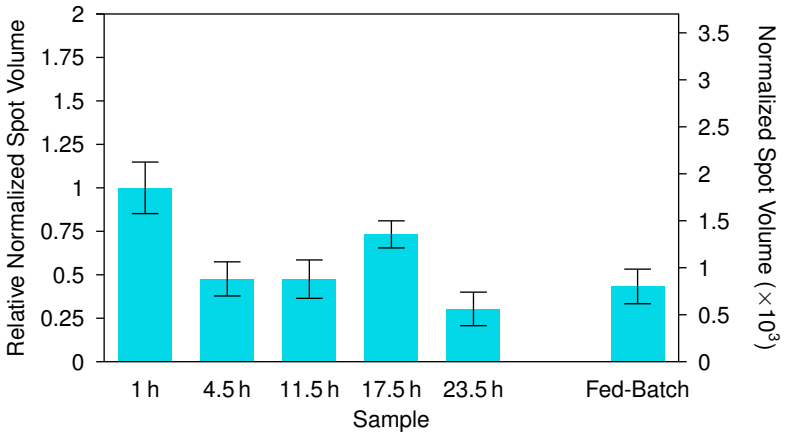

Figure B.26. Spot number 341 identified as Isocitrate dehydrogenase. Error bars depict the standard error of the mean normalized spot volume ($n = 3$).

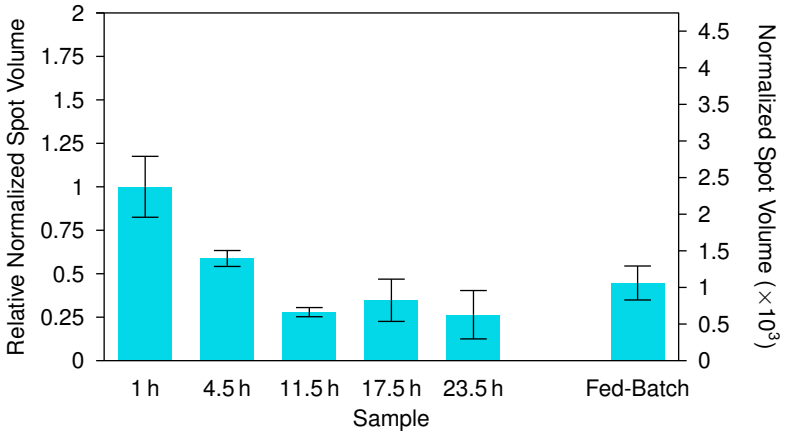

Figure B.27. Spot number 407 identified as Aldehyde dehydrogenase. Error bars depict the standard error of the mean normalized spot volume ($n = 3$).

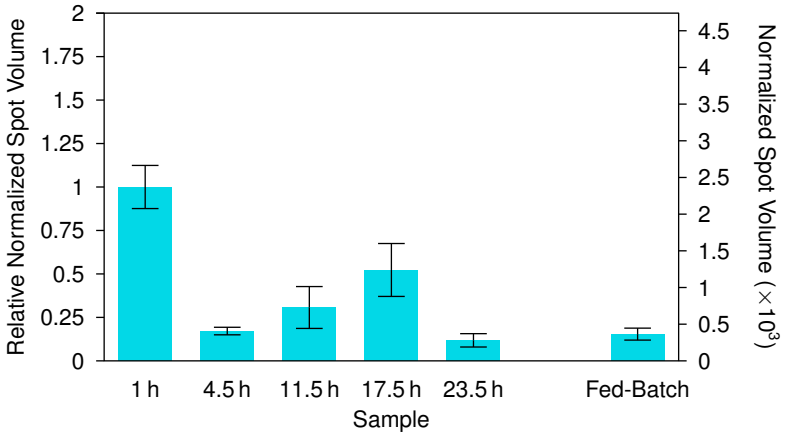

Figure B.28. Spot number 584 identified as Malate dehydrogenase. Error bars depict the standard error of the mean normalized spot volume ($n = 3$).

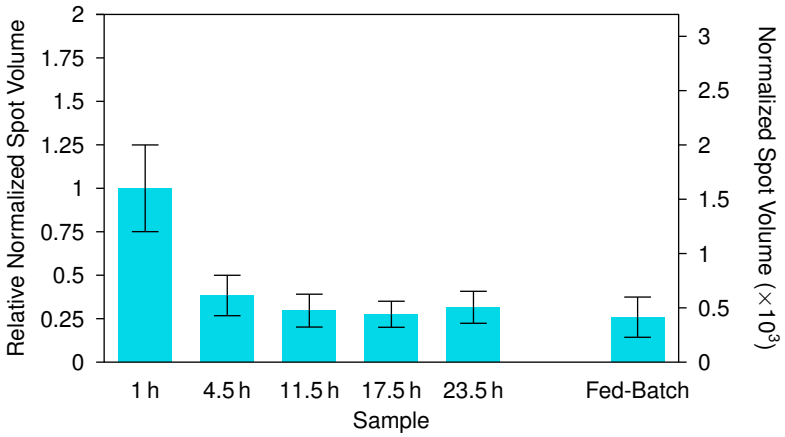

Figure B.29. Spot number 636 identified as Isocitrate dehydrogenase§. Error bars depict the standard error of the mean normalized spot volume ($n = 3$).

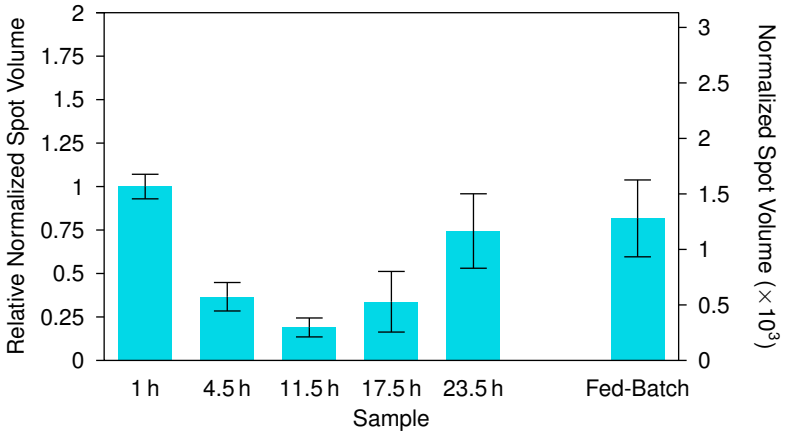

Figure B.30. Spot number 950 identified as Methylmalonate-semialdehyde dehydrogenase*. Error bars depict the standard error of the mean normalized spot volume ($n = 3$).

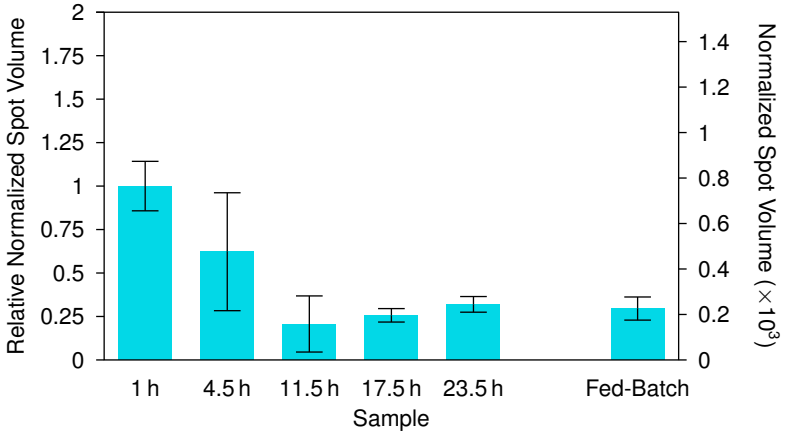

Figure B.31. Spot number 1196 identified as Aldehyde dehydrogenase. Error bars depict the standard error of the mean normalized spot volume ($n = 3$).

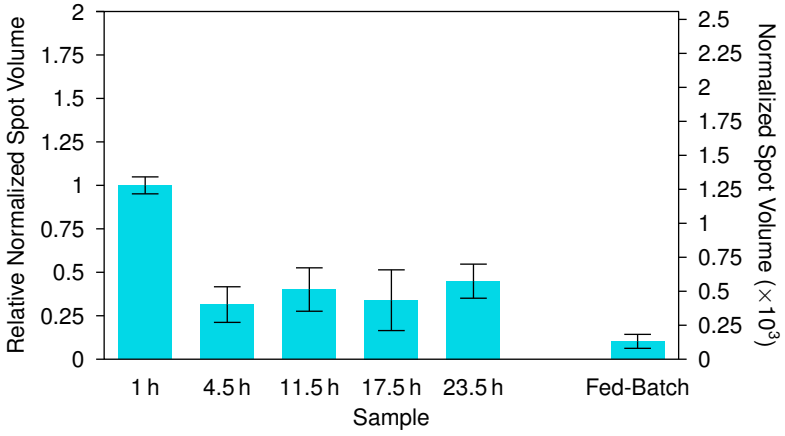

Figure B.32. Spot number 7274 identified as Malate dehydrogenase§. Error bars depict the standard error of the mean normalized spot volume ($n = 3$).

B.2.3 Protein synthesis

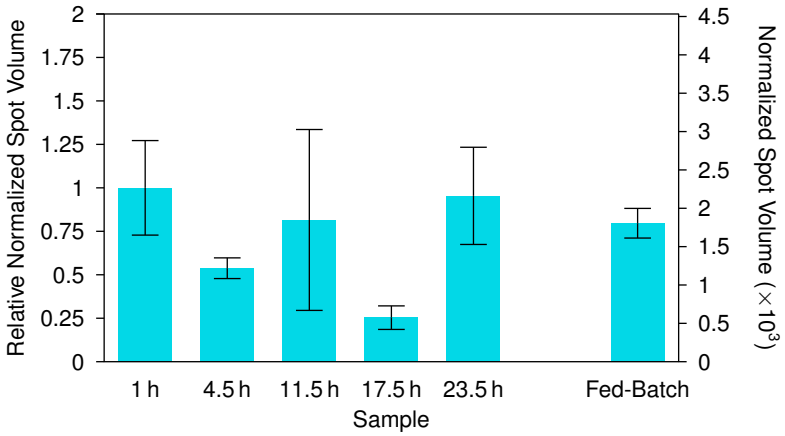

Figure B.33. Spot number 124 identified as Elongation factor Tu. Error bars depict the standard error of the mean normalized spot volume ($n = 3$).

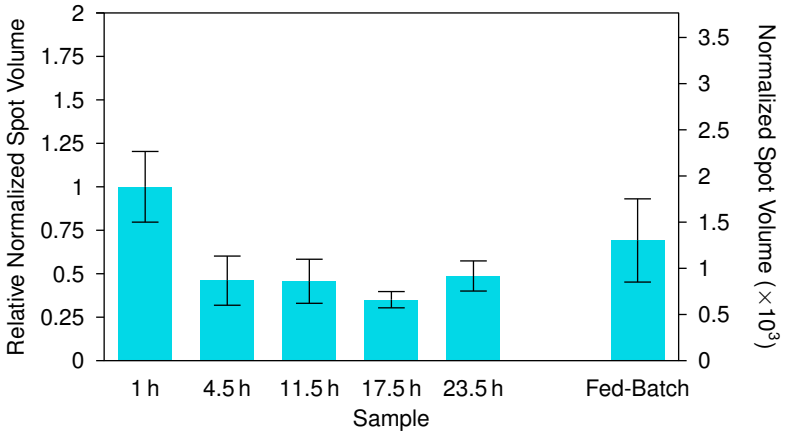

Figure B.34. Spot number 140 identified as Elongation factor Tu. Error bars depict the standard error of the mean normalized spot volume ($n = 3$).

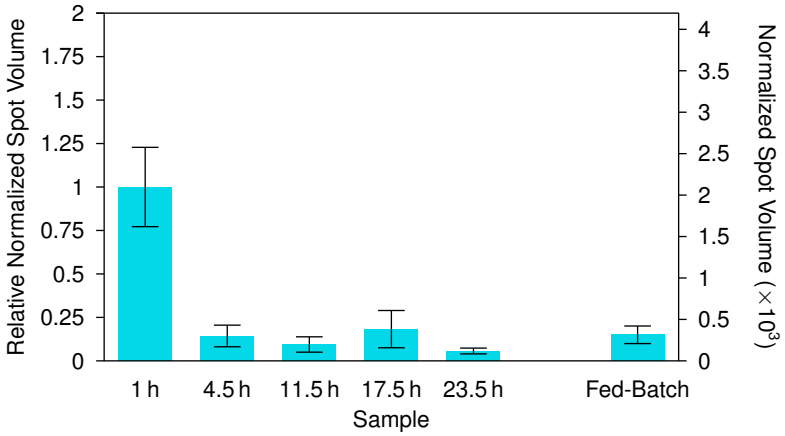

Figure B.35. Spot number 449 identified as 50S ribosomal protein L6. Error bars depict the standard error of the mean normalized spot volume ($n = 3$).

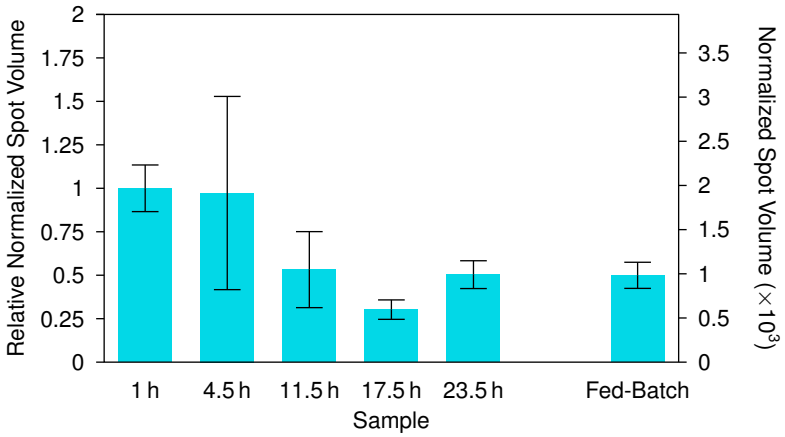

Figure B.36. Spot number 548 identified as Molecular chaperone GroEL. Error bars depict the standard error of the mean normalized spot volume ($n = 3$).

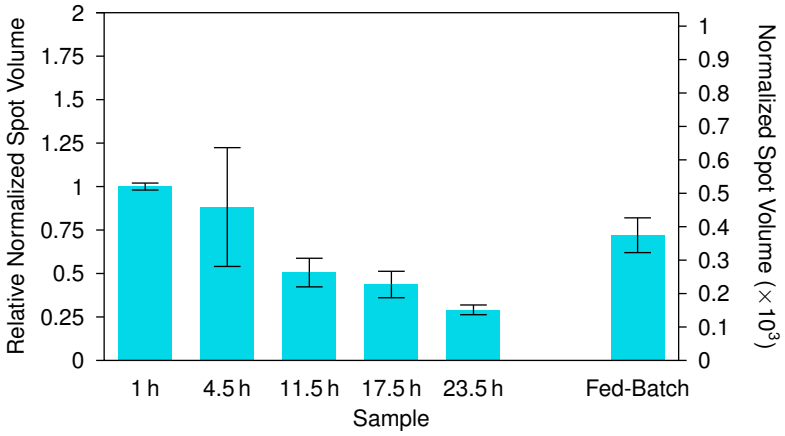

Figure B.37. Spot number 4657 identified as Molecular chaperone GroEL. Error bars depict the standard error of the mean normalized spot volume ($n = 3$).

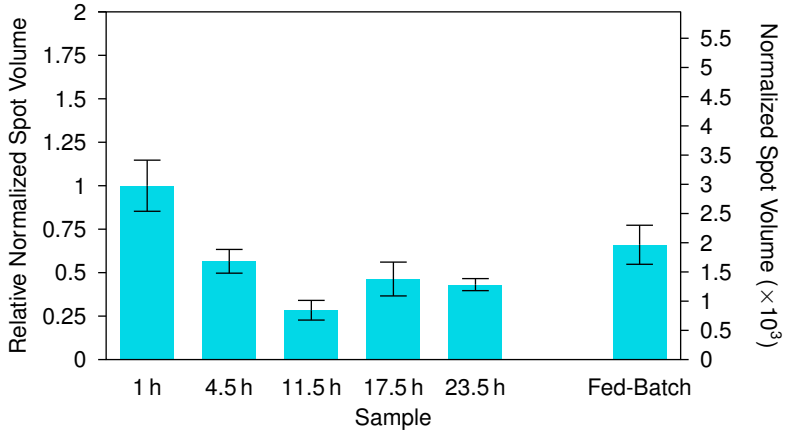

Figure B.38. Spot number 6395 identified as Elongation factor Tu. Error bars depict the standard error of the mean normalized spot volume ($n = 3$).

B.2.4 Other proteins

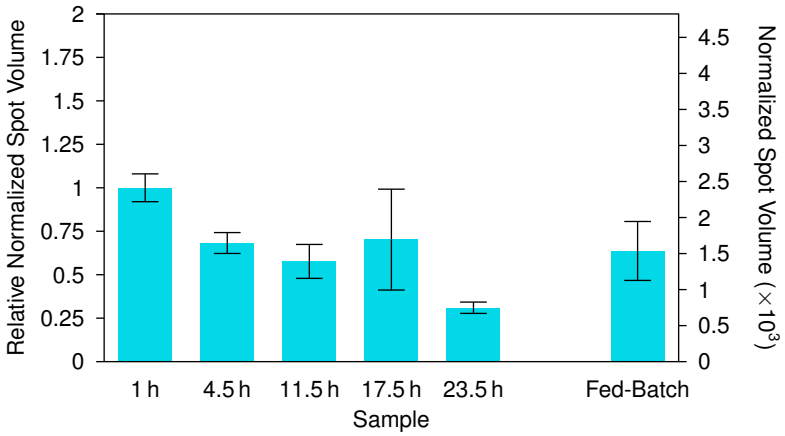

Figure B.39. Spot number 170 identified as Translocation protein TolB. Error bars depict the standard error of the mean normalized spot volume ($n = 3$).

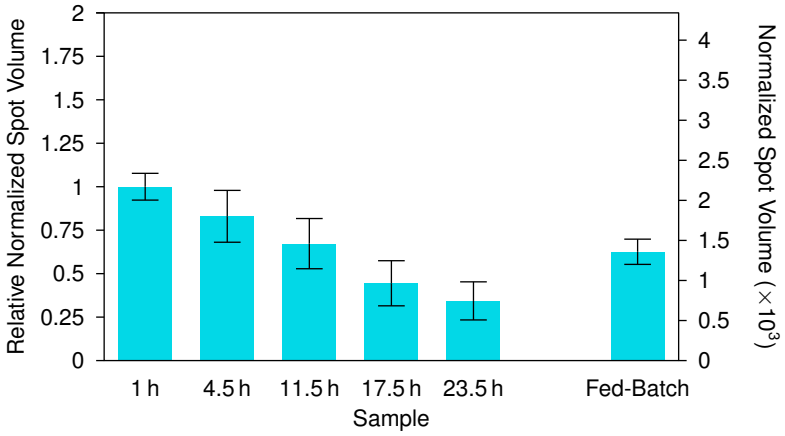

Figure B.40. Spot number 270 identified as Malyl-CoA lyase*. Error bars depict the standard error of the mean normalized spot volume ($n = 3$).

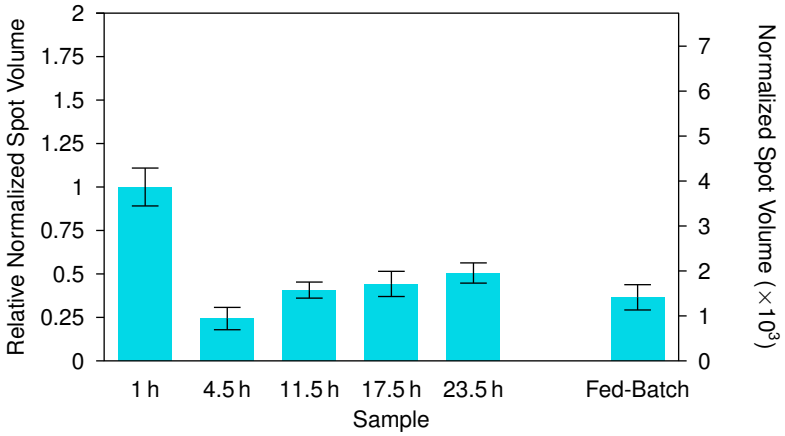

Figure B.41. Spot number 320 identified as 2,5-didehydrogluconate reductase*. Error bars depict the standard error of the mean normalized spot volume ($n = 3$).

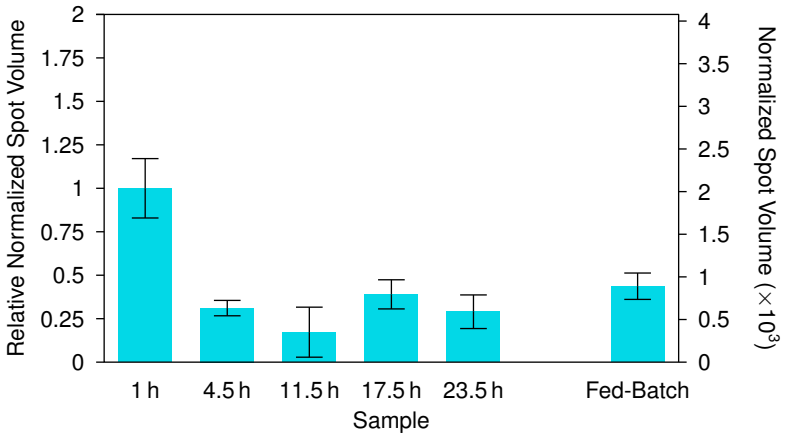

Figure B.42. Spot number 552 identified as Pentapeptide repeat-containing protein* . Error bars depict the standard error of the mean normalized spot volume ($n = 3$).

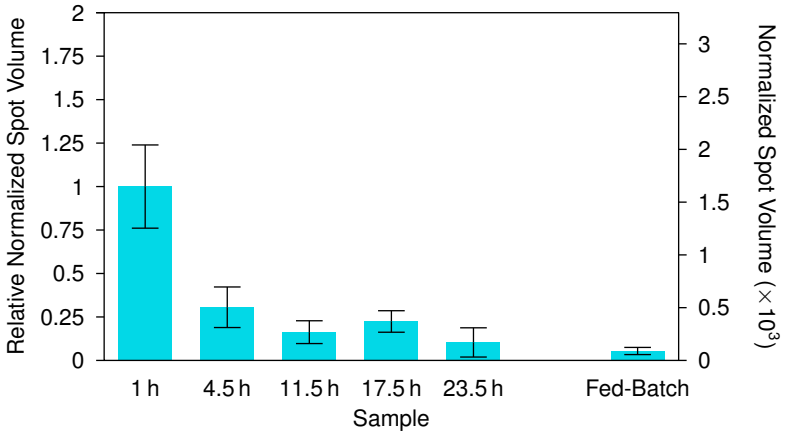

Figure B.43. Spot number 795 identified as Membrane protein. Error bars depict the standard error of the mean normalized spot volume ($n = 3$).

B.3 Famine phase proteins

These proteins each exhibited large, statistically-significant fold changes in the famine phase relative to the feast phase in the SBR cycle (i.e., they were more abundant in the famine than in the feast).

B.3.1 Nutrient transport

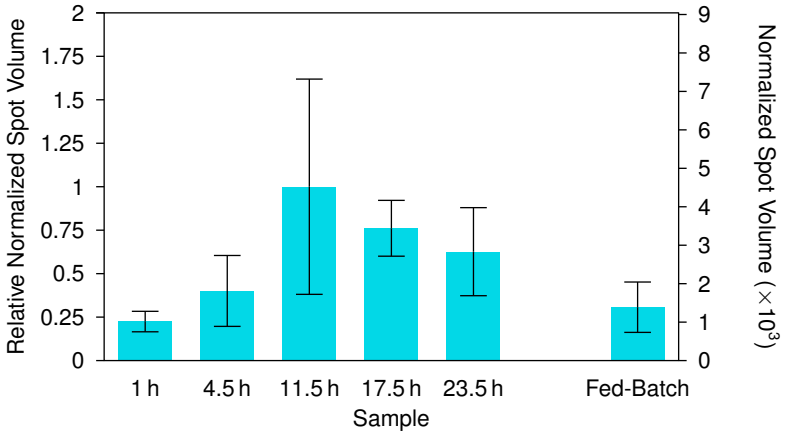

Figure B.44. Spot number 11 identified as Sulfate transporter subunit*. Error bars depict the standard error of the mean normalized spot volume ($n = 3$).

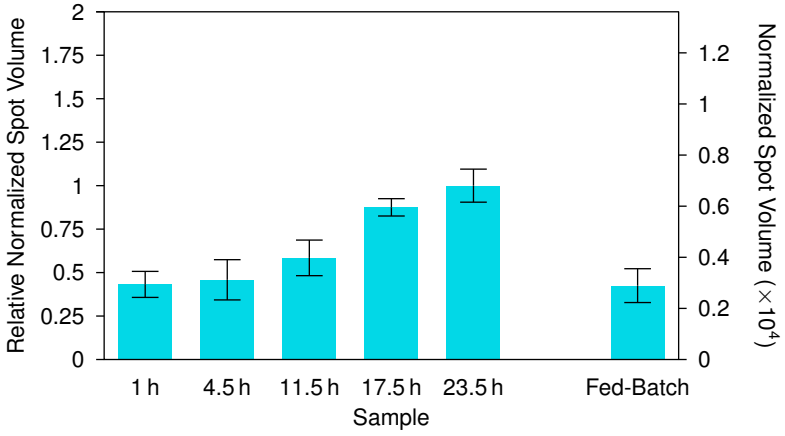

Figure B.45. Spot number 13 identified as ABC transporter permease. Error bars depict the standard error of the mean normalized spot volume ($n = 3$).

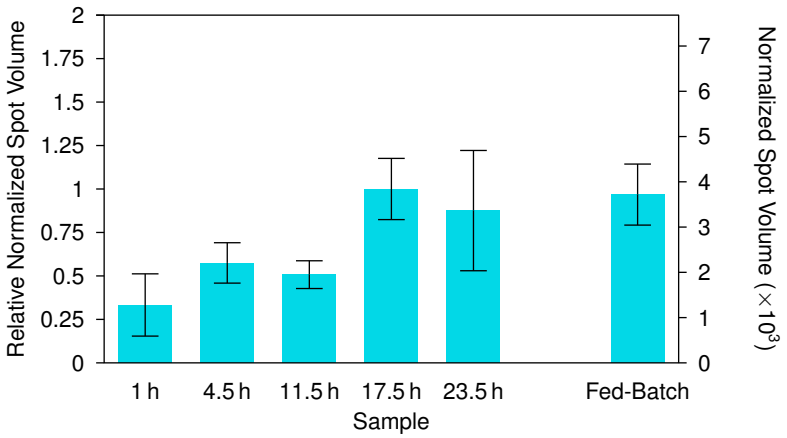

Figure B.46. Spot number 37 identified as ABC transporter substrate-binding protein*. Error bars depict the standard error of the mean normalized spot volume ($n = 3$).

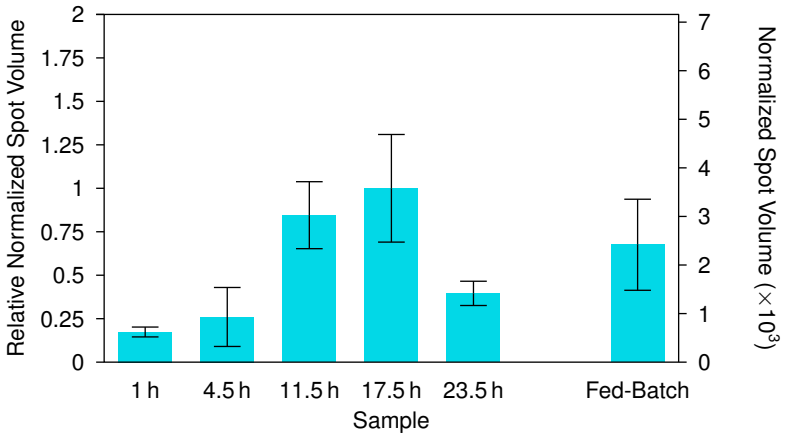

Figure B.47. Spot number 59 identified as ABC transporter substrate-binding protein*. Error bars depict the standard error of the mean normalized spot volume ($n = 3$).

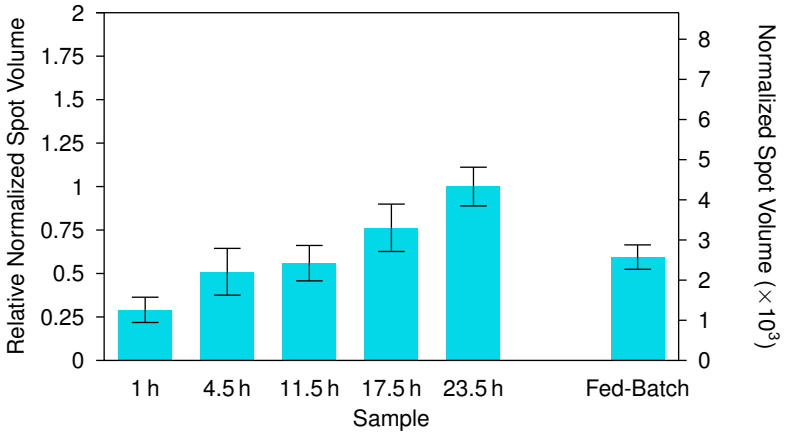

Figure B.48. Spot number 82 identified as ABC transporter substrate-binding protein. Error bars depict the standard error of the mean normalized spot volume ($n = 3$).

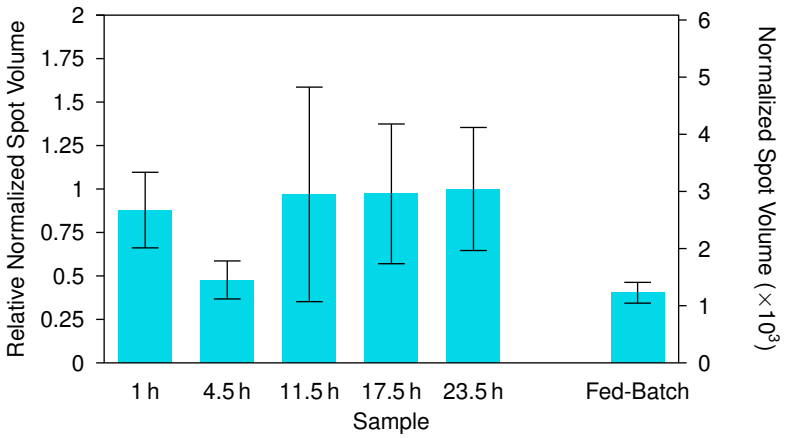

Figure B.49. Spot number 156 identified as ABC transporter substrate-binding protein*. Error bars depict the standard error of the mean normalized spot volume ($n = 3$).

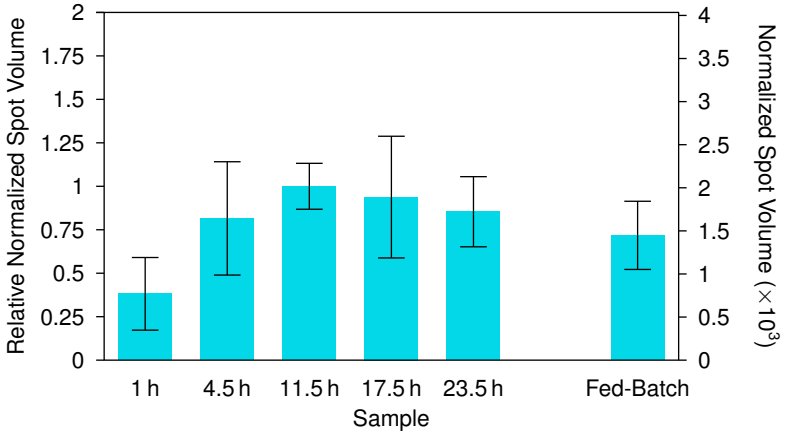

Figure B.50. Spot number 165 identified as Amino acid ABC transporter*. Error bars depict the standard error of the mean normalized spot volume ($n = 3$).

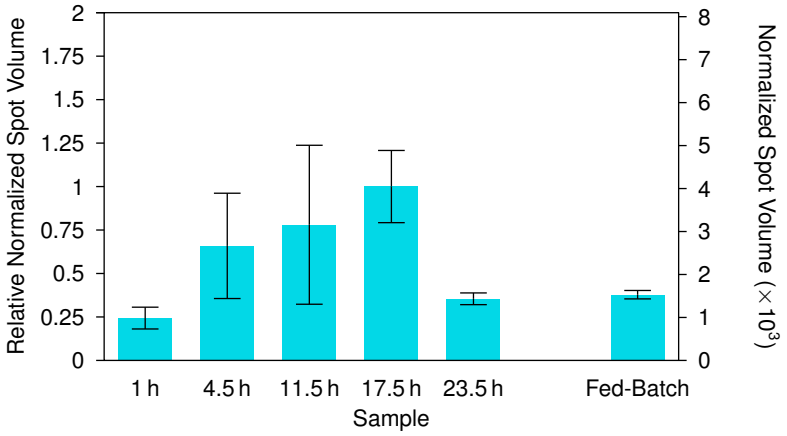

Figure B.51. Spot number 181 identified as Amino acid ABC transporter*. Error bars depict the standard error of the mean normalized spot volume ($n = 3$).

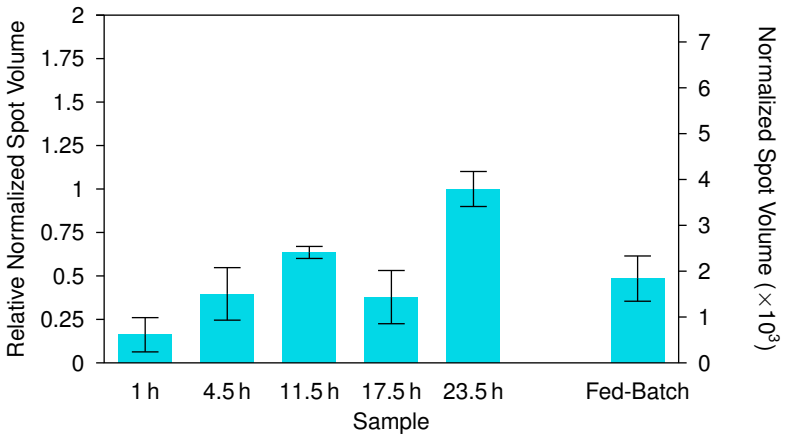

Figure B.52. Spot number 232 identified as ABC transporter substrate-binding protein*. Error bars depict the standard error of the mean normalized spot volume ($n = 3$).

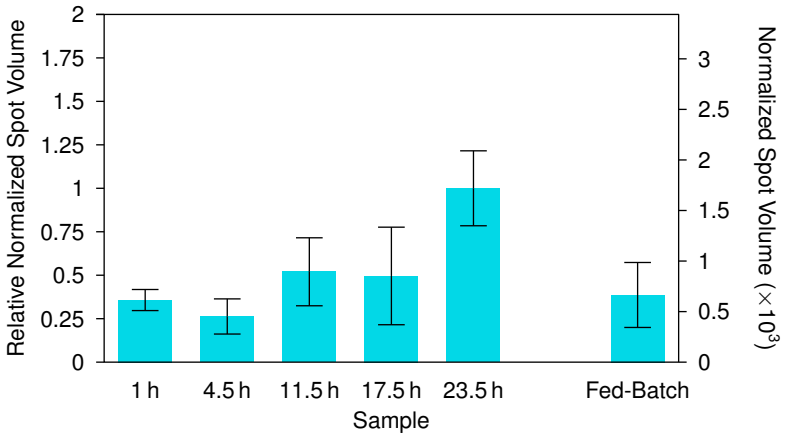

Figure B.53. Spot number 236 identified as ABC transporter substrate-binding protein*. Error bars depict the standard error of the mean normalized spot volume ($n = 3$).

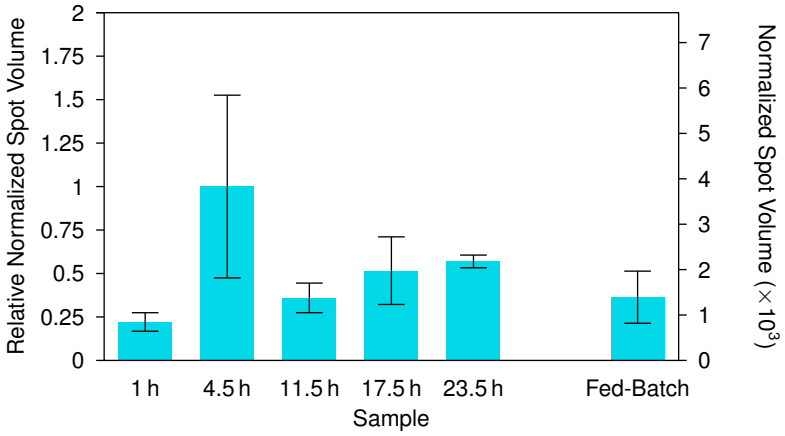

Figure B.54. Spot number 244 identified as Amino acid ABC transporter*. Error bars depict the standard error of the mean normalized spot volume ($n = 3$).

B.3.2 Energy generation/conversion

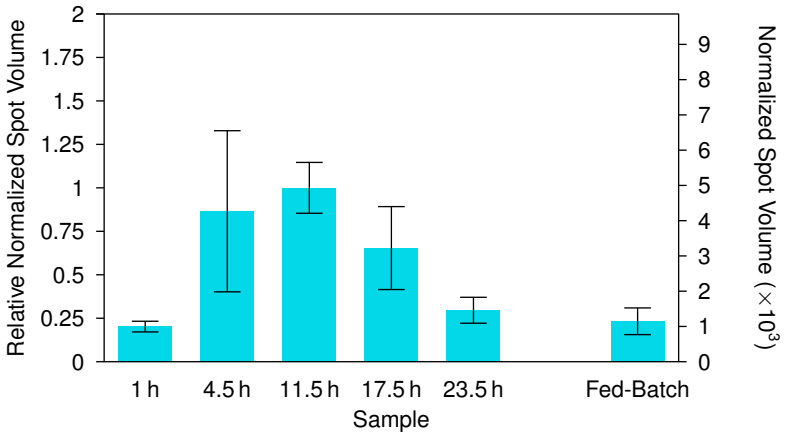

Figure B.55. Spot number 38 identified as Quinohemoprotein amine dehydrogenase*. Error bars depict the standard error of the mean normalized spot volume ($n = 3$).

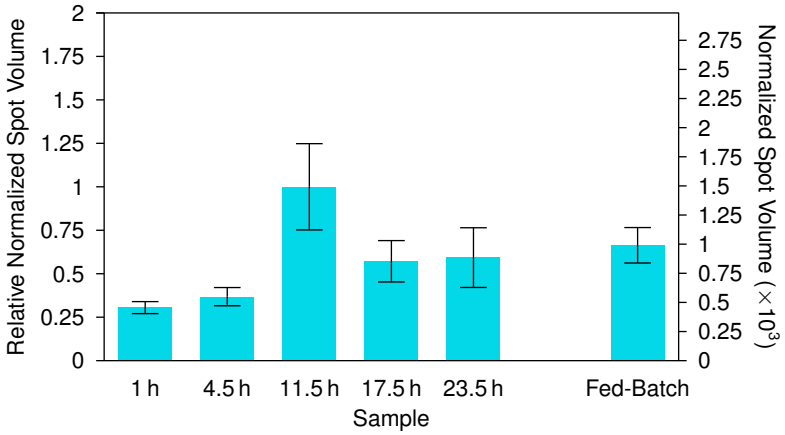

Figure B.56. Spot number 69 identified as Glycerol kinase*. Error bars depict the standard error of the mean normalized spot volume ($n = 3$).

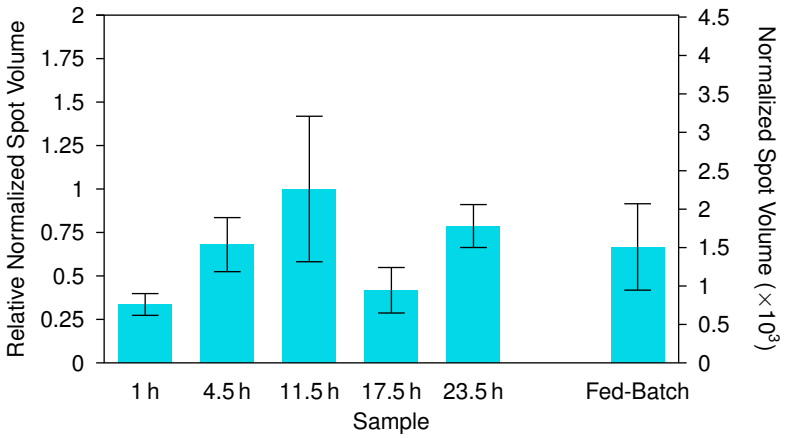

Figure B.57. Spot number 469 identified as F0F1 ATP synthase subunit beta. Error bars depict the standard error of the mean normalized spot volume ($n = 3$).

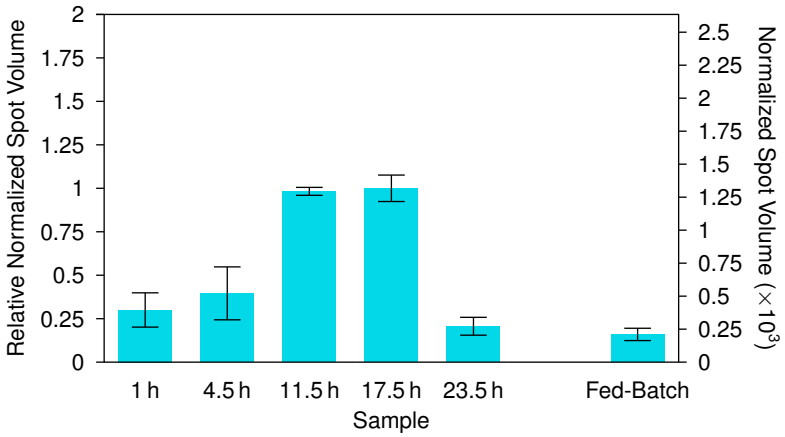

Figure B.58. Spot number 1809 identified as Fumarate hydratase. Error bars depict the standard error of the mean normalized spot volume ($n = 3$).

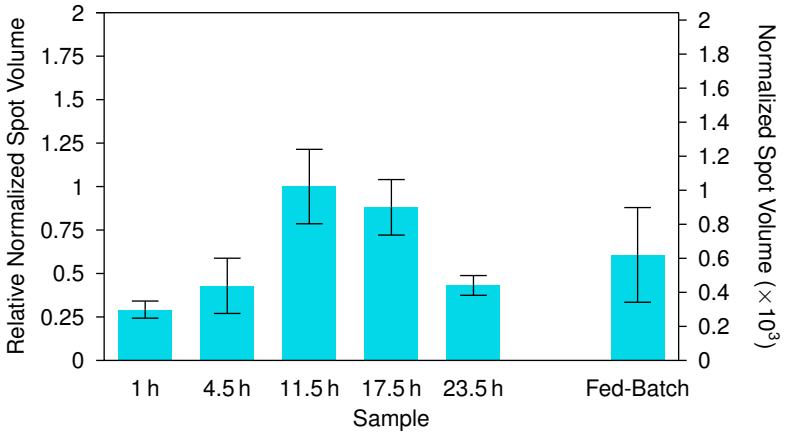

Figure B.59. Spot number 4746 identified as Quinone oxidoreductase. Error bars depict the standard error of the mean normalized spot volume ($n = 3$).

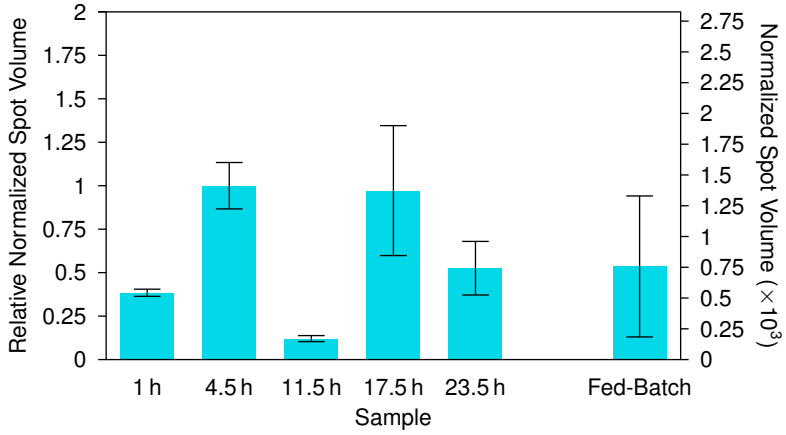

Figure B.60. Spot number 4960 identified as F0F1 ATP synthase subunit alpha§. Error bars depict the standard error of the mean normalized spot volume ($n = 3$).

B.3.3 Acyl-CoA metabolism

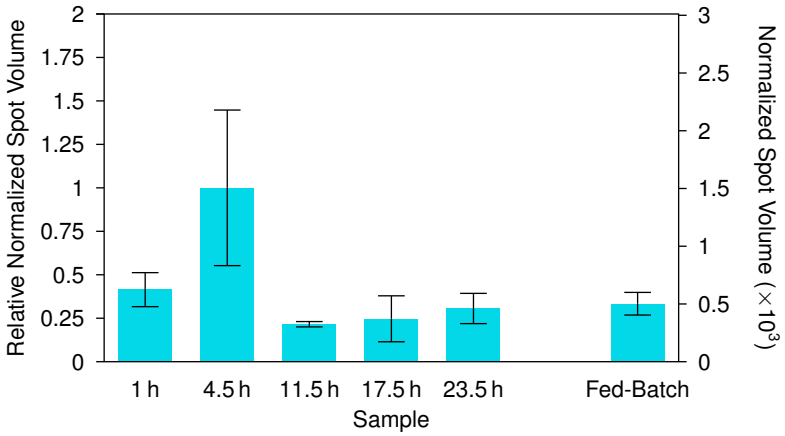

Figure B.61. Spot number 150 identified as Acetyl-CoA synthetase. Error bars depict the standard error of the mean normalized spot volume ($n = 3$).

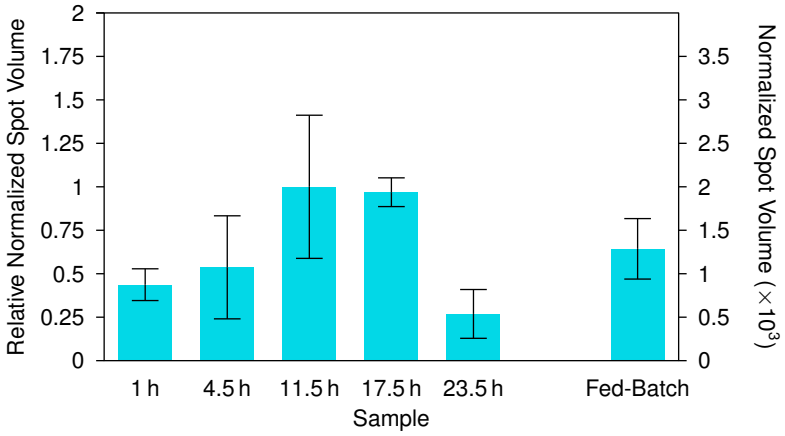

Figure B.62. Spot number 151 identified as Acetyl-CoA acetyltransferase. Error bars depict the standard error of the mean normalized spot volume ($n = 3$).

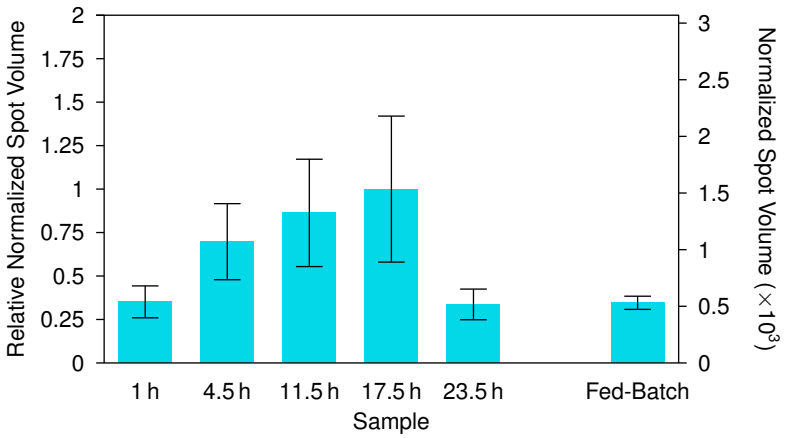

Figure B.63. Spot number 327 identified as Propionyl-CoA synthetase. Error bars depict the standard error of the mean normalized spot volume ($n = 3$).

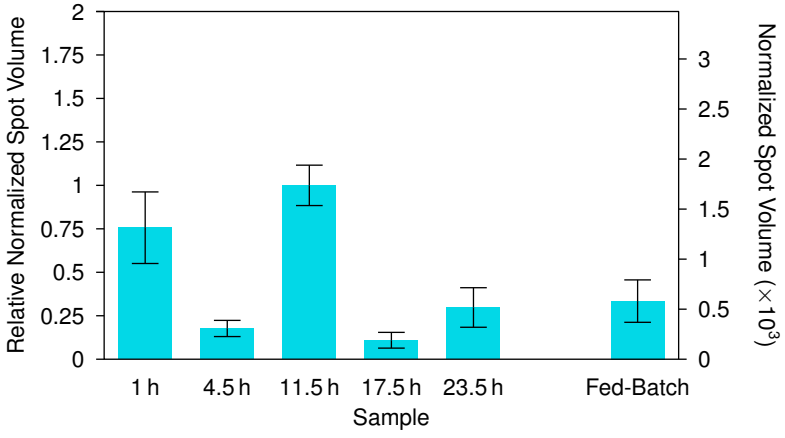

Figure B.64. Spot number 541 identified as Succinyl-CoA:3-ketoacid-CoA transferase. Error bars depict the standard error of the mean normalized spot volume ($n = 3$).

B.3.4 Housekeeping/cellular maintenance

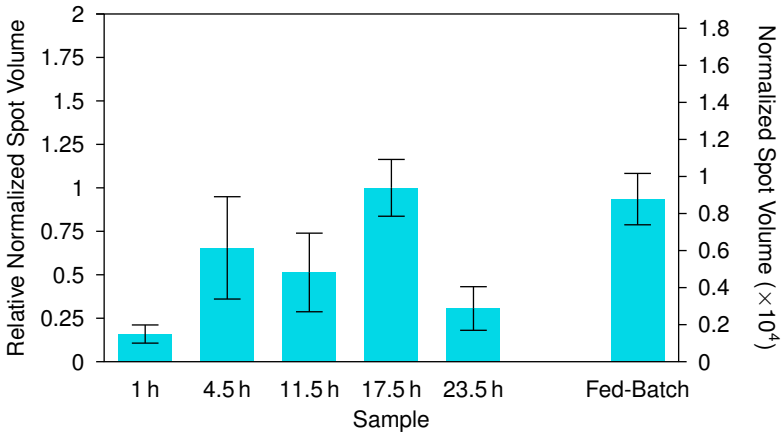

Figure B.65. Spot number 8 identified as Molecular chaperone GroEL. Error bars depict the standard error of the mean normalized spot volume ($n = 3$).

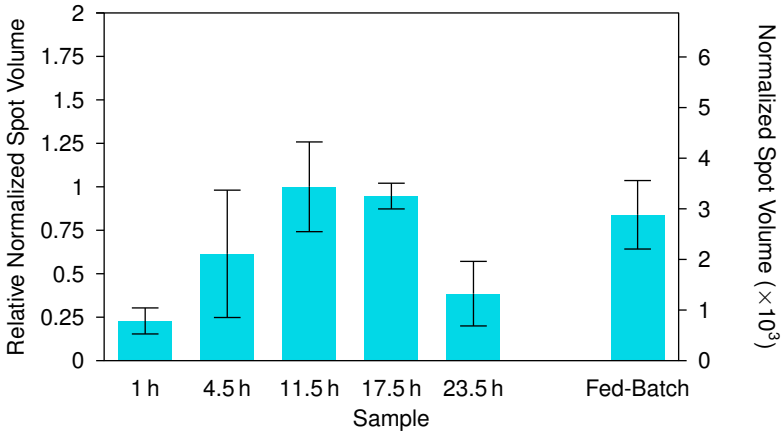

Figure B.66. Spot number 63 identified as Molecular chaperone GroEL. Error bars depict the standard error of the mean normalized spot volume ($n = 3$).

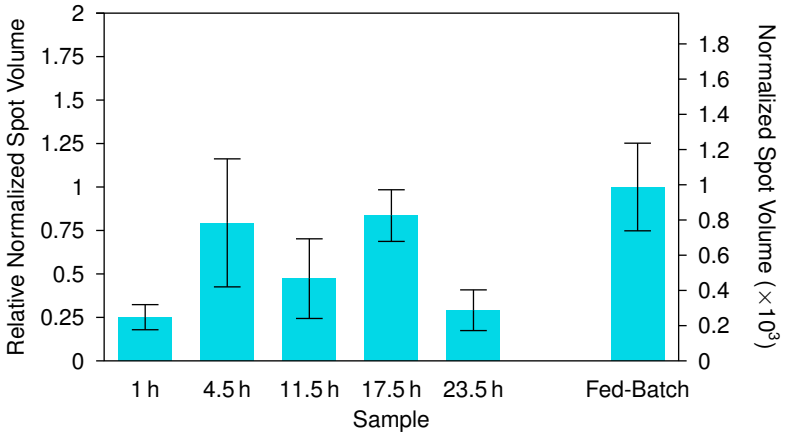

Figure B.67. Spot number 218 identified as Molecular chaperone GroEL. Error bars depict the standard error of the mean normalized spot volume ($n = 3$).

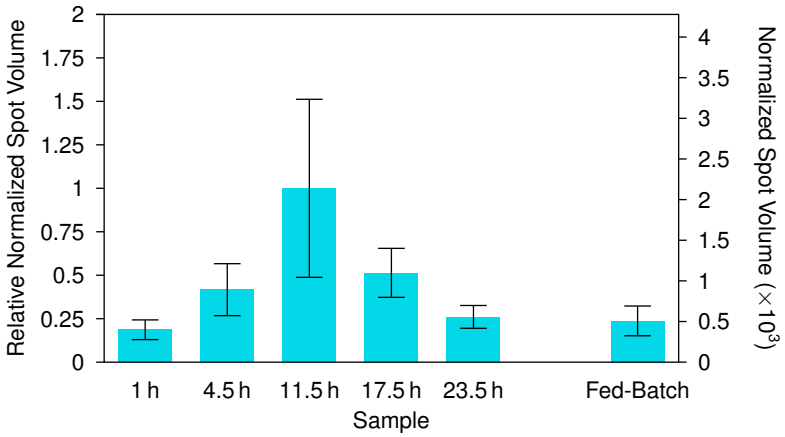

Figure B.68. Spot number 4978 identified as Molecular chaperone GroEL. Error bars depict the standard error of the mean normalized spot volume ($n = 3$).

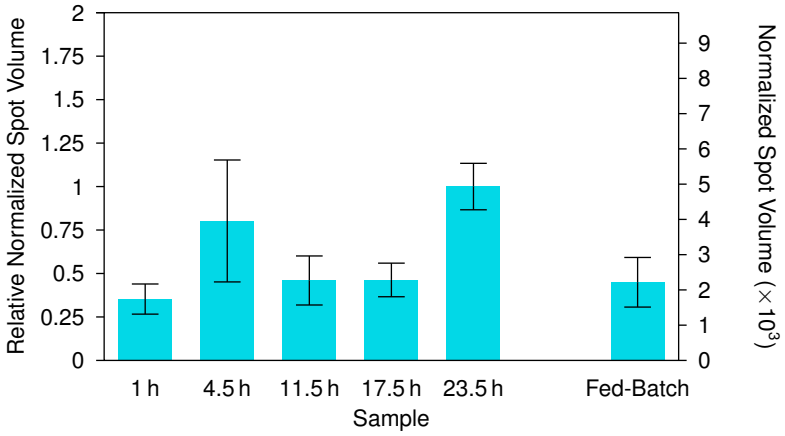

Figure B.69. Spot number 75 identified as Multifunctional 2'3'-cyclic-nucleotide 2'phosphodiesterase. Error bars depict the standard error of the mean normalized spot volume ($n = 3$).

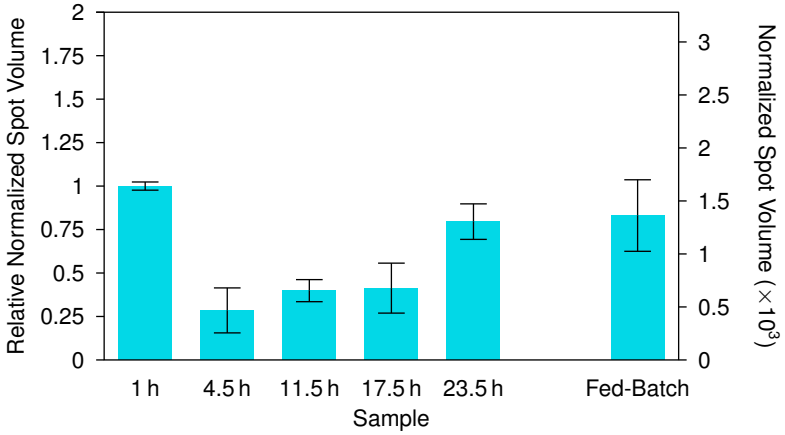

Figure B.70. Spot number 419 identified as Elongation factor Tu. Error bars depict the standard error of the mean normalized spot volume ($n = 3$).

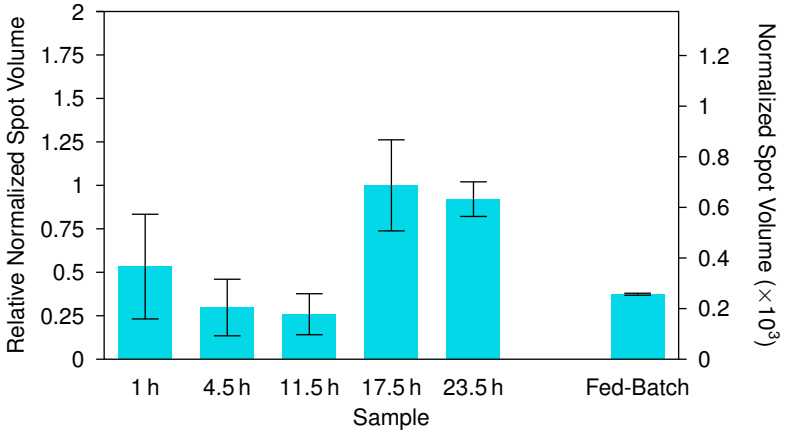

Figure B.71. Spot number 5837 identified as Sigma-54-dependent Fis family transcriptional regulator. Error bars depict the standard error of the mean normalized spot volume ($n = 3$).

B.3.5 Other proteins

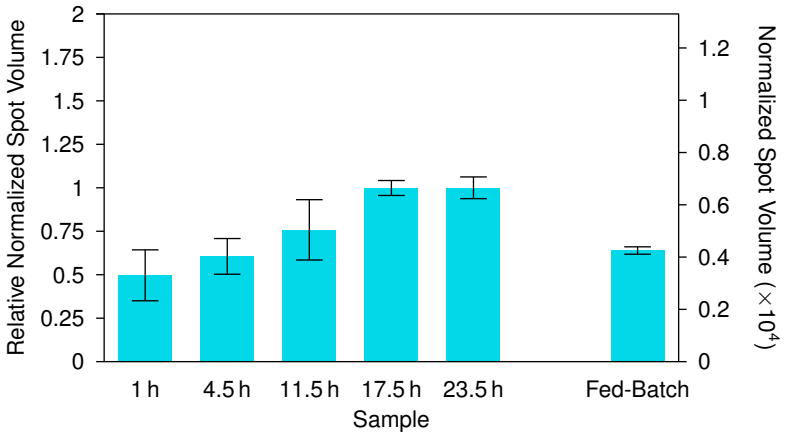

Figure B.72. Spot number 42 identified as Membrane protein*. Error bars depict the standard error of the mean normalized spot volume ($n = 3$).

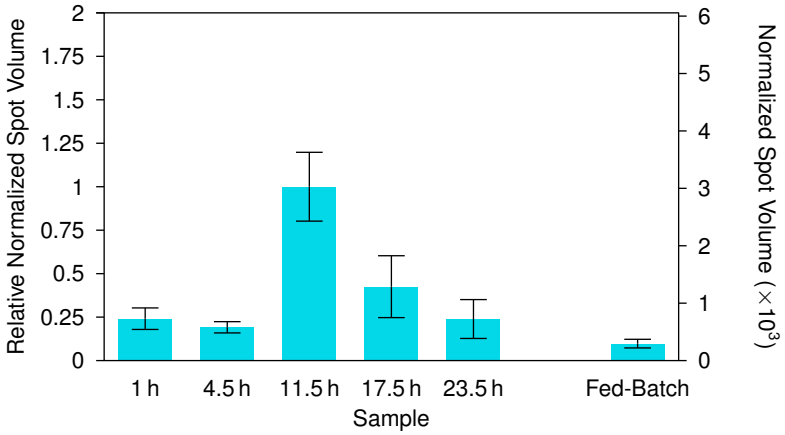

Figure B.73. Spot number 370 identified as TelA*. Error bars depict the standard error of the mean normalized spot volume ($n = 3$).

B.4 Fed-batch proteins

These proteins each exhibited large, statistically-significant fold changes in the fed-batch relative to the SBR (i.e., they were more abundant in the fed-batch than in the SBR).

B.4.1 PHA synthesis

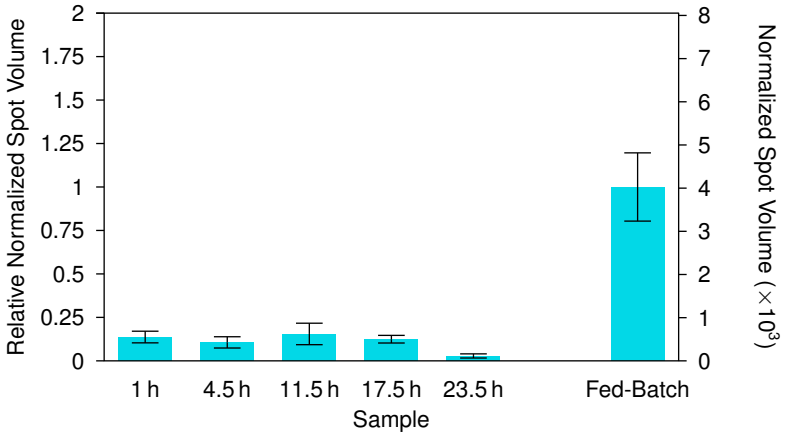

Figure B.74. Spot number 201 identified as Phasin*. Error bars depict the standard error of the mean normalized spot volume ($n = 3$).

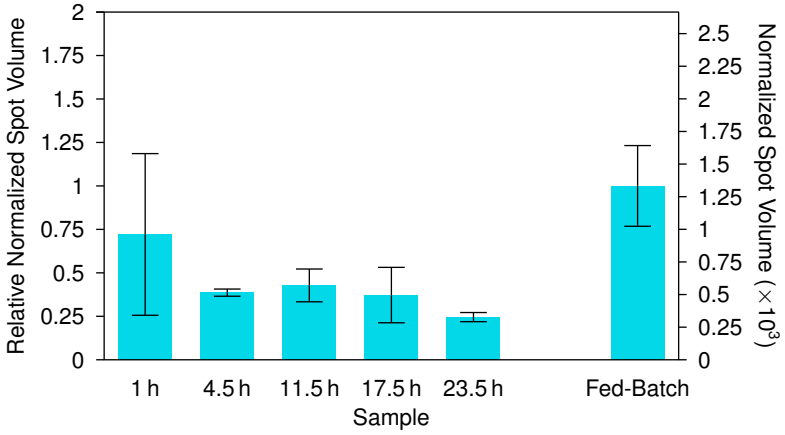

Figure B.75. Spot number 344 identified as Phasin*. Error bars depict the standard error of the mean normalized spot volume ($n = 3$).

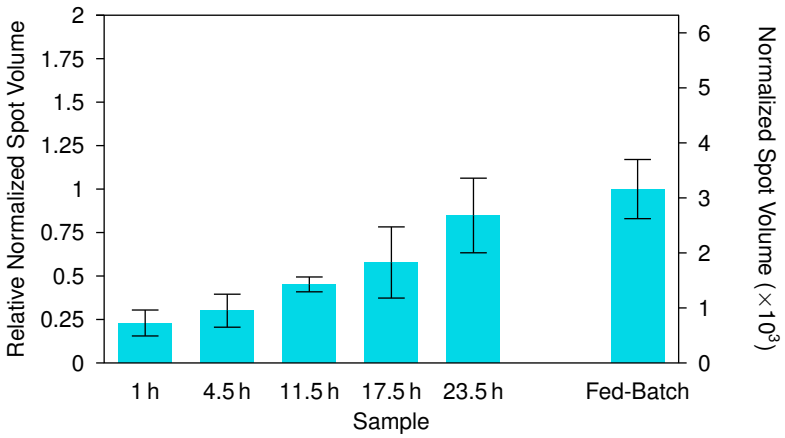

Figure B.76. Spot number 572 identified as Phasin*. Error bars depict the standard error of the mean normalized spot volume ($n = 3$).

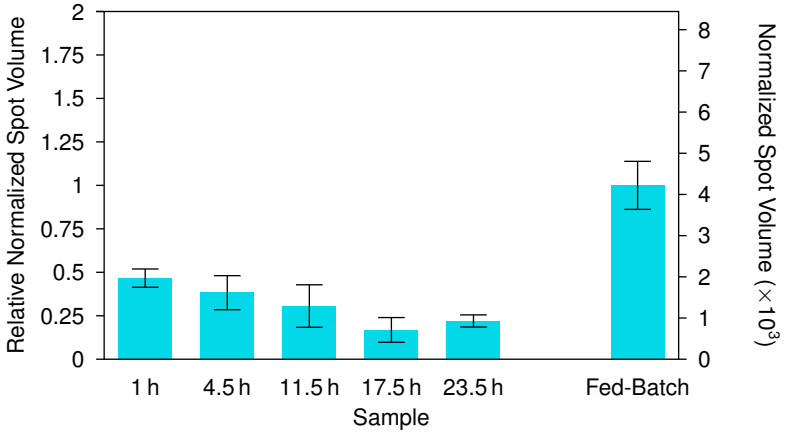

Figure B.77. Spot number 1956 identified as Phasin*. Error bars depict the standard error of the mean normalized spot volume ($n = 3$).

B.4.2 Energy generation/conversion

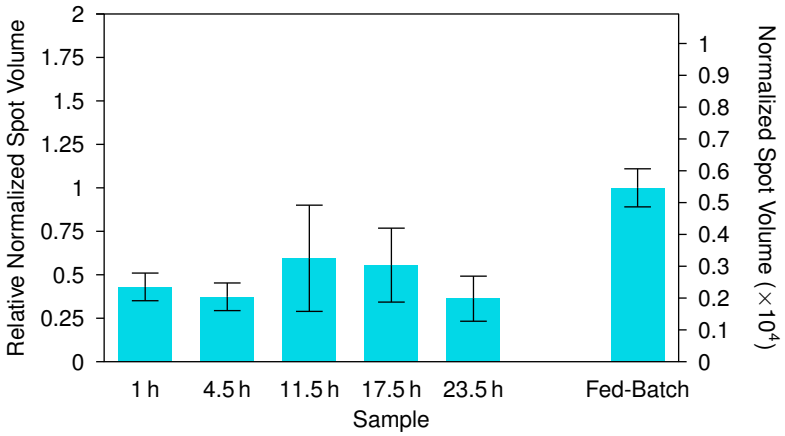

Figure B.78. Spot number 9 identified as F0F1 ATP synthase subunit alpha. Error bars depict the standard error of the mean normalized spot volume ($n = 3$).

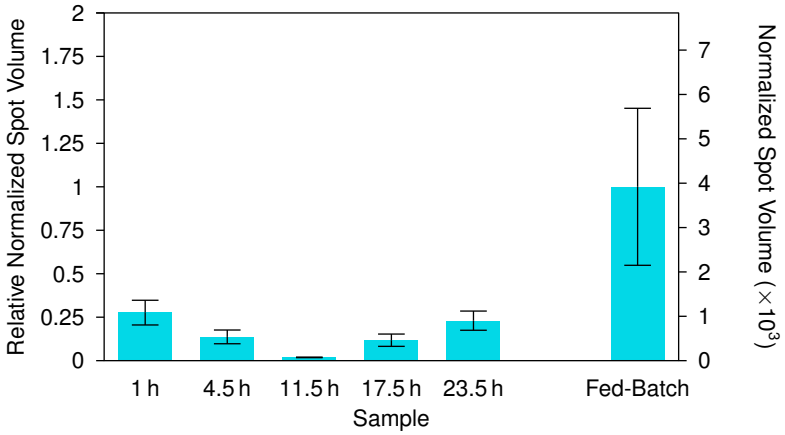

Figure B.79. Spot number 488 identified as ATP synthase epsilon chain*. Error bars depict the standard error of the mean normalized spot volume ($n = 3$).

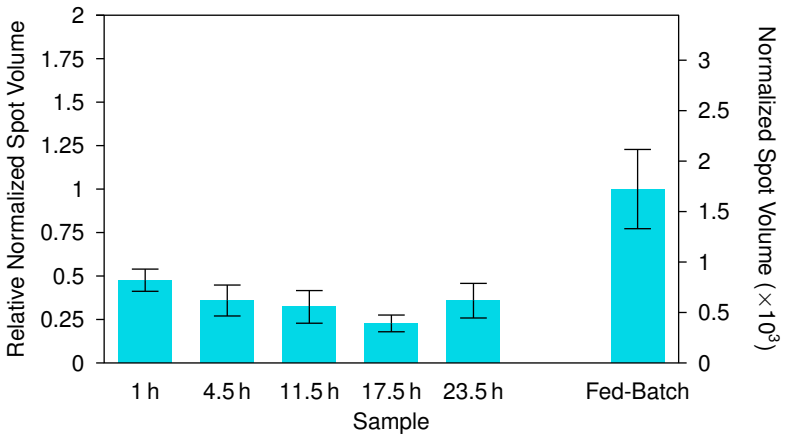

Figure B.80. Spot number 518 identified as Methylmalonate-semialdehyde dehydrogenase*. Error bars depict the standard error of the mean normalized spot volume ($n = 3$).

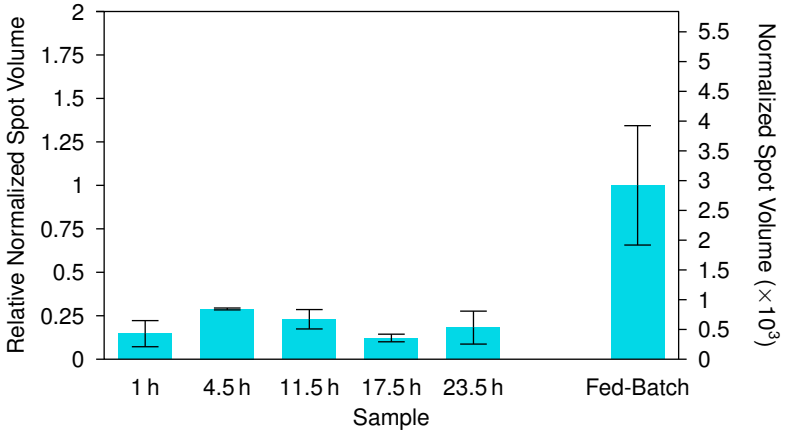

Figure B.81. Spot number 648 identified as Malate dehydrogenase. Error bars depict the standard error of the mean normalized spot volume ($n = 3$).

B.4.3 Other proteins

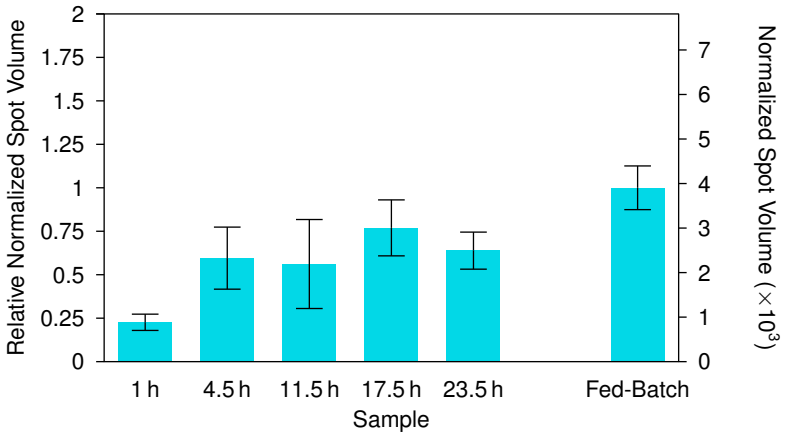

Figure B.82. Spot number 46 identified as ABC transporter substrate-binding protein*. Error bars depict the standard error of the mean normalized spot volume ($n = 3$).

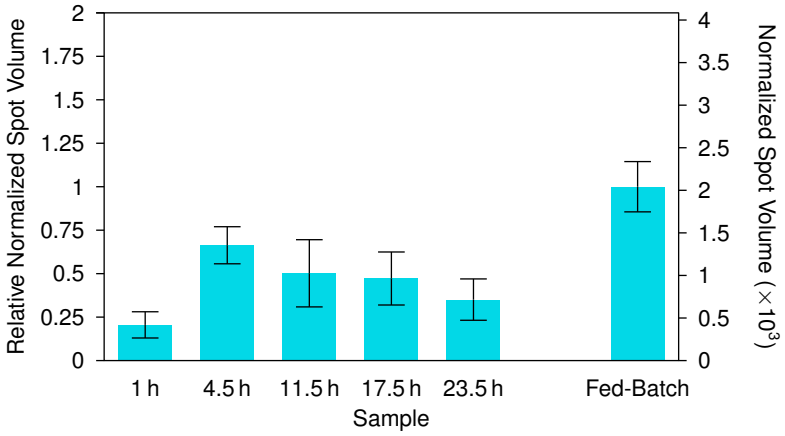

Figure B.83. Spot number 325 identified as Molecular chaperone GroEL. Error bars depict the standard error of the mean normalized spot volume ($n = 3$).

B.5 SBR proteins

These proteins each exhibited large, statistically-significant fold changes in the SBR relative to the fed-batch (i.e., they were more abundant in the SBR than in the fed-batch).

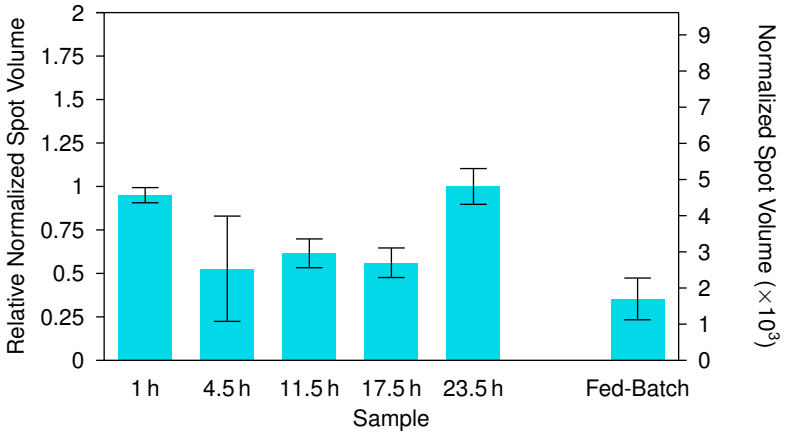

Figure B.84. Spot number 28 identified as Dihydrolipoamide dehydrogenase*. Error bars depict the standard error of the mean normalized spot volume ($n = 3$).

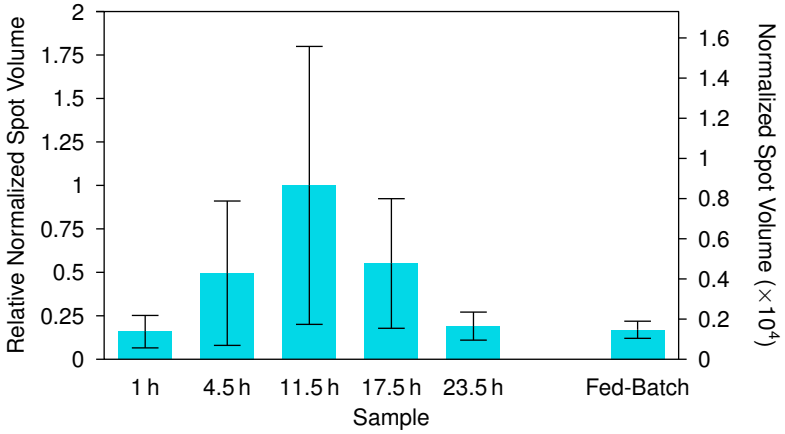

Figure B.85. Spot number 81 identified as Adenylate kinase. Error bars depict the standard error of the mean normalized spot volume ($n = 3$).

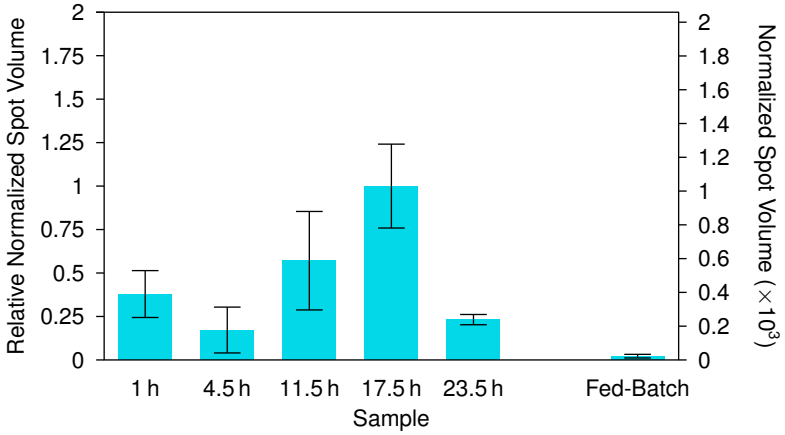

Figure B.86. Spot number 429 identified as Amino acid ABC transporter substrate-binding protein. Error bars depict the standard error of the mean normalized spot volume ($n = 3$).

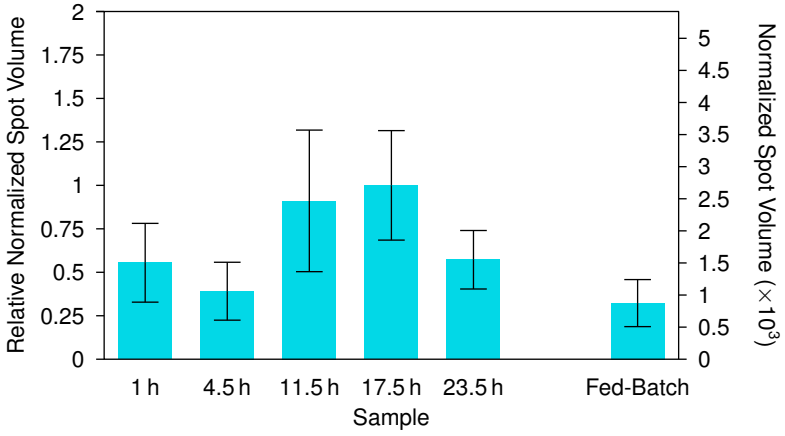

Figure B.87. Spot number 257 identified as Transcription termination/antitermination factor NusG. Error bars depict the standard error of the mean normalized spot volume ($n = 3$).

Table B.5. Identification of proteins excised from 2DE gels using LC-MS/MS and database search with Mascot. MS/MS peak list files were searched against the NCBInr database (October 2015, 73,055,898 protein sequences) with no species restriction and the following search parameters: (i) specific enzyme, trypsin; (ii) peptide window tolerance, ± 0.4 Da; (iii) fragment mass tolerance, ± 0.4 Da; (iv) missed cleavage sites, 1; and (v) variable modifications, carbamidomethyl C, deamidated NQ, and oxidized M. The decoy option was included for each search to include the false discovery rate. For protein identification, protein hits with at least two peptide matches and individual protein scores above the significance score calculated by Mascot ($p < 0.05$; the individual ion score is $-10 \times \log(p)$, where p is the probability that the observed match is the random match) were accepted.

Spot	Mascot Protein Name[a]	Accession	Score	Cut-off[b]	MW[c] (Da)	pI[d]	FDR[e]	Matched Peptides	% Protein Coverage
1	Hypothetical protein	WP_018631314	227	66	36221	4.53	0/14.29	4	14
2	Acetyl-CoA acetyltransferase	WP_018631634	764	66	40685	5.97	0	9	42
2	Isocitrate dehydrogenase	WP_018631946	207	66	44956	6.04	0	4	11
3	Hypothetical protein	WP_018632695	209	65	21878	5.89	0	4	18
4	Amino acid ABC transporter substrate-binding protein	WP_018632268	722	66	37781	4.89	0/9.09	8	30
5	Bacterioferritin	WP_026310284	227	65	18528	4.95	0	4	28
6	Hypothetical protein	WP_018631899	614	66	39576	6.36	0	9	32
8	Molecular chaperone GroEL	WP_018633070	1441	66	57962	5.05	0/5.56	19	47
9	F0F1 ATP synthase subunit alpha	WP_018631697	139	65	55571	5.7	0	3	7
11	Hypothetical protein	WP_018634284	672	65	36835	4.91	0	7	36
12	Molecular chaperone GroEL	WP_018633070	99	65	57962	5.05	0	2	4
13	ABC transporter permease	WP_018632451	533	66	42583	4.83	0	7	30
13	F0F1 ATP synthase subunit beta	WP_018631700	195	66	50791	4.79	0	4	14

Table B.5. Identification of proteins excised from 2DE gels using LC-MS/MS and database search with Mascot continued.

Spot	Mascot Protein Name[a]	Accession	Score	Cut-off[b]	MW[c] (Da)	pI[d]	FDR[e]	Matched Peptides	% Protein Coverage
15	Hypothetical protein	WP_018634051	493	66	18623	5.8	0	7	44
21	Acetyl-CoA acetyltransferase	WP_018631634	711	65	40685	5.97	0	9	42
27	Membrane protein	WP_018634320	197	63	35466	6.05	0	4	13
28	Hypothetical protein	WP_018632931	537	65	48291	5.79	0	8	23
32	Hypothetical protein	WP_018632161	124	66	40536	4.66	0/33.33	3	10
37	ABC transporter substrate-binding protein	WP_018633772	296	65	40130	4.6	0/11.76	3	14
37	Hypothetical protein	WP_018633424	896	65	38323	4.72	0/11.76	11	41
37	Hypothetical protein	WP_018631883	135	65	34845	6.46	0/11.76	3	12
37	Hypothetical protein	WP_018631314	114	65	36221	4.53	0/11.76	3	12
37	Multifunctional 2'3'-cyclic-nucleotide 2'phosphodiesterase	WP_018631853	168	65	58603	4.72	0/11.76	3	7
38	Hypothetical protein	WP_018634151	170	65	55372	4.81	0	4	7
38	Multifunctional 2'3'-cyclic-nucleotide 2'phosphodiesterase	WP_018631853	130	65	58603	4.72	0	2	4
42	Hypothetical protein	WP_018633522	623	65	34894	5	0/7.14	9	36
42	ATP synthase F1, beta subunit[f]	EEW24673	220	65	50542	4.91	0/7.14	4	11
46	Glutamyl-tRNA amidotransferase	WP_026310186	220	65	53121	4.93	0	3	8
46	Hypothetical protein	WP_018633957	344	65	54148	4.96	0	7	19
46	Molecular chaperone GroEL	WP_018633070	319	65	57962	5.05	0	6	15

Table B.5. Identification of proteins excised from 2DE gels using LC-MS/MS and database search with Mascot continued.

Spot	Mascot Protein Name[a]	Accession	Score	Cut-off[b]	MW[c] (Da)	pI[d]	FDR[e]	Matched Peptides	% Protein Coverage
59	Hypothetical protein	WP_018633424	577	63	38323	4.72	0	9	36
59	Hypothetical protein	WP_018634285	264	63	36927	4.89	0	5	19
59	Hypothetical protein	WP_018631314	126	63	36221	4.53	0	2	6
59	Multifunctional 2'3'-cyclic-nucleotide 2'phosphodiesterase	WP_018631853	184	63	58603	4.72	0	2	5
63	Molecular chaperone GroEL	WP_018633070	909	63	57962	5.05	14.29/7.69	15	30
69	Hypothetical protein	WP_018632171	265	62	54320	5.29	0	6	14
69	Polynucleotide phosphorylase/polyadenylase	WP_040788856	232	62	80328	4.53	0	4	6
75	Hypothetical protein	WP_018632268	442	63	37781	4.89	0	6	22
75	Hypothetical protein	WP_018631843	186	63	35024	6.28	0	4	15
75	Hypothetical protein	WP_018633424	130	63	38323	4.72	0	3	10
75	Multifunctional 2'3'-cyclic-nucleotide 2'phosphodiesterase	WP_018631853	801	63	58603	4.72	0	10	28
81	Adenylate kinase	WP_018631593	150	65	22738	5.46	0	3	18
82	ABC transporter substrate-binding protein	WP_018633400	406	63	58648	4.93	0/25	7	15
93	Hypothetical protein	WP_018634051	468	65	18623	5.8	0/16.67	7	36
124	Elongation factor Tu	WP_018631570	627	65	43422	5.42	0	11	35
124	Translation elongation factor Tu[g]	WP_002811703	258	65	43072	5.45	0	4	12

Table B.5. Identification of proteins excised from 2DE gels using LC-MS/MS and database search with Mascot continued.

Spot	Mascot Protein Name[a]	Accession	Score	Cut-off[b]	MW[c] (Da)	pI[d]	FDR[e]	Matched Peptides	% Protein Coverage
140	Elongation factor Tu	WP_018631570	369	65	43422	5.42	0	7	22
140	Enolase	WP_018632150	236	65	44819	4.93	0	3	11
150	Acetyl-CoA synthetase	WP_018631372	169	65	70657	5.88	0	3	5
151	Acetyl-CoA acetyltransferase	WP_018631634	328	61	40685	5.97	0	2	11
156	Hypothetical protein	WP_018631899	180	65	39576	6.36	0	3	9
165	Hypothetical protein	WP_018632269	258	64	37330	4.69	0/20	4	13
165	Hypothetical protein	WP_018631939	101	64	43788	5.81	0/20	2	4
170	Cysteine synthase	WP_018632506	112	65	32694	5.89	0	2	10
170	Translocation protein TolB	WP_026310348	182	65	47660	9.4	0	4	10
179	Hypothetical protein	WP_018632800	308	65	55550	5.73	0	6	12
181	ABC transporter substrate-binding protein	WP_018634210	217	64	28765	4.64	0	5	14
181	Hypothetical protein	WP_018632269	408	64	37330	4.69	0	7	23
183	Hypothetical protein	WP_018634051	348	65	18623	5.8	0	6	40
201	Hypothetical protein	WP_018634051	196	64	18623	5.8	0	3	23
218	Molecular chaperone GroEL	WP_018633070	574	65	57962	5.05	0	8	17
232	Hypothetical protein	WP_018633993	339	65	33128	4.53	0	6	25
232	Hypothetical protein	WP_018632269	327	65	37330	4.69	0	5	17
232	Hypothetical protein	WP_018633742	214	65	34178	4.57	0	4	18

Table B.5. Identification of proteins excised from 2DE gels using LC-MS/MS and database search with Mascot continued.

Spot	Mascot Protein Name[a]	Accession	Score	Cut-off[b]	MW[c] (Da)	pI[d]	FDR[e]	Matched Peptides	% Protein Coverage
236	Hypothetical protein	WP_018631899	117	62	39576	6.36	0	3	9
244	Hypothetical protein	WP_018632268	481	64	37781	4.89	0	8	24
244	Multifunctional 2'3'-cyclic-nucleotide 2'phosphodiesterase	WP_018631853	131	64	58603	4.72	0	2	4
257	Benzoate 1,2-dioxygenase subunit beta[h]	WP_005209338	106	64	21451	4.99	0	2	11
257	Transcription termination/antitermination factor NusG	WP_018631560	126	64	20049	5.16	0	3	18
258	ATP-dependent Clp protease proteolytic subunit	WP_018632247	140	65	23089	5.62	0/11.11	3	15
258	Fructose-6-phosphate aldolase	WP_018631694	122	65	23011	5.63	0/11.11	3	16
258	Hypothetical protein	WP_018632449	102	65	54008	5.94	0/11.11	2	5
270	Hypothetical protein	WP_018632386	137	65	34755	5.82	0	3	8
320	Hypothetical protein	WP_018633267	566	65	30332	5.81	9.09/11.11	7	35
320	Hypothetical protein, partial	WP_040789130	148	65	25201	6.16	9.09/11.11	2	12
320	Malate dehydrogenase	WP_018631935	132	65	33324	5.49	9.09/11.11	2	8
325	Molecular chaperone GroEL	WP_018633070	981	65	57962	5.05	0/8.33	14	34
327	Propionyl-CoA synthetase	WP_018632631	178	64	68489	5.73	0	4	6
341	Cysteine synthase	WP_018632506	170	63	32694	5.89	0	3	13
341	Isocitrate dehydrogenase	WP_018631946	237	63	44956	6.04	0	4	12
341	Malate dehydrogenase	WP_018631935	227	63	33324	5.49	0	4	17

Table B.5. Identification of proteins excised from 2DE gels using LC-MS/MS and database search with Mascot continued.

Spot	Mascot Protein Name[a]	Accession	Score	Cut-off[b]	MW[c] (Da)	pI[d]	FDR[e]	Matched Peptides	% Protein Coverage
344	Hypothetical protein	WP_018634051	311	62	18623	5.8	0	6	32
354	Acetoacetyl-CoA reductase	WP_012331188	99	65	25401	7.71	0/20	2	8
354	Hypothetical protein	WP_018634051	520	65	18623	5.8	0/20	7	42
370	Hypothetical protein	WP_018632854	296	65	45037	5.48	0	6	15
407	Aldehyde dehydrogenase	WP_018633284	302	63	55302	6.14	0	4	14
407	Elongation factor Tu	WP_018631570	267	63	43422	5.42	0	4	14
407	F0F1 ATP synthase subunit beta	WP_018631700	221	63	50791	4.79	0	5	11
407	Malate-CoA ligase subunit beta	WP_018631936	205	63	42646	5.38	0	4	14
407	Quinoprotein ethanol dehydrogenase	WP_018634195	172	63	66860	4.88	0	2	5
419	Elongation factor Tu	WP_018631570	154	63	43422	5.42	0	2	7
419	Hypothetical protein	WP_018631498	128	63	32596	7.75	0	3	11
419	Malate dehydrogenase	WP_018631935	85	63	33324	5.49	0	2	6
429	Amino acid ABC transporter substrate-binding protein	WP_018632268	366	63	37781	4.89	0	5	19
429	Malate-CoA ligase subunit beta	WP_018631936	180	63	42646	5.38	0	2	7
449	50S ribosomal protein L5	WP_018631584	138	62	21182	9.21	0	2	16
449	Hypothetical protein	WP_018631834	96	62	21639	6.4	0	3	19
469	F0F1 ATP synthase subunit beta	WP_018631700	297	63	50791	4.79	16.7/12.5	6	16
472	Hypothetical protein	WP_018634051	213	62	18623	5.8	0/12.5	4	30
472	Hypothetical protein	WP_018631719	201	62	20290	5.52	0/12.5	3	19

Table B.5. Identification of proteins excised from 2DE gels using LC-MS/MS and database search with Mascot continued.

Spot	Mascot Protein Name[a]	Accession	Score	Cut-off[b]	MW[c] (Da)	pI[d]	FDR[e]	Matched Peptides	% Protein Coverage
472	Hypothetical protein	WP_018634194	130	62	21188	5.89	0/12.5	3	15
472	Hypothetical protein	WP_018631899	129	62	39576	6.36	0/12.5	2	5
488	Hypothetical protein	WP_018631701	177	65	13935	4.89	0	2	18
518	Hypothetical protein	WP_018632449	151	62	54008	5.94	0	2	5
518	Hypothetical protein	WP_018634051	117	62	18623	5.8	0	3	16
541	Hypothetical protein	WP_026310169	98	62	85241	4.88	0	2	3
541	Succinyl-CoA:3-ketoacid-CoA transferase	WP_018634294	100	62	22360	4.69	0	2	14
548	ABC transporter substrate-binding protein	WP_040789902	107	63	57296	4.8	0/20	2	6
548	Hypothetical protein	WP_018633730	150	63	46308	4.79	0/20	2	6
548	Molecular chaperone GroEL	WP_018633070	184	63	57962	5.05	0/20	4	8
548	Quinoprotein ethanol dehydrogenase	WP_018634195	128	63	66860	4.88	0/20	4	7
552	Hypothetical protein	WP_018634194	116	63	21188	5.86	0	3	19
568	Acetyl-CoA acetyltransferase	WP_018631634	545	63	40685	5.97	0	8	38
572	Hypothetical protein	WP_018634051	318	62	18623	5.8	0	5	35
584	Malate dehydrogenase	WP_018631935	82	62	33324	5.49	0	2	8
636	Multispecies: isocitrate dehydrogenase[i]	WP_003813356	145	64	45249	5.24	0/33	2	5
648	Malate dehydrogenase	WP_018631935	122	65	33324	5.49	0	2	8

Table B.5. Identification of proteins excised from 2DE gels using LC-MS/MS and database search with Mascot continued.

Spot	Mascot Protein Name[a]	Accession	Score	Cut-off[b]	MW[c] (Da)	pI[d]	FDR[e]	Matched Peptides	% Protein Coverage
795	Membrane protein	WP_018634320	126	62	35466	6.05	0	3	9
795	Crp/Fnr family transcriptional regulator[j]	WP_030876847	100	62	50221	5.46	0	2	4
950	Hypothetical protein	WP_018632449	142	63	54008	5.94	0/50	2	5
950	Hypothetical protein	WP_018631640	115	63	28035	6.04	0/50	2	9
1196	Aldehyde dehydrogenase	WP_018633284	433	63	55302	6.14	0	7	16
1196	Hypothetical protein	WP_018632484	153	63	60642	5.58	0	2	5
1537	Hypothetical protein	WP_018634051	265	62	18623	5.8	0/11.1	4	32
1537	Hypothetical protein	WP_018632792	147	62	18979	5.81	0/11.1	2	16
1537	Multispecies: formaldehyde-activating enzyme Fae[k]	WP_002923426	149	62	17835	5.34	0/11.1	2	15
1809	Fumarate hydratase	WP_018633280	211	62	49297	5.74	0	4	10
1956	Beta-ketoacyl-ACP reductase	WP_018631633	67	63	25313	7.77	0	2	8
1956	Hypothetical protein	WP_018634051	486	63	18623	5.8	0	8	45
4193	Hypothetical protein	WP_018634051	268	64	18623	5.8	0	5	33
4657	Molecular chaperone GroEL	WP_018633070	214	63	57962	5.05	0	5	11
4657	Quinoprotein ethanol dehydrogenase	WP_018634195	169	63	66860	4.88	0	3	7
4746	Hypothetical protein	WP_018632319	220	62	35673	5.53	0	4	13
4960	F0F1 ATP synthase subunit alpha	WP_018631697	213	63	55571	5.7	0	5	10
4960	F0F1 ATP synthase subunit alpha[l]	WP_004261865	288	63	55268	5.59	0	5	11

Table B.5. Identification of proteins excised from 2DE gels using LC-MS/MS and database search with Mascot continued.

Spot	Mascot Protein Name[a]	Accession	Score	Cut-off[b]	MW[c] (Da)	pI[d]	FDR[e]	Matched Peptides	% Protein Coverage
4978	Molecular chaperone GroEL	WP_018633070	265	63	57962	5.05	0	5	11
5242	Hypothetical protein	WP_018631899	379	62	39576	6.36	0	5	20
5242	Malate-CoA ligase subunit beta	WP_018631936	160	62	42646	5.38	0	4	13
5837	Hypothetical protein	WP_018633103	80	62	53526	5.41	0	2	4
6395	Elongation factor Tu	WP_018631570	286	63	43422	5.42	0	5	16
6395	Malate-CoA ligase subunit beta	WP_018631936	254	63	42646	5.38	0	5	13
7274	Malate dehydrogenase[m]	WP_020951282	189	63	33433	5.34	0	3	11
CS1	Hypothetical protein	WP_018632695	466	62	21878	5.89	0/8.33	6	54
CS1	Hypothetical protein	WP_018633178	349	62	25775	6	0/8.33	4	30
CS1	Hypothetical protein	WP_018634094	309	62	23728	5.86	0/8.33	5	34
CS1	Hypothetical protein	WP_018633228	275	62	24319	5.82	0/8.33	5	33
CS2	Acetyl-CoA synthetase	WP_018631372	391	62	70657	5.88	0/3.33	6	11
CS2	F0F1 ATP synthase subunit alpha	WP_018631697	536	62	55571	5.7	0/3.33	8	20
CS2	Hypothetical protein	WP_018632931	286	62	48291	5.79	0/3.33	4	16
CS2	Propionyl-CoA synthetase	WP_018632631	487	62	68489	5.73	0/3.33	8	19
CS3	Acetyl-CoA acetyltransferase	WP_018631634	695	63	40685	5.97	0/5.13	12	47
CS3	Cysteine synthase	WP_018632506	966	63	32694	5.89	0/5.13	10	59
CS3	Hypothetical protein	WP_018632302	734	63	45367	5.96	0/5.13	8	29
CS3	Hypothetical protein	WP_018631899	391	63	39576	6.36	0/5.13	6	12
CS3	Malate dehydrogenase	WP_018631935	719	63	33324	5.49	0/5.13	9	44

Table B.5. Identification of proteins excised from 2DE gels using LC-MS/MS and database search with Mascot continued.

Spot	Mascot Protein Name[a]	Accession	Score	Cut-off[b]	MW[c] (Da)	pI[d]	FDR[e]	Matched Peptides	% Protein Coverage
CS3	Membrane protein	WP_018634320	758	63	35466	6.05	0/5.13	9	42
CS3	Poly(3-hydroxyalkanoate) synthetase, partial	WP_040789154	121	63	62122	5.96	0/5.13	2	4

[a] Of the 157 identitied proteins, 149 belonged to *M. perideroedes*. Those belonging to a different taxa are denoted.

[b] The Mascot cut-off score indicates the minimum score for an acceptable protein match.

[c] The calculated molecular weight of the protein from Mascot.

[d] The calculated isoelectric point of the protein from Mascot.

[e] False discovery rate. Peptide matches above identity threshold/Peptide matches above homology or identity threshold.

[f] Belongs to *Rhodobacter* sp. SW2

[g] Belongs to *Xanthomonas fragariae*

[h] Belongs to *Gordonia sputi*

[i] Belongs to *Bifidobacterium*

[j] Belongs to *Streptomyces* sp. NRRL S-1868

[k] Belongs to *Thauera*

[l] Belongs to *Thauera* sp. 63

[m] Belongs to *Paracoccus aminophilus*

Table B.6. Homology based identification of hypothetical proteins from Mascot using Blastp. The protein accession listed was searched using Blastp; the protein match with the highest percentage of amino acid identity to a known bacterial protein was accepted.

Spot	Mascot Taxonomy	Accession	Mascot Score	Blast Protein Name	Blast Taxonomy	Amino Acid Identity (%)
1	*M. perideroedes*	WP_018631314	227	Porin	*Thalassospira lucentensis*	31
3	*M. perideroedes*	WP_018632695	209	Superoxide dismutase	*Paracoccus halophilus*	64
6	*M. perideroedes*	WP_018631899	614	ABC transporter substrate-binding protein	*Microvirga* sp. BSC39	69
11	*M. perideroedes*	WP_018634284	672	Sulfate transporter subunit	*Hyphomicrobium* sp. 99	75
15	*M. perideroedes*	WP_018634051	493	Phasin	*Rhodospirillum centenum*	39
28	*M. perideroedes*	WP_018632931	537	Dihydrolipoamide dehydrogenase	*Proteobacteria*	72
32	*M. perideroedes*	WP_018632161	124	Putrescine/spermidine ABC transporter substrate-binding protein	*Oceanimonas* sp. GK1	56
37	*M. perideroedes*	WP_018633424	896	DNA-binding protein	*Thalassospira* sp. HJ	67
37	*M. perideroedes*	WP_018631883	135	Phosphoribosylpyrophosphate synthetase	alpha proteobacterium Mf 1.05b.01	66
37	*M. perideroedes*	WP_018631314	114	Porin	*Thalassospira lucentensis*	31
38	*M. perideroedes*	WP_018634151	170	Quinohemoprotein amine dehydrogenase	*Paracoccus* sp. J39	64
42	*M. perideroedes*	WP_018633522	623	Membrane protein	*Thalassospira* sp. HJ	72
46	*M. perideroedes*	WP_018633957	344	ABC transporter substrate-binding protein	*Ochrobactrum* sp. UNC390CL2Tsu3S39	72
59	*M. perideroedes*	WP_018633424	577	DNA-binding protein	*Thalassospira* sp. HJ	67

Table B.6. Homology based identification of hypothetical proteins from Mascot using Blastp continued.

Spot	Mascot Taxonomy	Accession	Mascot Score	Blast Protein Name	Blast Taxonomy	Amino Acid Identity (%)
59	*M. perideroedes*	WP_018634285	264	Thiosulfate transporter subunit	*Thauera linaloolentis*	64
59	*M. perideroedes*	WP_018631314	126	Porin	*Thalassospira lucentensis*	31
69	*M. perideroedes*	WP_018632171	265	Glycerol kinase	*Labrenzia*	68
75	*M. perideroedes*	WP_018632268	442	Amino acid ABC transporter substrate-binding protein	SAR116 cluster alpha proteobacterium HIMB100	68
75	*M. perideroedes*	WP_018631843	186	3-beta hydroxysteroid dehydrogenase	*Falsirhodobacter* sp. alg1	60
75	*M. perideroedes*	WP_018633424	130	DNA-binding protein	*Thalassospira* sp. HJ	67
93	*M. perideroedes*	WP_018634051	468	Phasin	*Rhodospirillum centenum*	39
156	*M. perideroedes*	WP_018631899	180	ABC transporter substrate-binding protein	*Microvirga* sp. BSC39	69
165	*M. perideroedes*	WP_018632269	258	Amino acid ABC transporter	*Stappia aggregata* IAM 12614	62
165	*M. perideroedes*	WP_018631939	101	2-oxoglutarate dehydrogenase E2 component	*Paracoccus aminophilus*	70
179	*M. perideroedes*	WP_018632800	308	D-3-phosphoglycerate dehydrogenase	*Phaeospirillum fulvum*	61
181	*M. perideroedes*	WP_018632269	408	Amino acid ABC transporter	*Stappia aggregata* IAM 12614	62
183	*M. perideroedes*	WP_018634051	348	Phasin	*Rhodospirillum centenum*	39
201	*M. perideroedes*	WP_018634051	196	Phasin	*Rhodospirillum centenum*	39

Table B.6. Homology based identification of hypothetical proteins from Mascot using Blastp continued.

Spot	Mascot Taxonomy	Accession	Mascot Score	Blast Protein Name	Blast Taxonomy	Amino Acid Identity (%)
232	*M. perideroedes*	WP_018633993	339	ABC transporter substrate-binding protein	*Paracoccus halophilus*	82
232	*M. perideroedes*	WP_018632269	327	Amino acid ABC transporter	*Stappia aggregata* IAM 12614	62
232	*M. perideroedes*	WP_018633742	214	Taurine ABC transporter substrate-binding protein	*Paracoccus aminophilus*	68
236	*M. perideroedes*	WP_018631899	117	ABC transporter substrate-binding protein	*Microvirga* sp. BSC39	69
244	*M. perideroedes*	WP_018632268	481	Amino acid ABC transporter substrate-binding protein	SAR116 cluster alpha proteobacterium HIMB100	68
258	*M. perideroedes*	WP_018632449	102	Methylmalonate-semialdehyde dehydrogenase	*Tistrella mobilis*	68
270	*M. perideroedes*	WP_018632386	137	Malyl-CoA lyase	*Tistrella mobilis*	67
320	*M. perideroedes*	WP_018633267	566	2,5-didehydrogluconate reductase	*Sinorhizobium meliloti*	66
320	*M. perideroedes*	WP_040789130	148	N-acetylglucosamine kinase	*Nitratireductor pacificus*	40
344	*M. perideroedes*	WP_018634051	311	Phasin	*Rhodospirillum centenum*	39
354	*M. perideroedes*	WP_018634051	520	Phasin	*Rhodospirillum centenum*	39
370	*M. perideroedes*	WP_018632854	296	Tellurium resistance protein	*Pseudorhodobacter aquimaris*	68
419	*M. perideroedes*	WP_018631498	128	Fructose-bisphosphate aldolase	*Loktanella* sp. S4079	71

Table B.6. Homology based identification of hypothetical proteins from Mascot using Blastp continued.

Spot	Mascot Taxonomy	Accession	Mascot Score	Blast Protein Name	Blast Taxonomy	Amino Acid Identity (%)
449	*M. perideroedes*	WP_018631834	96	Ketohydroxyglutarate aldolase	*Rhodobacter* sp. CACIA14H1	72
472	*M. perideroedes*	WP_018634051	213	Phasin	*Rhodospirillum centenum*	39
472	*M. perideroedes*	WP_018631719	201	Ubiquinol-cytochrome C reductase	*Labrenzia aggregata*	72
472	*M. perideroedes*	WP_018634194	130	Hypothetical protein	*Paracoccus* sp. J55	49
472	*M. perideroedes*	WP_018631899	129	ABC transporter substrate-binding protein	*Microvirga* sp. BSC39	69
488	*M. perideroedes*	WP_018631701	177	ATP synthase epsilon chain	*Rhodobacter blasticus*	61
518	*M. perideroedes*	WP_018632449	151	Methylmalonate-semialdehyde dehydrogenase	*Tistrella mobilis*	68
518	*M. perideroedes*	WP_018634051	117	Phasin	*Rhodospirillum centenum*	39
541	*M. perideroedes*	WP_026310169	98	Membrane protein	*Inquilinus limosus*	48
548	*M. perideroedes*	WP_018633730	150	Peptidase inhibitor	*Synechococcus* sp. JA-3-3Ab	32
552	*M. perideroedes*	WP_018634194	116	Hypothetical protein	*Paracoccus* sp. J55	49
572	*M. perideroedes*	WP_018634051	318	Phasin	*Rhodospirillum centenum*	39
950	*M. perideroedes*	WP_018632449	142	Methylmalonate-semialdehyde dehydrogenase	*Tistrella mobilis*	68
950	*M. perideroedes*	WP_018631640	115	Enoyl-CoA hydratase	*Rhodovulum* sp. NI22	70
1196	*M. perideroedes*	WP_018632484	153	Dihydrolipoamide dehydrogenase	*Microvirga* sp. JC119	68

Table B.6. Homology based identification of hypothetical proteins from Mascot using Blastp continued.

Spot	Mascot Taxonomy	Accession	Mascot Score	Blast Protein Name	Blast Taxonomy	Amino Acid Identity (%)
1537	*M. perideroedes*	WP_018634051	265	Phasin	*Rhodospirillum centenum*	39
1537	*M. perideroedes*	WP_018632792	147	Acetyltransferase	*Methylocystis* sp. SB2	70
1956	*M. perideroedes*	WP_018634051	486	Phasin	*Rhodospirillum centenum*	39
4193	*M. perideroedes*	WP_018634051	268	Phasin	*Rhodospirillum centenum*	39
4746	*M. perideroedes*	WP_018632319	220	Quinone oxidoreductase	*Rhodobacteraceae* bacterium PD-2	64
5242	*M. perideroedes*	WP_018631899	379	ABC transporter substrate-binding protein	*Microvirga* sp. BSC39	69
5837	*M. perideroedes*	WP_018633103	80	Fis family transcriptional regulator	alpha proteobacterium MA2	62
CS1	*M. perideroedes*	WP_018632695	466	Superoxide dismutase	*Paracoccus halophilus*	64
CS1	*M. perideroedes*	WP_018633178	349	Glutathione S-transferase	*Maricaulis* sp. JL2009	69
CS1	*M. perideroedes*	WP_018634094	309	Ribulose-phosphate 3-epimerase	*Defluviimonas* sp. 20V17	70
CS1	*M. perideroedes*	WP_018633228	275	Carbonic anhydrase	*Rhodobacteraceae* bacterium HTCC2150	56
CS2	*M. perideroedes*	WP_018632931	286	Dihydrolipoamide dehydrogenase	*Proteobacteria*	72
CS3	*M. perideroedes*	WP_018632302	734	O-acetylhomoserine aminocarboxypropyltransferase	*Azospirillum halopraeferens*	68
CS3	*M. perideroedes*	WP_018631899	391	ABC transporter substrate-binding protein	*Microvirga* sp. BSC39	69

Appendix C

Supplementary material for:

Chapter 4. Microbial Community Dynamics in a Sequencing Batch Reactor Operated under Aerobic Feast-Famine Conditions for the Synthesis of Polyhydroxyalkanoates from Fermented Dairy Manure

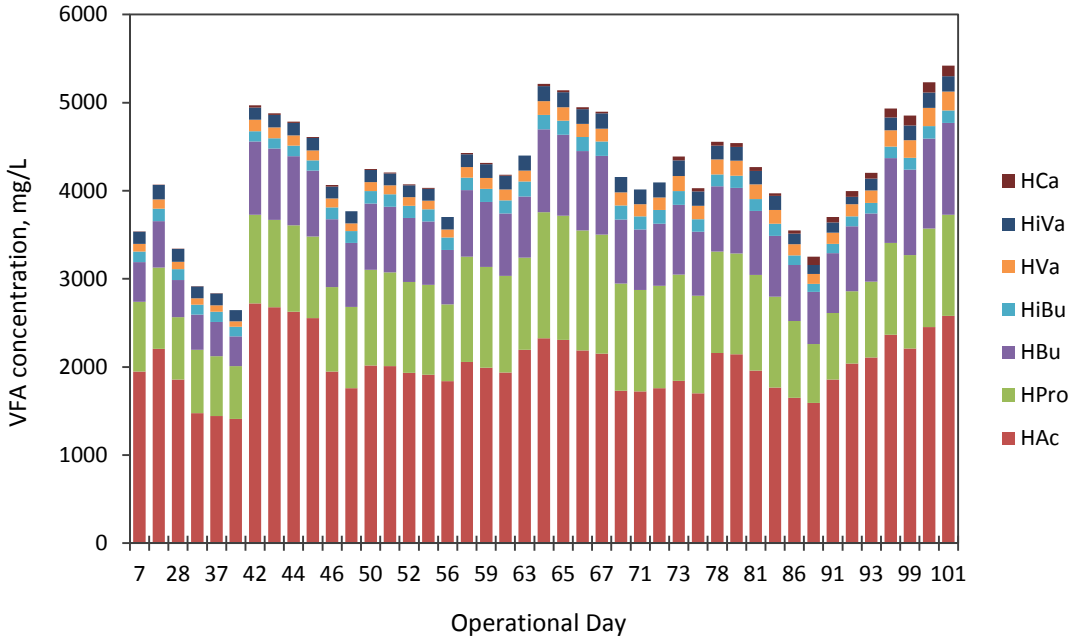

Figure C.1. Total influent VFA content during SBR monitoring.

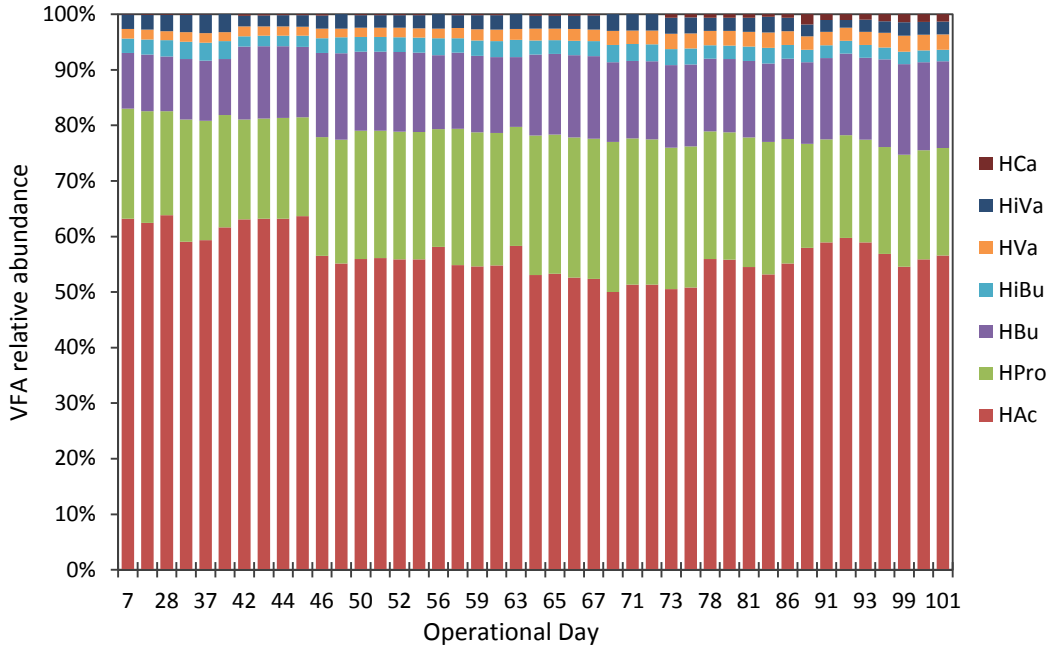

Figure C.2. Influent VFA relative abundance during SBR monitoring.

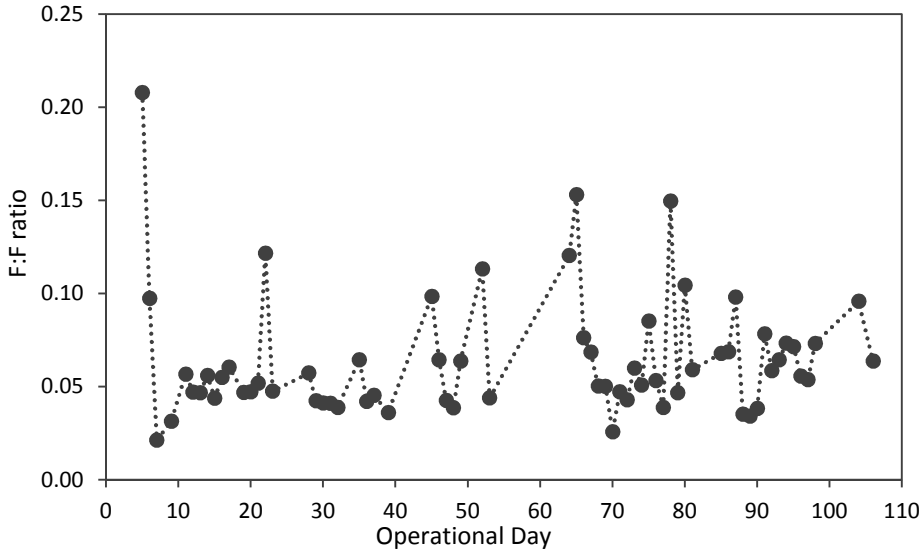

Figure C.3. Measured F:F ratios during SBR monitoring.

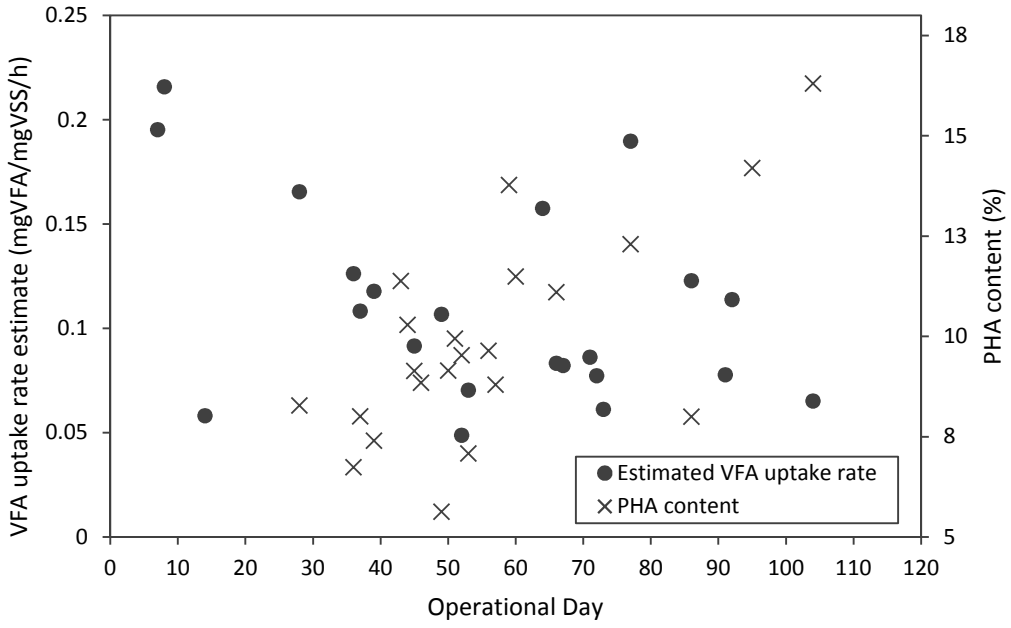

Figure C.4. Estimated VFA uptake rates and PHA content during SBR monitoring.

Table C.1. Quantity and quality of genomic DNA extracted from MMC biomass.

Operational Day	Quantity nucleic acids (ng/µL)	Quality nucleic acids (260/280)
Day 1	96.6 ± 1.4	1.878 ± 0.007
Day 8	176.9 ± 3.8	1.890 ± 0.004
Day 11	150.9 ± 0.7	1.981 ± 0.003
Day 14	184.4 ± 5.8	1.879 ± 0.004
Day 18	238.1 ± 1.2	1.879 ± 0.002
Day 26	179.8 ± 4.4	1.907 ± 0.003
Day 29	203.8 ± 0.1	1.879 ± 0.001
Day 34	148.9 ± 14.2	1.877 ± 0.004
Day 38	276.4 ± 19.4	1.907 ± 0.001
Day 42	196.1 ± 2.1	1.875 ± 0.001
Day 50	163.8 ± 5.3	1.925 ± 0.001
Day 54	156.8 ± 4.3	1.886 ± 0.003
Day 59	205.4 ± 0.7	1.942 ± 0.003
Day 66	130.4 ± 1.3	1.891 ± 0.001
Day 70	220.2 ± 1.4	1.886 ± 0.001
Day 74	222.2 ± 4.5	1.903 ± 0.001
Day 77	146.9 ± 0.6	1.880 ± 0.002
Day 79	216.8 ± 8.2	1.888 ± 0.000
Day 86	171.7 ± 2.2	1.873 ± 0.006
Day 88	219.4 ± 5.6	1.907 ± 0.007
Day 91	256.9 ± 14.0	1.890 ± 0.000
Day 93	198.4 ± 1.3	1.886 ± 0.004
Day 95	217.6 ± 5.1	1.891 ± 0.002
Day 99	215.4 ± 5.6	1.910 ± 0.003
Day 103	220.6 ± 0.4	1.921 ± 0.004
Day 104	247.0 ± 3.0	1.890 ± 0.001
Day 107	246.1 ± 6.0	1.914 ± 0.009
Day 111	201.3 ± 2.0	1.892 ± 0.000
Day 115	190.9 ± 2.9	1.894 ± 0.000
Day 119	202.6 ± 0.1	1.893 ± 0.006

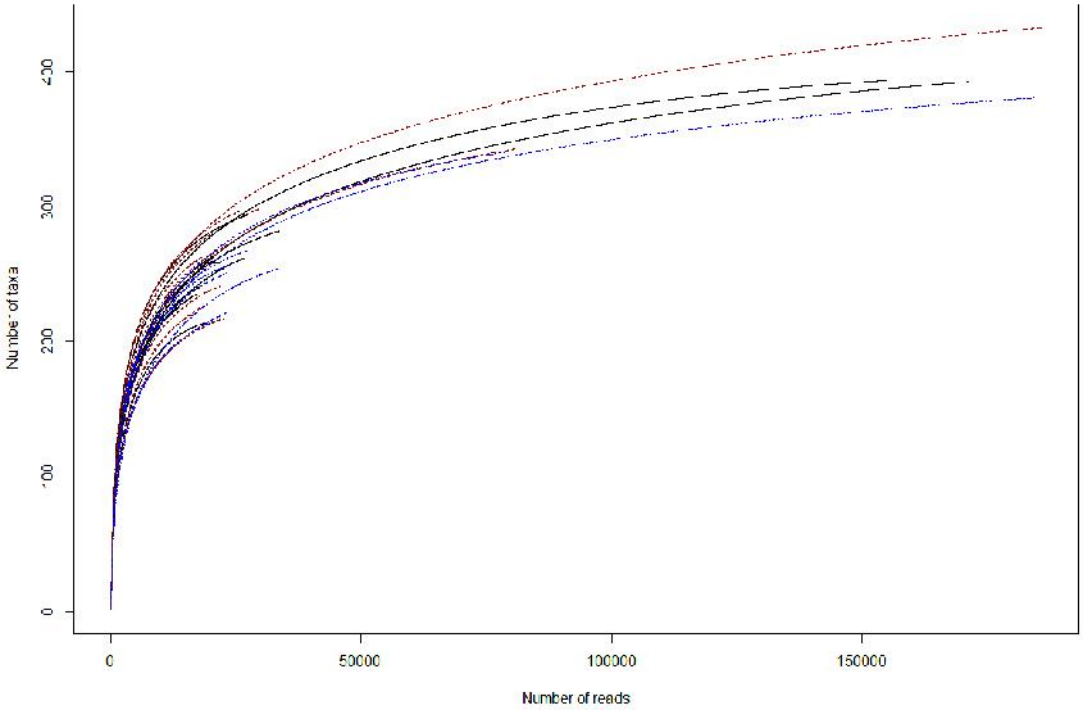

Figure C.5. Rarefaction analysis of samples sequenced during SBR monitoring.

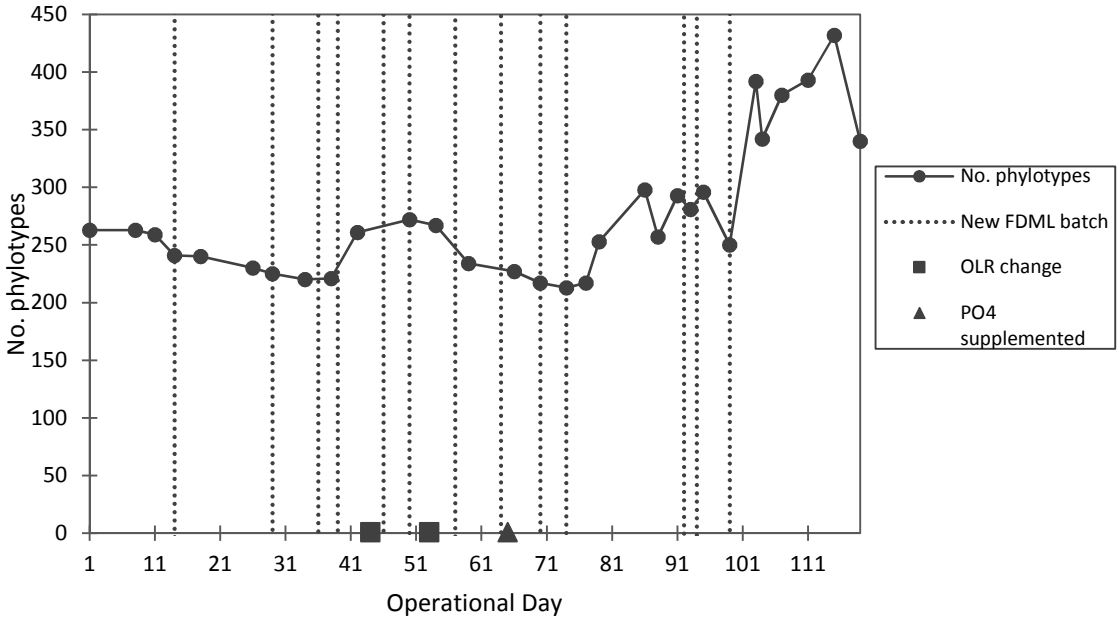

Figure C.6. Number of phylotypes identified during SBR monitoring. Operational changes are denoted, and dashed lines indicate the time at which a "fresh" batch of FDML was substituted.

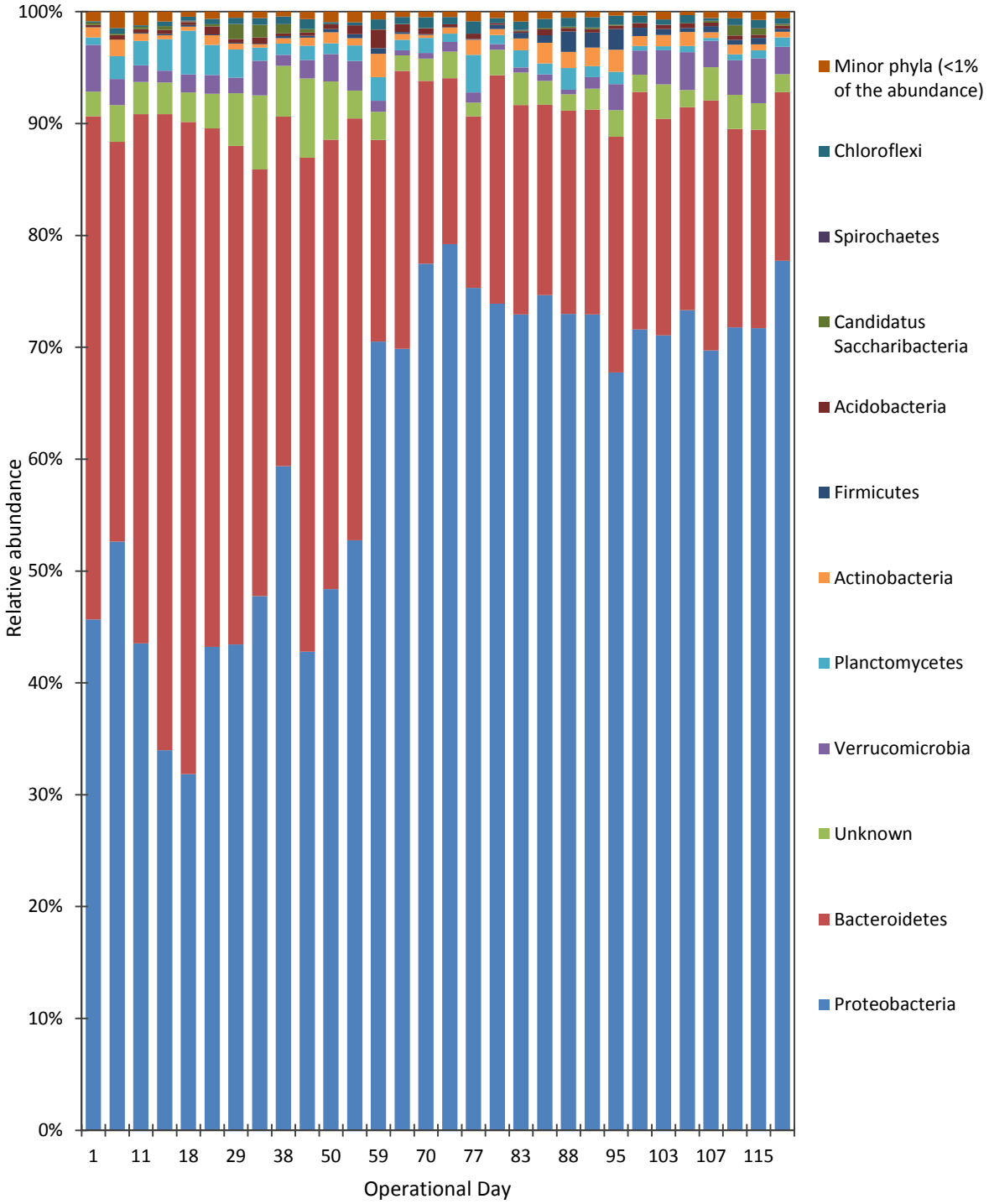

Figure C.7. Phylum level abundance during SBR monitoring.

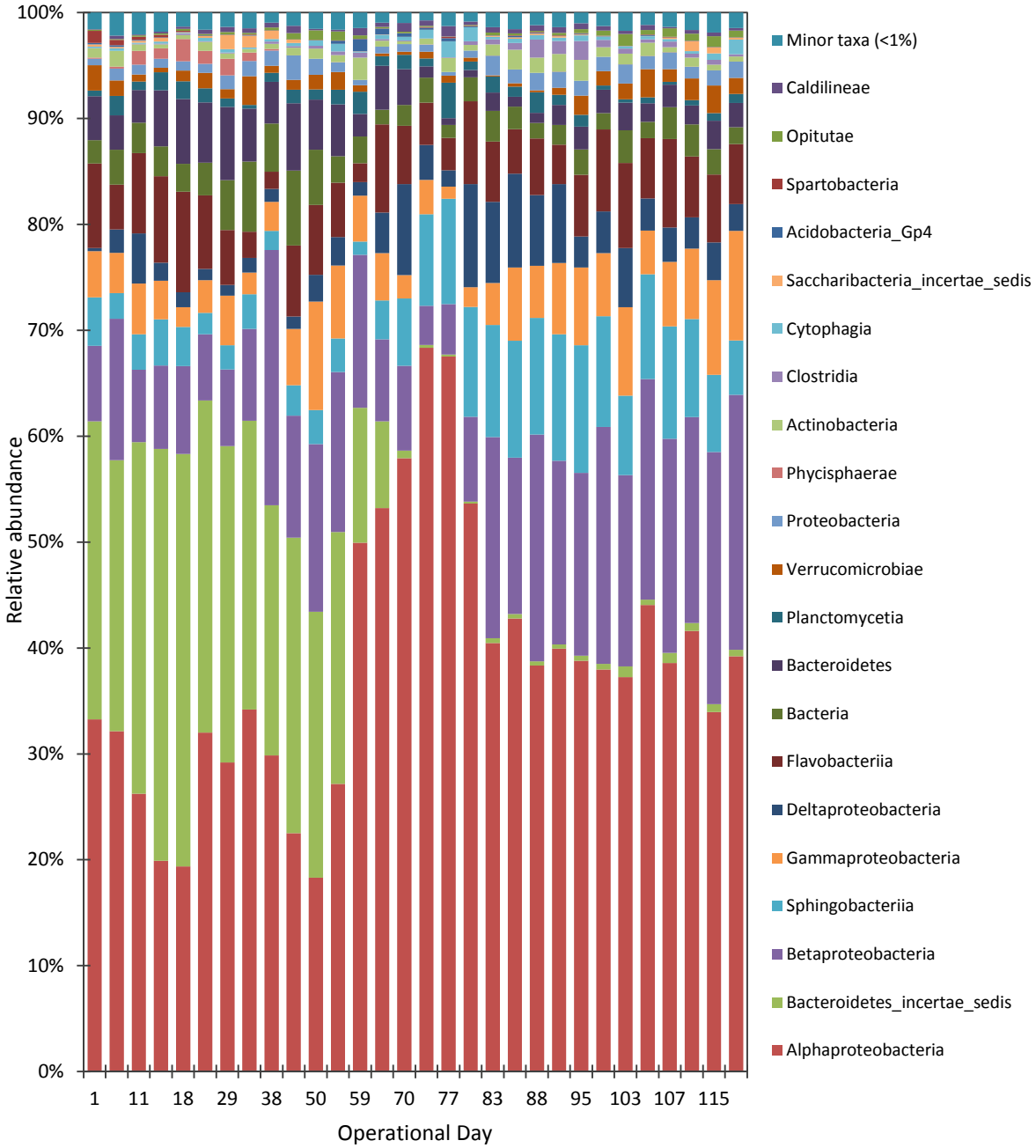

Figure C.8. Class level abundance during SBR monitoring.

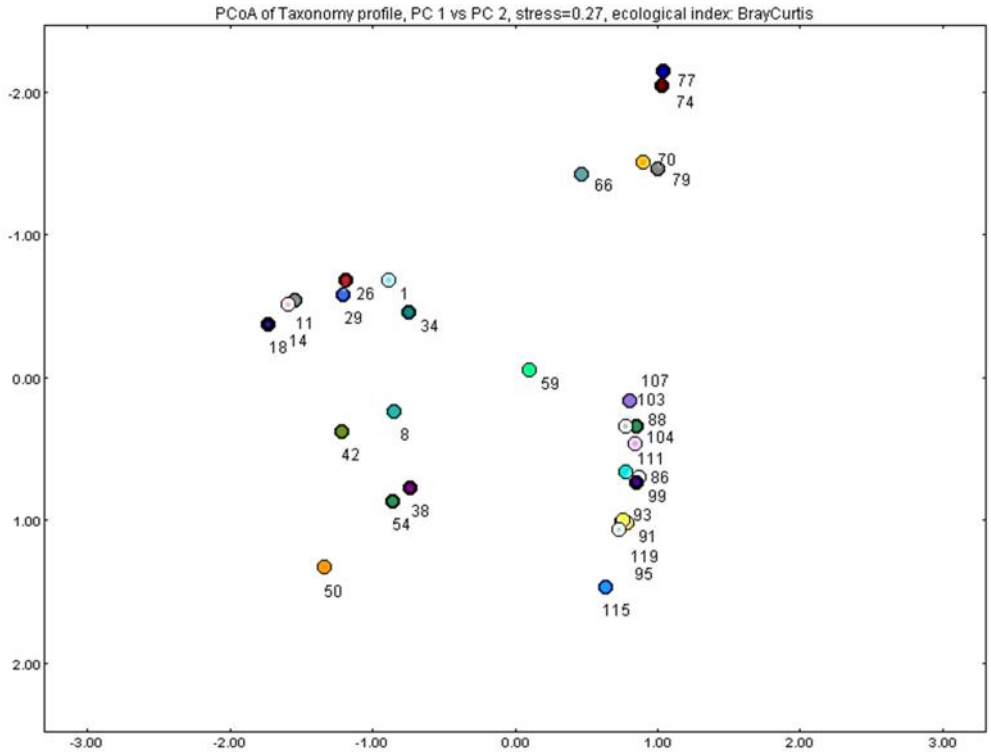

Figure C.9. Principal coordinate analysis of MMC samples collected during the SBR evaluation period. Operational days are indicated by the numbers.

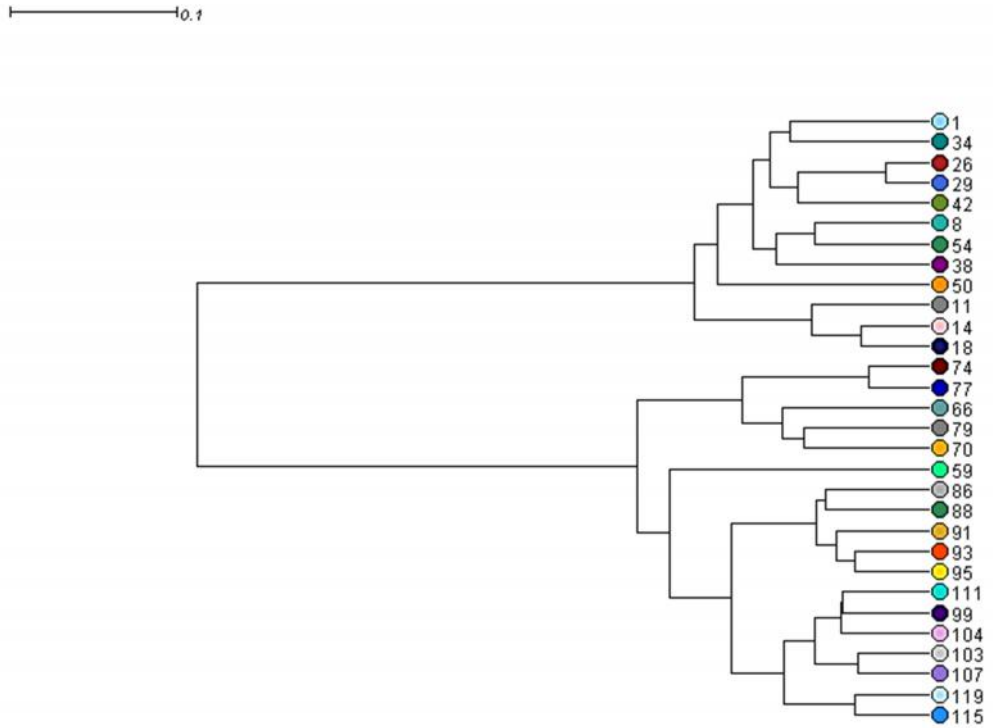

Figure C.10. Cluster analysis of MMC samples collected during the SBR evaluation period. Distances are based on Bray-Curtis dissimilarities, and operational days are indicated by the numbers.